

Modelling the Estuarine Circulation of the Port of Saint John: Applications in

Hydrographic Surveying

by

Ian Church

B.Sc. Eng GGE, University of New Brunswick, 2006

M.Sc.Eng GGE, University of New Brunswick, 2008

A Dissertation Submitted in Partial Fulfillment
of the Requirements for the Degree of

Doctor of Philosophy

in the Graduate Academic Unit of Geodesy and Geomatics Engineering

Supervisor: John Hughes-Clarke, Ph.D., Geodesy and Geomatics Eng.

Examining Board: Katy Haralampides, Ph.D., Civil Engineering

Susan Haigh, Ph.D., Department of Fisheries and Oceans

David Wells, Ph.D., Geodesy and Geomatics Eng.

External Examiner: Fred Page, Ph.D., Department of Fisheries and Oceans

This dissertation is accepted by the
Dean of Graduate Studies

THE UNIVERSITY OF NEW BRUNSWICK

May, 2014

© Ian Church, 2014

ABSTRACT

A 3D baroclinic hydrodynamic model has been developed to investigate the estuarine circulation within the Port of Saint John, in southern New Brunswick. The model simulates the movement and interaction between fresh waters from the Saint John River and saline waters from the Bay of Fundy over four seasonal periods of river flood stages. An improved understanding of sediment dynamics in the harbour is established from the model output, which is critical for understanding the sources of sedimentation and prediction of dredge requirements.

The model describes both the longitudinal and lateral estuarine flow within the harbour. This allows for improved estimates of sediment flux through the primary channels, which reveals annual variations in the relative contributions of the river and salt wedge borne sediments to harbour sedimentation rates. Integration of the near seabed flow patterns over a tidal cycle explains regions of deposition and erosion of fine grained sediments and corridors of sediment motion through examination of the residual current velocity fields.

The model simulation periods coincide with a dense physical oceanographic observation campaign. The validity of the model output has been verified through statistical comparison to the physical observation data. An innovative practical application of the model output to the assessment and prediction of hydrographic multibeam echosounder depth uncertainty is also examined.

ACKNOWLEDGEMENTS

I would like to thank Dr. Susan Haigh, Dr. John Hughes Clarke, Alex Ketchum and others at the Saint John Port Authority, NSERC, Reenu Toodesh, Jeff Melanson, Steve Brucker, James Muggah and other students and staff of the Ocean Mapping Group and department of Geodesy and Geomatics Engineering.

Table of Contents

	Page
ABSTRACT	ii
ACKNOWLEDGEMENTS	iii
List of Tables	vii
List of Figures	ix
CHAPTER 1: Introduction	1
CHAPTER 2: Study Area	6
2.1. Main Harbour Channel	9
2.2. Courtney Bay	13
2.3. Estuarine Mixing	14
2.4. Previous Studies of Saint John	14
CHAPTER 3: Data and Methods	21
3.1. Archived High Density Oceanographic Data for Model Validation	22
3.2. Derivation of Sound Speed from Model Data Output	25
3.3. Bathymetric Surveys	26
3.4. Three Dimensional Baroclinic Hydrodynamic Model	28
3.4.1. Mesh Construction	29
3.4.2. Boundary and Initial Conditions	31
3.4.3. Finite-Volume Coastal Ocean Model	34
CHAPTER 4: Assessing Model Uncertainty	37
4.1. Qualitative Model Comparison with Observed Data	39
4.1.1. Main Harbour Channel Section	40
4.1.1.1. April 2008	41
4.1.1.2. November 2008	44
4.1.1.3. March 2009	47
4.1.1.4. June 2009	50
4.1.2. Courtney Bay Channel Section	53
4.1.2.1. April 2008	54
4.1.2.2. November 2008	57
4.1.2.3. March 2008	60

4.1.2.4. June 2009	63
4.2. Quantitative Model Comparison with Observed Data	65
4.2.1. April 2008	69
4.2.2. November 2008	71
4.2.3. March 2009	73
4.2.4. June 2009	76
4.2.5. Water Mass Analysis	78
4.3. Discussion	79
CHAPTER 5: Model Estuarine Circulation	85
5.1. Estuarine Circulation Observation Overview	86
5.2. Model Contribution to Understanding Cross-Channel Flow	89
5.2.1. Harbour Bridge	92
5.2.1.1. April 2008	92
5.2.1.2. November 2008	95
5.2.1.3. March 2009	98
5.2.1.4. June 2009	101
5.2.2. End of Courtney Bay Breakwater	104
5.2.2.1. April 2008	105
5.2.2.2. November 2008	109
5.2.2.3. March 2009	112
5.2.2.4. June 2009	115
5.2.3. Salt Wedge Residency in Courtney Turning Basin	118
5.3. Optical Backscatter Observation Overview	120
5.3.1. April 2008	121
5.3.2. November 2008	126
5.3.3. March 2009	130
5.4. Estuarine Circulation and Optical Backscatter Upstream of Harbour Bridge ..	134
5.4.1. April 2008	134
5.4.2. November 2008	139
5.4.3. March 2009	142
5.4.4. June 2009	145
5.5. Discussion of Circulation	147
CHAPTER 6: Residual Model Circulation	151
6.1. April 2008	152
6.2. November 2008	154
6.3. March 2009	157
6.4. June 2009	159
6.5. Bathymetry Difference Correlation to Residual Circulation	160
6.5.1. Main Harbour Channel	163
6.5.2. Courtney Bay Channel	170
6.5.3. Short Term Seabed Change Analysis	172
6.6. Discussion of Residual Circulation	176

CHAPTER 7: Volume Flux Estimation.....	179
7.1. Calculation of Model Volume Flux	183
7.2. Model vs. Observation Flux Comparison	187
7.2.1. Main Harbour Channel Section	188
7.2.1.1. April 2008	189
7.2.1.2. November 2008.....	191
7.2.1.3. March 2009	194
7.2.1.4. June 2009	197
7.2.2. Courtney Bay Section	199
7.2.2.1. April 2008	200
7.2.2.2. November 2008.....	202
7.2.2.3. March 2009	204
7.2.2.4. June 2009	207
7.3. Discussion of Model Flux Estimates	208
CHAPTER 8: Hydrographic Vertical Uncertainty Assessment	212
8.1.1. Model Surface Elevations	214
8.1.2. Model Sound Speed Comparison to Observations	216
8.1.3. Model vs. Observations	218
8.1.3.1. Estimating Potential Error Distributions.....	222
8.2. Discussion	225
CHAPTER 9: Discussion.....	227
9.1. Recommendations for Future Work.....	233
CHAPTER 10: Conclusions	236
Bibliography	239
Appendix A.....	243
Curriculum Vitae	

List of Tables

Table 1 – Open Boundary Conditions	33
Table 2 – Constant Values for Initial Conditions of Temperature and Salinity	34
Table 3 – Model Assessment Statistics, from [Hess et al., 2003].....	67
Table 4 – April 2008 MVP vs. Model Assessment	69
Table 5 – April 2008 ADCP vs. Model Assessment	70
Table 6 – November 2008 MVP vs. Model Assessment.....	72
Table 7 – November 2008 ADCP vs. Model Assessment.....	72
Table 8 – March 2009 MVP vs. Model Assessment	74
Table 9 – March 2009 ADCP vs. Model Assessment	75
Table 10 – June 2009 MVP vs. Model Assessment.....	76
Table 11 – June 2009 ADCP vs. Model Assessment.....	77
Table 12 – Central Frequency for each Simulation Period Categorized by Water Mass .	78
Table 13 – Average Salinity Central Frequency by Area	81
Table 14 – Residual Flux Results for April 2008 in Main Harbour Channel. Positive flux indicates downstream direction, towards the Bay of Fundy.	190
Table 15 – Residual Sediment Flux Results for April 2008 in Main Harbour Channel. Positive flux indicates downstream direction, towards the Bay of Fundy.....	190
Table 16 – Flux Results for November 2008 in Main Harbour Channel. Positive flux indicates downstream direction, towards the Bay of Fundy.	192

Table 17 – Residual Sediment Flux Results for November 2008 in Main Harbour Channel. Positive flux indicates downstream direction, towards the Bay of Fundy.	193
Table 18 – Flux Results for March 2009 in Main Harbour Channel. Positive flux indicates downstream direction, towards the Bay of Fundy.	195
Table 19 – Residual Sediment Flux Results for March 2008 in Main Harbour Channel. Positive flux indicates downstream direction, towards the Bay of Fundy.	196
Table 20 – Flux Results for June 2009 in Main Harbour Channel. Positive flux indicates downstream direction, towards the Bay of Fundy.	198
Table 21 – Flux Results for April 2008 in Courtney Bay	200
Table 22 – Sediment Flux Results for April 2008 in Courtney Bay	201
Table 23 – Flux Results for November 2008 in Courtney Bay	203
Table 24 – Sediment Flux Results for November 2008 in Courtney Bay	203
Table 25 – Flux Results for March 2009 in Courtney Bay	205
Table 26 – Sediment Flux Results for March 2009 in Courtney Bay	206
Table 27 – Flux Results for June 2009 in Courtney Bay	207
Table 28 – Relative Influence of Fresh water in Courtney Bay from Main Harbour	211
Table 29 – Cumulative Statistics up to 60 deg of MVP-30 Casts vs. Model Output	219

List of Figures

Figure 1 – The Port of Saint John Overview. Modified from Canadian Hydrographic Service (CHS) Chart 4117 (2009) and Service New Brunswick Softcopy Orthophotomap Data Base (2002).....	8
Figure 2 – Dredge Volumes vs. Maximum Annual River Levels at Saint John [Saint John Port Authority, 2013].....	8
Figure 3 – Seasonal Saint John River Levels with Saint John Harbour Tides (Reference to Chart Datum at Saint John) [Toodesh, 2012]	10
Figure 4 – The Port of Saint John Bathymetry. Topographic Background Map from Toporama WMS (2003).....	11
Figure 5 – Saint John River Watershed (modified from Natural Resources Canada (2013)).....	12
Figure 6 – Proposed Breakwater Locations from Neu (1960).....	16
Figure 7 – Saint John River Levels from River Gauge 01AP005 for 2008 and 2009 with Observation Times (Elevation Reference to CGVD28)	21
Figure 8 – April 2008 MVP-30 Deployments	24
Figure 9 – Port of Saint John Survey Overview with Multibeam Survey Coverage Polygons. Topographic Background Map from Toporama WMS (2003).....	28
Figure 10 – Vertical Terrain-Following Layers.....	30
Figure 11 – Model Mesh and Domain Overview	31
Figure 12 – Reversing Falls Bathymetry and Model Boundary	32

Figure 13 – Quantitative Analysis Areas	38
Figure 14 – April 2008 Main Harbour Section Comparison. Observed sections in first column, model sections in second column. The Section starts near the Harbour Bridge and terminates near the Harbour Entrance.....	42
Figure 15 – April 2008 Main Harbour Profile Comparison	43
Figure 16 – November 2008 Main Harbour Section Comparison. Observed sections in first column, model sections in second column. The Section starts near the Harbour Bridge and terminates near the Harbour Entrance.....	45
Figure 17 – November 2008 Main Harbour Profile Comparison	47
Figure 18 – March 2009 Main Harbour Section Comparison. Observed sections in first column, model sections in second column. The Section starts near the Harbour Bridge and terminates near the Harbour Entrance.....	48
Figure 19 – March 2009 Main Harbour Profile Comparison	50
Figure 20 – June 2009 Main Harbour Section Comparison. Observed sections in first column, model sections in second column. The Section starts near the Harbour Bridge and terminates near the Harbour Entrance.....	51
Figure 21 – June 2009 Main Harbour Profile Comparison.....	53
Figure 22 – April 2008 Courtney Bay Section Comparison. Observed sections in first column, model sections in second column. The Section starts in the Turning Basin and terminates near the intersection with the Main Harbour.....	55
Figure 23 – April 2008 Courtney Bay Profile Comparison.....	57

Figure 24 – November 2008 Courtney Bay Section Comparison. Observed sections in first column, model sections in second column. The Section starts in the Turning Basin and terminates near the intersection with the Main Harbour	58
Figure 25 – November 2008 Courtney Bay Profile Comparison	60
Figure 26 – March 2009 Courtney Bay Section Comparison. Observed sections in first column, model sections in second column. The Section starts in the Turning Basin and terminates near the intersection with the Main Harbour	61
Figure 27 – March 2009 Courtney Bay Profile Comparison	62
Figure 28 – June 2009 Courtney Bay Section Comparison. Observed sections in first column, model sections in second column. The Section starts in the Turning Basin and terminates near the intersection with the Main Harbour	63
Figure 29 – June 2009 Courtney Bay Profile Comparison	65
Figure 30 -- Turbulence Closure Comparison for April 2008 Flood Tide	82
Figure 31 – Observed vs. Model Representation of Interfacial Turbulence	83
Figure 32 – Circulation Overview of Main Harbour Channel. (Derived from observations in Toodesh (2012)).....	87
Figure 33 – Circulation Overview of Courtney Bay Channel. (Derived from observations in Toodesh (2012)).....	89
Figure 34 – Circulation Analysis Areas.....	91
Figure 35 – April 2008 Seabed Current Velocities over a Tidal Cycle in Main Harbour	93
Figure 36 – April 2008 Surface Current Velocities over a Tidal Cycle in Main Harbour	94
Figure 37 – April 2008 Seabed Salinity Distribution over a Tidal Cycle in Main Harbour	95

Figure 38 – November 2008 Seabed Current Velocities over a Tidal Cycle in Main Harbour	96
Figure 39 – November 2008 Surface Current Velocities over a Tidal Cycle in Main Harbour	97
Figure 40 – November 2008 Seabed Salinity Distribution over a Tidal Cycle in Main Harbour	98
Figure 41 – March 2009 Seabed Current Velocities over a Tidal Cycle in Main Harbour	99
Figure 42 – March 2009 Surface Current Velocities over a Tidal Cycle in Main Harbour	100
Figure 43 – March 2009 Seabed Salinity Distribution over a Tidal Cycle in Main Harbour	100
Figure 44 – June 2009 Seabed Current Velocities over a Tidal Cycle in Main Harbour	102
Figure 45 – June 2009 Surface Current Velocities over a Tidal Cycle in Main Harbour	103
Figure 46 – June 2009 Seabed Salinity Distribution over a Tidal Cycle in Main Harbour	104
Figure 47 – April 2008 Seabed Current Velocities over a Tidal Cycle at end of Courtney Bay Breakwater.....	106
Figure 48 – April 2008 Surface Current Velocities over a Tidal Cycle at end of Courtney Bay Breakwater.....	107
Figure 49 – Velocity Magnitude Profile on Flood Tide at Courtney Bay Entrance	108
Figure 50 – April 2008 Seabed Salinity Distribution over a Tidal Cycle at Courtney Bay	109

Figure 51 – November 2008 Seabed Current Velocities over a Tidal Cycle at end of Courtney Bay Breakwater.....	110
Figure 52 – November 2008 Surface Current Velocities over a Tidal Cycle at end of Courtney Bay Breakwater.....	111
Figure 53 – November 2008 Seabed Salinity Distribution over a Tidal Cycle at Courtney Bay	112
Figure 54 – March 2009 Seabed Current Velocities over a Tidal Cycle at end of Courtney Bay Breakwater.....	113
Figure 55 – March 2009 Surface Current Velocities over a Tidal Cycle at end of Courtney Bay Breakwater.....	114
Figure 56 – March 2009 Seabed Salinity Distribution over a Tidal Cycle at Courtney Bay	115
Figure 57 – June 2009 Seabed Current Velocities over a Tidal Cycle at end of Courtney Bay Breakwater.....	116
Figure 58 – June 2009 Surface Current Velocities over a Tidal Cycle at end of Courtney Bay Breakwater.....	117
Figure 59 – June 2009 Seabed Salinity Distribution over a Tidal Cycle at Courtney Bay	118
Figure 60 – Salt Wedge Distribution in Courtney Bay Turning Basin at Low Tide	119
Figure 61 – April 2008 Optical Backscatter Profiles from Main Harbour Channel	123
Figure 62 – April 2008 Optical Backscatter Profiles from Courtney Bay Channel	125
Figure 63 – November 2008 Optical Backscatter Profiles from Main Harbour Channel	127

Figure 64 – November 2008 Optical Backscatter Profiles from Courtney Bay Channel	129
Figure 65 – March 2009 Optical Backscatter Profiles from Main Harbour Channel	131
Figure 66 – March 2009 Optical Backscatter Profiles from Courtney Bay Channel	133
Figure 67 – April 2008 Model Salinity Output Upstream of Harbour Bridge at Low and Flood Tide. Section begins at the Reversing Falls sill and terminates at the Harbour Bridge.....	135
Figure 68 – April 2008 Oceanographic Observations Upstream of Harbour Bridge at High Tide. Section begins at the Reversing Falls sill and terminates at the Harbour Bridge.....	136
Figure 69 – April 2008 Oceanographic Observations Upstream of Harbour Bridge at the start of the Ebb Tide. Section begins at the Reversing Falls sill and terminates at the Harbour Bridge.	137
Figure 70 – April 2008 Model Salinity Output Upstream of Harbour Bridge at the Start of Ebb Tide. Section begins at the Reversing Falls sill and terminates at the Harbour Bridge.	138
Figure 71 – April 2008 Modelled Salt Wedge at High Tide at Reversing Falls.....	138
Figure 72 – April 2008 Model Salinity Output Upstream of Harbour Bridge on Ebb Tide. Section begins at the Reversing Falls sill and terminates at the Harbour Bridge.	139
Figure 73 – November 2008 Model Salinity Output Upstream of Harbour Bridge at Low and Flood Tide. Section begins at the Reversing Falls sill and terminates at the Harbour Bridge.....	139

Figure 74 – November 2008 Oceanographic Observations Upstream of Harbour Bridge at end of Flood Tide. Section begins at the Reversing Falls sill and terminates at the Harbour Bridge.	140
Figure 75 – November 2008 Model Salinity Output Upstream of Harbour Bridge at High Tide and the Start of Ebb Tide. Section begins at the Reversing Falls sill and terminates at the Harbour Bridge.....	141
Figure 76 – November 2008 Oceanographic Observations Upstream of Harbour Bridge on Ebb Tide. Section begins at the Reversing Falls sill and terminates at the Harbour Bridge.....	142
Figure 77 – March 2009 Model Salinity Output Upstream of Harbour Bridge at Low, Flood and High Tide. Section begins at the Reversing Falls sill and terminates at the Harbour Bridge.	143
Figure 78 – March 2009 Oceanographic Observations Upstream of Harbour Bridge on Ebb Tide. Section begins at the Reversing Falls sill and terminates at the Harbour Bridge.	144
Figure 79 – March 2009 Model Salinity Output Upstream of Harbour Bridge at the Start of Ebb and Ebb Tide. Section begins at the Reversing Falls sill and terminates at the Harbour Bridge.	145
Figure 80 – June 2009 Model Salinity Output Upstream of Harbour Bridge at Low, Flood and High Tide. Section begins at the Reversing Falls sill and terminates at the Harbour Bridge.....	146

Figure 81 – June 2009 Oceanographic Observations Upstream of Harbour Bridge on the start of the Ebb Tide. Section begins at the Reversing Falls sill and terminates at the Harbour Bridge.	147
Figure 82 – June 2009 Model Output Upstream of Harbour Bridge on Ebb Tide. Section begins at the Reversing Falls sill and terminates at the Harbour Bridge.	147
Figure 83 – April 2008 Model Tidal Residual Currents at the Seabed.....	153
Figure 84 – November 2008 Model Tidal Residual Currents at the Seabed	157
Figure 85 – March 2009 Model Tidal Residual Currents at the Seabed.....	159
Figure 86 – June 2009 Model Tidal Residual Currents at the Seabed.....	160
Figure 87 – Saint John Multibeam Survey Times relative to Saint John River level. Line thickness indicates survey duration.	162
Figure 88 – Bathymetry Difference Main Harbour Channel (Spring 2009 vs. Spring 2008)	164
Figure 89 – Bathymetry Difference Main Harbour Channel (Fall 2009 vs. Spring 2009)	167
Figure 90 – Bathymetry Difference Main Harbour Channel (Fall 2010 vs. Spring 2009)	168
Figure 91 – Bathymetry Difference Main Harbour Channel (Fall 2010 vs. Fall 2009) .	169
Figure 92 – Bathymetry Difference Main Harbour Channel (Spring 2008 vs. Spring 2000)	170
Figure 93 – Bathymetry Difference Courtney Bay Channel (Fall 2008 vs. Spring 2008)	171

Figure 94 – Bathymetry Difference Courtney Bay Channel (Spring 2009 vs. Fall 2008)	172
Figure 95 – Spring 2008 Survey Times	173
Figure 96 – Bathymetry Difference Main Harbour Channel (Spring 2008, JD120 vs. JD113)	174
Figure 97 – Bathymetry Difference Main Harbour Channel (Spring 2008, JD150 vs. JD120)	175
Figure 98 – Bathymetry Difference Profile (Spring 2008, JD150 vs. JD120). Negative differences correspond to areas of erosion, while positive differences correspond to areas of deposition.	176
Figure 99 – West Pier Berth Dredge Volumes vs. Maximum Annual River Levels [Saint John Port Authority, 2013]	177
Figure 100 – Flux Section Location Overview for Main Harbour Channel and Courtney Bay	180
Figure 101 – April 2008 Main Harbour Volume Flux Section at four Stages of the Tide. Section is Presented from West to East Across the Channel. Depths Referenced to Mean Sea Level.	182
Figure 102 – April 2008 Courtney Bay Volume Flux Section at four Stages of the Tide. Section is Presented from West to East Across the Channel. Depths Referenced to Mean Sea Level.	183
Figure 103 – Flux Segment Node and Element Averaging	185
Figure 104 – Volume Flux Calculation, Modified from Ip and Lynch [1995]	186
Figure 105 – April 2008 Volume Flux over a Tidal Cycle in Main Harbour	191

Figure 106 – November 2008 Volume Flux over a Tidal Cycle in Main Harbour	194
Figure 107 – March 2009 Volume Flux over a Tidal Cycle in Main Harbour	197
Figure 108 – June 2009 Volume Flux over a Tidal Cycle in Main Harbour	199
Figure 109 – April 2008 Volume Flux over a Tidal Cycle in Courtney Bay	202
Figure 110 – November 2008 Volume Flux over a Tidal Cycle in Courtney Bay	204
Figure 111 – March 2009 Volume Flux over a Tidal Cycle in Courtney Bay	206
Figure 112 – June 2009 Volume Flux over a Tidal Cycle in Courtney Bay	208
Figure 113 – Beam Angle Standard Deviation based on Difference Statistics	220
Figure 114 – April 2008 Absolute and Percentage Depth Error Histograms	221
Figure 115 – November 2008 Absolute and Percentage Depth Error Histograms	221
Figure 116 – March 2009 Absolute and Percentage Depth Error Histograms	222
Figure 117 – June 2009 Absolute and Percentage Depth Error Histograms	222
Figure 118 – November 2008 IHO Order Distribution	224

List of Symbols, Nomenclature or Abbreviations

ADCP: Acoustic Doppler Current Profiler

AINS: Aided Inertial Navigation System

CF: Central Frequency

CHS: Canadian Hydrographic Service

CRI: Canadian Rivers Institute

DOY: Day of the Year

INRS: Institut National de la Recherche Scientifique

MBES: Multibeam Echosounder

MVP: Moving Vessel Profiler

NOF: Negative Outlier Frequency

OMG: Ocean Mapping Group

POF: Positive Outlier Frequency

PSU: Practical Salinity Units

SD: Standard Deviation

SJPA: Saint John Port Authority

RMSE: Root Mean Squared Error

TVU: Total Vertical Uncertainty

UNB: University of New Brunswick

CHAPTER 1: Introduction

The Port of Saint John, located in southern New Brunswick on the east coast of Canada, is an active industrial port, important economic centre and a natural estuary at the confluence of the Saint John River and the Bay of Fundy. The estuary is very highly stratified as the river flows over the salt wedge that is pushed into the harbour by strong semi-diurnal tides from the bay [Baird, 1987]. The tides at Saint John can reach a spring range of over nine metres. Both the river and the residual tidal circulation from offshore are potential sources of sedimentation in the harbour [Baird, 1987], which must be removed each year through dredging to allow access to most of the berthing areas.

A multidisciplinary project was started in 2008 to better discern the sources of the excess sedimentation in the harbour. The project is a collaboration between the Ocean Mapping Group (OMG), Canadian Rivers Institute (CRI), department of Civil Engineering at the University of New Brunswick (UNB), Institut National de la Recherche Scientifique (INRS) and Saint John Port Authority (SJPA). The OMG's role is to study tidal and seasonal changes in seabed bathymetry, estuarine circulation and oceanography. This thesis expands on previous observational work by Toodesh (2012) by further interpreting those observations and correlating them to the output of a three-dimensional baroclinic hydrodynamic model of the harbour developed as part of this work. The model is able to predict the distribution of salt and fresh waters in the estuary and the three dimensional

current velocities. The model is tested against the observations (Chapter 4) to assess its validity.

Previous studies of the estuarine circulation and sedimentation of the Port of Saint John have been based on limited spatial and temporal observations. These studies have all concluded that the observations do not capture the full estuarine environment and that the movement of salt and fresh water in the port must be better understood. The observational data have been restricted by logistical constraints on sampling due to vessel traffic, the large tidal range and strong tidal currents. An overview of previous studies is presented in Chapter 2. This thesis is designed to resolve the complex estuarine circulation in the Port of Saint John without the restrictions of physical sampling through the use of high resolution three-dimensional numerical modelling. Knowledge of the estuarine circulation provides essential information towards understanding the erosion and deposition of sediment in the harbour, and estimating and predicting sound speed uncertainty for hydrographic surveying.

Salinity, temperature, speed of sound, optical backscatter, current velocities and acoustic backscatter data were collected from the OMG research vessel, the Heron, over a period of a semi-diurnal tidal cycle at four times of the year when characteristic flow regimes were present [Toodesh, 2012]. The data were collected underway along the axes of the major channels of the port. The hydrodynamic model was built to coincide with the

observation periods and was used to understand the circulation within the port away from the observations, as presented in Chapters 5 and 6.

Toodesh (2012) estimated the volume fluxes through a section of the main harbour channel through lateral extrapolation of repeat observations at a single point on that section over a tidal cycle. With the model the flux of salt and fresh waters over a cross section of the harbour can now be calculated properly taking into account the lateral variations in salinity and current velocities. The volume fluxes across a section can be evaluated at any location within the model domain, including areas where current velocities are below the noise threshold of the ADCP instrumentation, as was the case in Courtney Bay in Toodesh (2012). The model sediment and volume flux estimates for the Main Harbour Channel and Courtney Bay are presented in Chapter 7.

Precise bathymetry is required to monitor the dredge volumes removed. Performing accurate multibeam echosounder (MBES) hydrographic surveys in the port is, however, particularly difficult due to the rapidly changing oceanographic conditions. As the salt wedge moves throughout the harbour with the flood and ebb tide, the sound speed structure changes dramatically. To cope with the complex environment, traditionally MBES surveys have been completed using narrow swath widths and tight line spacing to limit sound speed related data artifacts. With a hydrodynamic model of the Port of Saint John the effects of performing MBES surveys at different stages of the tide can now be evaluated in order to minimize sound speed errors and improve survey efficiency. The consequences of using the model outputs of temperature and salinity to calculate the

sound speed structure in the port are assessed in terms of subsequent vertical ray-tracing uncertainty, as described in Chapter 8. The accuracy of the model can then be evaluated in terms of potential MBES vertical error associated with using the model rather than actual observations for acoustic ray-tracing.

MBES surveys on the Port of Saint John were completed by the OMG's research vessel, the Heron, in the springs of 2008 and 2009 and fall of 2010. MBES data were also collected by the CHS vessels Plover and Pipit during the falls of 2008 and 2009. The primary difference between these surveys and the MBES surveys completed by port's survey vessel, the Hawk, is that these surveys extend outside of the dredged areas.

Through examination of changes in the seabed bathymetry, the seasonal and annual variations in the seabed morphology within the domain of the port can be examined and correlated to the variations in oceanography and model output, as described in Chapter 6.

The Port of Saint John is a complex environment that requires a multidisciplinary approach to understanding the circulation and potential sources of sedimentation. The hydrodynamic model allows for the density structure and current velocities to be predicted throughout the port. The oceanographic observations are required to validate the model and provide insight into the quantities and distribution of suspended sediment. The analysis of changes in seabed bathymetry gives an indication of how the physical environment is changing in response to the oceanographic circulation over time. It is with the amalgamation of these tools that the dynamics in the Port of Saint John is starting to be understood.

This thesis accomplishes three primary objectives: (1) development of methods for assessment of high resolution hydrodynamic model output to observational data, (2) develop an understanding of the estuarine dynamics and three dimensional circulation of the Port of Saint John, and (3) examining methods to use model output to plan and model sound speed variations during a MBES hydrographic survey.

CHAPTER 2: Study Area

The Port of Saint John is New Brunswick's largest port, bringing in over 26 million metric tonnes of cargo and hosting approximately 80 cruise ships with over 200,000 passengers each year [Saint John Port Authority, 2009]. As shown in Figure 1, there are two principal channels and berthing areas in the harbour; the Main Harbour channel to the west and the Courtney Bay channel to the east. Sections of both channels are dredged each year to maintain minimum under keel clearances. The principal difference between the two areas is fresh water input. The Main Harbour Channel is also the mouth of the Saint John River and must cope with the entire fresh water load of the river watershed. Courtney Bay, on the other hand, has no significant input of fresh water and with reduced current velocities is a natural location for deposition of sediments [Neu, 1960].

The amount of dredging required within the port is unpredictable from year to year. There is little to no correlation with the maximum flood levels of the Saint John River near the port, as shown in Figure 2, with a correlation coefficient R^2 of 0. Figure 2 shows that over the past 10 years, the amount of annual dredged material has varied from a minimum of 120,000 m³ in 2007 to a maximum of 375,000 m³ in 2006 [Saint John Port Authority, 2013]. Analysis of dredging records from the Saint John Port Authority reveals that approximately 70% of dredging is performed in Courtney Bay and is therefore the primary area of concern for the Saint John Port Authority. Large amounts of sediments move into Courtney Bay and must be removed so that vessel traffic is not impeded [Leys,

2007]. It is unknown whether the source of the majority of the sediments which enter the bay are from the river or from tidal offshore resuspension [Neu, 1960]. This thesis is designed to better resolve that unknown.

A comprehensive overview of the study area may be found in Toodesh (2012), which investigates the offshore wave activity, local climate, river water level and tides. All these factors may influence the overall sediment distribution and redistribution in the Port of Saint John, although the river levels and tides certainly have the most influence on estuarine circulation. The role of winter storms was addressed in Melanson (2012) who found that there was a correlation between storm surge events and sediment concentrations in the salt wedge.

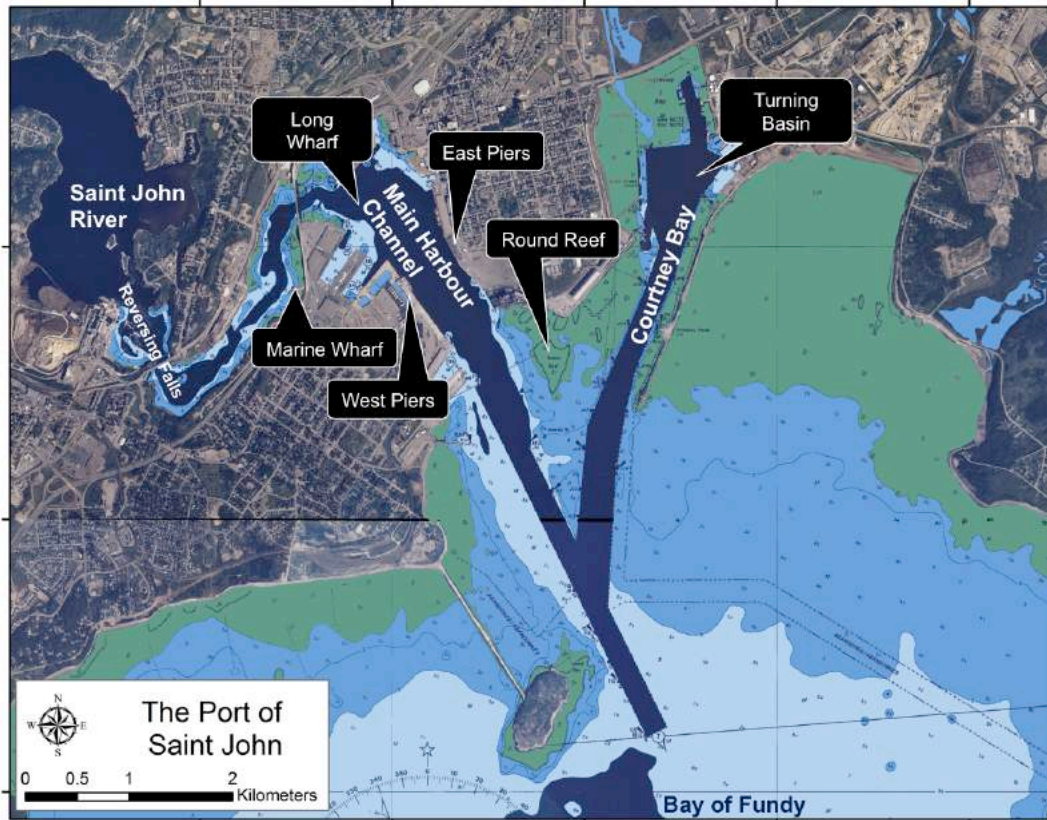


Figure 1 – The Port of Saint John Overview. Modified from Canadian Hydrographic Service (CHS) Chart 4117 (2009) and Service New Brunswick Softcopy Orthophotomap Data Base (2002)

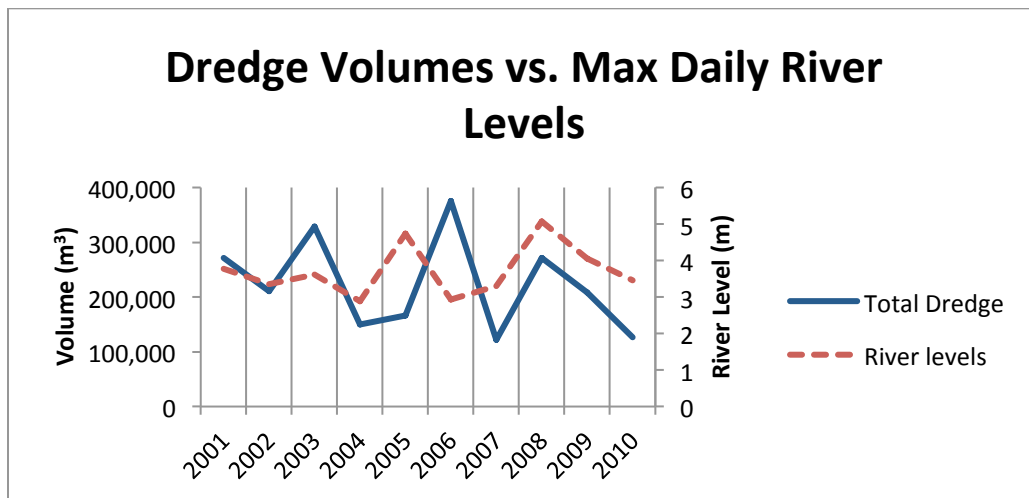


Figure 2 – Dredge Volumes vs. Maximum Annual River Levels at Saint John [Saint John Port Authority, 2013]

2.1. Main Harbour Channel

The Main Harbour Channel is the natural connection between the Saint John River and the Bay of Fundy. Upstream of the harbour is the Reversing Falls which influences mixing and limits the intrusion of the salt wedge upstream of the falls at certain periods of river discharge through a lateral and bathymetric constriction. The range of the tides is reduced by an order of magnitude as the tidal wave propagates through the falls, but the river is still classified as tidal over 90 km upstream [Godin, 1991]. Due to the reduction in tidal amplitudes between the bay and the river the rapids generated by the constriction at the Reversing Falls appear to either flow up river, or down into the harbour depending on the stage of the tide. The reversal of flow is dependent on the river level. At times of very high river levels, such as those experienced during the spring freshet, the tidal amplitude in the harbour may not be sufficient to surpass the elevation of the river, as shown in the top right panel of Figure 3.

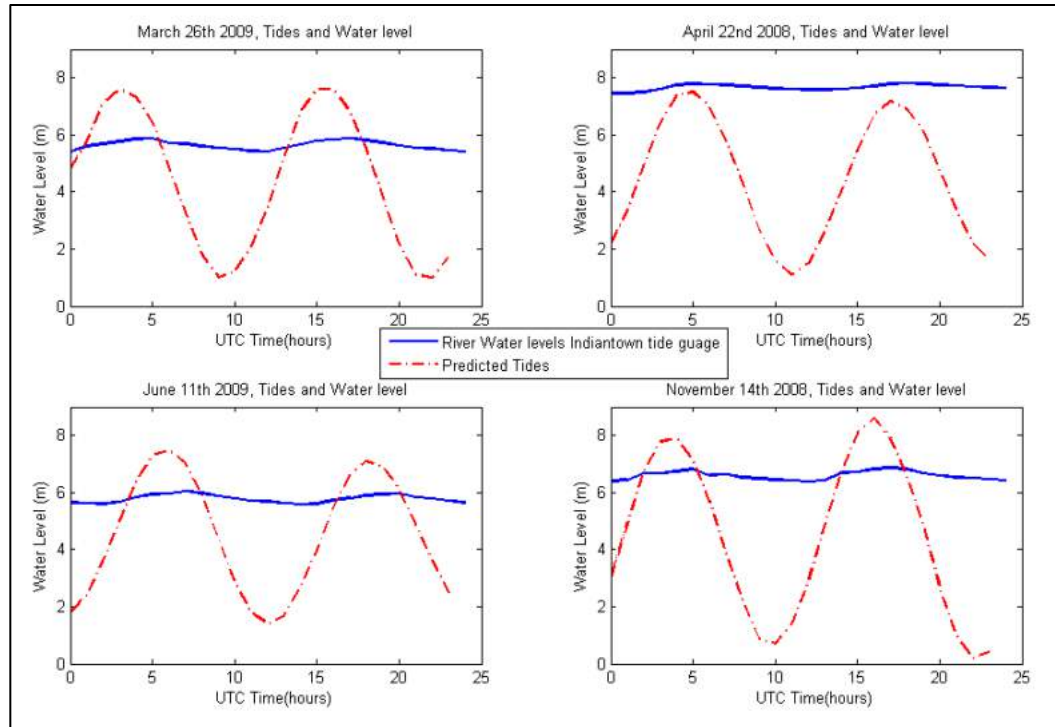
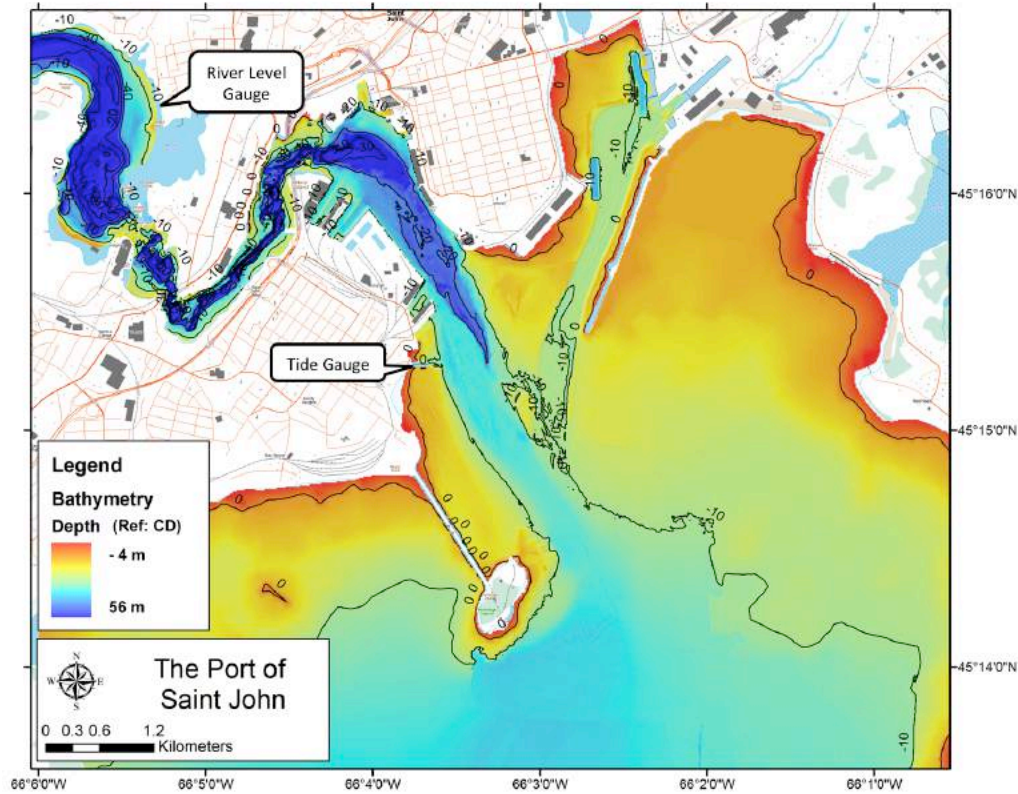


Figure 3 – Seasonal Saint John River Levels with Saint John Harbour Tides (Reference to Chart Datum at Saint John) [Toodesh, 2012]

Depths in the Main Harbour channel extend to a maximum of over 45 metres, as shown in Figure 4. Sediments in the Main Harbour are naturally eroded in the centre of the channel, but berth areas require dredging annually to maintain minimum under keel clearance [Leys and Mulligam, 2011]



**Figure 4 – The Port of Saint John Bathymetry. Topographic Background Map from Toporama
WMS (2003).**

The Saint John River has a drainage area of 60,000 km² and extends up into northern Maine and Quebec [Neu, 1960]. Discharge rates of the river have only been measured in a small number of locations, the closest to the Reversing Falls being Environment Canada gauge 01AK004 downstream of the Mactaquac Generating Station. Discharge rates were measured at this location from 1961 to 1995 with a maximum mean discharge of 2360 m³/s in April and a minimum mean discharge of 376 m³/s in February [Environment Canada, 2012]. W.F. Baird (1987) suggested that in Saint John the river discharge rate

varies from a spring high of 3,000 m³/s to a winter minimum of 200 m³/s. The limit of the watershed of the Saint John River is shown as the red area of Figure 5.

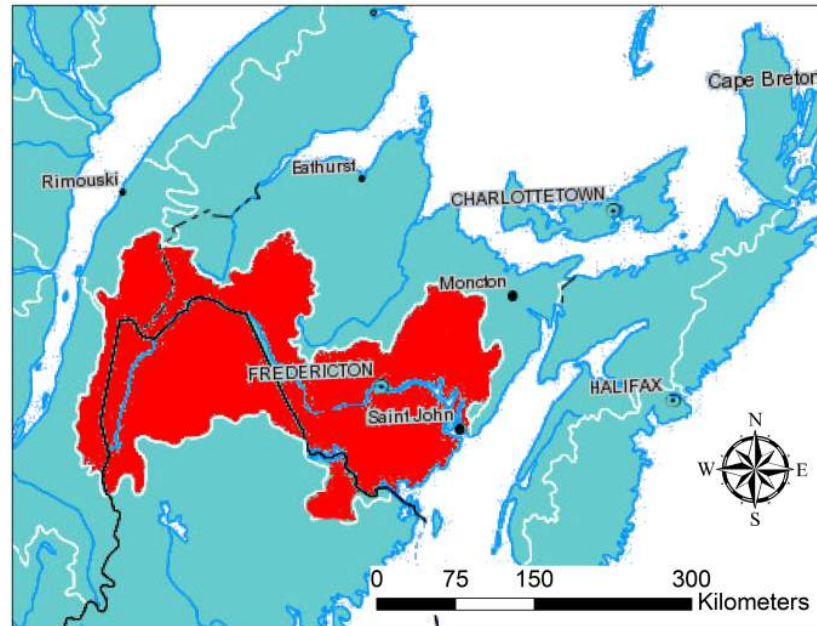


Figure 5 – Saint John River Watershed (modified from Natural Resources Canada (2013))

A permanent tide gauge located in the Port of Saint John (Figure 4) measures the observed tides at the location of the Ferry Terminal at the entrance of the Main Harbour channel. It is maintained by the Department of Fisheries and Ocean Canada and is the only tide gauge in continuous operation in the Bay of Fundy. Data have been logged at the gauge since 1936. The spring tidal range at the gauge is approximately 9.1 metres while the neap range is approximately 6.7 metres [Baird, 1987].

River levels are recorded upstream of the Reversing Falls by Environment Canada at the Saint John River at Saint John, NB, 01AP005 river level gauge. The gauge is located at an approximate WGS84 latitude of $45^{\circ}16'24''N$ and longitude of $66^{\circ}05'20''W$ (Figure 4) and has been in operation since 1965 [Environment Canada, 2012].

2.2. Courtney Bay

The Courtney Bay Turning Basin, located at the head of the Courtney Bay Channel (Figure 1), and the Courtney Bay Channel were created by the construction of a breakwater in the early 1900s. The natural circulation of water in the estuary was further disrupted by the construction of the breakwater between Partridge Island and the nearby shoreline in the early 1960's, after recommendations for flow control structures in Neu (1960) shown in Figure 6 [Baird, 1987].

Courtney Bay has a very small input of fresh water from Marsh Creek at the northern tip of the Turning Basin. Tidal gates block the flow of salt water from entering the creek at high tide, but allow some fresh water to flow back into the bay at low tide. Discharge rates for Marsh Creek are very low, but have not been measured. Depths in Courtney Channel and the berths in Courtney Bay are dredged annually to maintain a minimum under keel clearance of 5.5 metres.

2.3. Estuarine Mixing

Two types of interfacial mixing are expected in the Port of Saint John and include entrainment and turbulent diffusion [Toodesh, 2012]. Entrainment is the process of injecting denser bottom layer waters into the less dense surface waters through progressive interfacial Holmboe waves [Dyer, K. R., 1997]. Turbulent diffusion occurs when unstable flows generate Kelvin-Helmholtz instabilities [Dyer, K. R., 1997; Pond, S. and G. L. Pickard, 1983]. These waves can be large, with wavelengths of over a metre, and tend to break along the density interface causing eddies to form which mixes within the upper and lower layers broadening the pycnocline. While entrainment only moves denser lower waters into the less dense upper layer, turbulent diffusion may move water between both layers.

2.4. Previous Studies of Saint John

The excess sedimentation problem within the Port of Saint John is an issue that has existed since the construction of the Courtney Bay breakwater. A number of relevant previous studies have been conducted which examined the source of the sedimentation and some suggestions were put forth to remedy the problem. A comprehensive literature review on the Port of Saint John was prepared by Baird (1987) for Transport Canada, which examined available relevant material on the circulation and sedimentation in the port. The synopsis includes, but is not limited to, an overview of Rogers' 1936 report on

“The Estuary of the Saint John River”, Hachey’s 1939 report on “Hydrographic Features of the waters of Saint John Harbour”, Neu’s 1960 report on a “Hydrographic survey of Saint John Harbour, N.B.” for the National Research Council, and Metcalfe’s 1976 report on “Physical, Chemical and Biological Parameters of the Saint John River Estuary”.

The literature review of Baird (1987) provides a summary of existing research within the Port of Saint John at the time and future recommendations for additional research and remediation. Based on the reports on the hydrographic and estuarine conditions of the Port of Saint John, it was determined that the principal source of the sediments in Courtney Bay is likely the waters of the Saint John River. Baird (1987) also notes that many of the physical observations in previous studies may no longer be valid as various construction projects have changed the circulation patterns within the port. These projects include the construction of the breakwater connecting Partridge Island to the main land and changes to the dock faces in the Main Harbour Channel. The construction projects have likely increased the speed of water as it flows through the Harbour, but not the direction of the waters. It is observed that river waters are still moving over the mudflats to the west of the Courtney Bay channel on the ebb and low tide.

The breakwater connection to Partridge Island was built after recommendations provided in Neu (1960) during the early 1960’s [Baird, 1987]. The break water was one of many flow control structures suggested by Neu (1960), as shown in Figure 6. His proposed control structures were designed to train the river into flowing away from the area known

as Round Reef (Figure 1) and to limit erosion in the Courtney Bay Channel with spur dykes.

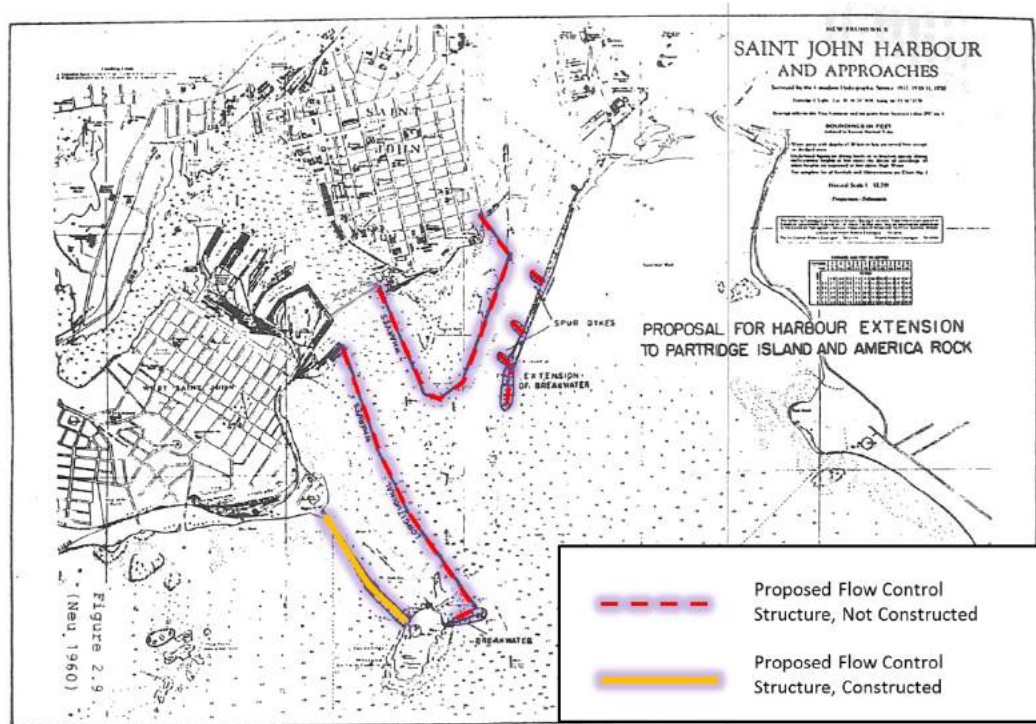


Figure 6 – Proposed Breakwater Locations from Neu (1960).

Baird (1987) states that a reduction in dredge quantities in Courtney Bay will be achieved if structures are built to redirect the sediment rich flows of the Saint John River away from the mudflats west of the Courtney Bay channel. This recommendation is accompanied by a caution that the exact location of the redirection structures requires additional knowledge of the estuarine circulation, which could be achieved through numerical modelling. To calibrate the models and improve our understanding of the present day circulation, Baird (1987) recommends that physical observations be made of

the temperature, salinity and current velocities throughout a tidal cycle during both the spring freshet and average flow conditions.

Twenty years later Leys (2007) generated a hydrodynamic and sediment transport model focused on the Marine Wharf in the Reversing Falls Channel upstream of the Harbour Bridge (Figure 1). The model was bounded by the entrance to the Main Harbour Channel, downstream of the Harbour Bridge, and the Saint John River, upstream of the Environment Canada river level gauge. The model simulation was completed for the middle of November, 2006, to correspond to field measurements. Leys (2007) discovered that tidal and density currents likely contribute more sedimentation than the river water for areas of the port downstream of the Reversing Falls. Physical observations throughout the Reversing Falls channel also describe the circulation during the fall freshet condition for that area.

Through examination of seabed and suspended sediments, Matheron (2010) found that suspended sediments are mostly contained in the salt wedge entering the port on the flood tide. This observation correlates with the findings of Leys (2007), but not with the synopsis of Baird (1987). It was found that the larger suspended sediment particles deposit at the entrance to the Courtney Bay Channel, while the finer grain sediments make their way to the Courtney Bay Turning Basin as current velocities decrease.

In Leys (2011) the modeling domain of the Port of Saint John was increased in size from the model presented previously in Leys (2007) to include Courtney Bay. The relatively

low resolution model was developed to examine the effects of sedimentation throughout the port, extending beyond the previous study of Leys (2007). Annual sedimentation rates were estimated based on dredging records and a 15 day model run was simulated where the river and Bay of Fundy sediment fractions were analyzed separately. It was found that 50% of the transport and deposition within the harbour are a result of tidal currents, indicating that the river water and salt wedge may have an equal influence on the sedimentation. It was also found that the spring freshet may have very little effect on deposition rates as the increase in fresh water is compensated by the decrease in the reach of the salt wedge. Leys (2011) recommended that additional field data collection and modelling efforts be conducted in an effort to predict annual variations in sedimentation.

Melanson (2012) observed high suspended sediment concentrations in the salt wedge based on ADCP acoustic backscatter observations, which agrees with the observations of Leys (2007) and Matheron (2010). Two bottom mounted ADCPs were moored in the Harbour to observe the long term variations in currents velocities. One system was placed in the Main Harbour channel, while the other was located near the end of the Courtney Bay breakwater, but for logistical reasons, unfortunately, outside the Courtney Bay Channel. The highest levels of suspended sediment in the salt wedge were observed in the Main Harbour Channel on spring tides and during storm surges in the winter months. The presence of a cross channel current at the end of the Courtney Bay breakwater coming from the intertidal mudflats to the east of the breakwater is observed in the ADCP data, but the levels of suspended sediment are lower than observed in the Main

Harbour Channel. As the ADCP was not located in the Courtney Bay channel thalweg, results were subsequently skewed.

Through the most extensive harbour physical oceanographic sampling to date, Toodesh (2012) provides an overview of the estuarine circulation within the Port of Saint John over a semi-diurnal tidal cycle for four periods of the year which represent the range of circulation conditions. An along channel section of the Main Harbour channel was observed approximately 20 times over a semi-diurnal tidal cycle as the data collection vessel steamed throughout the harbour. By extrapolating these observables across the channel the tidal variations in volume flux of sediment was calculated using current velocities from vessel mounted ADCP observations and sediment estimates from a profiling optical backscatter probe. As also observed by Melanson (2012), high concentrations of suspended sediment were observed in the salt wedge throughout the year in the Main Harbour Channel, but at times of high river discharge the flux of suspended sediment was highest in the fresh river waters leaving the harbour. In Courtney Bay, Toodesh (2012) observed that high levels of suspended sediment were entering the channel through the salt wedge on the rising tide. The source of the sediment observed in the salt wedge was assumed to be from around the end of the breakwater from the intertidal area east of the channel, a similar observation to Melanson (2012). During the spring freshet, elevated levels of suspended sediment were observed in the fresh water entering Courtney Bay on the rising tide.

A common thread through all relevant previous studies of the Port of Saint John is that the circulation and deposition and suspension of sediment depend heavily on the interplay between the tide and the river discharge. Toodesh (2012) showed that the annual, fortnightly and diurnal variations in estuarine circulation arrest the salt wedge at varying locations throughout the harbour, which greatly affects the erosion and accretion of seabed sediment. The ultimate source of deposited sediments in the Courtney Bay channel and Turning Basin remains imperfectly understood as observed data alternatively supports both the river and salt wedge as potential sources.

CHAPTER 3: Data and Methods

The hydrodynamic modelling undertaken as part of this thesis was developed for four representative periods of the year, which describe the range of water levels of the Saint John River. As shown in Figure 7, the times included April 22nd 2008, a spring freshet condition with spring tides; November 8th 2008, a fall freshet condition with neap tides; March 18th 2009, a winter minimum condition with neap tides; and June 3rd, 2009, a summer minimum condition with spring tides. During each of these times a previous observational campaign [Toodesh, 2012] had been undertaken to analyze the oceanographic conditions of the port over the period of a semi-diurnal tidal cycle. Each of the surveys covered the Courtney Bay Turning Basin and channel, Main Harbour Channel and the Reversing Falls at slack water. A more detailed overview of the sampling campaign, including a detailed explanation of the oceanographic instrumentation, is provided in Toodesh (2012).

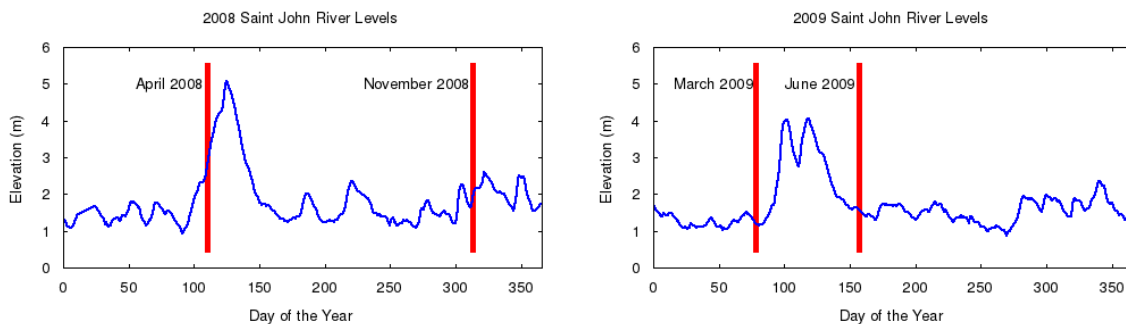


Figure 7 – Saint John River Levels from River Gauge 01AP005 for 2008 and 2009 with Observation Times (Elevation Reference to CGVD28)

3.1. Archived High Density Oceanographic Data for Model Validation

Oceanographic sections of the Main Harbour Channel and Courtney Bay were observed from the CSL Heron, a 10 metre research vessel, over a 13 hour period at four times of the year [Toodesh, 2012]. These sections covered the entire Courtney Bay and Main Harbour channels over a semi-diurnal tidal cycle, as the M2 constituent, with a period of 12.42 hours, is the dominant component of the tide in the area. Between 22 and 25 transects were completed in each area per observation period.

The vessel recorded seabed bathymetry and backscatter and watercolumn backscatter from a Kongsberg EM3002 300 KHz multibeam system; watercolumn backscatter from a 200 KHz Knudsen 320 B/P single beam; current velocities and water column backscatter at 600 KHz from an RDI ADCP; and temperature, salinity and optical backscatter data from a Moving Vessel Profiler (MVP) 30. All data was collected underway at a speed of approximately 8 knots. Using these sensors, the along channel component of the estuarine circulation of the Port of Saint John could be viewed quantitatively and qualitatively throughout the domain over a tidal cycle.

For each of the oceanographic surveys, the MVP-30 was deployed approximately 800 times, as shown in Figure 8 for the April 2008 survey. The horizontal distance between successive deployments varied between 190 and 440 metres with recovery time being a function of depth [Toodesh, 2012]. With each deployment, optical backscatter, salinity, temperature and associated depth information was collected from near the surface to

within 2 metres of the seabed at a resolution of 0.1 metres. The depth, salinity and temperature data could be used to calculate the speed of sound in water at each cast location. The major limitation of the MVP data was the lack of information close to the water surface and seabed. The MVP instrument must be towed below the water surface away from the turbulent wash of the vessel propeller and cannot come too close to the seabed during free fall as it could be damaged if it impacts the bottom. As will be demonstrated later, the portion of the volume fluxes associated with the surface fresh and near seabed saline layers are critical to understanding overall circulation and are missed by MVP observations.

The optical backscatter data from the MVP could be roughly correlated with sediment concentration using a calibration curve calculated by Natural Resources Canada in 2004 [Natural Resources Canada, 2004] [Toodesh, 2012]. The sensor becomes saturated at a concentration of 60 mg/l, which occurs regularly during a tidal cycle in the Main Harbour Channel, as will be discussed in Chapter 5. The optical backscatter probe was functional for the April 2008, November 2008 and March 2009 surveys, but not for the June 2009 survey.

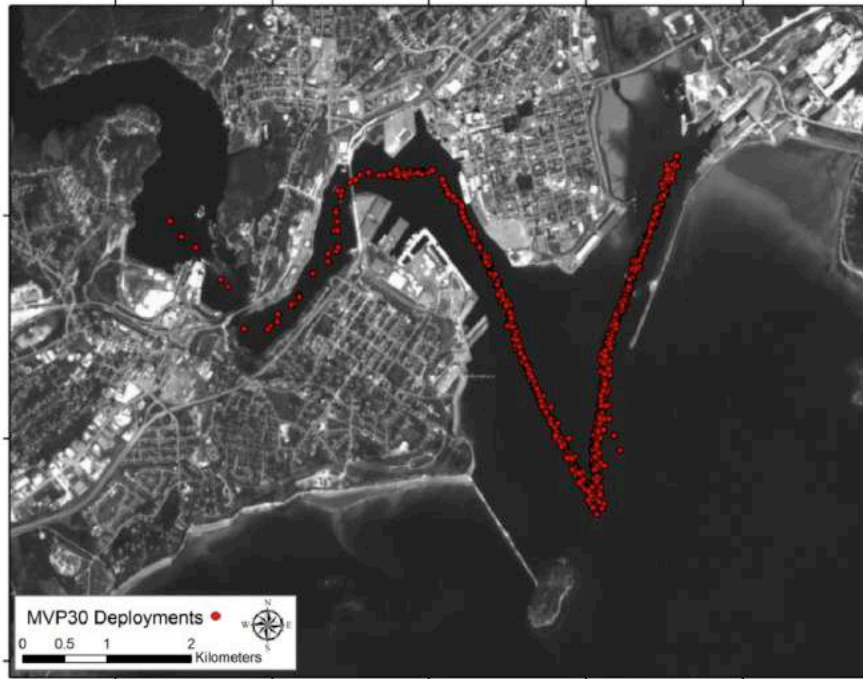


Figure 8 – April 2008 MVP-30 Deployments

The ADCP was mounted on a rigid pole on the port side of the CSL Heron. It provided measurements of current velocities and acoustic backscatter throughout the water column. Due to the draft of the transducer below the waterline (1.2 metres) and the blanking distance (0.5 metres) observations begin at a depth of 1.7 metres below the surface. Current velocities at the seabed cannot be measured due to the acoustic side lobe interference associated with the 20 degree beam angle of the ADCP [Gordon, 1996]. The near seabed interference equates to a distance of approximately 6% of the water depth. Again, the inability to measure near surface and seabed velocity data has a critical impact on understanding the circulation.

Horizontal averaging of the ADCP observations was completed on 10 ping ensembles to reduce noise. The ping rate of the ADCP was 1 Hz and the vessel speed was approximately 4 m/s during transects which roughly equated to a 40 meter sampling interval [Toodesh, 2012]. Vertical averaging was completed using the model derived sigma level coordinate system, as discussed in section 3.4.1.

The internal compass bias of the ADCP was determined through examination of the difference between the vessel heading from the Aided Inertial Navigation System and the compass direction from the ADCP at each ensemble location. The compass bias was applied to the ADCP heading and the u and v velocity components were corrected.

Current velocity data were collected from the ADCP through the domain of the port during the oceanographic observations, but the signal to noise ratio was too low for velocities to be interpreted from the data within Courtney Bay. Only the observations in the Main Harbour channel could be used for analysis of volume fluxes in Toodesh (2012).

3.2. Derivation of Sound Speed from Model Data Output

Understanding acoustic propagation in a body of water requires knowledge of both the mean and gradient of the speed of sound in water. The sound speed gradient controls the refraction of the path of the acoustic energy as the signal propagates from a transmitter

down to the seafloor and back to the receiver of a sonar system. Knowledge of the refraction of the acoustic energy is especially important in oblique beams, such as those within a multibeam echosounder.

The MVP instrument collects information about the temperature and salinity of the water column. These values are then converted to sound speed using Chen & Millero's equations, which require pressure, salinity and temperature as input [Fofonoff and Millard, 1983]. The baroclinic hydrodynamic model also outputs temperature and salinity throughout the model domain and sound speed can then be derived for subsequent analysis.

3.3. Bathymetric Surveys

Various multibeam echosounder bathymetric surveys were completed throughout the domain of the Port of Saint John during a time period similar to that of this projects oceanographic observations. The primary difference between the surveys explained here and the traditional multibeam surveys completed by the SJPA vessel, the Hawk, is that these surveys extended beyond the limits of the dredging areas. The purpose of examining these areas is to understand the natural seasonal variability of sedimentation throughout the port and their correlation with residual tidal circulation.

Multibeam surveys were completed by the OMG's vessel, the Heron, and the CHS vessels, Pipit and Plover, in spring 2000, fall 2001, spring 2008, fall 2008, spring 2009,

fall 2009 and fall 2010. The extents of the surveys are shown in Figure 9. For the 2000 and 2001 surveys, the Plover CHS vessel was equipped with a 300 kHz Kongsberg-Simrad EM3000 multibeam system, a POS/MV 320 motion sensor, a DGPS for horizontal positioning, and an AML-SVP16 sound speed probe. For the spring 2008 and spring 2009 surveys, the Heron was equipped with an EM3002 multibeam system, a F185 motion sensor, a MVP-30 sound speed profiler, and a C-Nav GPS receiver for horizontal positioning. During the fall 2008 and fall 2009 surveys, the Pipit and Plover operated with an EM3002 multibeam system, a POS/MV 320, and an Omni-Star GPS for horizontal positioning. The fall 2010 survey was conducted from the Heron with a 70 kHz EM710 multibeam system, a POS/MV 320 motion sensor, a MVP-30 sound speed profiler, and a C-Nav GPS for horizontal positioning. All surveys were vertically referenced using observed tides from the tide gauge in the Port of Saint John.

In differencing the seasonal bathymetry surveys, changes in morphology can be observed which describe, within the accuracy limits of the integrated multibeam sonar, how the seabed is evolving over time. The erosional and depositional changes of the sediments in the port can be determined and can be correlated with the residual current velocities derived from the model output as will be discussed in Chapter 6

As will be discussed in Section 6.5, systematic biases in the difference maps are seen resulting in faint false along ship track ridging. This primarily reflects the uncertainty due to imperfect compensation of sound speed. Secondary systematic biases were also from

the impulse response during and after turns, which is a characteristic of some heave sensors.

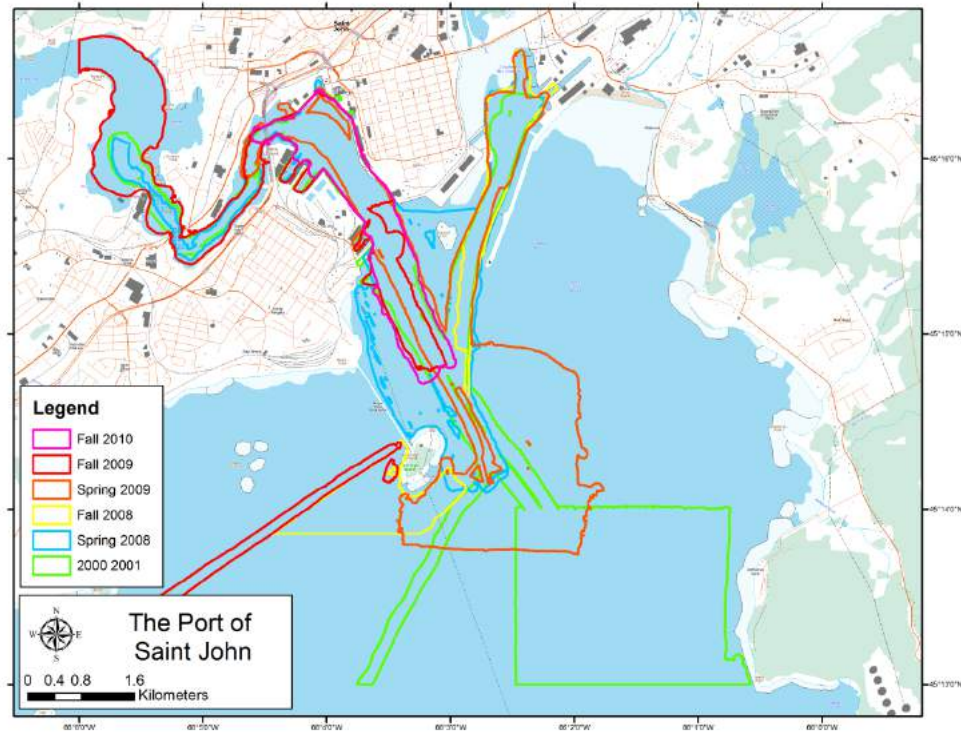


Figure 9 – Port of Saint John Survey Overview with Multibeam Survey Coverage Polygons.
Topographic Background Map from Toporama WMS (2003).

3.4. Three Dimensional Baroclinic Hydrodynamic Model

Numerical hydrodynamic models can be constructed for bodies of water to simulate the amplitude and phase of the tides, examine the internal density distributions in the water column and observe the changes in three dimensional circulation patterns. If surface

fluctuations are the primary interest, the models can use an isodensity assumption (barotropic), which ignores sub-surface conditions of estuarine circulation. If the distributions of temperature and salinity of an area are of interest, the model can be constructed to capture the three dimensional density distribution (baroclinic). A baroclinic model allows the structure and variability of the physical properties of the water column to be examined.

To complement the two-dimensional data from the four oceanographic channel section surveys, a baroclinic hydrodynamic model was developed of the Port of Saint John, which examined the three dimensional density distributions in the port. The model allows prediction of the current velocities and estuarine circulation at any point within the model domain and at any stage of the tide. Temperature and salinity fields were calculated throughout the model domain for the duration of the model run. Dr. Susan Haigh initiated the model setup for the Port of Saint John for the April 2008 simulation period.

3.4.1. Mesh Construction

The model grid was constructed using a high resolution coastline of the Port of Saint John and a combination of multibeam bathymetry and CHS chart soundings, as shown in Figure 4, by Dr. Susan Haigh. The coastline and the bathymetry were input to Resolute, a semi-automated finite-element ocean model mesh generation routine, to obtain a finite element grid suitable for input to the modelling software [Chaffey and Greenberg, 2003].

The result of the mesh generation was a triangular irregular network of nodes and elements with variable spacing. The nodes describe the intersection points of the triangles in the mesh, while the elements are the triangles themselves. The element sizes, and corresponding node spacing, correlates to depth and depth gradients within the area. The mesh included 20 evenly spaced vertical terrain-following layers (Figure 10), 16471 nodes and 30679 triangles and had a horizontal resolution which varied between 3 and 128 metres, as shown in Figure 11.

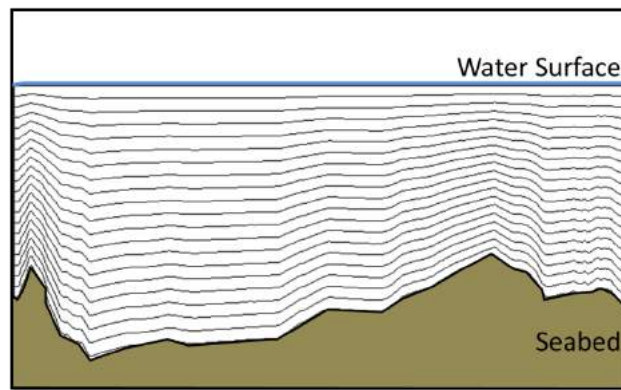


Figure 10 – Vertical Terrain-Following Layers

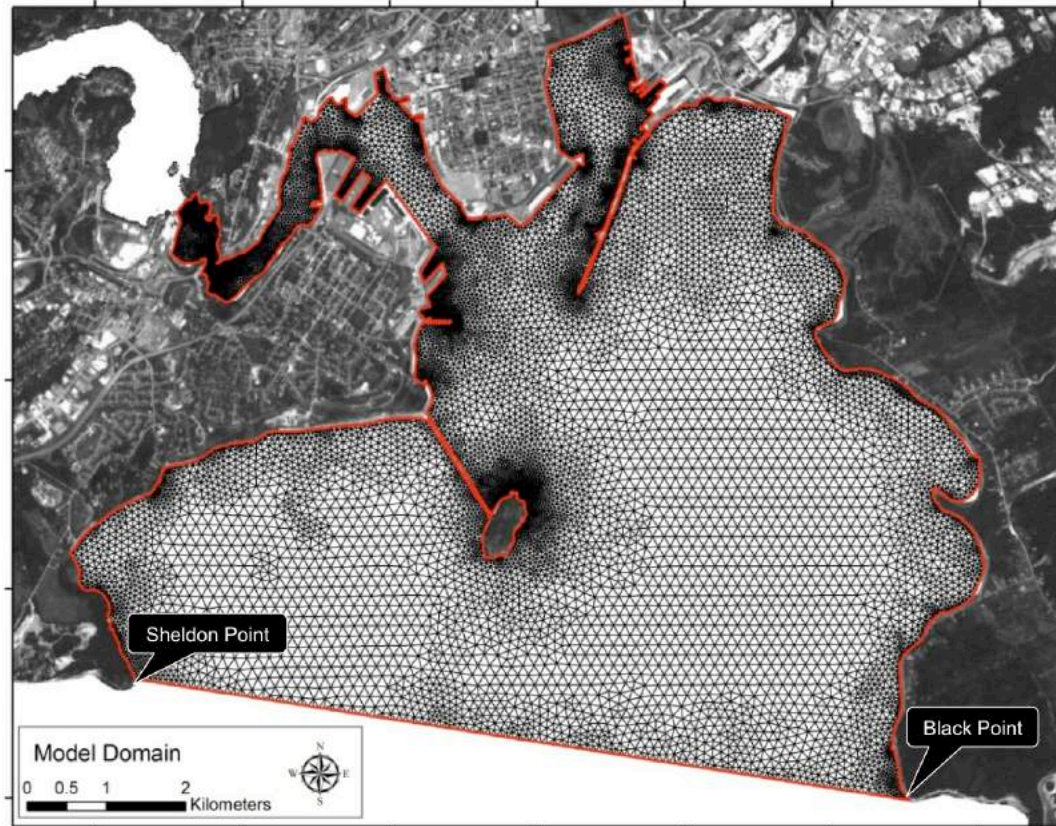


Figure 11 – Model Mesh and Domain Overview

3.4.2. Boundary and Initial Conditions

Two open boundaries were defined in the mesh. The open boundaries require two sources of input information; water levels and temperature and salinity distributions. The first open boundary is located at the sill of the Reversing Falls, as shown in Figure 12. This location was chosen as it represented the upstream limit of the area of interest, the spatial extent of the physical observations. Additionally it is an area with strong turbulent mixing and is well mixed vertically [Leys, 2007]. Water levels recorded at the nearby river level gauge (Environment Canada gauge 01AP005) were used as the source of elevation

forcing for the model at this open boundary. Examining the surface waters of the MVP data obtained close to the boundary provided a source of temperature and salinity data for the open boundary.

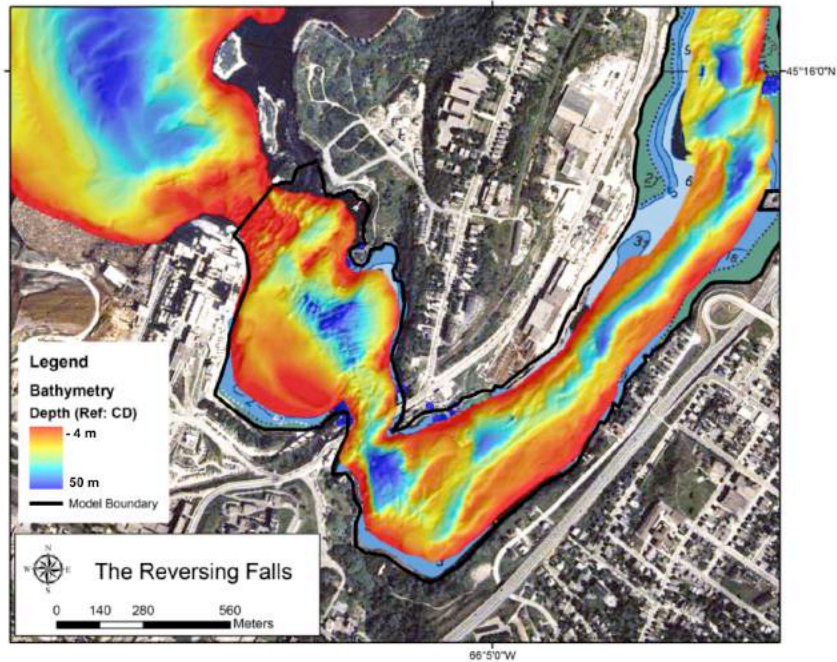


Figure 12 – Reversing Falls Bathymetry and Model Boundary

The second open boundary represents the intersection of the Saint John Harbour and the Bay of Fundy and is represented by a straight line between Sheldon Point and Black Point, as shown in Figure 11. Water levels for this boundary were sourced from the observed tides at the Port of Saint John tide gauge, when available. As the tide gauge was located in the centre of the model domain, the observations were phase shifted based on the estimated phase shift of the M2 constituent from the WebTide Scotian Shelf hydrodynamic model [Dupont et al., 2005]. This allows for a representation of the propagation of the tide both up the bay and across the boundary. Observed tides for the

port were available for April 2008, and March and June 2009, but not for November 2008. For the November 2008 time period, phase shifted predicted tides for the Port of Saint John tide gauge were used as the reference for the open boundary water levels. The temperature and salinity structure of the water entering the domain was assumed to be well mixed vertically along the Bay of Fundy open boundary. Values for the input variables of temperature and salinity along the open boundary were obtained from the near-bottom water data of the MVP profiles in the harbour. The open boundary initial conditions for the four observation and simulation periods are shown in Table 1.

Table 1 – Open Boundary Conditions

Simulation Time	Reversing Falls Boundary		Bay of Fundy Boundary	
	<i>Salinity (psu)</i>	<i>Temperature (°C)</i>	<i>Salinity (psu)</i>	<i>Temperature (°C)</i>
April 2008	0.7	3.0	31.4	2.7
November 2008	3.3	8.3	31.8	10.5
March 2009	10.4	2.3	31.4	1.5
June 2009	7.6	13.5	30.8	7.3

The grid nodes throughout the model domain were set to constant initial conditions. The depth averaged salinity and temperature values from the MVP observations for the area were used. Alternatively, the salinity and temperature observations from the MVP could have been extrapolated spatially and vertically to describe the oceanographic structure of the model domain. Testing revealed that the large tides of the Bay of Fundy and the high river discharge of the Saint John River caused the model to stratify naturally in less than one tidal cycle. Initial constant condition values of temperature and salinity are shown in Table 2.

Table 2 – Constant Values for Initial Conditions of Temperature and Salinity

Simulation Time	<i>Salinity (psu)</i>	<i>Temperature (C)</i>
April 2008	32	3
November 2008	15	9
March 2009	20	2
June 2009	19	10

3.4.3. Finite-Volume Coastal Ocean Model

The mesh and initial conditions were input to the Finite-Volume Coastal Ocean Model (FVCOM) for simulation. FVCOM is an open source ocean model developed at the University of Massachusetts-Dartmouth and Woods Hole Oceanographic Institution. It was chosen for this project due to its capability of handling areas of complex coastlines and bathymetry, intertidal zones through a wet/dry treatment and accounting for vertical density distributions through a baroclinic mode [Chen et al., 2006]. The model takes as input the model grid (Figure 11), an elevation time series along each of the open, non-coastal, boundaries, and prescribed temperature and salinity conditions at the open boundaries and throughout the domain. FVCOM is widely used for coastal modelling studies, has a large user group of academic and government organizations throughout the world and encourages user contributions to aid in development. Applications of FVCOM in the coastal environment are demonstrated in the Northern Gulf of Mexico [Wei et al., 2014]; the Skagit River estuary in Puget Sound, Washington [Yang and Khangaonkar, 2009]; Tampa Bay, Florida [Weisberg and Zheng, 2006]; Rookery Bay and Naples Bay,

Florida [Zheng and Weisberg, 2010]; Mount Hope Bay, Massachusetts; and Narragansett Bay, Rhode Island [Zhao et al., 2006].

FVCOM is able to use a variety of vertical layering coordinate solutions. For this project the vertical sigma layers were divided into equally spaced layers. The number of layers stays constant throughout the domain, but the layer thickness is variable depending on water depth and water level. The depth of a layer is variable throughout the grid and follows the bathymetry, as shown previously in Figure 10.

The governing equations in FVCOM are based on the fundamental equations for the conservation of mass, momentum, temperature, salinity and density [Chen, 2013]. The equations are able to be applied to either Cartesian or spherical coordinate systems depending on the reach of the model domain. Due to the limited spatial extent of the Port of Saint John, the Cartesian coordinate system was used for this application.

To allow the model to stratify naturally away from the constant initial conditions, as described above, the model run was initiated between five and seven days prior to the specific oceanographic observation period. The water levels at the open boundaries were ramped up from zero at the beginning of the simulation to full amplitude after six hours into the model run. The ramping of open boundary water levels allowed the model to slowly adjust based on the temperature and salinity boundary conditions. The final 24 hour period of the model simulation was analyzed for comparison to the observations.

FVCOM is able to take advantage of a Message Parsing Interface (MPI) parallelization to maximize efficiency [Chen et al., 2006]. Model runs were done using the Atlantic Computational Excellence Network (ACEnet) high performance computing network [ACEnet, 2011]. A seven day simulation running on 128 processors took 40 hours to complete, which is equivalent to 5120 CPU-hours. The model outputs a series of NETCDF files that include water surface elevations, horizontal and vertical velocities, salinity and temperature at each level of each node and prescribed output time-step of the duration of the model run. Any of these variables can be extracted for a desired location, depth and time period within the model domain.

FVCOM version 3.1.4 was used for the simulations. Input and output files used Cartesian coordinates for calculations of the governing equations with specified node latitudes for inclusion of the Coriolis Effect. Wetting and drying was used to allow for the model sea level to change relative to the bathymetry during different tidal stages, which is important in the Port of Saint John due to the large tidal ranges and the expansive areas of intertidal mudflats. The General Ocean Turbulence Model (GOTM) was chosen as the turbulence model to use for the simulations in the Port of Saint John. The standard Mellor-Yamada 2.5 implementation was found to not perform as well as the GOTM model in areas of strong stratification to define the mixing between salt and fresh water [Foreman, 2012].

CHAPTER 4: Assessing Model Uncertainty

The results of the hydrodynamic model simulation during the March 2009, April 2008, June 2009 and November 2008 time periods must be assessed to determine the validity of the model output in comparison to the observed natural conditions of the harbour. A model will never perfectly represent the physical observations, but the differences between the model output variables and the observations can be examined both qualitatively and quantitatively. The ultimate consequence of the differences must be assessed to determine the practical effect of the model uncertainty on any interpretation of real physical processes.

The observed temperature, salinity, sound speed and ADCP velocity throughout the watercolumn from Toodesh (2012) was compared to the model data for each of the four observational periods. The sound speed variable was not calculated directly within the model, but was derived from output temperature and salinity. The relevance of the sound speed assessment becomes apparent in Chapter 8 where the application of the model output to hydrographic data collection is examined. It is important to note that none of the observational data from Toodesh (2012) were assimilated into the model. Only the prescribed conditions of temperature and salinity along the river and Bay of Fundy open boundaries were determined from the observations and the model was allowed to stratify naturally. The observations then did not influence the distribution of salinity, temperature and velocity throughout the model domain.

The quantitative analysis was first performed for the entire model domain and then subsequently for each of the defined quantitative analysis areas, as shown in Figure 13. The Main Harbour area is divided into a section which spans the waters upstream of the Saint John Harbour Bridge to the Reversing Falls and a section downstream of the bridge to Partridge Island. Courtney Bay is divided into the Courtney Bay Channel, marked by the dredged navigation channel, and the Turning Basin at the head of the bay. Statistics were calculated to provide an evaluation of compatibility of the model to the observations. The qualitative analysis examines the ability of the model to reproduce the oceanographic sections described in Toodesh (2012), as shown in Figure 13.

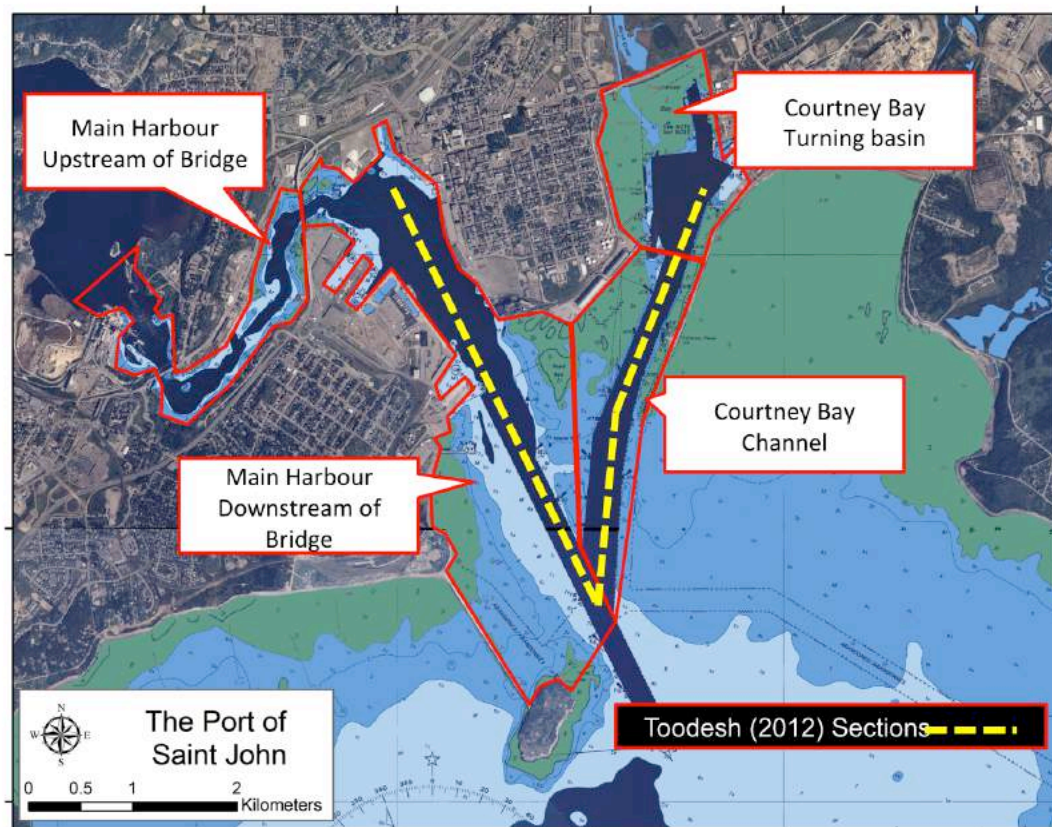


Figure 13 – Quantitative Analysis Areas

A qualitative analysis is described to illustrate how well the main oceanographic structure is represented. Subsequently a quantitative analysis is performed to measure the scale of the discrepancies. Finally the reasons behind the observed differences will be discussed.

4.1. Qualitative Model Comparison with Observed Data

The model output through the Main Harbour and Courtney Bay Channels were examined and compared with the sections and profiles described in Toodesh (2012). The Main Harbour section from Toodesh (2012) is restricted to an along-channel line through the area defined as the Main Harbour Downstream of Bridge in Figure 13, while The Courtney Bay section is restricted to an along-channel line through the areas of the Courtney Bay Channel and Courtney Bay Turning Basin.

The salinity stratification in the harbour is very difficult to accurately simulate. The gradient along the halocline is strong and in some cases may be narrower than a single output layer of the model. The turbulence along that interface is also very complex, especially within the Main Harbour Channel, and may not be properly described by the GOTM parameters within the model.

The output sections for April 2008, November 2008, March 2009 and June 2009 were compared herein. April 22, 2008, represents the period when the greatest velocity shear is apparent between the salt and fresh water layers. The discharge from the river is maximized due to the spring freshet condition, which competes with the incoming salt

wedge. The tidal range is approximately 6 metres, which represents a weak spring tide. A fall freshet is apparent on November 8, 2008, but river discharge is less than observed in April 2008. November 8, 2008, also represents a period of neap tides with a tidal range of approximately 5m. March 18, 2009, represents the minimum river discharge condition with neap tides driving the salt wedge. The tidal range in on March 18, 2009, is approximately 4.5 metres. On June 3, 2009, river discharge falls between November 2008 and March 2009 levels and weak spring tides are present with a tidal range of 6 metres.

A comparison between observed and modelled profiles was also completed for April 2008, November 2008, March 2009 and June 2009. The profiles provide a detailed examination of differences between the observations and the model data at each stage of the tide for a chosen location. The comparison emphasises the model estimation of the halocline within the estuary that significantly affects the quantitative statistics. To understand the similarities and differences in the data, the variables of density and velocity were examined and to facilitate comparison, the observed data was averaged to 1 metre bins.

4.1.1. Main Harbour Channel Section

Qualitatively the advance and retreat of the salt wedge in the Main Harbour Channel over a tidal cycle is well described by the model. The primary differences noted below can be

explained by the variations in the timing of the arrival of the salt wedge and the degree of mixing along the halocline.

4.1.1.1. April 2008

The observed and modelled sections for April 2008 within the Main Harbour Channel are shown in Figure 14 for low, flood, high and ebb tide. The right hand side of the figure represents the downstream extent of the section, closest to the Bay of Fundy, while the left hand side represents the upstream extent, closest to the Saint John River. At low tide (first row of Figure 14) the observed salt wedge is shown to advance more rapidly than the model prediction. The concentration of salt and the thickness of the layer are similar. On the flood tide (second row of Figure 14), the salt wedge of the model is still lagging relative to the observations and the concentration of the salt below the halocline is lower in the model. The location of the halocline looks similar for both profiles. By high tide (third row of Figure 14), the halocline is still in the correct location, although the salinity concentration within the salt wedge beneath the harbour bridge in the model section is too low. The salinity concentration near the harbour entrance is very similar. At ebb tide (fourth row of Figure 14), the model and observation profiles provide a close match with similar representations of the halocline beneath the Harbour Bridge and comparable salinity concentrations.

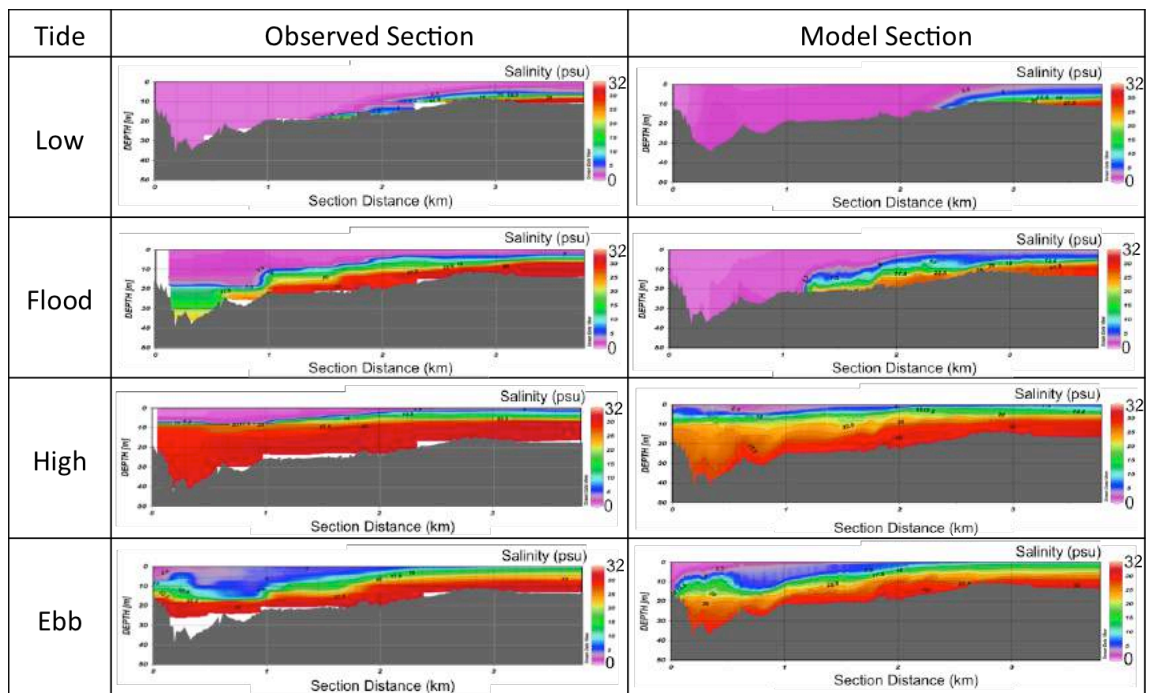


Figure 14 – April 2008 Main Harbour Section Comparison. Observed sections in first column, model sections in second column. The Section starts near the Harbour Bridge and terminates near the Harbour Entrance.

The profile comparison of the observed and model data for a location within the Main Harbour Channel for is shown in Figure 15 for April 2008. At low tide the waters near the seabed are slightly too dense and hence too saline in the model output, but there is a very close match overall. The velocity magnitude of the model output is too low compared to the observed ADCP data at low tide. At flood tide the model describes too much salinity in the near seabed waters and displaces the halocline and pycnocline towards the surface. This likely results from a small timing problem with the propagation of the salt wedge upstream on the flood tide. At high tide the observed and modeled water masses provide a closer match than on the flood tide. The near surface and seabed

densities provide a close match while the primary discrepancy lies along the halocline and pycnocline. The velocity profiles provide a close match at high tide. The ebb tide shows a discrepancy between the model and the observations in density, much like on the flood tide. This again is likely caused by a small timing problem in the retreat of the salt wedge. The velocity profiles are of a similar average magnitude, but there is more variation in the observed profile.

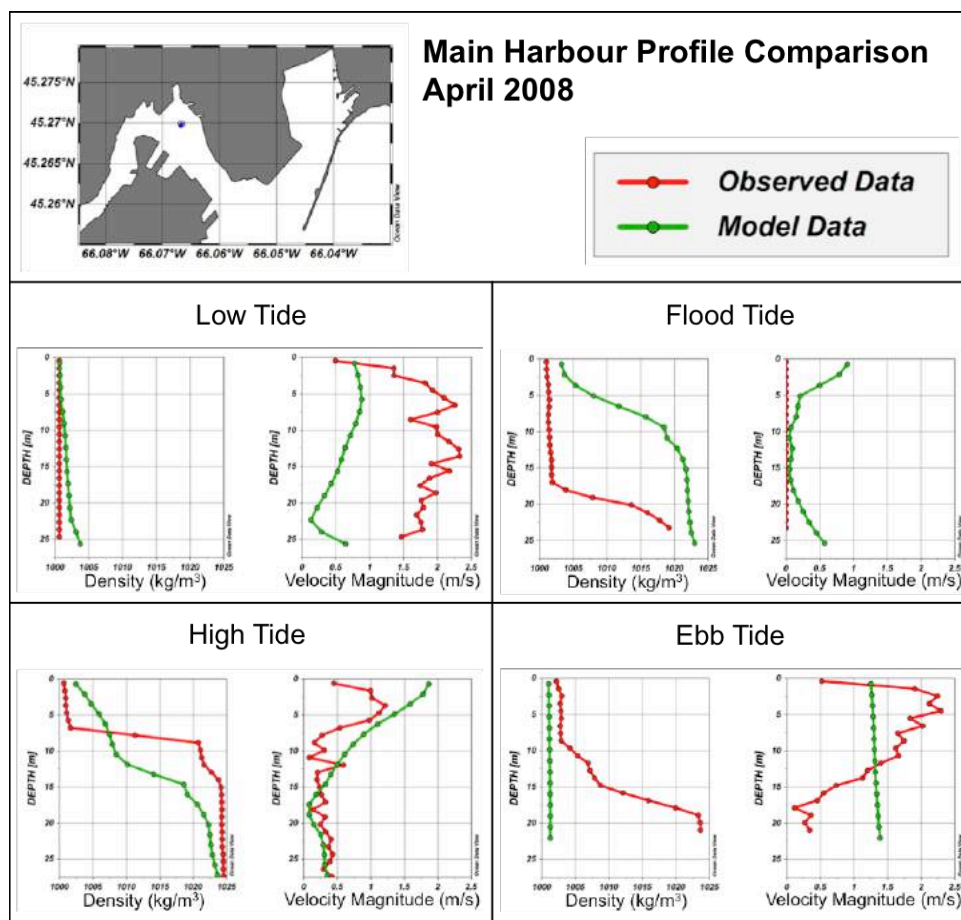


Figure 15 – April 2008 Main Harbour Profile Comparison

The model provides the best match to the observation at high tide in April 2008. The discrepancies observed at low, flood and ebb tide may be related to timing of the progression of the salt wedge through the harbour, as noted previously in section 4.1.1.

4.1.1.2. November 2008

The November 2008 section, shown in Figure 16, displays that the model and observed sections provide a close match throughout the tidal cycle. At low tide similar concentrations of fresh water on the left hand side of the section and salt water on the right hand side of the section are visible. The model preserves the location of the halocline, but as the observations don't extend to the seabed it's difficult to assess if similar seabed salinity concentrations are present in the harbour as described by the model. A discrepancy between the model and the observations becomes apparent at high tide, where the fresh surface layer observed in the observations is not apparent in the model output.

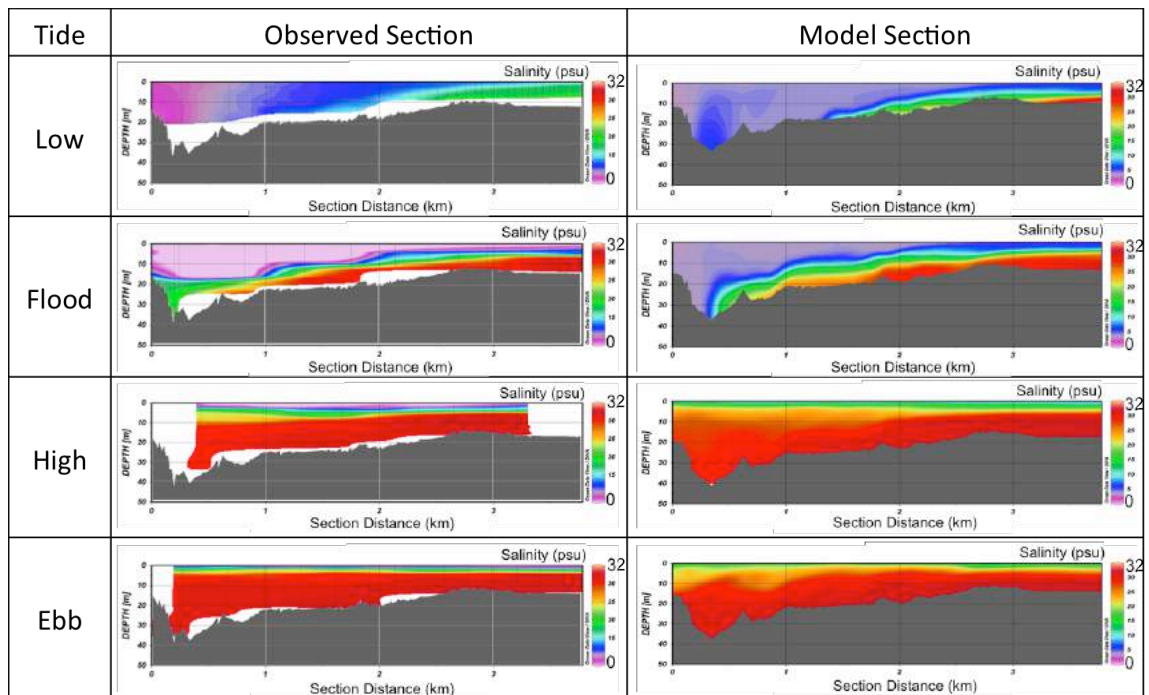


Figure 16 – November 2008 Main Harbour Section Comparison. Observed sections in first column, model sections in second column. The Section starts near the Harbour Bridge and terminates near the Harbour Entrance.

The profile comparison of the observed and model data for a location within the Main Harbour Channel for is shown in Figure 16 for November 2008. The density profiles exhibit similar gradients but are shifted in magnitude at low tide. The magnitude of the velocity profiles is similar for model and observed data, but the observations suggest more variation along the profile. On the flood tide the density profiles provide a close match for the near surface and seabed areas of the profile. A discrepancy in the profiles exists within the gradient of the pycnocline. The observations suggest a sharp transition between salt and fresh waters while the model shows a more gradual transition. The model velocity profile shows that the lower saline waters are moving faster than the fresh surface waters, but the observations suggest that the magnitude of the velocity is similar

throughout the water column. At high tide the model and observed profiles provides a close match in density. The velocity profiles do not provide as close of a match as the density profiles, but the observed velocities may be incorrect as the profile ends short at approximately 20 metres. On the ebb tide the model and observations continue to provide a close match in density. The model velocity profile indicates that the fresher surface waters are moving faster than the lower saline waters. The observed ADCP velocity profile is relatively noisy with a similar magnitude throughout the water column.

The model and observed profiles provide a close match for all stages of the tide in November, with the primary discrepancy being the shift in density at low tide.

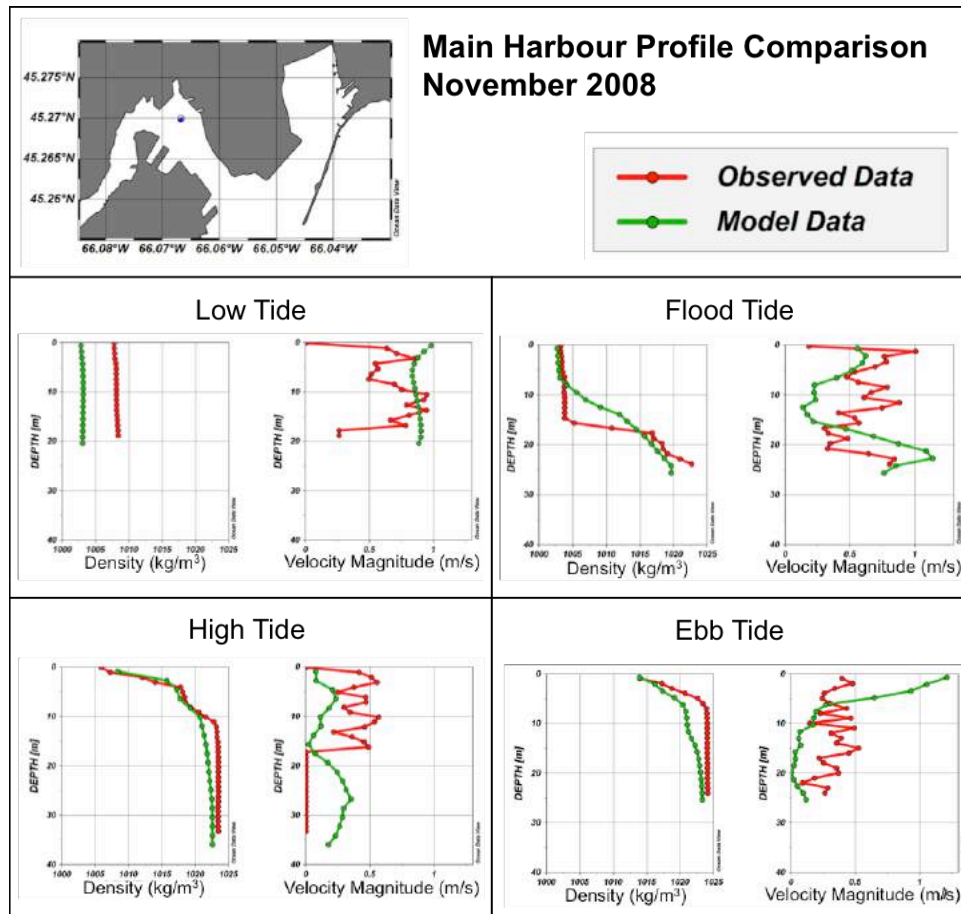


Figure 17 – November 2008 Main Harbour Profile Comparison

4.1.1.3. March 2009

The observed and modelled sections for March within the Main Harbour Channel are shown in Figure 18 for low, flood, high and ebb tide. At low tide the salt wedge of the model has advanced beyond the visible salt wedge of the observations. This is the opposite to the conditions observed in April at this stage of the tide. Caution must be taken with the observations as they do not extend to the seabed, so the true concentration

of the salt wedge near the seabed is not sampled. The location of the halocline is at the same depth for both the observed and model sections. At flood tide the salt wedge within the model profile has advanced to beneath the Harbour Bridge, while the observations are lagging further down the channel. The halocline is generally in the correct location and the concentration of salinity near the Harbour Entrance provides a close match between the two sections. At both high and ebb tide the model and observational sections provide a very close match as the salt wedge has advanced up the channel to fill the section domain.

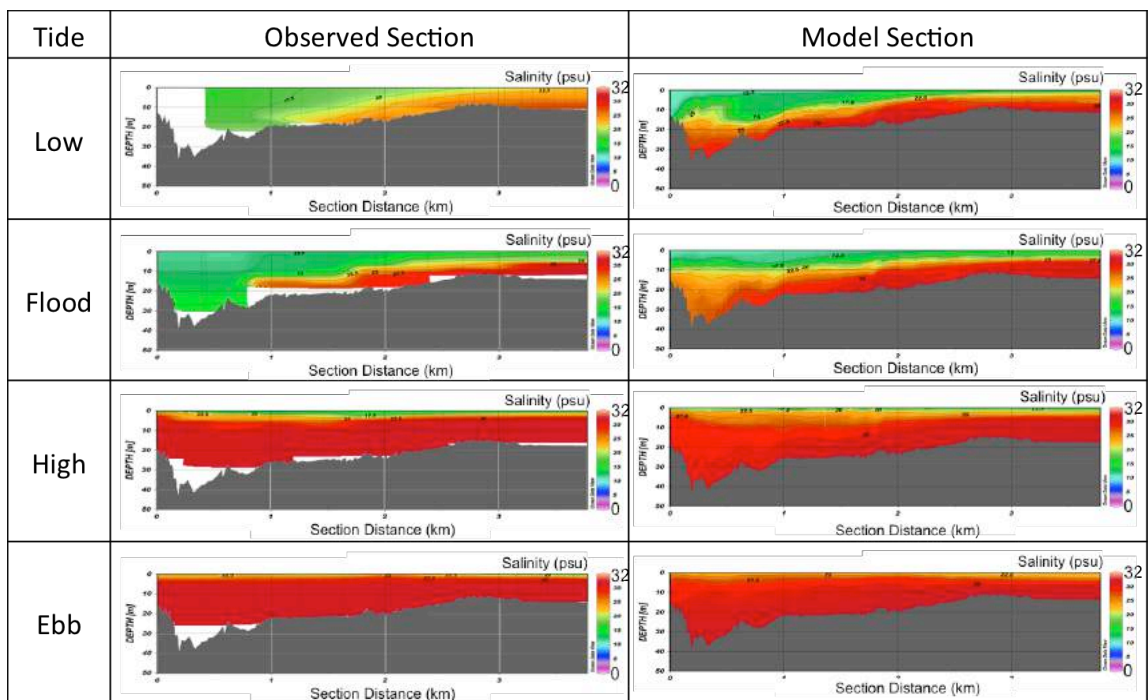


Figure 18 – March 2009 Main Harbour Section Comparison. Observed sections in first column, model sections in second column. The Section starts near the Harbour Bridge and terminates near the Harbour Entrance.

The profile comparison of the observed and model data for a location within the Main Harbour Channel for is shown in Figure 19 for March 2009. At low tide there is an offset in the density values through the water column. The model indicates the presence of too much dense saline water, while under estimating the magnitude of the velocities. On the flood tide an offset in density still exists between the model and observed profiles. The model over-estimates the value of the salinity through the water column. The ADCP was not functioning at this time; therefore a comparison in velocity was not possible. At high tide the density of the observed water mass increases and is now greater than the model estimate for the central portion of the profile, although the near surface and near seabed densities provide a close match. At high tide the model also estimates that the dense near seabed waters are moving faster than the surface waters, while the observations suggest that the entire water mass is moving at near constant velocity. On the ebb tide, the model and the observations begin to show very similar characteristics in their density profiles.

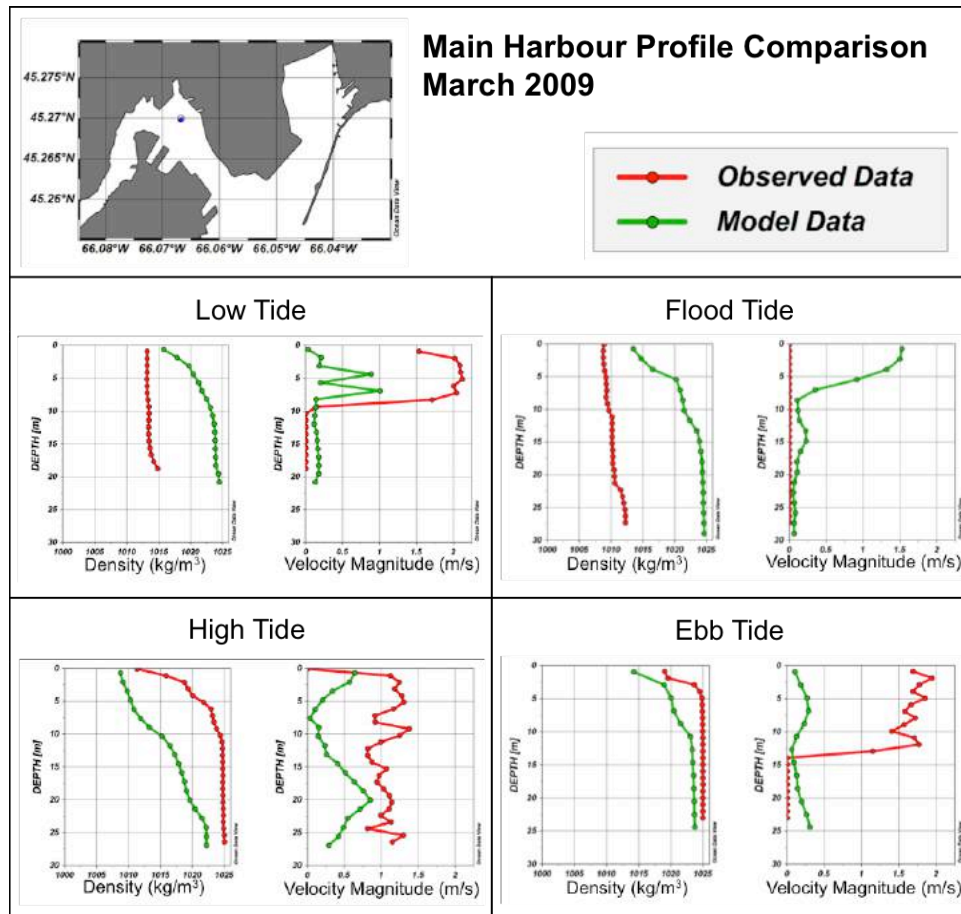


Figure 19 – March 2009 Main Harbour Profile Comparison

4.1.1.4. June 2009

The June 2009 sections are compared over a tidal cycle in Figure 20. The model provides a good estimation of the halocline location throughout at each stage of the tide. The primary discrepancy between the model and the observations is observed at low tide where the fresh river waters to the left of the section are too fresh within the model

output. This may indicate that the model is not sufficiently mixing the fresh river water and the saline Bay of Fundy water further upstream.

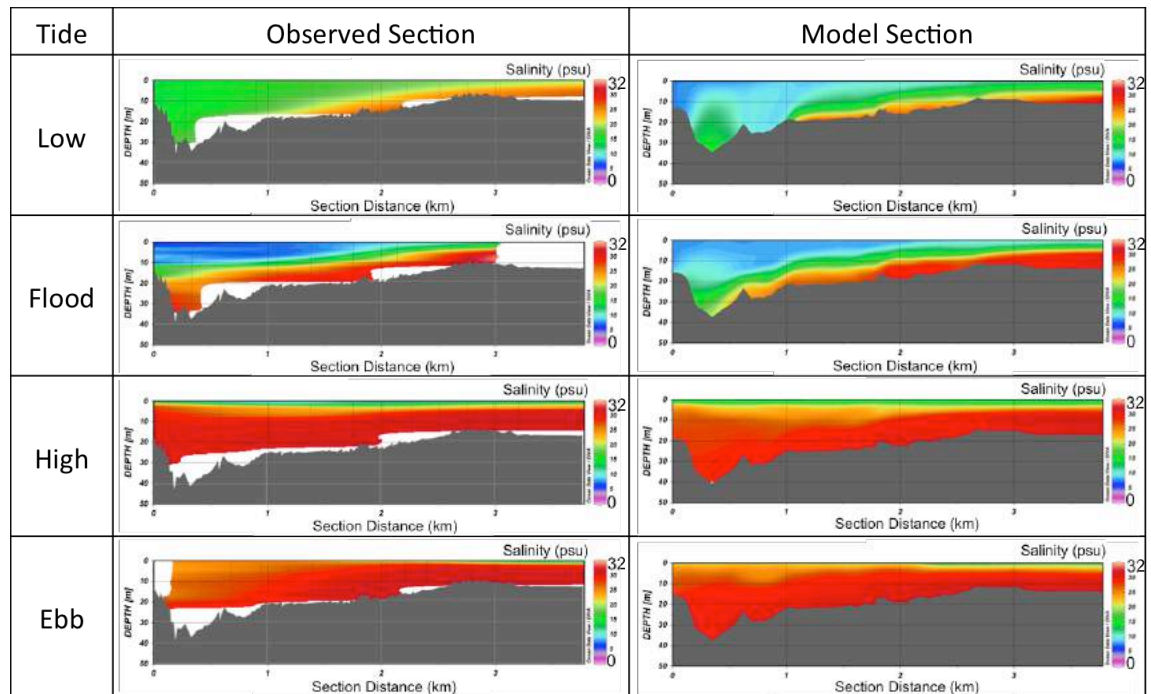


Figure 20 – June 2009 Main Harbour Section Comparison. Observed sections in first column, model sections in second column. The Section starts near the Harbour Bridge and terminates near the Harbour Entrance.

The profile comparison of the observed and model data for a location within the Main Harbour Channel for is shown in Figure 21 for June 2009. At low tide the model is underestimating the density of the water column. The gradients of the profiles are similar. The magnitudes of the velocities are similar, but there is more variation in the observed velocity profiles. On the flood tide the model and observed profiles begin to converge. The near surface and seabed salinity and densities are similar with a variation in the

shape of the halocline. The observations suggest the presence of a fresh less dense surface layer with an elevated velocity, which is not reproduced by the model. At high tide the model and observed density profiles provide a very close match. The model underestimates the magnitude of the velocities at this time. On the ebb tide the model and observed density profiles begin to diverge. The model describes a rapid return to fresh less dense water after high tide, which is not shown in the observed profile. Alternatively the observed velocity profile shows a close match with the model output at this time with a near linear transition in magnitude from the surface to the seabed.

In June 2009 the model provides a close match to the observation on the flood and high tide. Discrepancies at those times exist primarily in the description of the pycnocline.

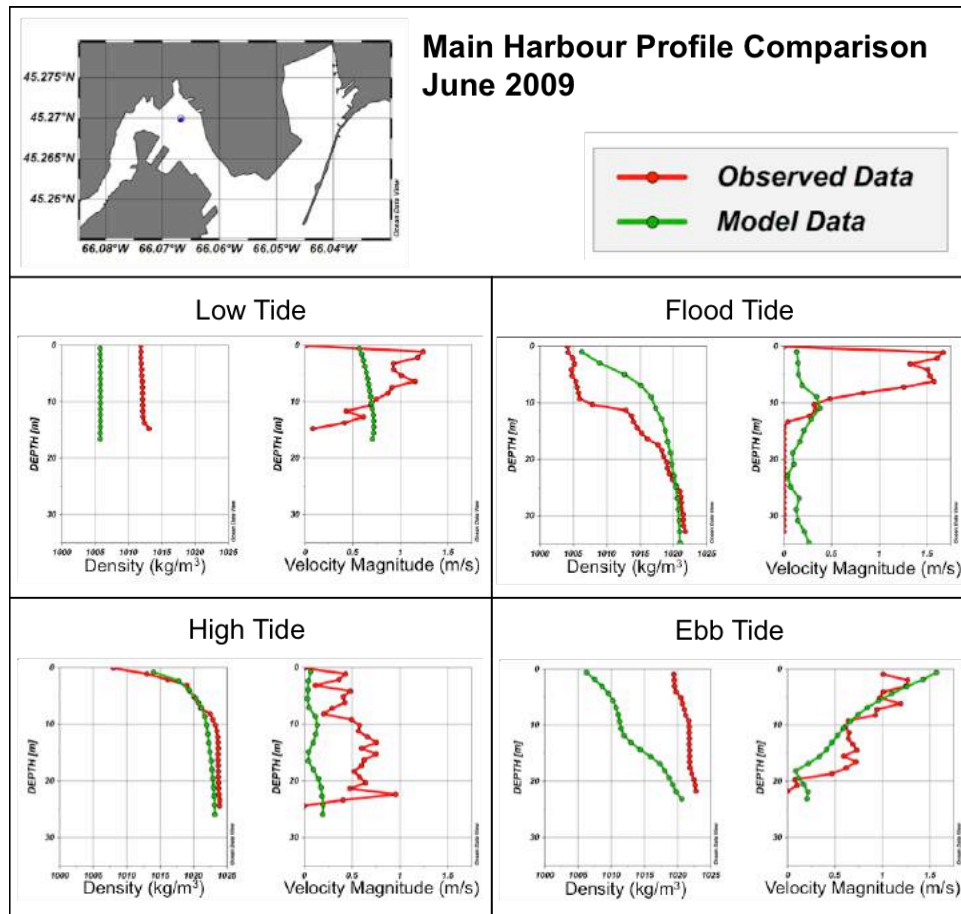


Figure 21 – June 2009 Main Harbour Profile Comparison

4.1.2. Courtney Bay Channel Section

The Courtney Bay channel is an inlet with no significant input of fresh water. Circulation within the channel is driven entirely by the near seabed and surface waters which enter through the channel entrance from the Bay of Fundy and the Main Harbour channel.

For the profile comparison in Courtney Bay only the variable of density was examined as the velocity magnitude within the channel is too low to be measured with the ADCP, as discussed previously in section 3.1.

Qualitatively the advance and retreat of the salt wedge in Courtney Bay over a tidal cycle is well described by the model. The primary differences noted below can be explained by the variations in penetration of the salt wedge and the degree of mixing along the halocline. At low river discharge the diminished quantity of fresh water entering the channel improves the mixing estimate within the model output, while at higher discharges the gradient of the halocline is too weak relative to the observations indicating over estimated mixing levels in the model output.

4.1.2.1. April 2008

The oceanographic observations and model output sections within Courtney Bay are compared for April 2008 in Figure 22 where the left hand side of each panel in the figure represents the Courtney Bay Turning Basin and the right hand side describes the intersection of the Courtney Bay Channel and the Main Harbour Channel. The common observed difference between the sections at all stages of the tide is the deficiency of salt water in the model output. At low tide (first row of Figure 22), both the model and observations show the orphaned plug of salt water within the Turning Basin. At flood tide (second row of Figure 22), there is a noticeable difference in the shape of the halocline

between the two profiles near the centre of the section, although the advancing salt wedge is visible at the channel entrance within both sections. At high tide (third row of Figure 22), the modelled advancing salt wedge is lagging behind the observed salt wedge. On the ebb tide (fourth row of Figure 22), the model salt wedge has mixed with the surface waters and a weak halocline is observed, unlike the observations which show predominantly salt water within the section.

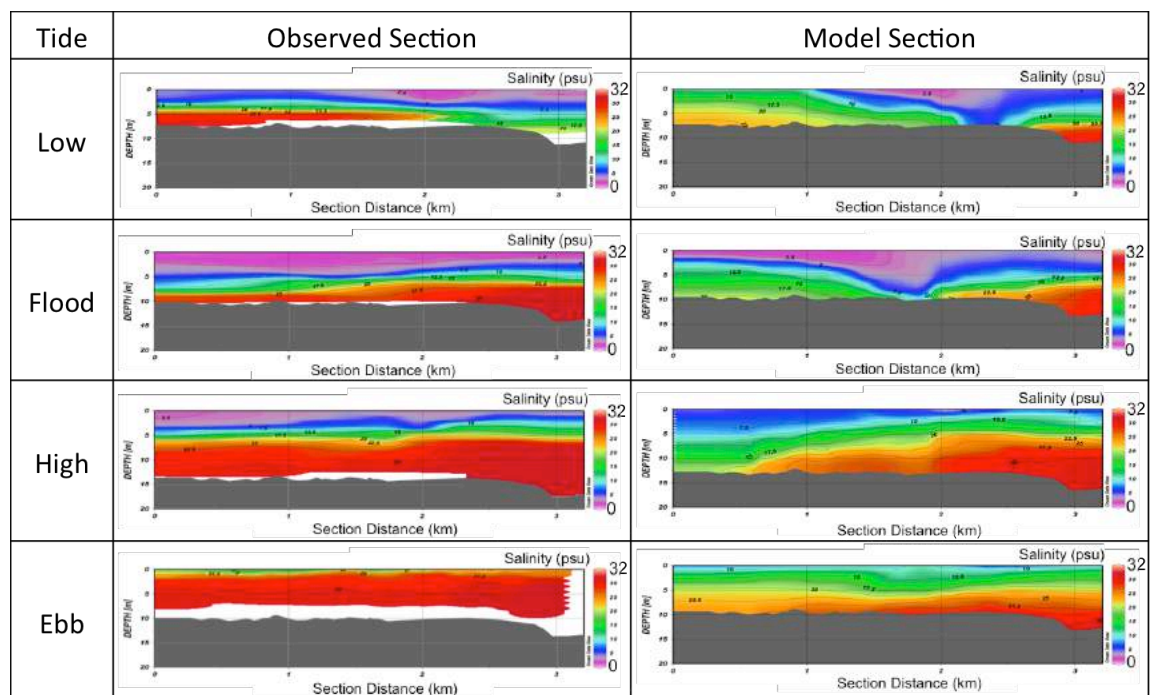


Figure 22 – April 2008 Courtney Bay Section Comparison. Observed sections in first column, model sections in second column. The Section starts in the Turning Basin and terminates near the intersection with the Main Harbour.

The profile comparison of the observed and model data for a location within the Courtney Bay Channel for is shown in Figure 23 for April 2008. At low tide the density of the

model is lower than the observations, which corresponds to the conclusions drawn from examination of the salinity section comparisons above. The increase in density from surface to seabed is observed in both profiles. On the flood tide the model and observed density profiles provide a closer match than previously shown at low tide. At high tide the formation of a pycnocline is shown in the observed profile. The model does not describe the formation of a sharp pycnocline but shows a gradual increase in density from the surface to the seabed. On the ebb tide the observed pycnocline has weakened and the model and observed profiles provide a close match.

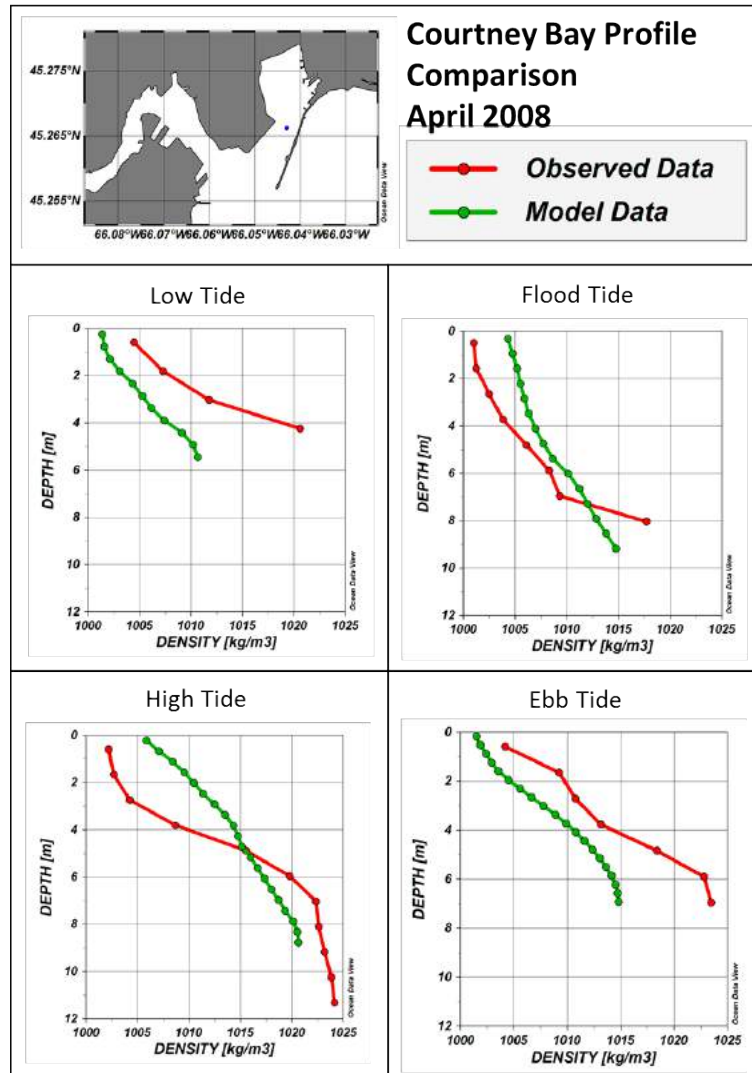


Figure 23 – April 2008 Courtney Bay Profile Comparison

4.1.2.2. November 2008

The November section, as shown in Figure 24, shows an overall salinity deficiency which is similar to the April sections. The observed waters in the channel are less saline than observed in April and provide a closer match to the model output. The location of the

halocline provides a close match between the model and the observations at all stages of the tide, with the primary difference being the gradient along the interface. The model salinity gradient is consistently weaker than the observed gradient.

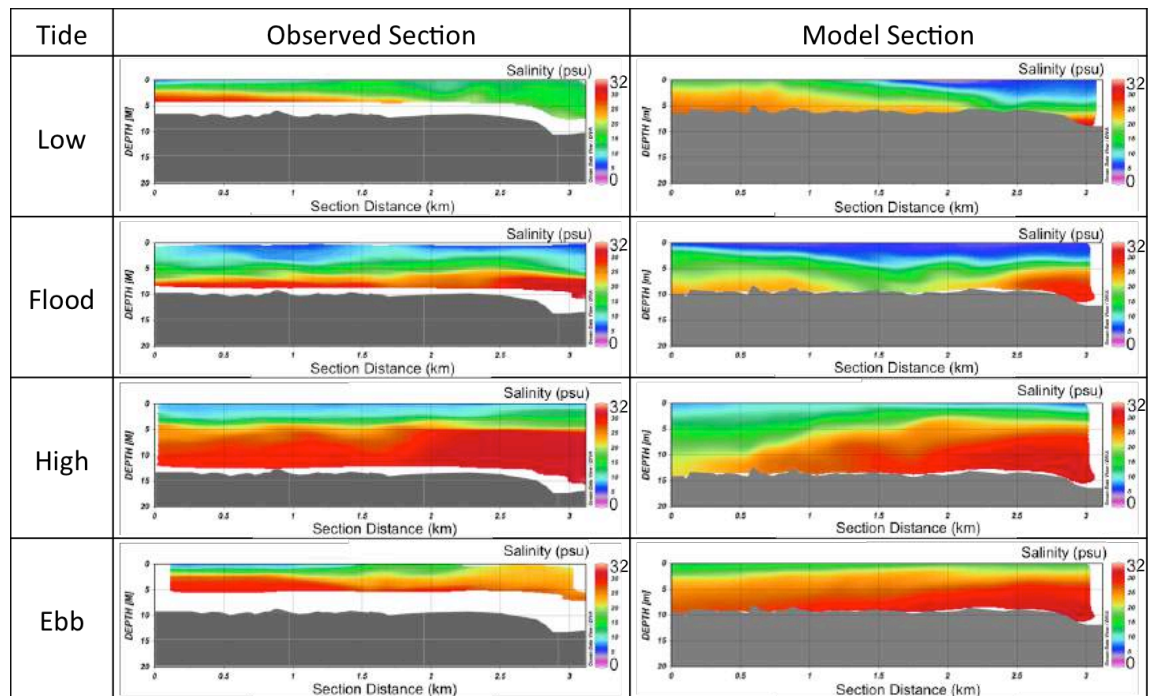


Figure 24 – November 2008 Courtney Bay Section Comparison. Observed sections in first column, model sections in second column. The Section starts in the Turning Basin and terminates near the intersection with the Main Harbour

The profile comparison of the observed and model data for a location within the Courtney Bay Channel is shown in Figure 25 for November 2008. Throughout the tide, there is a strong correlation between the model and observed density profiles. At low tide the density profiles and gradients are nearly identical. The density profiles on the flood tide overlap for most of the watercolumn. The difference in the profiles is near the seabed

where the rate of density increase in the model lowers and diverges from the observations. At high tide the observations describe the formation of a pycnocline. A similar formation was previously observed at high tide in April. Like in the April 2008 comparison, the model does not correctly define the pycnocline, but the near surface and seabed density provides a close match. On the ebb tide the near surface and seabed model densities start to diverge from the observed values but the average density provides a close match.

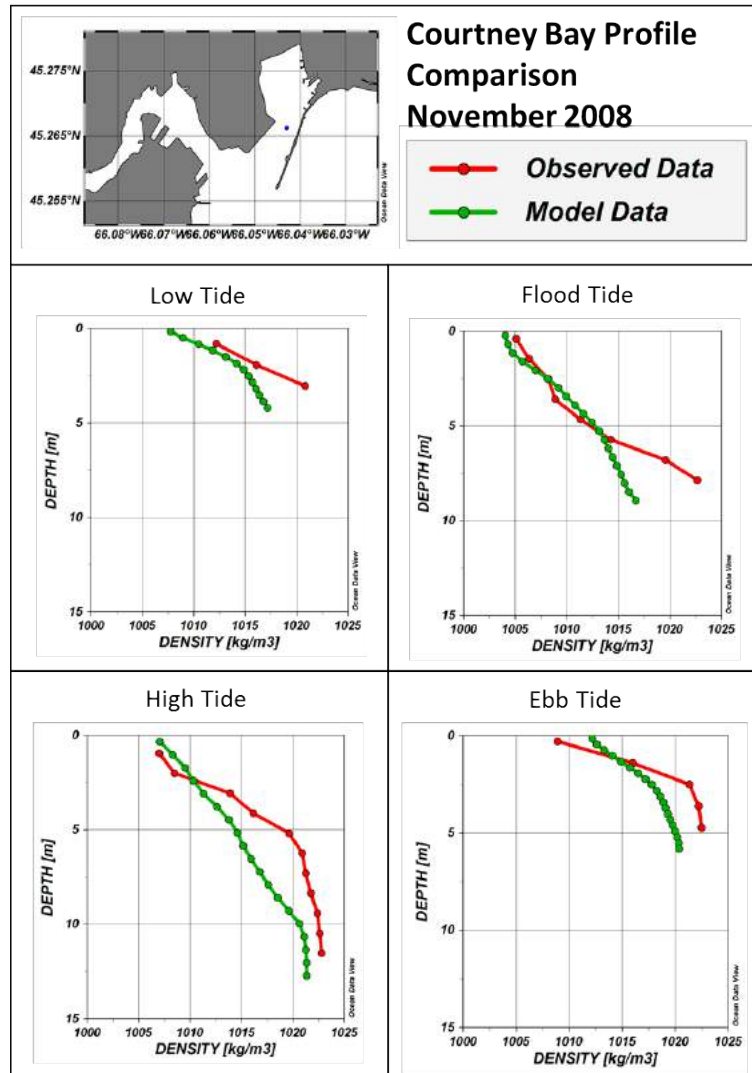


Figure 25 – November 2008 Courtney Bay Profile Comparison

4.1.2.3. March 2008

The model and observation sections in Courtney Bay provide a closer match for March than they do in April, as shown in Figure 26. Less fresh water is input into the system from the Main Harbour Channel in March and the circulation is driven largely by the

tides. Figure 26 shows that for low, flood, high and ebb tide the salinity concentrations and halocline location provide a close match between the model and observational sections.

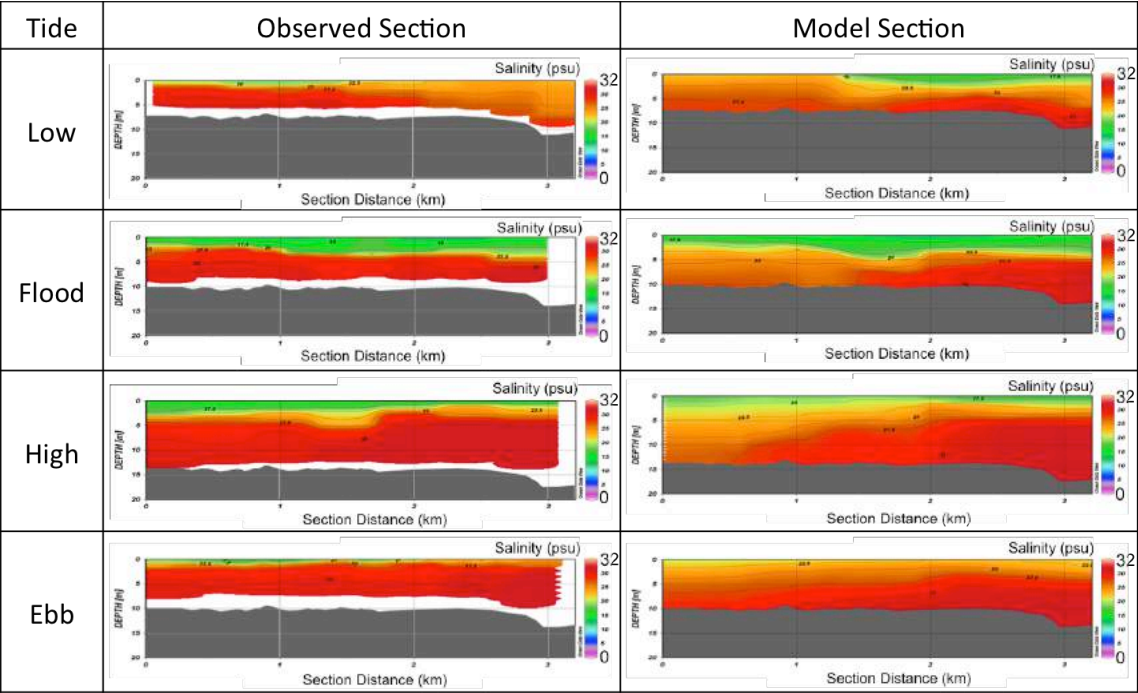


Figure 26 – March 2009 Courtney Bay Section Comparison. Observed sections in first column, model sections in second column. The Section starts in the Turning Basin and terminates near the intersection with the Main Harbour

The profile comparison of the observed and model data for a location within the Courtney Bay Channel is shown in Figure 27 for March 2009. At low tide the model density provides a very close match at the surface but diverges slightly towards the seabed. On the flood tide the average model density approaches the observed profile and a pycnocline is formed in the observed profile. As noted previously in April and

November, the model does not reproduce the observed sharp pycnocline. At high tide the model develops a pycnocline, which resembles the observed profile. The near seabed density of the model is slightly too low when compared to the observations. On the ebb tide the comparison of the profiles resembles the structure at low tide. The surface density provides a very close match between the observed and model profiles, but they diverge slightly with depth.

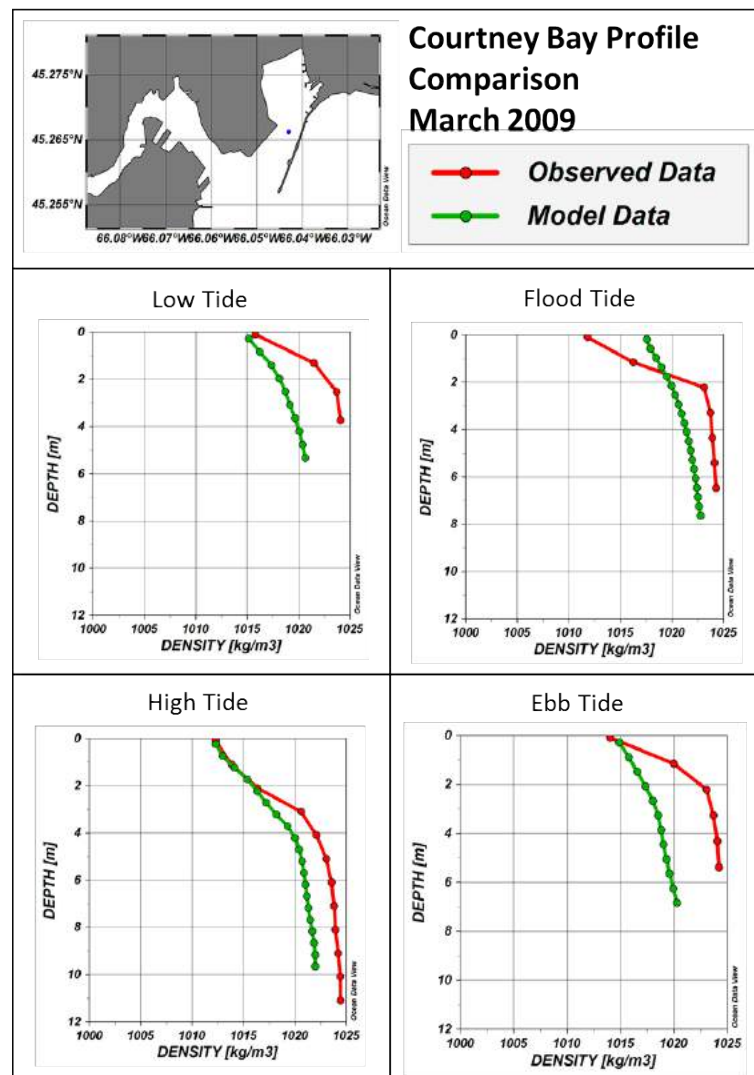


Figure 27 – March 2009 Courtney Bay Profile Comparison

4.1.2.4. June 2009

The June 2009 section, as shown in Figure 28, exhibits similar structure and failings as observed in the previous comparisons within the Courtney Bay Channel. Throughout the tidal cycle the structure of the water mass is preserved with the approximate correct location of the halocline. The primary deficiency is the salinity gradient along the halocline. The model indicates that too much mixing is occurring along the interface which reduces the near seabed salinity concentrations in the Turning Basin.

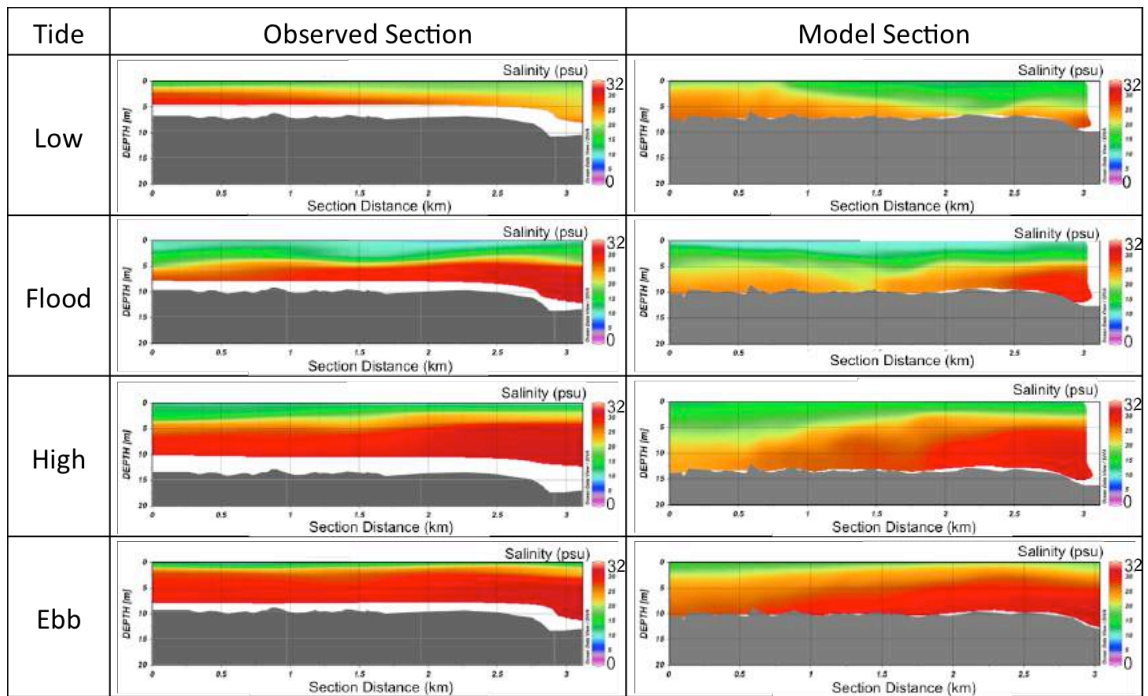


Figure 28 – June 2009 Courtney Bay Section Comparison. Observed sections in first column, model sections in second column. The Section starts in the Turning Basin and terminates near the intersection with the Main Harbour

The profile comparison of the observed and model data for a location within the Courtney Bay Channel for is shown in Figure 29 for June 2009. At low tide there is a near static offset in density between the observed and modelled profiles. On the flood tide the near surface density now provides a near perfect match between the observed and model profiles but the profiles diverge as they approach the seabed. At high tide the two profiles begin to converge towards an improved match. A discrepancy is still observed in the lower half of the water column where the model profile is less dense than the observed profile. This difference is in the development of the pycnocline, similar to observations in April, November and March. On the ebb tide the surface waters of the model provide a good match to the observations, but the seabed water of the model is lower in density than the observations.

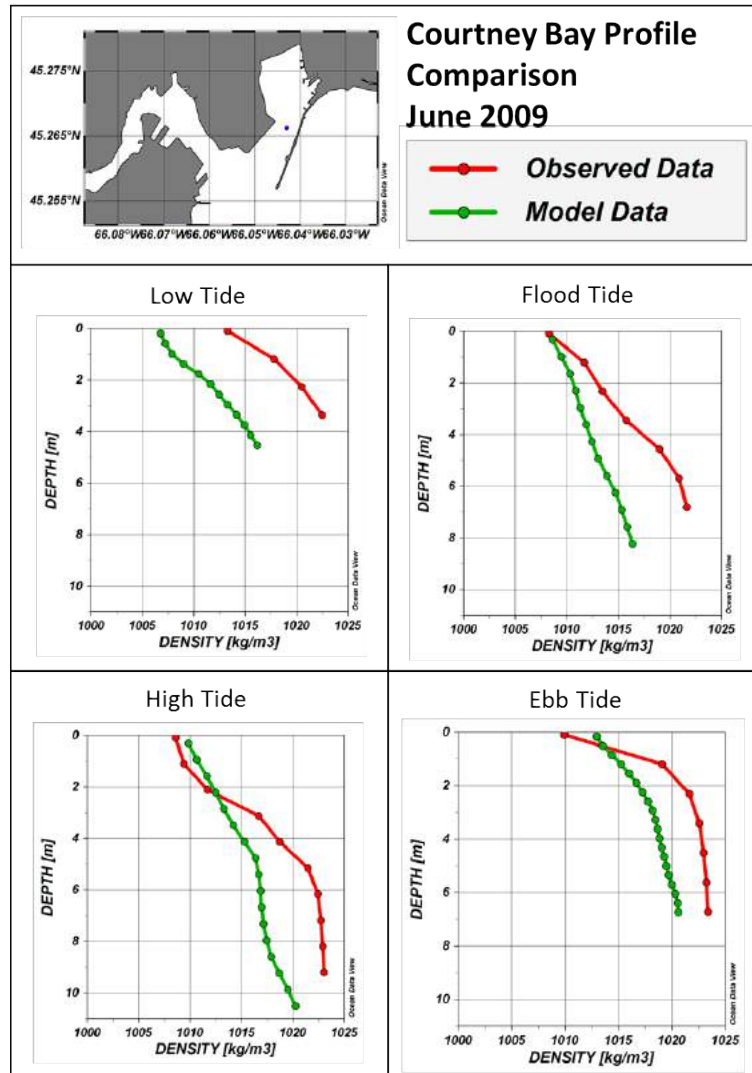


Figure 29 – June 2009 Courtney Bay Profile Comparison

4.2. Quantitative Model Comparison with Observed Data

To augment the qualitative differences of section 4.1, the differences in temperature, salinity, sound speed and current velocities between the model output and observed quantities from the campaign of Toodesh (2012) can be quantified for the observational

periods. The differences are analyzed based on a selection of statistics from Hess et al. (2003), which provides an objective judgement of the model performance. These statistics have been widely used to evaluate a variety of models, including the Tampa Bay Operational Forecast System (TBOFS) and the Northeast and Northwest Gulf of Mexico Operational Forecast System (NEGOFS & NWGOFS) [Wei and Zhang, 2011; Wei et al., 2014]. The statistics include the mean difference between the model and the observation, standard deviation (SD), root mean squared error (RMSE), central frequency (CF), positive outlier frequency (POF) and negative outlier frequency (NOF), as described in Table 3. The selection of limit criteria for the central frequency and negative and positive outlier frequency statistics, as described in Table 3, is arbitrary but for this evaluation a limit of approximately 15% of the maximum range was chosen for the variables of temperature, salinity, and sound speed, while a value of 1 m/s was chosen for the ADCP velocity comparison. The 15% salinity, temperature and sound speed and 1m/s velocity limit criteria could be altered depending on the application of the model, but was deemed as an appropriate reference for describing the oceanographic conditions within the port due to the dynamically complex and highly stratified environment.

Within the domain of the Port of Saint John, there can be large spatial variations in the observed fields; therefore the statistics were computed separately for each of the areas outlined previously in Figure 13. The tables described in this section correspond to the overall difference scheme for the entire model domain, while the statistical tables for the defined zones of circulation are available in Appendix A.

Table 3 – Model Assessment Statistics, from [Hess et al., 2003]

Variable	Explanation
<i>Error</i>	The model value minus the observed data value: y_i
<i>Mean</i>	The mean value of the error values: $\bar{y} = \frac{1}{N} \sum_{i=1}^N y_i$
<i>Standard Deviation (SD)</i>	$SD = \sqrt{\frac{1}{N-1} \sum_{i=1}^N (y_i - \bar{y})^2}$
<i>Root Mean Square Error(RMSE)</i>	$RMSE = \sqrt{\frac{1}{N} \sum_{i=1}^N (y_i)^2}$
<i>Central Frequency(CF)</i>	Percentage of Errors (y_i) which lie within limits $\pm(Limit Value)$
<i>Positive Outlier Frequency (POF)</i>	Percentage of Errors (y_i) which are greater than the limit $+(Limit Value)$
<i>Negative Outlier Frequency(NOF)</i>	Percentage of Errors (y_i) which are less than the limit $-(Limit Value)$

At the location of each physical oceanographic observation, the node closest to the observation is determined and used as the source of model data. The model is output in projected grid coordinates; therefore the observation data must be projected to the same coordinate system for analysis. The Proj.4 API c libraries were used for coordinate projection. The WGS84 datum was used for model and observational coordinates. The ADCP velocities are compared using a similar procedure, with the exception being that the velocities are output from the model at the centre of the elements instead of at the nodes.

The model outputs temperature, salinity and current velocity at each of the 20 vertical layers. For the temperature and salinity variables the observation closest to the centre of each layer is used for comparison. For the ADCP velocities, the data were averaged into vertical bin segments which match the model level thicknesses. As a layer in the model is defined as the vertical area between two levels, the binned ADCP velocities match the location of the model velocities output at each level.

Model results are saved at 30 minute time intervals; therefore the two closest model result times to the observation time are determined and an inverse time weighted average value of temperature, salinity and sound speed at the node and velocity at the element is calculated for comparison to the observational data. An example calculation is shown in Equation (1), where S' represents the time averaged salinity, S_1 the model salinity at the closest node from the previous output model result in time and S_2 the model salinity at the closest node from the next output model result in time. The weights ω_1 and ω_2 are calculated as the difference in time between the observation and the previous model result and next model result respectively.

$$S' = \frac{\omega_1 S_1 + \omega_2 S_2}{\omega_1 + \omega_2} \quad (1)$$

As discussed in Section 3.1, the signal to noise ratio of the ADCP observations in the Courtney Bay area was too low to resolve the current data from the background noise. Therefore, the comparison between model and observational data was not performed for the ADCP within either the Courtney Bay Turning Basin or the Courtney Bay channel.

4.2.1. April 2008

Table 4 outlines the statistical results of the comparison between the April MVP data observations and the model output data. The statistics described in the table corresponds to analysis with 750 MVP dips over a semi-diurnal tidal cycle, at each of the matching depth layers which equates to a total sample size of 12109 observations. The table shows that, on average, the temperature, salinity and sound speed model variables are very close to the observations, with mean differences of 0.17 degrees C, 0.01 psu and 0.88 m/s respectively. Using the limits described in Table 4, the positive and negative outlier frequencies for salinity and sound speed are relatively equal indicating that there is no bias in these data. The temperature variable has a small negative bias of 11%.

Table 4 – April 2008 MVP vs. Model Assessment

Variable	Sound speed (m/s)	Limit (m/s)	Temp (deg C)	Limit (deg C)	Sal (psu)	Limit (psu)
<i>Mean</i>	-0.88		-0.17		-0.01	
<i>SD</i>	10.85		0.36		8.70	
<i>RMSE</i>	10.88		0.40		8.70	
<i>Min</i>	-38.06		-2.41		-29.87	
<i>Max</i>	33.84		0.24		27.41	
<i>CF</i>	69.30 %	10	88.17 %	0.5	50.22 %	5
<i>POF</i>	14.60 %	10	0.00 %	0.5	26.87 %	5
<i>NOF</i>	16.10 %	10	11.83 %	0.5	22.91 %	5

Table 5 outlines the statistical results of the comparison between the April ADCP data observations and the model output data. The mean difference between the model results and the observed north and east velocities is very close to zero and within the

measurement noise of the ADCP observations [Toodesh, 2012]. The positive and negative outlier frequencies are close to equal, but there may be a small bias in the south and west directions.

Table 5 – April 2008 ADCP vs. Model Assessment

Variable	North (m/s)	Limit (m/s)	East (m/s)	Limit (m/s)
<i>Mean</i>	0.03		-0.10	
<i>SD</i>	1.22		0.79	
<i>RMSE</i>	1.22		0.79	
<i>Min</i>	-10.69		-11.66	
<i>Max</i>	10.21		11.87	
<i>CF</i>	85.27 %	1	92.23 %	1
<i>POF</i>	6.40 %	1	1.84 %	1
<i>NOF</i>	8.34 %	1	5.94 %	1

Examination of the tables for April 2008 of Appendix A, which describe the statistics associated with the individual circulation areas, reveals the spatial skill assessment of the model. Within the Courtney Bay Turning Basin, only 45 % of the salinity variables are within the CF limit of 5psu and there is a positive bias of 36%. This indicates that in this area there may be too much salt water in the model output. Examining the qualitative comparisons of Figure 22 reveals that for Courtney Bay in April this bias results from the absence of fresh water in the near surface layer of the model output. Moving down into the channel, the salinity CF variable increases to 51% and the NOF and POF values are nearly equal indicating that there is no bias in the data. Similar values are observed in the Main Harbour Channel with a salinity CF at 48% and a bias free NOF and POF.

The assessment of the ADCP data in the Main Harbour Channel provides a bias free CF of 85% and 93% for north and east velocities respectively. Within the Reversing Falls channel, upstream of the harbour bridge, the salinity CF percentage increases to 71 % with no bias towards the POF or NOF. ADCP results in this area show a negative bias with a CF of 61% and 78% for north and east velocities respectively. The negative bias indicates that the model is under predicting the north and east velocities present in this channel.

4.2.2. November 2008

Table 6 outlines the statistical assessment of the model results for November 2008. The statistics described in the table corresponds to analysis with 906 MVP dips over a semi-diurnal tidal cycle at each of the matching depth layers which equates to a total sample size of 14501 observations. The model provides a good fit to the observed data with a CF value of salinity at 65% as the minimum CF value for all variables. The NOF value for each variable indicates that there may be a negative bias in the model data overall, indicating that there is a deficiency of salt water, temperatures are too cold and sound speed is too slow. The CF values for sound speed and salinity are both higher than the values observed in April, while temperature is lower.

Table 6 – November 2008 MVP vs. Model Assessment

Variable	Sound speed (m/s)	Limit (m/s)	Temp (deg C)	Limit (deg C)	Sal (psu)	Limit (psu)
<i>Mean</i>	-1.95		-0.09		-1.24	
<i>SD</i>	7.98		0.46		5.19	
<i>RMSE</i>	8.21		0.47		5.33	
<i>Min</i>	-24.97		-3.99		-16.52	
<i>Max</i>	23.81		1.26		15.90	
<i>CF</i>	73.96 %	10	69.54 %	0.5	65.36 %	5
<i>POF</i>	9.26 %	10	11.81 %	0.5	12.99 %	5
<i>NOF</i>	16.79 %	10	18.65 %	0.5	21.65 %	5

Table 7 describes the statistics associated with the ADCP data assessment for November.

As with the April statistics, the ADCP data provides a close match to the model current velocities with CF value of 79% and 90% for the north and east current velocities respectively.

Table 7 – November 2008 ADCP vs. Model Assessment

Variable	North (m/s)	Limit (m/s)	East (m/s)	Limit (m/s)
<i>Mean</i>	0.01		-0.02	
<i>SD</i>	0.95		0.66	
<i>RMSE</i>	0.95		0.66	
<i>Min</i>	-10.73		-7.72	
<i>Max</i>	10.15		7.13	
<i>CF</i>	79.05 %	1	89.96 %	1
<i>POF</i>	12.13 %	1	3.01 %	1
<i>NOF</i>	8.82 %	1	7.03 %	1

Examination of the tables for November 2008 of Appendix A, which describe the statistics associated with the individual circulation areas, reveals the spatial skill assessment of the model. The model results for November provide a closer match to the

observations of salinity and sound speed than April, with the exception of the Reversing Falls channel. Within the Courtney bay Turning Basin, the CF reveals that 71% of the salinity values are within the prescribed limits of 5 psu. Associated with the CF, a positive bias is present for this area, indicating that the model is either over estimating the salinity or underestimating the fresh water concentrations. Within the Courtney Channel, the CF of salinity has fallen to 66%, but the bias is now slightly negative. In the Main Harbour Channel the CF is higher than April for salinity, at 62%, but a negative bias is present in the data. The lowest CF value for salinity is found in the Reversing Falls channel, at 46%, with a negative bias in the results indicating either that an insufficient quantity of saltwater is propagating up towards the falls or too much freshwater is coming downstream.

The ADCP data in the Main Harbour Channel provides a good fit with the model output, with CF values of 75% and 89% for north and east velocities respectively. The ADCP data in the Reversing Falls channel upstream of the bridge still provides good agreement with the model data with relatively bias free CF values of 63% and 73% for north and east velocities respectively.

4.2.3. March 2009

Table 8 outlines the statistical assessment of the model results for March 2009. The statistics described in the table corresponds to analysis with 685 MVP dips over a semi-

diurnal tidal cycle at each of the matching depth layers, which equates to a total sample size of 12389 observations. The mean differences for temperature, salinity and sound speed are small and the CF for salinity is at 78% with a positive bias. The sound speed CF is high at 78 % with a positive bias. The assessment for temperature provides the weakest CF value, and shows a strong positive bias of 34 % indicating temperatures are too warm in the model output.

Table 8 – March 2009 MVP vs. Model Assessment

Variable	Sound speed (m/s)	Limit (m/s)	Temp (deg C)	Limit (deg C)	Sal (psu)	Limit (psu)
<i>Mean</i>	2.04		0.38		0.29	
<i>SD</i>	7.83		0.47		5.23	
<i>RMSE</i>	8.09		0.60		5.24	
<i>Min</i>	-24.97		-4.02		-18.15	
<i>Max</i>	26.86		1.61		17.70	
<i>CF</i>	78.45 %	10	62.04 %	0.5	66.83 %	5
<i>POF</i>	19.14 %	10	34.34 %	0.5	19.76 %	5
<i>NOF</i>	2.41 %	10	3.62 %	0.5	13.41 %	5

The mean difference in the ADCP velocities in Table 9 shows little difference between the observed and model velocities. Further examination reveals that weak CF values are apparent for this period. The values are lower than previously observed in April or November, but no bias exists in the data. The weak current magnitudes observed in March approach the signal to noise limits of the ADCP data based on a depth cell size to match model levels and ensemble averaging in Toodesh (2012), which could explain the low CF values.

Table 9 – March 2009 ADCP vs. Model Assessment

Variable	North (m/s)	Limit (m/s)	East (m/s)	Limit (m/s)
<i>Mean</i>	-0.03		0.02	
<i>SD</i>	0.92		1.10	
<i>RMSE</i>	0.92		1.10	
<i>Min</i>	-5.83		-4.38	
<i>Max</i>	9.74		3.85	
<i>CF</i>	74.87 %	1	51.54 %	1
<i>POF</i>	12.07 %	1	26.09 %	1
<i>NOF</i>	13.06 %	1	22.37 %	1

Examination of the tables for March 2009 of Appendix A, which describe the statistics associated with the individual circulation areas, reveals the spatial skill assessment of the model. Examination of the CF for salinity in the Courtney Bay Turning Basin and channel reveals statistics of 60% and 74% respectively. The primary difference between the two areas is the bias which in the Turning Basin represents a NOF value of 8% more than the POF and in the channel represents a POF value of 10% more than the NOF. This indicates that too much salt water is observed in the channel, while not quite enough is arriving in the Turning Basin. The CF value for salinity in the Main Harbour channel is 64% with a positive bias of 10%. ADCP CF values in the Main Harbour channel are 55% and 70% in the east and north directions respectively, with no bias observed. In the Reversing Falls channel, the mean difference of -5 psu is reflected in the near equal CF and NOF values of 52% and 48% respectively. In general the waters of the model are too fresh in the Reversing Falls channel. A positive bias in the ADCP eastward velocities is observed in this area with a POF value of 45% with a CF value of 54%. This indicates that the current velocities of the model should be stronger in the westward, upstream direction.

4.2.4. June 2009

Table 10 outlines the statistical assessment of the model results for June 2009. The statistics described in the table corresponds to analysis with 667 MVP dips over a semi-diurnal tidal cycle at each of the matching depth layers which equates to a total sample size of 12412 observations. The June salinity model output provides a close match to the observations with a CF value of 63%. There is a negative bias in the salinity comparison indicating that too little salt water is present overall in the model data. By contrast there is no bias in the temperature data, but temperature prediction is poor based on the CF of only 33%. The model sound speed data displays a very close fit to the observations with a CF value of 99 %.

Table 10 – June 2009 MVP vs. Model Assessment

Variable	Sound speed (m/s)	Limit (m/s)	Temp (deg C)	Limit (deg C)	Sal (psu)	Limit (psu)
<i>Mean</i>	-2.76		-0.10		-1.93	
<i>SD</i>	1.95		1.51		4.92	
<i>RMSE</i>	3.38		1.51		5.28	
<i>Min</i>	-21.96		-4.81		-16.55	
<i>Max</i>	2.39		4.14		15.60	
<i>CF</i>	98.95 %	10.00	32.86 %	0.50	63.48 %	5.00
<i>POF</i>	0.00 %	10.00	33.35 %	0.50	9.40 %	5.00
<i>NOF</i>	1.05 %	10.00	33.79 %	0.50	27.12 %	5.00

The ADCP velocities provide a very close match to the model output, as shown in Table 11. The CF values are higher than any other time period with CF values for the North and East directions at 96% and 98% respectively.

Table 11 – June 2009 ADCP vs. Model Assessment

Variable	North (m/s)	Limit (m/s)	East (m/s)	Limit (m/s)
<i>Mean</i>	-0.03		-0.04	
<i>SD</i>	0.57		0.41	
<i>RMSE</i>	0.57		0.42	
<i>Min</i>	-10.21		-4.22	
<i>Max</i>	4.92		8.36	
<i>CF</i>	96.45 %	1.00	97.67 %	1.00
<i>POF</i>	1.37 %	1.00	0.41 %	1.00
<i>NOF</i>	2.18 %	1.00	1.92 %	1.00

Examination of the tables for June 2009 of Appendix A, which describe the statistics associated with the individual circulation areas, reveals the spatial skill assessment of the model. June is the period when the best fit for salinity and sound speed between the observations and the model is observed in the Reversing Falls Channel. This is represented as a salinity CF value of 88%. The lowest CF values are observed in the Courtney Bay Channel and the Main Harbour Channel both with a CF value of 63%. The Courtney Bay Turing Basin observed slightly higher statistics with a CF value of 69%. A negative bias is observed in the all areas which implies that the model water mass is deficient of saline waters.

The ADCP values fit well with the model output in the Main Harbour Channel with a CF value of 97% and 98% for the north and east directions respectively. The discrepancies within the Reversing Fall channel increase, with a minimum CF value of 65% in the north direction.

4.2.5. Water Mass Analysis

The qualitative analysis demonstrated that the predominant discrepancy between the model output and the observations was in the model misrepresentation of the halocline or pycnocline. To illustrate the consequence to the statistics of the model generalization of the halocline, the CF value for salinity was examined for the fresh, brackish and salt water layers for the April and November simulation periods. These periods are representative of times of strong salinity gradient due to the spring and fall freshets. Salt water was classified as having salinity greater than 20 psu and fresh water was classified as having a salinity of less than 10 psu. The waters of March and June are sufficiently mixed that a comparison within those limits could not be made. The results of the comparison, shown in Table 12, demonstrate the relative agreement between the model and the observations for each area of the water column. The CF values in the salt and fresh water layers are shown to be greater than the values for the brackish layer. The mismatch along the halocline in the brackish waters lowers the overall CF value described in the previous sections for each simulation period.

Table 12 – Central Frequency for each Simulation Period Categorized by Water Mass

Central Frequency by Water Mass	April 2008 Sal (psu)	Nov. 2008 Sal (psu)	Limit (psu)
<i>Fresh <10 psu</i>	57.55 %	67.42 %	5.00
<i>Brackish >10 && <20 psu</i>	30.80 %	38.24 %	5.00
<i>Salt >20 psu</i>	48.62 %	84.01 %	5.00

4.3. Discussion

The qualitative sections and profiles and the quantitative statistics reveal the fit of the observations to the model output. The discrepancies observed in the model output are shown to evolve over a tidal cycle and the structure of the water masses is described. The significance of the differences is shown in terms of the sound speed variable, used in hydrographic survey data reduction and discussed in Chapter 8.

The qualitative comparisons between the model and observational data reveal that within the Main Harbour and Courtney Bay Channels the model generally provides a close match to the observations. The predominant discrepancy between the model and the observations is shown to exist in the model development of the halocline or pycnocline. In the Courtney Bay Channel comparisons the general structure of the water masses is correct, but the weak pycnocline gradient over-mixes the water column changing the salinity concentrations at the surface and near the seabed. Near low tide in Courtney Bay there is almost always a deficiency of saline waters in the model output, which is likely related to the development of the halocline near high tide. The circulation in the Courtney Bay Channel is heavily influenced by the interaction of the fresh waters originating from the Main Harbour Channel and the tides from the Bay of Fundy. The fresh surface waters must flow over the intertidal area between the two channels before reaching the Courtney Channel; therefore any deficiencies in the model representation of the bathymetry in the intertidal area, due to incomplete multibeam coverage, or the hydrodynamics of the water flowing over it will influence the resultant circulation. The

three dimensional current velocities within the intertidal area between the channels are complex and depend of the velocity of the currents leaving the Main Harbour Channel and the subsequent interaction with the Courtney Bay breakwater. This area will be discussed further in Chapter 5 through examination of the evolving model current fields.

The quantitative comparison shows that the model output data provides a close match to the observed data in most areas with an overall central frequency statistic of at least 50% for salinity within the prescribed limits for April, November, March and June. The central frequency statistic for sound speed for June of 99% shows that the difference in salinity has very little effect on the potential application to acoustic ray-tracing, to be discussed in Chapter 8, as the two water masses have similar sound speed values with warm fresh water overlaying cold salt water. The resultant vertical sound speed gradient in the area is minimized and any errors in the location of the halocline do not greatly influence the sound speed field, while it does significantly affect the salinity statistics.

When the model output is compared to the individual areas described in Figure 13, the spatial correlation of the goodness of fit between the model and the observations can be observed. Overall the model best described the salinity structure within the Reversing Falls Channel, while providing slightly lower but similar statistics in the Courtney Channel, Courtney Bay Turning Basin and Main Harbour Channel, as shown in Table 13. This fact is observed through averaging the salinity CF value, within a limit of 5 psu, for each area over the simulation periods.

Table 13 – Average Salinity Central Frequency by Area

Area	Average Salinity CF (%)
Reversing Falls	64
Main Harbour	59
Courtney Channel	63
Courtney Turning Basin	61

Almost exclusively, the model describes too much mixing between the fresh and salt water, which increases the salinity in the surface layer and lowers the salinity in the bottom layer. Both the MY2.5 [Mellor and Yamada, 1982] and GOTM [Umlauf et al., 2012] turbulence closure model implementations were examined and tested in an effort to improve the mixing estimate. The models provided different representations of the halocline, as shown in Figure 30, and the GOTM turbulence closure model was determined to provide a better estimate of the salinity interface through analysis of the qualitative statistics for both methods. The vertical Prandtl number, which defines the ratio of vertical thermal diffusion to vertical eddy viscosity, was lowered from default values of 0.1 to 0.000001 in an effort to reduce the interfacial mixing in temperature and salinity but little difference was observed in the results. The inability of the model to accurately capture the halocline mixing affects the achievable accuracy of the model output data in both the Main Harbour and the Courtney Bay channels for practical applications.

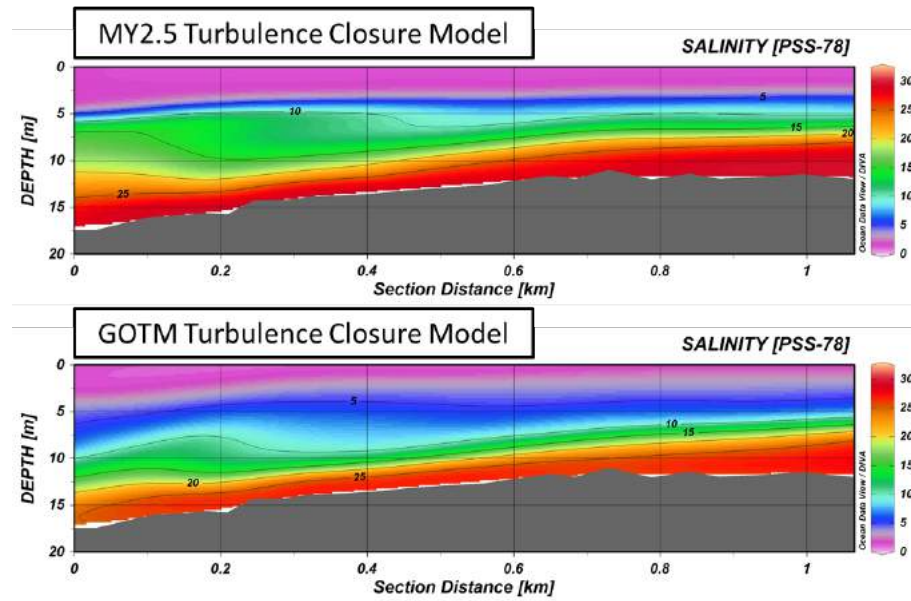


Figure 30 -- Turbulence Closure Comparison for April 2008 Flood Tide

The majority of differences observed in the comparison of model output with observations are a result of incorrect interfacial mixing along the halocline, as shown below in Figure 31. In order to emphasise the scale and intensity of the internal waves on the halocline the observed interfacial turbulence from the single beam echosounder acoustic backscatter is compared to the model salinity field in Figure 31. The figure represents the interaction between the salt wedge and the fresh water on the flood tide for April. The acoustic backscatter clearly shows the complexity of the mixing along the halocline.

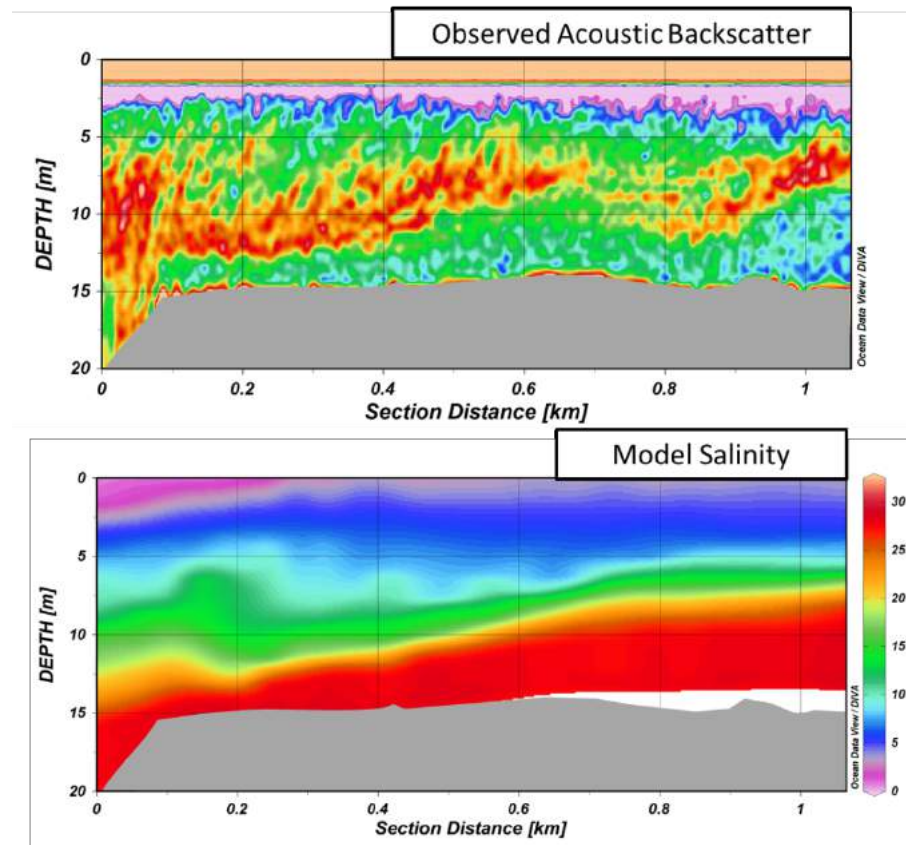


Figure 31 – Observed vs. Model Representation of Interfacial Turbulence

Considering the estuarine dynamics of the Port of Saint John, the model provides a good representation of the observations. Small changes in the location and thickness of the halocline will negatively affect the salinity statistics, while still allowing the model to represent the three dimensional movement of the water masses over a tidal cycle.

Altering the limits associated with the CF, NOF and POF variables also impact the statistical fit of the model to the observations. Based on the criteria chosen for this investigation, the model successfully estimates the flow conditions and interactions of the salt and fresh water within the Port of Saint John and their effects on the seabed, and is able to establish lateral circulation patterns for the first time. The ability of the model to

be implemented in the practical application of MBES data reduction, and the associated uncertainty, is investigated in Chapter 8.

CHAPTER 5: Model Estuarine Circulation

Oceanographic data collected from the Heron were examined at four times of the year over a semidiurnal tidal cycle along narrow sections through the centre line of the two principal areas of the port, the Main Harbour Channel and Courtney Bay [Toodesh, 2012]. The result was a two-dimensional profile of the physical oceanographic conditions that ignored the lateral variations of temperature and salinity throughout the domain and missed the near surface and seabed conditions. As the baroclinic hydrodynamic modelling simulations were completed for the same times of year, they can provide additional information on the circulation and temperature and salinity distributions away from the observations. Chapter 4 revealed that the imperfections in the model output are sufficiently small to be considered acceptable for this project and the model is able to reproduce the primary oceanographic circulation throughout the area. Furthermore, in the low velocity environment of Courtney Bay, the model velocities provide an estimate of the flow in the area unlike the vessel mounted ADCP observations that were hampered by low signal to noise levels.

The model output is used to investigate the areas of missing observational data and extends the understanding of the oceanographic conditions to all areas of the harbour. The model outputs temperature, salinity and velocity over 20 vertical layers at more than 16000 nodes distributed throughout the domain of the Port of Saint John. The 20 vertical layers are terrain following and therefore can resolve near seabed structure independent

of depth. The ability of the model to simulate the surface layer allows for an improved understanding of the buoyant fresh water movement within the area, which is often constrained to a thin surface sheet.

5.1. Estuarine Circulation Observation Overview

A synthesis of the oceanographic profile observations of Toodesh (2012) are schematically represented in Figure 32 and Figure 33 for the Main Harbour Channel and Courtney Bay respectively. The Main Harbour Channel figure is representative of the salinity structure in the water column at low, flood, high and ebb tide. The section covers the Main Harbour area from the Harbour Bridge (left hand side of the sections in Figure 32) to the entrance to the Harbour, which is defined as the intersection of the Main Harbour and Courtney Bay navigation channels (right hand side of the sections in Figure 32). High salinity corresponds to a range of 20 to 30 psu, moderate salinity to a range of 10 to 20 psu and low salinity to a range of 0 to 10 psu.

The Main Harbour Channel section schematic, described in Figure 32, shows the variations in the location of the halocline over a tidal cycle at each stage of the tide for each observational period. The salt wedge is arrested at different locations within the harbour depending on the fresh water discharge at that time of the year. At low, flood and high tide there is always at least a moderately fresh surface layer visible within the profile. On the ebb tide, the fresh surface waters disappear for the March and June

observation periods. This indicates that at times of low river discharge the incoming salt wedge mixes completely with the river water before the falls start to reverse and the river waters, which are mixed upstream in the lower Saint John River estuary, appear again at low tide.

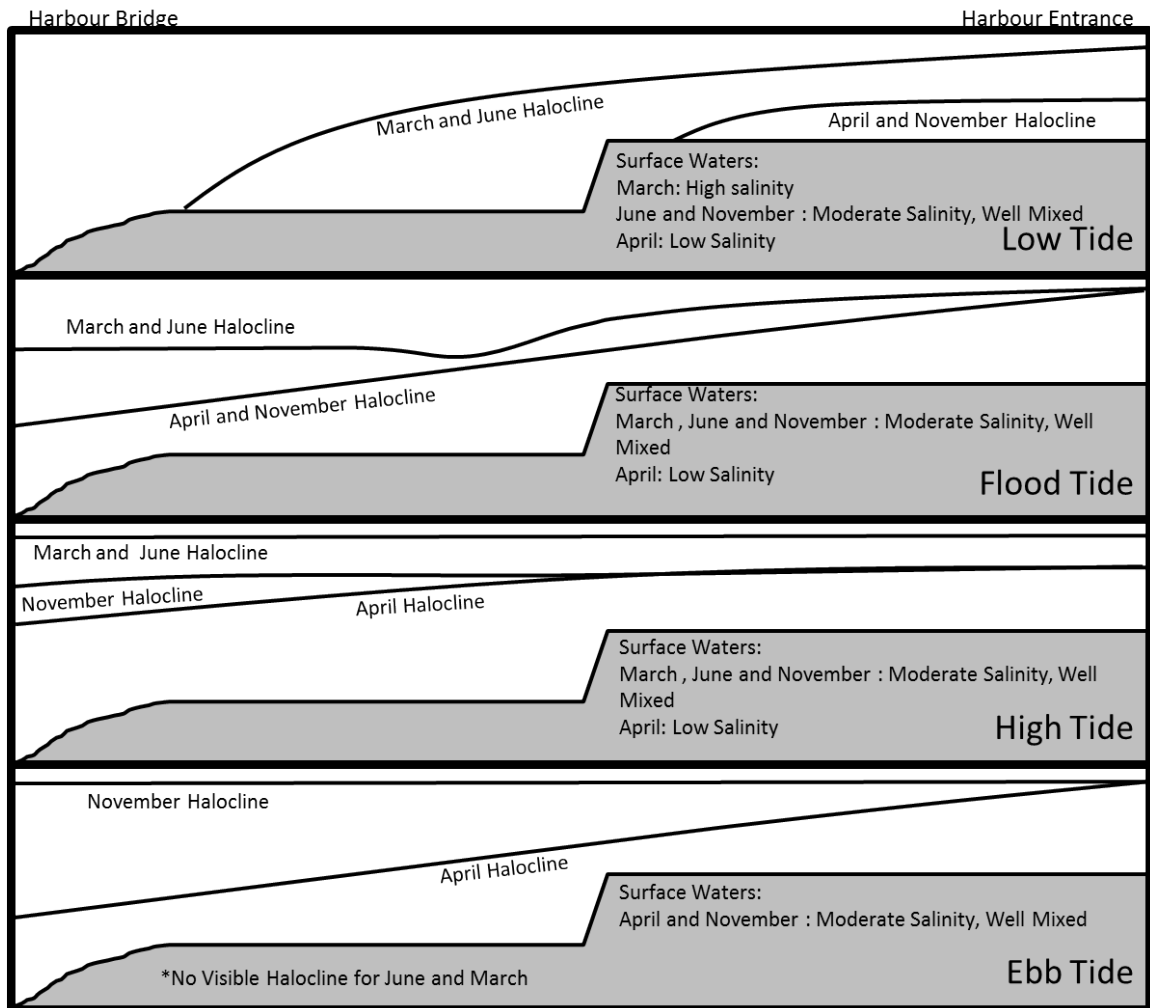


Figure 32 – Circulation Overview of Main Harbour Channel. (Derived from observations in Toodesh (2012))

The Courtney Bay Channel section schematic, described in Figure 33, shows the variations in the interaction between the salt wedge and the fresh water input from the Main Harbour Channel. The section covers the channel area from the Turning Basin (left hand side of the sections in Figure 33) to the entrance to the channel, which is defined as the intersection of the Main Harbour and Courtney Bay navigation channels (right hand side of the sections in Figure 33). At low tide, independent of the time of year, a plug of salt water is left within the Turning Basin of the Courtney Bay Channel. The salinity of the surface waters above the halocline vary and are dependent on the quantity of fresh water input to the channel, which is directly proportional to discharge of the Saint John river. As the flood tide begins, the location of the halocline varies according to the quantity of fresh water within the channel as the incoming salt wedge interacts with the existing water mass. At high and ebb tide, the halocline is relatively level and the elevation of the surface depends on the river level discharge. On the ebb tide in March, the river discharge is sufficiently low that the fresh water layer either becomes too thin to be visible by the equipment or disappears completely.

Although the Courtney Bay Channel has no significant source of input fresh water, the circulation in the area is still heavily driven by the interaction of the salt and fresh water which both enter the area through the channel entrance. The relative quantities of fresh and salt water which flow through this area, and their resultant mixing, will be examined further in Chapter 7.

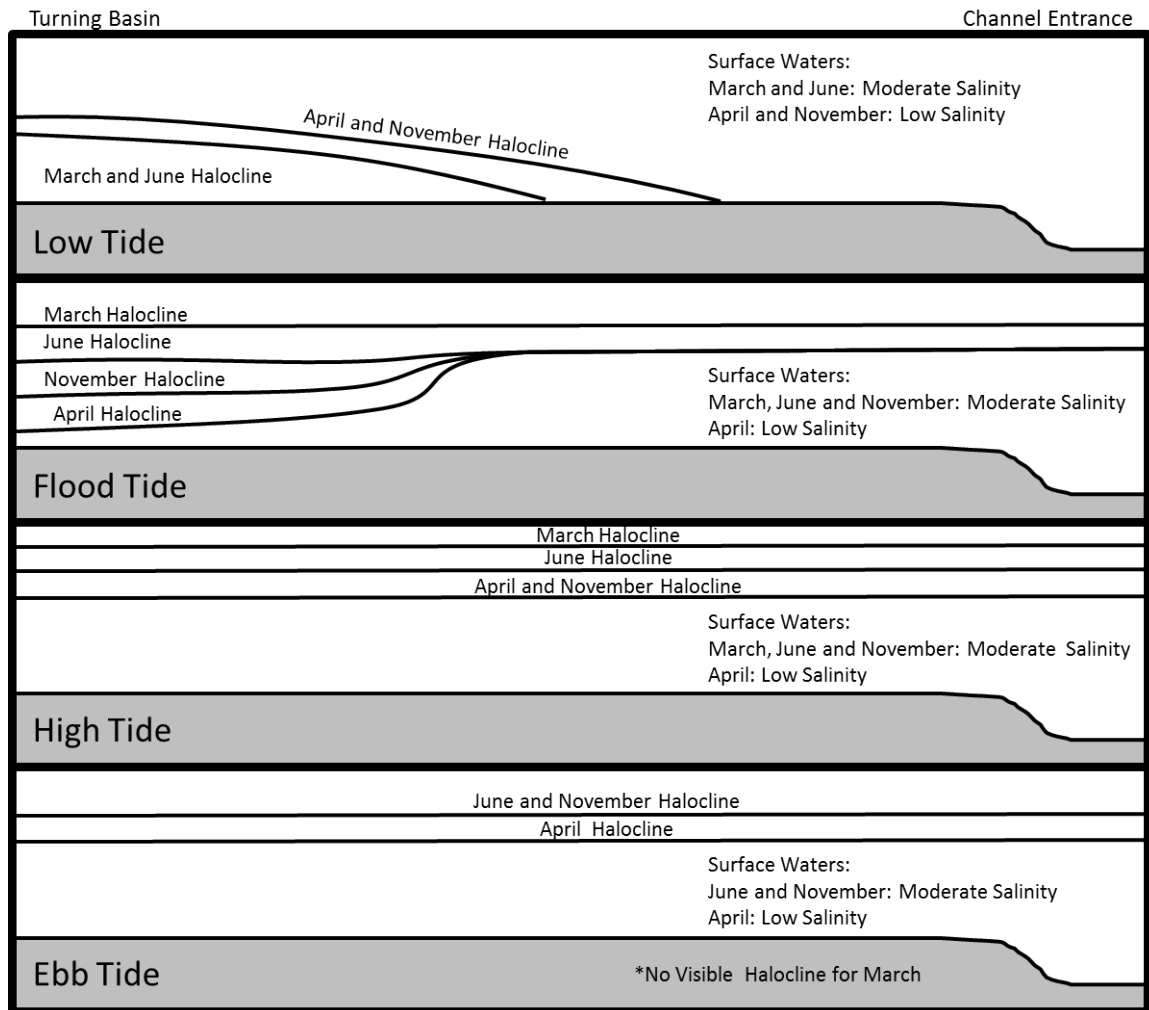


Figure 33 – Circulation Overview of Courtney Bay Channel. (Derived from observations in Toodesh (2012))

5.2. Model Contribution to Understanding Cross-Channel Flow

The estuarine circulation observations can be supplemented through examination of the model output at each of the simulation periods. The model delivers the lateral variations in temperature, salinity and current velocities at each of the vertical layers. The lateral

variations in circulation are particularly important in the Port of Saint John due to the complex geometries (curvature and protrusions) of the Main Harbour Channel and the interaction between the Main Harbour Channel and the Courtney Bay Channel over the intertidal mud flats of Round Reef.

Two areas which are important in controlling the circulation in the Port of Saint John are identified in Figure 34. The northernmost area titled “Harbour Bridge Area” encompasses the area of interaction between the salt wedge and the fresh water identified as the upstream extent of the observations in Toodesh (2012). Within this area, there are strong cross channel variations in salinity distribution and current velocities due to the tight curvature and abrupt change in cross section of the channel. The sudden change in direction changes the hydrodynamics of the salt and fresh water masses as they move throughout the area creating eddies and cross channel gradients. The southernmost area titled “End of Courtney Bay Breakwater” covers two important flow regimes that can only be understood through examination of the three dimensional current field. The first is the inter-channel flow from the Main Harbour Channel to the Courtney Bay Channel over the area known as Round Reef. This flow controls the timing and quantity of fresh water input to the Courtney Bay system. The second condition is the flow present at the end of the Courtney Bay breakwater, which originates from the intertidal area to the east of the breakwater and pushes salt water into the Courtney Bay Channel.

Within each of the areas, the seabed and surface model velocities will be examined at each node along with generalized representations over a tidal cycle. The salinity at the seabed will also be displayed to show the extent of the salt wedge.

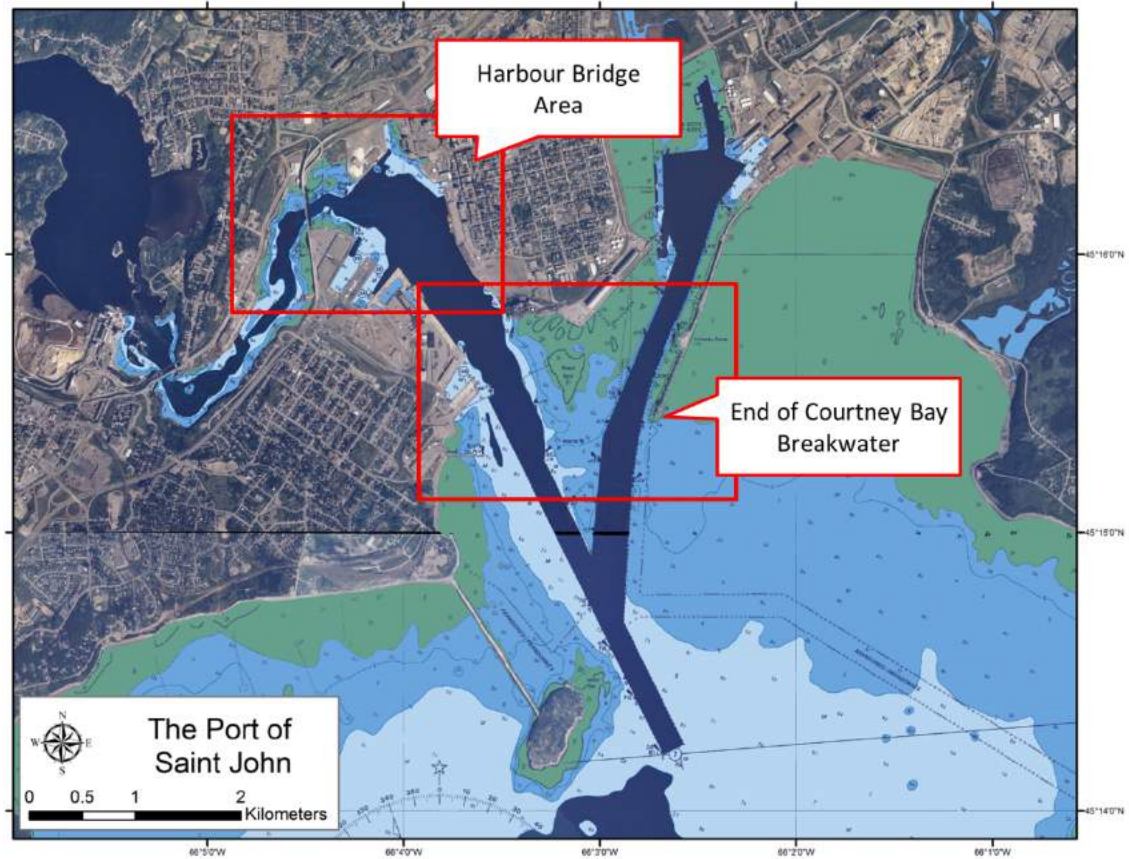


Figure 34 – Circulation Analysis Areas

In section 5.1 a plug of salt water is described as being orphaned within the Courtney Bay breakwater at low tide. The lateral extent of the saline plug can be examined for the Courtney Bay Turning Basin through examination of the salinity distribution from the model output.

5.2.1. Harbour Bridge

The first area examined was the Harbour Bridge Area identified in Figure 34. Within this area the model output variables of salinity and current velocity were examined. Current velocities were extracted from the model for the surface and the seabed layers of the terrain following vertical coordinate system. Salinity distribution was examined at the seabed as a proxy for the extent of the salt wedge. The output variables were plotted in the sections below for the low, flood, high and ebb tidal stages.

5.2.1.1. April 2008

During April 2008, water levels from the Saint John River are at an annual maximum with the occurrence of the spring freshet, as shown in Figure 7 and discussed in Chapter 2. Figure 35 shows the variation in seabed current velocities for April over a tidal cycle along with overlaid arrows providing a not-to-scale generalization of the flow regime to aid the user in comprehension. The influence of the incoming salt wedge and the outgoing fresh water plume are shown through the direction and magnitude of the velocity vectors. At low tide the flow is dominated by the outgoing fresh water. A large eddy is formed in the centre of the Main Harbour Channel that reverses the predominant flow along the face of the west piers. A small eddy is also visible along the face of Long Wharf at the North end of the channel. Anytime an eddy is developed within the harbour it causes the flow to decelerate and some suspended sediment to deposit. The quantity of

sediment coming out of suspension will depend on the sediment concentration of the waters, the deceleration of the flow and the settling velocity of the sediment. At flood tide the flow regime is almost the same as low tide, but the magnitude of the vectors has been reduced. On high tide the general inflow of salt water is visible at the seabed and a small eddy is developed along the west piers. The advancing fresh water outflow from the river is visible on the ebb tide downstream of the Harbour Bridge.

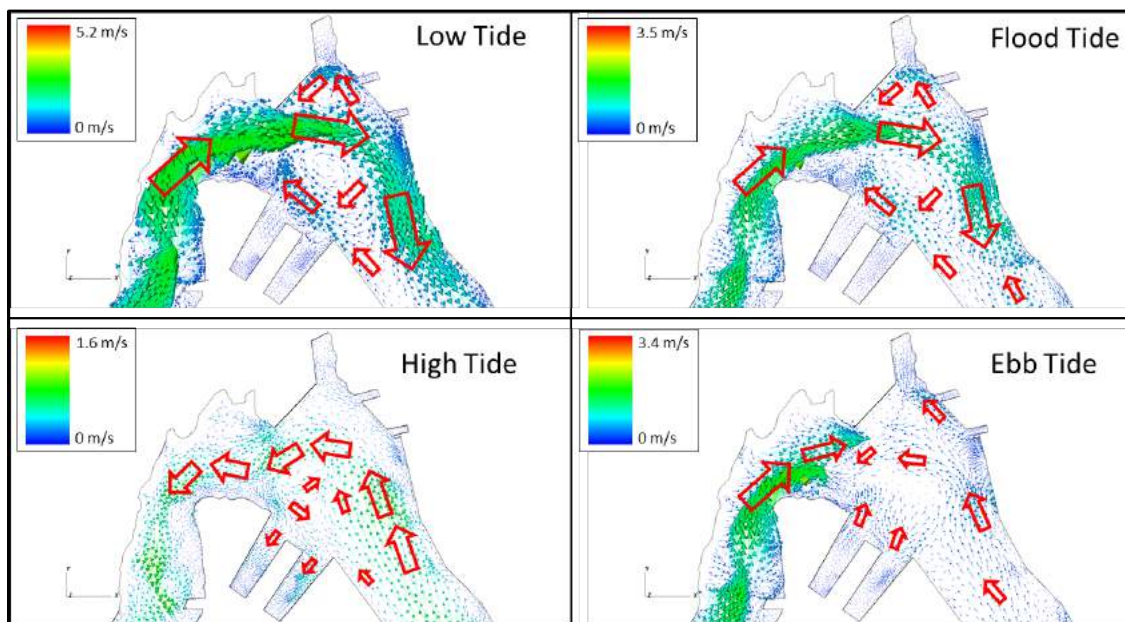


Figure 35 – April 2008 Seabed Current Velocities over a Tidal Cycle in Main Harbour

The surface currents over a tidal cycle, as shown in Figure 36, always flow in the downstream direction as there is always a surface influence of fresh water in the channel. The magnitude of the velocities changes over a tidal cycle, as would be expected, and the formation of mid channel eddies are also variable. At both low and flood tide a large clockwise eddy is formed in the centre of the Main Harbour Channel. At high and ebb

tide, the eddy disappears. This phenomenon is not solely related to flow magnitude as current speeds are similar on the flood and ebb tide.

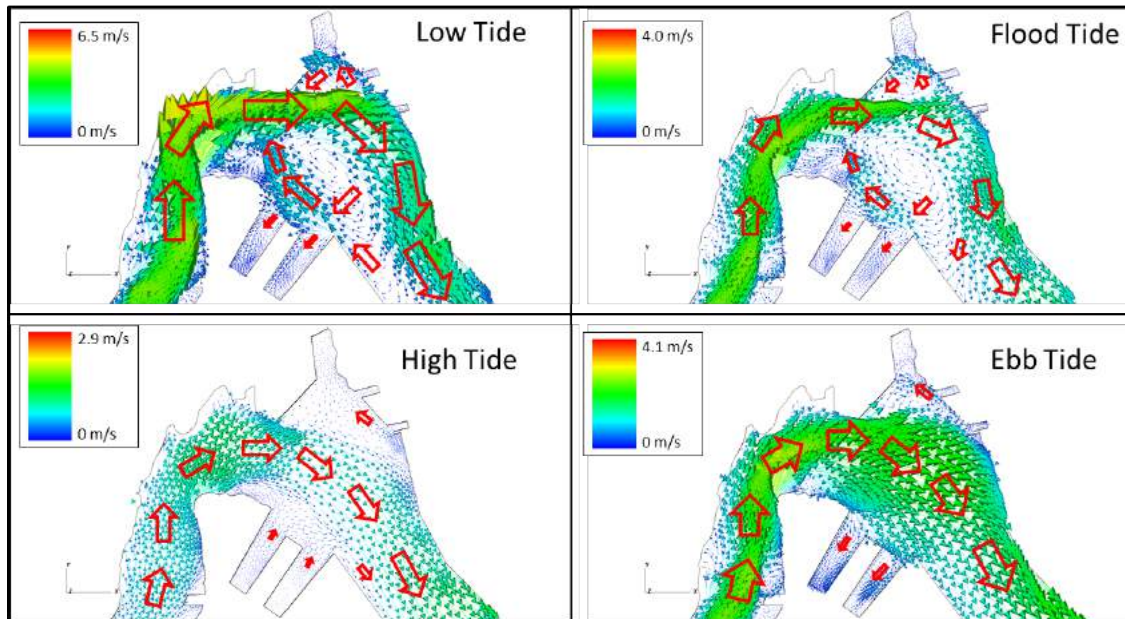


Figure 36 – April 2008 Surface Current Velocities over a Tidal Cycle in Main Harbour

The distribution of salt water at the seabed is shown in Figure 37 as a proxy for the extent of the salt wedge. The location of the salt wedge varies over a tidal cycle and correlates with the seabed current velocities discussed previously. The salinity distribution displays a non-uniform cross channel concentration as it progresses up the harbour which approximately follows the bathymetry of the channel. The salinity correlates with current velocity and the significance of the abrupt changes in spatial geometry of the port can be observed. The lateral variations in salinity are notably visible on the ebb tide. It is important to recognise that the salt wedge protects the underlying sediments from the extreme bed shear stress associated with the strong downstream fresh water currents.

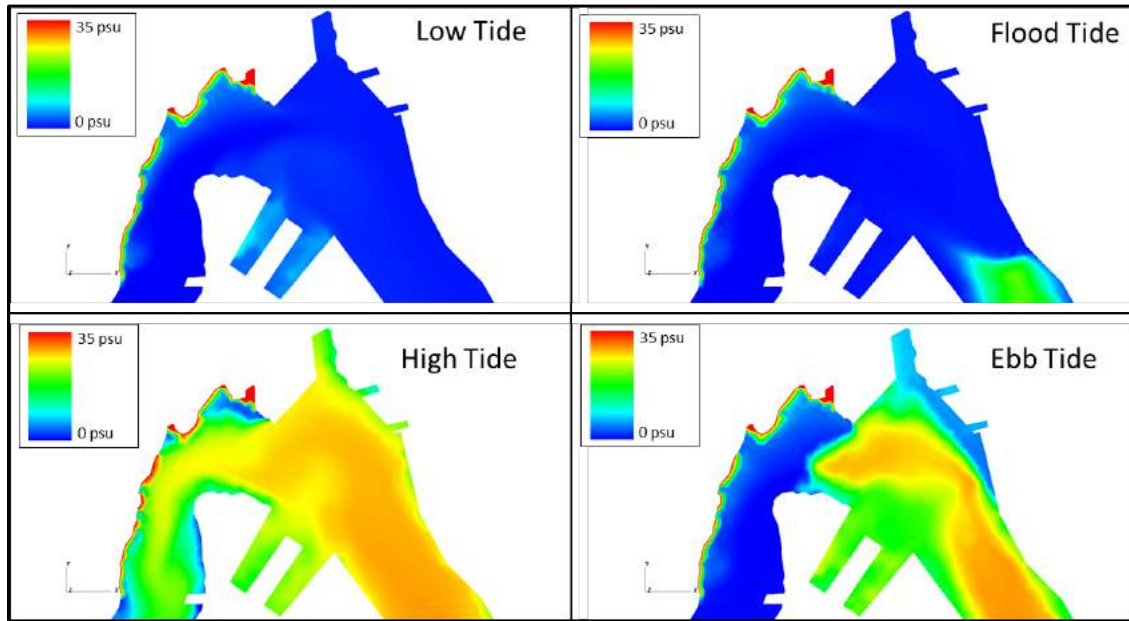


Figure 37 – April 2008 Seabed Salinity Distribution over a Tidal Cycle in Main Harbour

5.2.1.2. November 2008

During November, water levels from the Saint John River are near the fall maximum with the occurrence of the fall freshet, as shown in Figure 7 and discussed in Chapter 2. Figure 38 shows the variation in seabed current velocities for November over a tidal cycle. At low tide the modelled current pattern is very similar to April (Figure 35), with the formation of a large clockwise eddy, but the overall magnitude of the velocities are lower. At flood tide the seabed current velocities for November are in the upstream direction, unlike April where the currents were still flowing downstream. At high tide a small and weak counter clockwise eddy forms near the western berths, while the flow

direction is generally upstream. The downstream flow begins to reappear on the ebb tide beneath the Harbour Bridge.

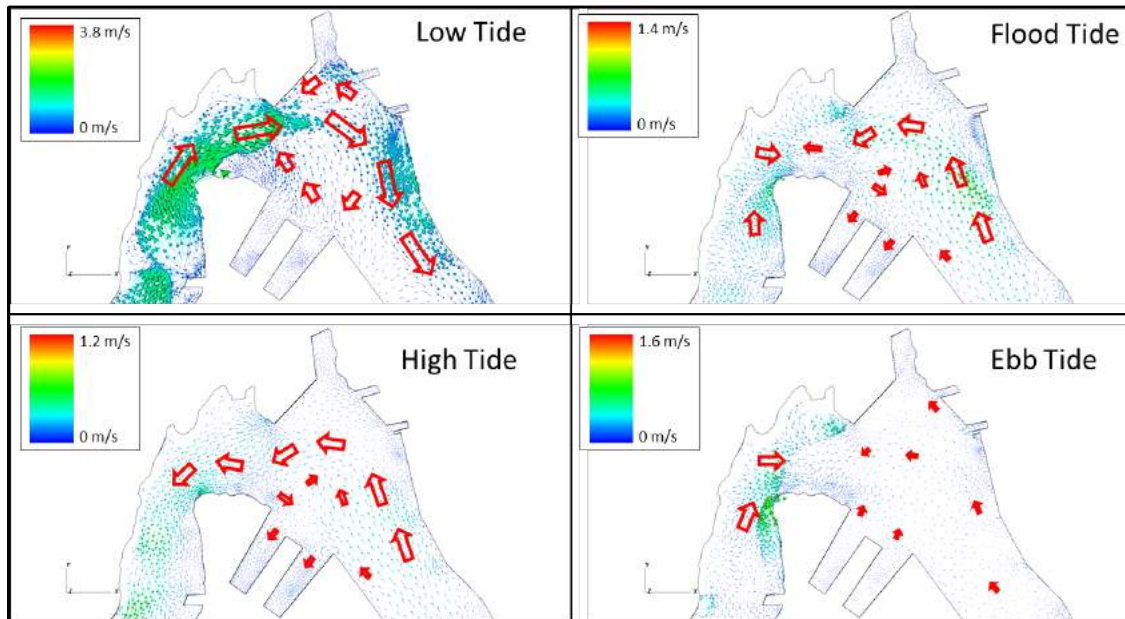


Figure 38 – November 2008 Seabed Current Velocities over a Tidal Cycle in Main Harbour

The surface current velocities for November are shown in Figure 39. The low tide pattern in November is similar to April (Figure 36) with the formation of the large mid channel clockwise eddy. However, in November that eddy is not present on the flood tide. The primary difference between the surface currents for November in comparison to April is the reversal of flow at high tide, as the river level is not as high in November. At this stage of the tide the influence of the salt wedge has reached the surface layer in November.

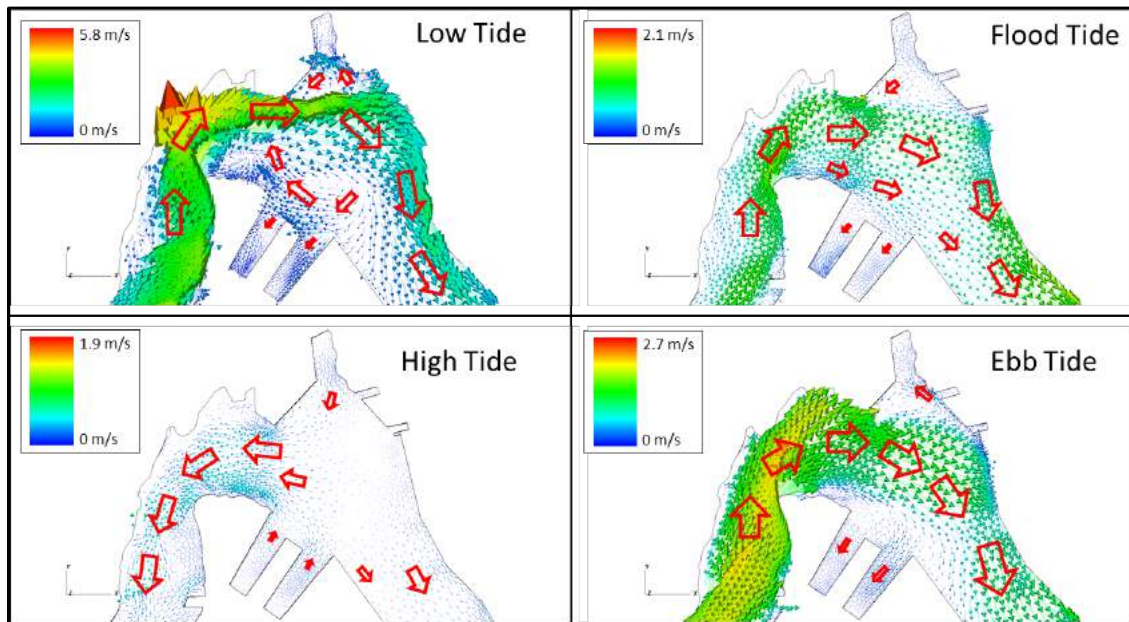


Figure 39 – November 2008 Surface Current Velocities over a Tidal Cycle in Main Harbour

Figure 40 displays the variations in progression of the salt wedge over a tidal cycle for November 2008. Similar to April (Figure 37), the importance of the cross channel component of the salinity distribution is visible, especially on the flood tide. The incoming salt wedge correlates with the variations in current velocities. Notably however the upstream penetration of the salt wedge is more developed throughout the tidal range and is thus shielding the seabed more than in April.

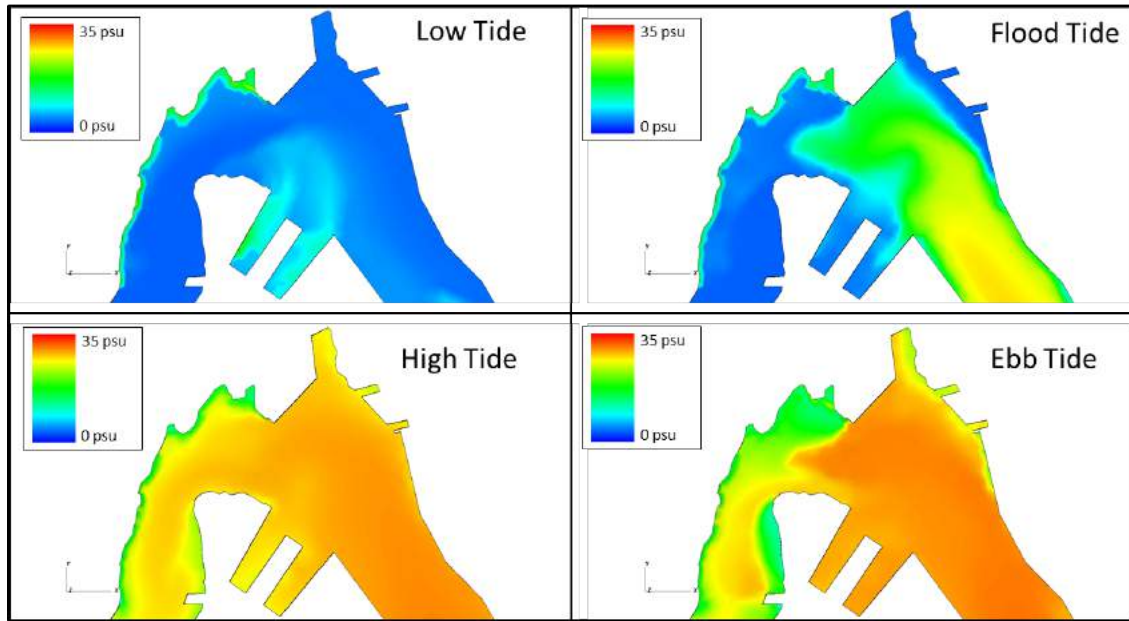


Figure 40 – November 2008 Seabed Salinity Distribution over a Tidal Cycle in Main Harbour

5.2.1.3. March 2009

During March, water levels from the Saint John River are at a minimum, as shown in Figure 7 and discussed in Chapter 2, and significant differences would be expected at the surface and seabed compared to April and November. The current velocities throughout the area over a tidal cycle are at a minimum annual level at both the seabed and surface, as shown in Figure 41 and Figure 42 respectively. At the seabed the low velocities and the direction of the currents are a reflection of the constant presence of the salt wedge (Figure 43), which therefore masks the seabed from the net-outgoing freshwater layer. The magnitude of the velocities at the seabed is lowest on the ebb tide and the clockwise eddy is not developed in the centre of the channel which reduces the likelihood of

decelerating waters depositing sediment into the western berths. The surface currents are flowing downstream with the outflow of the river, except for high tide where the vertical extent of the salt wedge is maximized and the surface flow changes direction.

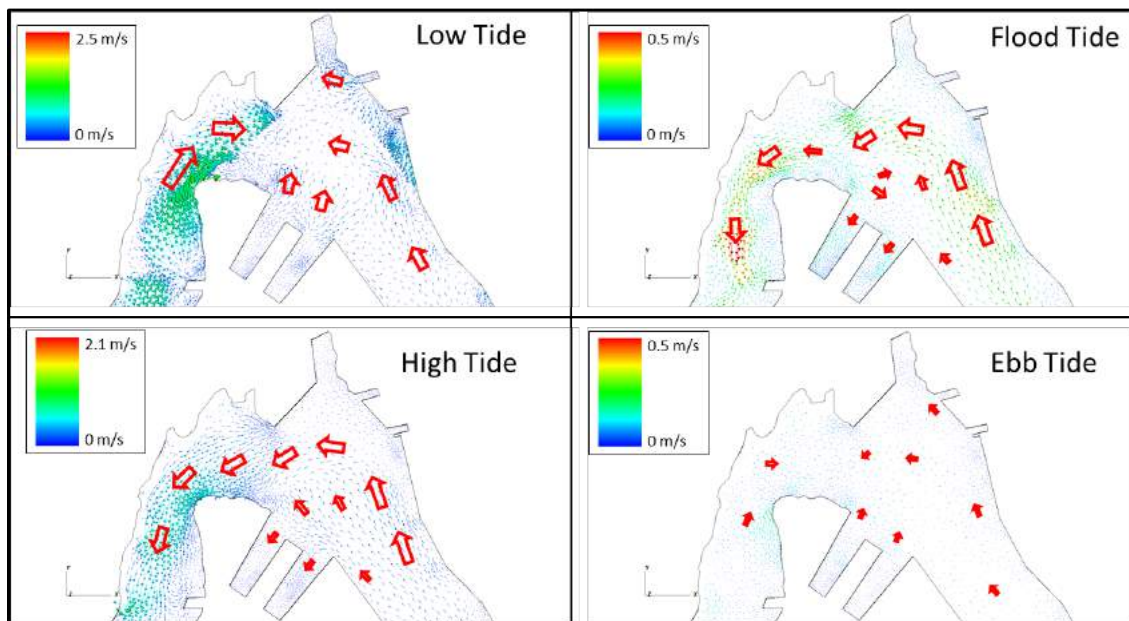


Figure 41 – March 2009 Seabed Current Velocities over a Tidal Cycle in Main Harbour

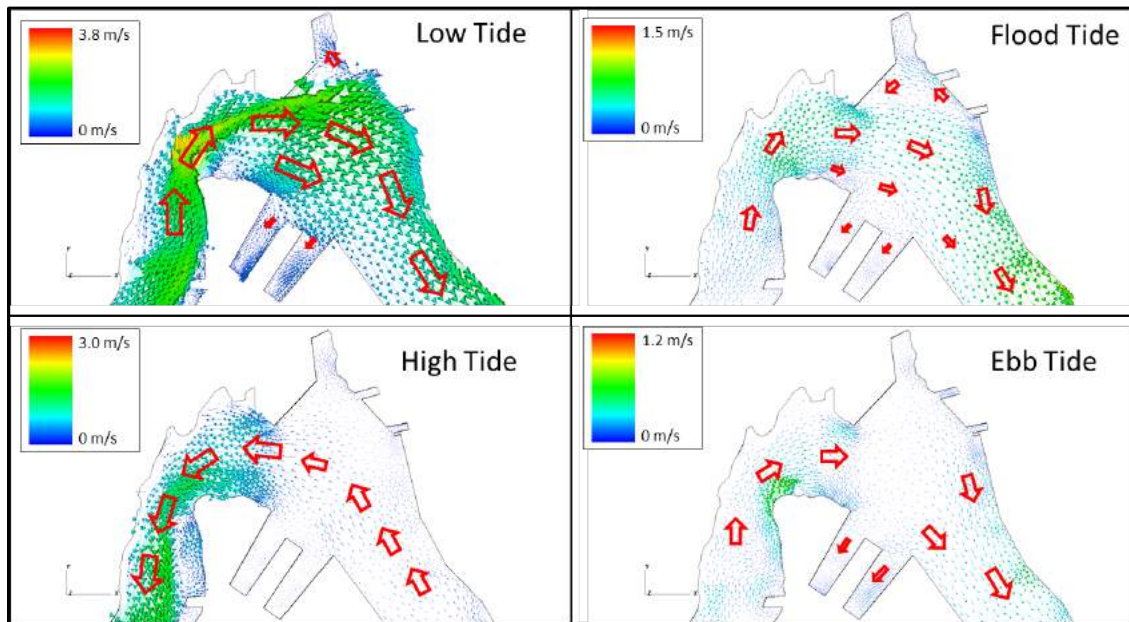


Figure 42 – March 2009 Surface Current Velocities over a Tidal Cycle in Main Harbour

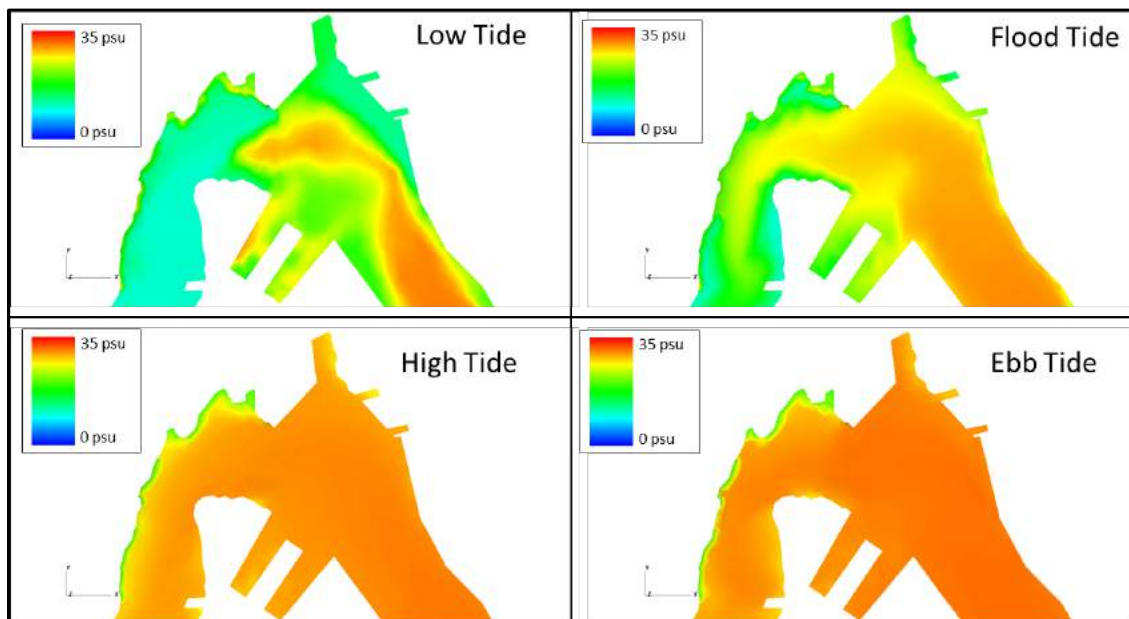


Figure 43 – March 2009 Seabed Salinity Distribution over a Tidal Cycle in Main Harbour

5.2.1.4. June 2009

Water levels from the Saint John River in June are at a summer minimum, as shown in Figure 7 and discussed in Chapter 2. The semidiurnal variations in current velocities and reach of the salt wedge in June are most similar to the model output in March. Both periods exhibit low river levels, but the June simulation is during spring tides while the March simulation is during neap tides. The seabed current velocities over a tidal cycle shown in Figure 44 show the interaction of the fresh and salt water. At low tide the effect of the fresh water on the seabed is visible under the harbour bridge and along the eastern piers. There is a general outflow of waters from the western berths at this time. On the flood and high tide a weak counter-clockwise eddy is observed to develop in the centre of the channel. This eddy influences the current velocities within the western berths and directs sediment rich salt waters into the berths. On the ebb tide, the current velocities are very weak downstream of the harbour bridge.

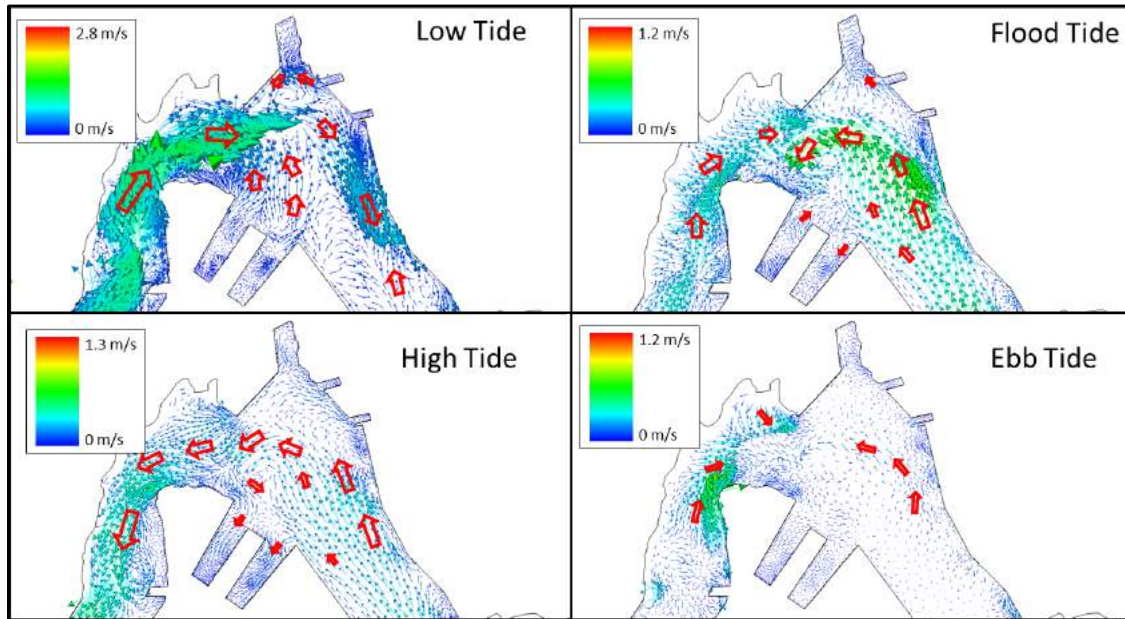


Figure 44 – June 2009 Seabed Current Velocities over a Tidal Cycle in Main Harbour

Figure 45 displays the surface current velocities for June. The surface currents resemble the observed field in March, with the exception of low tide, but with stronger magnitudes. At low tide a small eddy has developed close to the western berths. Suspended sediment in the fresh surface waters at this time could become trapped in the eddy, quickly decelerate and deposit into the berths. At the entrance to the harbour at high tide the currents have maintained their downstream direction from the flood tide while the velocities in the channel upstream of the Harbour Bridge are directed upstream.

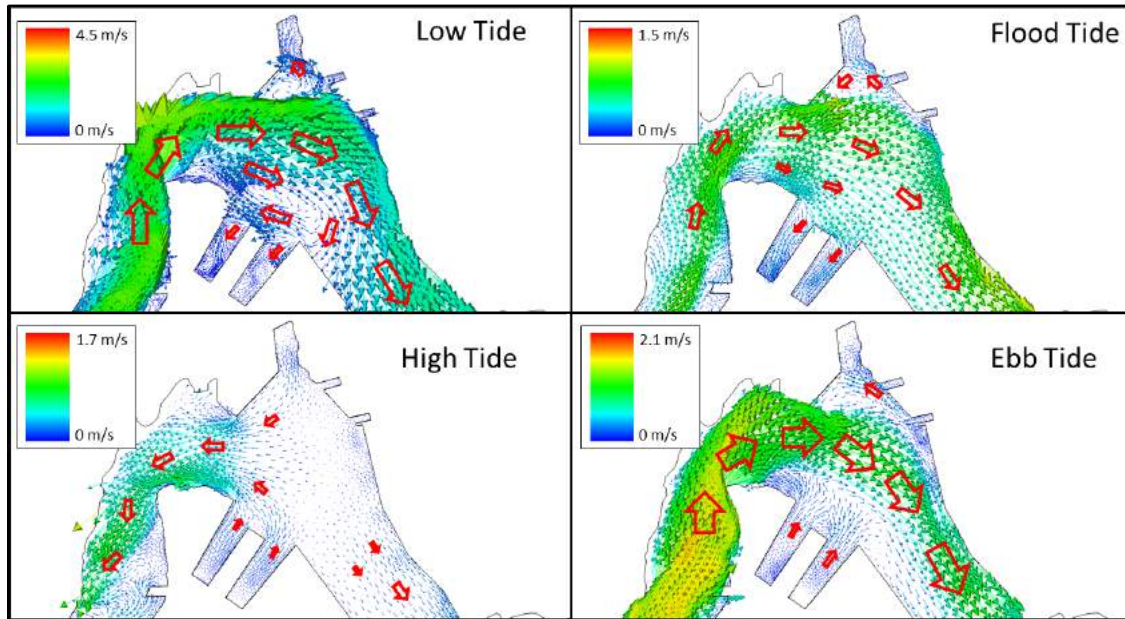


Figure 45 – June 2009 Surface Current Velocities over a Tidal Cycle in Main Harbour

Figure 46 displays the salt wedge at the seabed for June over a tidal cycle. The timing of the progression of the salt wedge is very similar to March. Cross channel variations in the concentration of salinity are visible through the channel. The fresh water visible at low and flood tide is mixed from the previous tidal cycle at approximately 12 psu.

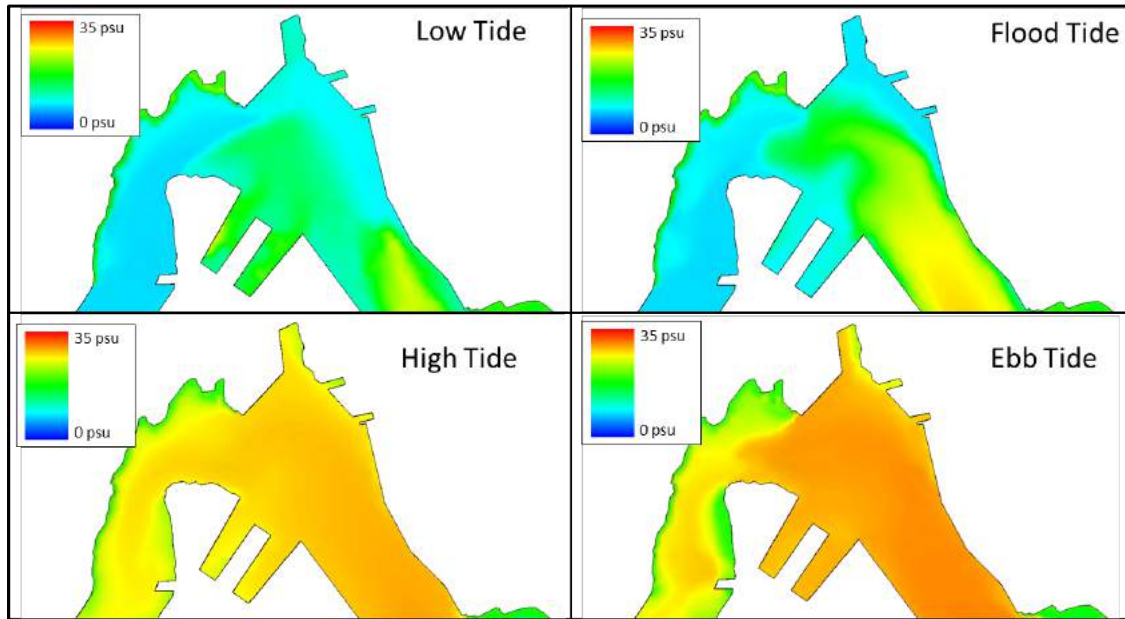


Figure 46 – June 2009 Seabed Salinity Distribution over a Tidal Cycle in Main Harbour

5.2.2. End of Courtney Bay Breakwater

The area which covers the intersection of the Main Harbour and Courtney Bay Channels (See Figure 34) is important for understanding the circulation in Courtney Bay. Almost all the fresh water which enters Courtney Bay originates from the Main Harbour Channel, with the exception of the relatively small discharge of Marsh Creek. The fresh water flows over the intertidal mud flats between the two channels and is redirected upstream in the Courtney Bay Channel by the breakwater. The variation in this process along with other flow regimes will be examined below. Current velocities are extracted from the model for the surface and the seabed layers of the terrain following vertical coordinate

system. As with the previous examples, the output variables are plotted in the sections below for the low, flood, high and ebb tidal stages.

5.2.2.1. April 2008

The seabed currents over a tidal cycle for April are shown in Figure 47. At low tide, outgoing downstream flow is observed for both the Main Harbour and Courtney Bay Channels. At flood tide the seabed currents are now flowing into the Main Harbour Channel on the western side of the harbour. The flow is still downstream for the eastern side of the Main Harbour Channel, but, notably, the strength of the currents over the intertidal mudflats between the channels is beginning to increase from almost zero to approximately 1 m/s indicating increased diversion of the river water into the mouth of Courtney Channel. Note the near seabed flow velocities decelerate abruptly on reaching the Courtney Channel, which could result in rapid localized suspended sediment deposition. The flow is still moving out of Courtney Bay on the flood tide. At high tide the flow in the Main Harbour Channel is predominately upstream and the flow in Courtney Bay has changed direction. The seabed currents entering Courtney Channel are arriving from around the end of the breakwater in a flow pattern which is bringing waters from the eastern side of the breakwater around and into the channel. At ebb tide, the flow regime is similar to the modelled flow on the flood tide, with the exception of the flow over the inter-channel area of Round Reef which is now diverted away from the Courtney Channel.

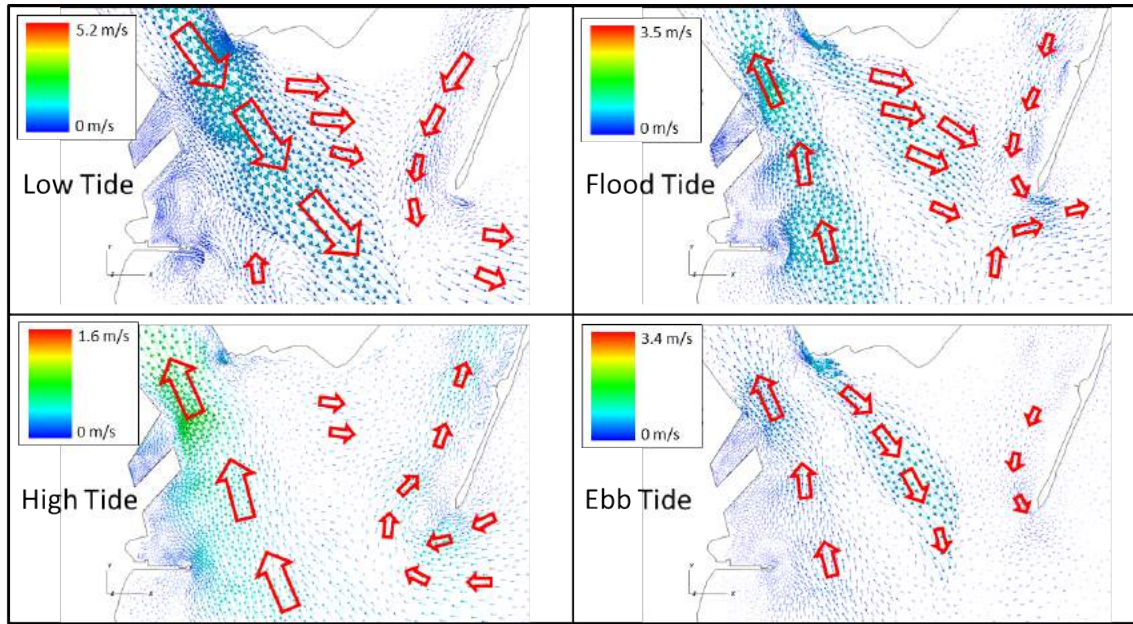


Figure 47 – April 2008 Seabed Current Velocities over a Tidal Cycle at end of Courtney Bay Breakwater

At the surface at all stages of the tide, the predominant flow direction within the Main Harbour Channel is downstream as shown in Figure 48. The primary variation in the surface currents over a tidal cycle is the interaction between the waters of Courtney Bay and the Main Harbour channel. At low and flood tide, the surface currents from the Main Harbour Channel pass over the Round Reef area and flow into Courtney Bay. At high tide, the waters within the bay start to flow downstream and deflect the waters passing over Round Reef so that they are not able to enter the channel.

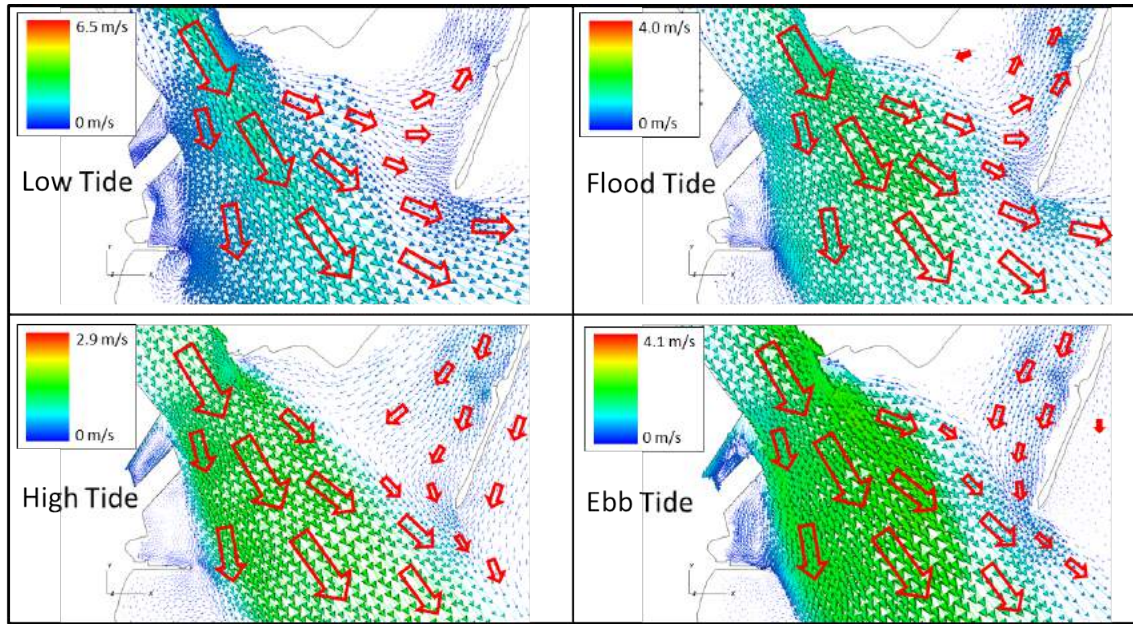


Figure 48 – April 2008 Surface Current Velocities over a Tidal Cycle at end of Courtney Bay Breakwater

The abrupt deceleration of current magnitude of waters travelling from the Main Harbour Channel to Courtney Bay, over Round Reef, can be visualized in profile as shown in Figure 49. The current speed on the flood tide reaches over 1 m/s (to a maximum of 1.8 m/s) as the water travels downstream over Round Reef. As the waters enter the Courtney Bay Channel their speed is quickly reduced to less than 0.5 m/s.

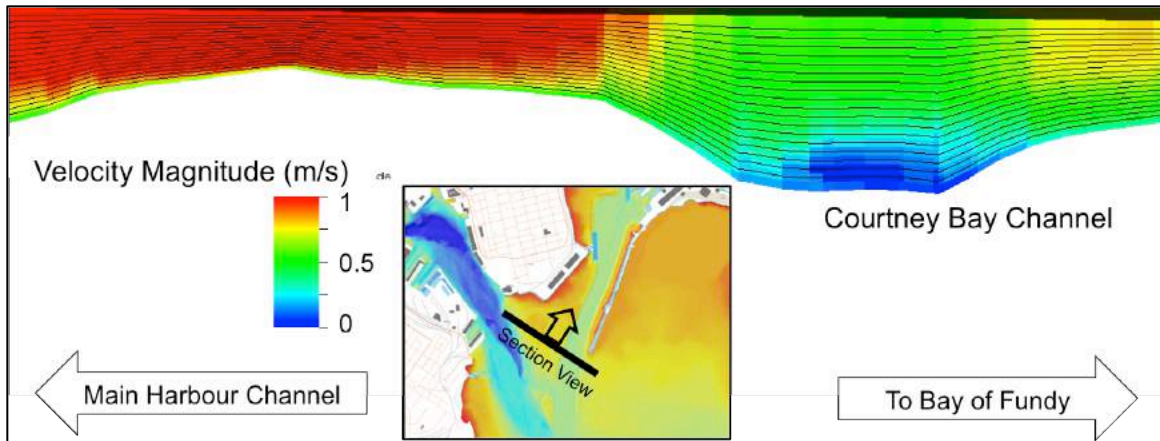


Figure 49 – Velocity Magnitude Profile on Flood Tide at Courtney Bay Entrance

The salinity at the seabed is shown for the intersection of the Courtney Bay and Main Harbour Channels in Figure 50. The salinity concentrations follow the bathymetry of the channels and the relative interaction of the fresh and salt water throughout the tidal cycle is observed. At both low and flood tide the fresh water moving over Round Reef is apparent at the seabed.

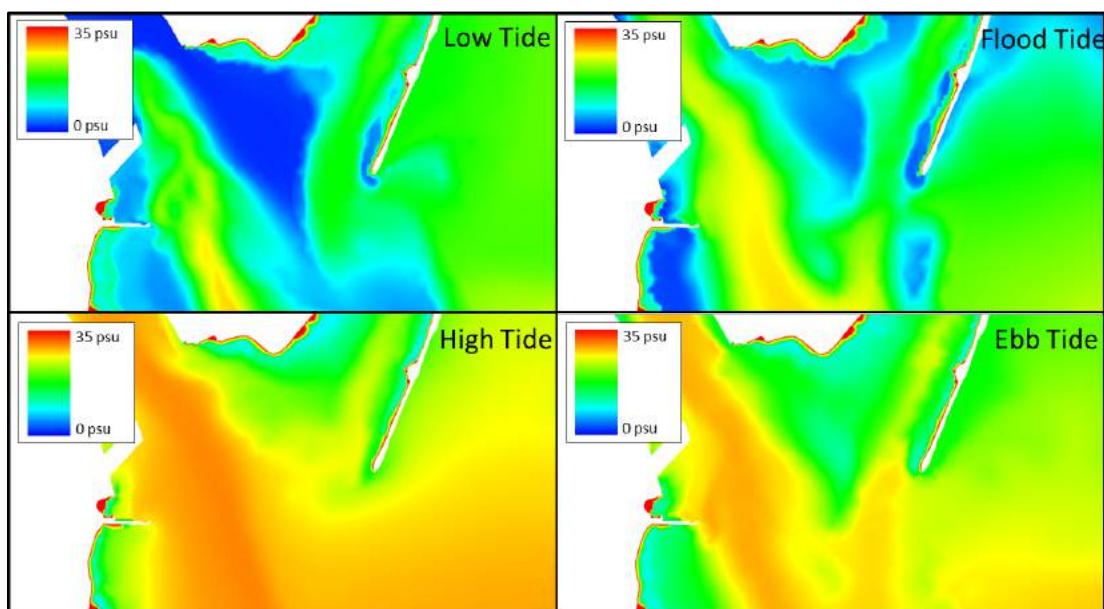


Figure 50 – April 2008 Seabed Salinity Distribution over a Tidal Cycle at Courtney Bay

5.2.2.2. November 2008

The seabed currents over a tidal cycle for November are shown in Figure 51. At low tide the seabed current velocities within Courtney Bay are very weak. Significant flow within the area is constrained to a downstream movement of waters along the eastern side of the Main Harbour Channel. By flood tide the flow direction within the Main Harbour Channel has already changed and waters are now moving upstream. Current velocity magnitudes within Courtney Bay have increased and the around breakwater flow observed only at high tide in April (Figure 47) is already apparent on the flood tide in November indicating a longer period when offshore derived near-seabed waters are entering the channel. A cross channel flow from the Main Harbour Channel over Round

Reef is also visible at flood and high tide. A similar flow regime is observed at the seabed on high tide as April. On the ebb tide, current magnitudes in both the Main Harbour and Courtney Bay channels have decreased.

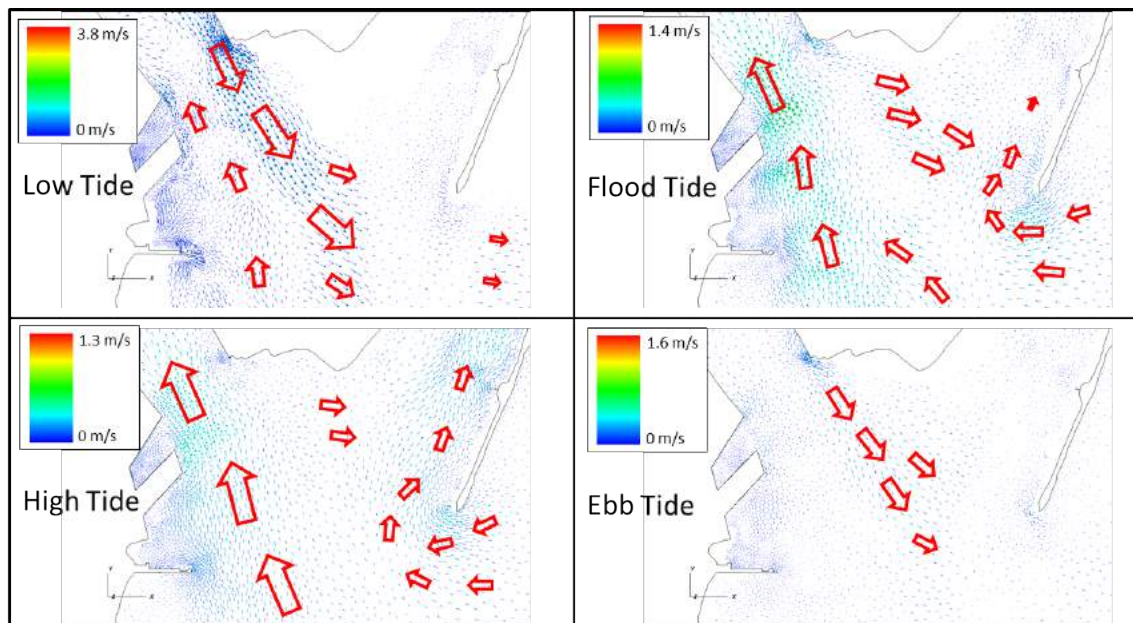


Figure 51 – November 2008 Seabed Current Velocities over a Tidal Cycle at end of Courtney Bay Breakwater

At the surface in November, as shown in Figure 52, the flow conditions are very similar to April (Figure 48). The flow is always downstream for the Main Harbour Channel and the waters moving over the tidal mud flats of Round Reef propagate into Courtney Bay on low and flood tide. At high and ebb tide the downstream flow of the waters of Courtney Bay deflect the waters of the Main Harbour Channel. As the magnitude of the downstream surface currents of the Main Harbour Channel in November are weaker than those of April, the ebbing Courtney Bay waters are able to have a greater influence on the

redirection of those currents and prevent less fresh water from entering the Courtney Channel.

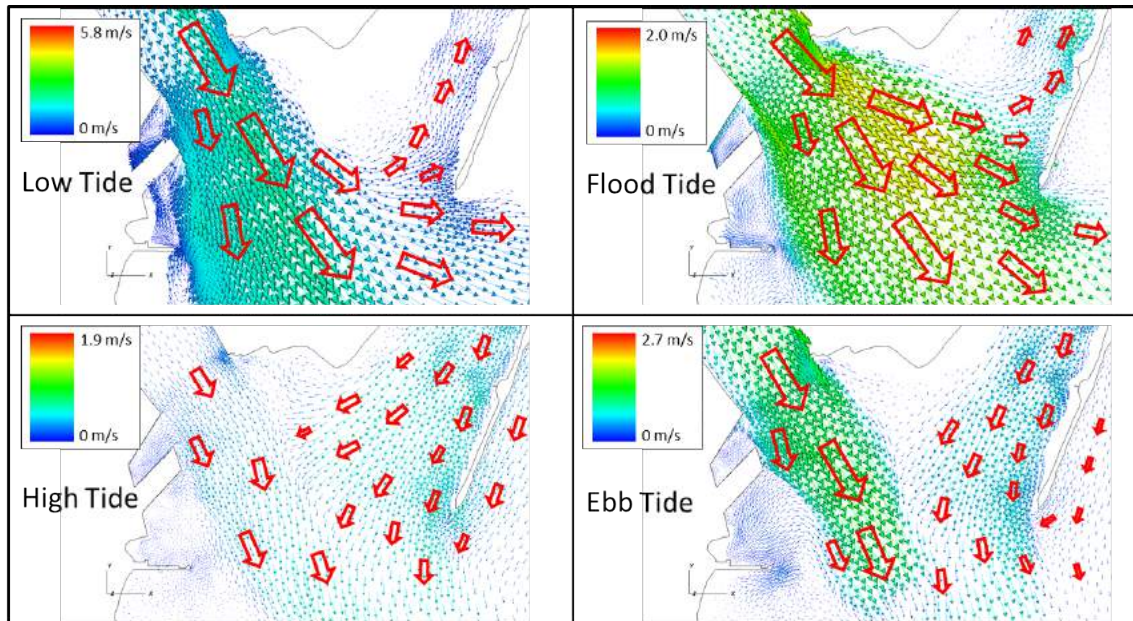


Figure 52 – November 2008 Surface Current Velocities over a Tidal Cycle at end of Courtney Bay Breakwater

The salinity at the seabed is shown for the intersection of the Courtney Bay and Main Harbour Channels in Figure 53. Fresh water is observed over Round Reef at low tide, as was observed previously in April (Figure 50). The salt water then enters the area on the flood tide and remains for the remainder of the tidal cycle.

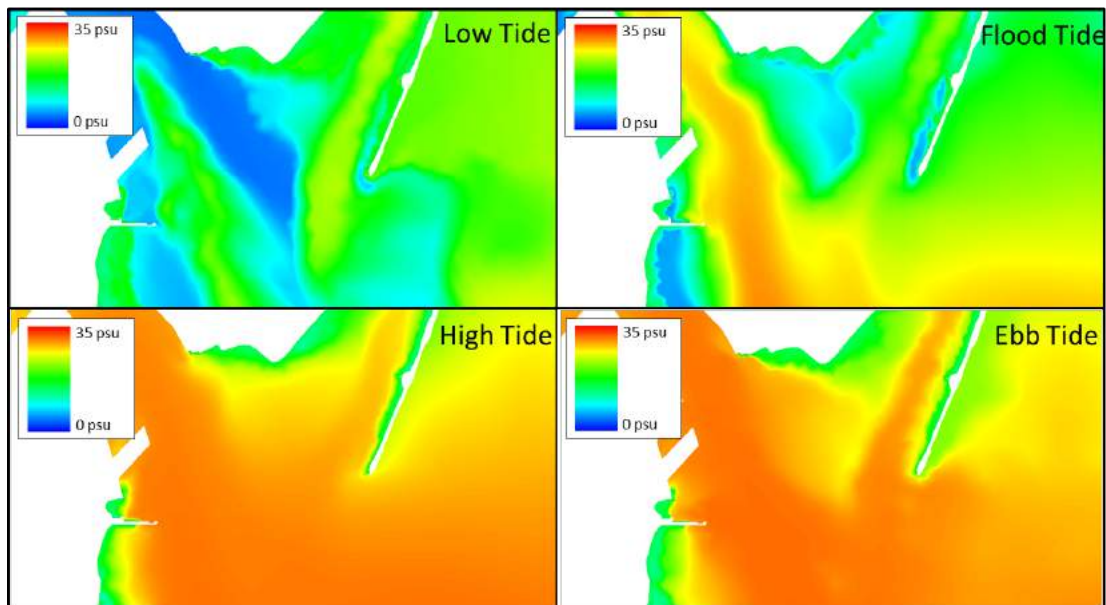
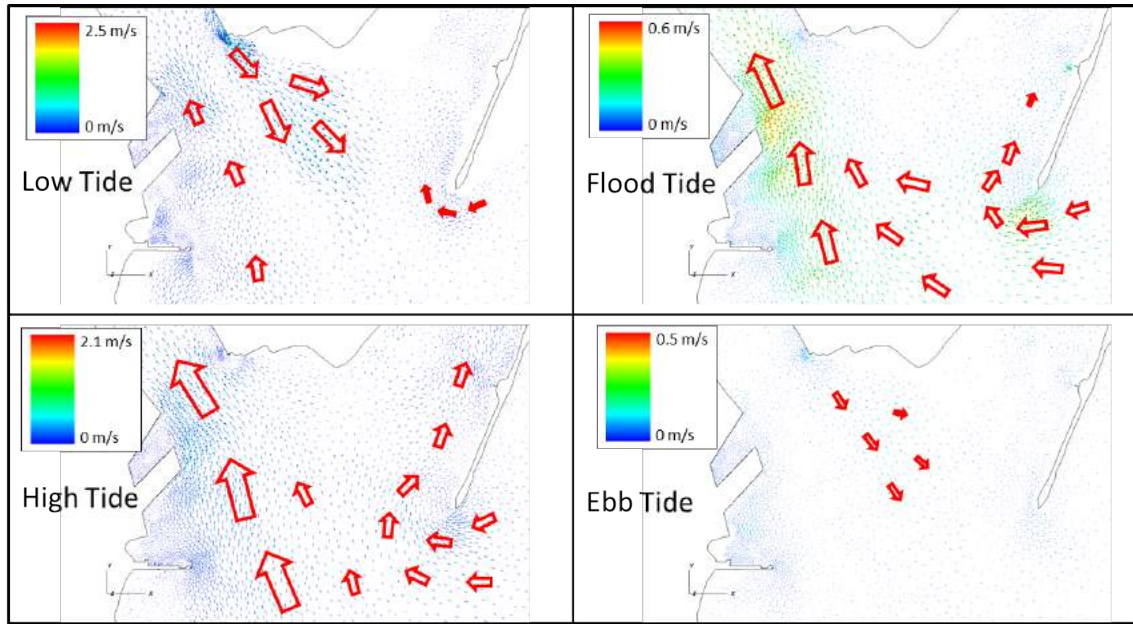


Figure 53 – November 2008 Seabed Salinity Distribution over a Tidal Cycle at Courtney Bay

5.2.2.3. March 2009

As shown in Figure 54, the March seabed current velocities near the intersection of the two channels are very similar to those observed in November (Figure 51). On the flood and high tides the salt wedge propagates into the Courtney Bay channel through a similar circulation pattern around the end of the breakwater as observed in November. Much of the salt water entering Courtney Bay is originating from the intertidal area east of the breakwater. This is particularly important as, during the winter months, storm wave activity will significantly resuspend seabed sediments in the shallows immediately to the east of the breakwater. The majority of water is still passing through the area between the end of the breakwater and Partridge Island continuing into the Main Harbour Channel.



**Figure 54 – March 2009 Seabed Current Velocities over a Tidal Cycle at end of Courtney Bay
Breakwater**

The surface currents for March, as shown in Figure 55, display many similarities to November (Figure 52) in that the waters from the Main Harbour channel are moving over the inter-channel Round Reef area and into Courtney Bay on low and flood tide. The ebb tide also shows that the outflow of Courtney Bay deflects the outflow from the Main Harbour Channel. The primary difference in March is shown during high tide. At this time some of the outflow of Courtney Bay is not limited by the competing flow of the Main Harbour Channel and propagates up into the Main Harbour area.

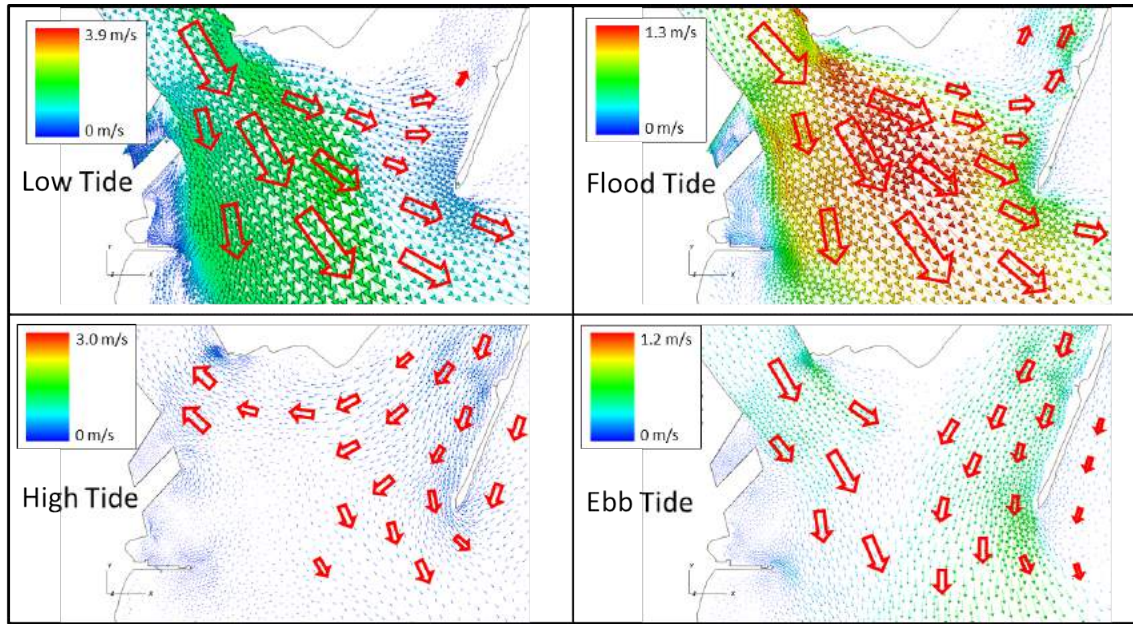


Figure 55 – March 2009 Surface Current Velocities over a Tidal Cycle at end of Courtney Bay Breakwater

The salinity at the seabed is shown for the intersection of the Courtney Bay and Main Harbour Channels in Figure 56. At low tide the highest salinity concentrations follow channels in the bathymetry of the area. As the salt wedge progresses upstream over the tidal cycle, the area gains a near constant seabed salinity value.

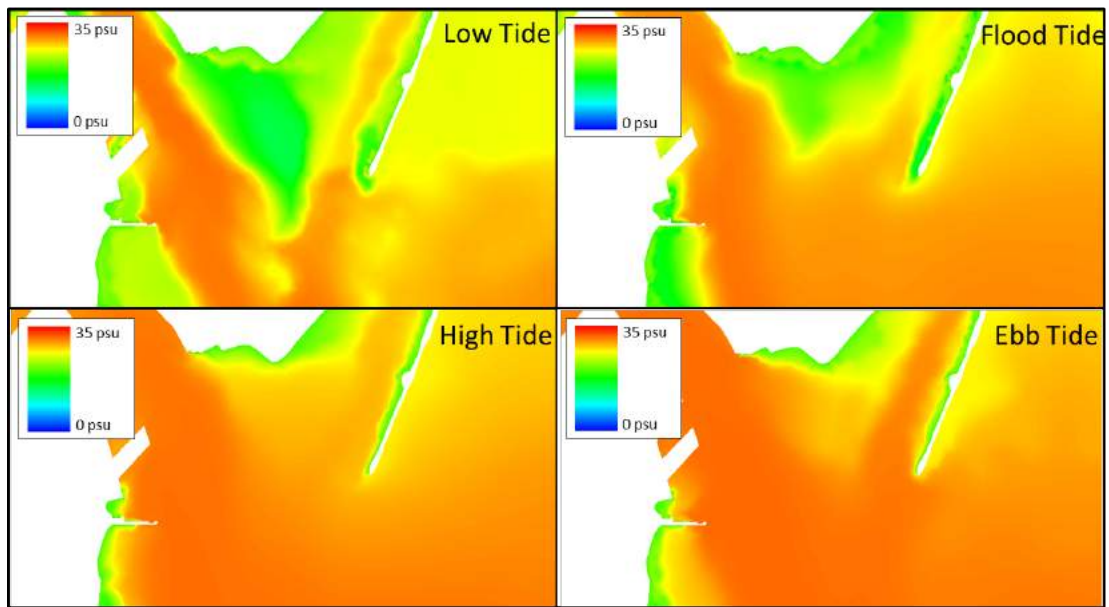
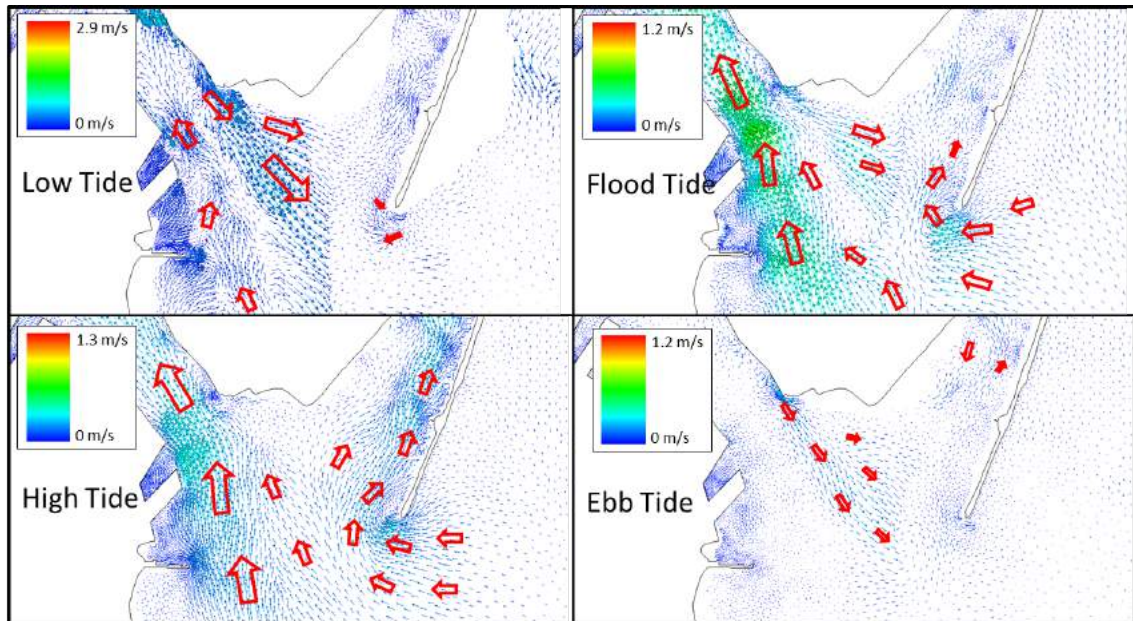


Figure 56 – March 2009 Seabed Salinity Distribution over a Tidal Cycle at Courtney Bay

5.2.2.4. June 2009

The seabed currents for June, as shown in Figure 57, offer a unique circulation pattern over a tidal cycle. Moderately strong current velocities are visible over the Round Reef area at low tide. Along the seabed these current velocities quickly decelerate as they approach the Courtney Bay Channel, which could deposit sediment recently put into suspension from the Main Harbour Channel and the Round Reef. On the flood tide the upstream currents increase in magnitude and the cross channel currents over Round Reef weaken. The current velocities around the end of the breakwater begin to increase. At high tide the inflowing salt wedge decelerates as it approaches Round Reef and likely deposits sediment in the area. Well-defined flow around the end of the Courtney Bay

Breakwater continues on high tide, transporting near seabed waters from offshore into Courtney Bay.



**Figure 57 – June 2009 Seabed Current Velocities over a Tidal Cycle at end of Courtney Bay
Breakwater**

The surface currents, as shown in Figure 58, reveal the influence of the fresh waters of the Main Harbour Channel on Courtney Bay. At low and flood tide the waters of the Main Harbour Channel are able to flood the Courtney Bay Channel. The flow is redirected on high and ebb tide by the ebbing waters of Courtney Bay. Unlike March, the waters of Courtney Bay in June do not flow into the Main Harbour Channel at high tide.

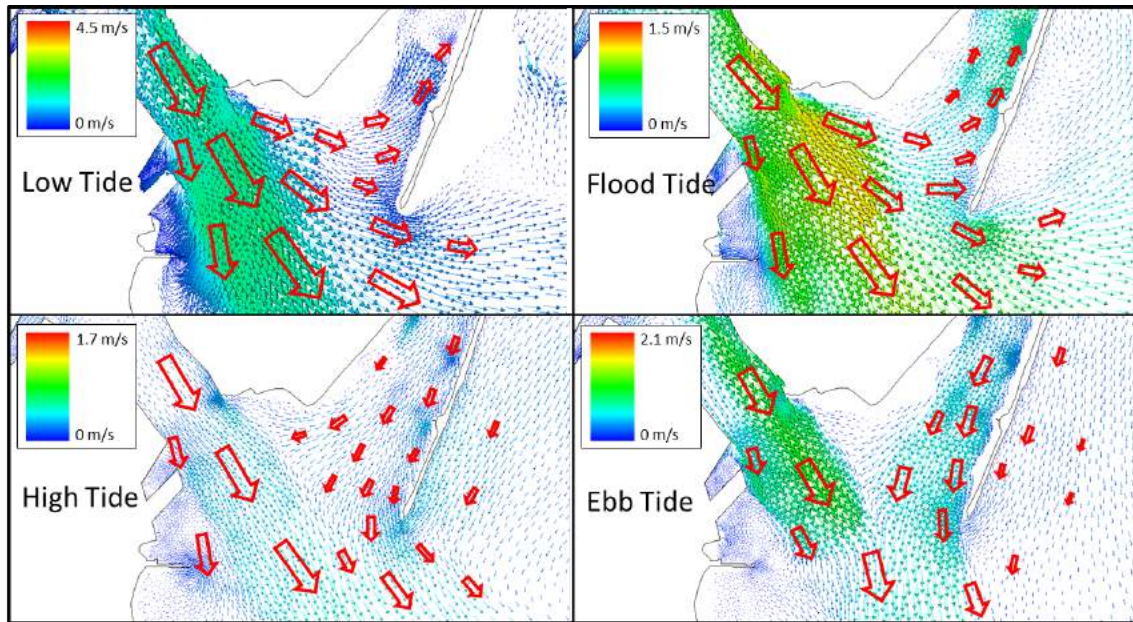


Figure 58 – June 2009 Surface Current Velocities over a Tidal Cycle at end of Courtney Bay Breakwater

The salinity at the seabed is shown for the intersection of the Courtney Bay and Main Harbour Channels in Figure 59. In June the fresh water interaction with Round Reef is maintained for low and flood tide before being displaced by the incoming salt wedge. As observed at other periods, the salinity concentration correlates to the bathymetry.

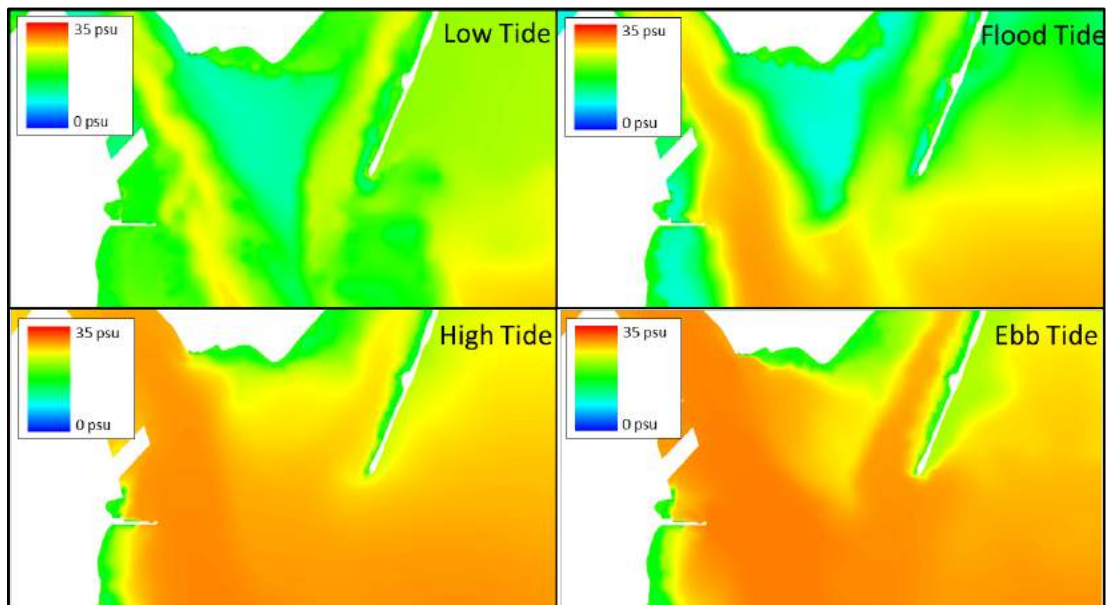


Figure 59 – June 2009 Seabed Salinity Distribution over a Tidal Cycle at Courtney Bay

5.2.3. Salt Wedge Residency in Courtney Turning Basin

As mentioned previously in section 5.1, a plug of salt water is abandoned in the Turning Basin of Courtney Bay at low tide. This phenomenon is present at all times of the year, but there are annual variations in its extent. The model salinity field is able to reproduce the zone of saline waters in the Turning Basin and augments the observations through enabling analysis of its lateral extent. Understanding the extent of the saline waters is important as the salt water in Courtney Bay carries much of the suspended sediment, as discussed in Toodesh (2012), Melanson (2012) and below in section 5.3. By being left orphaned, without any bed shear stress, that sediment is most likely to settle out of suspension. March is a particularly significant simulation period as Melanson (2012)

noted that the incoming salt water holds especially high suspended sediment load during winter storm activity.

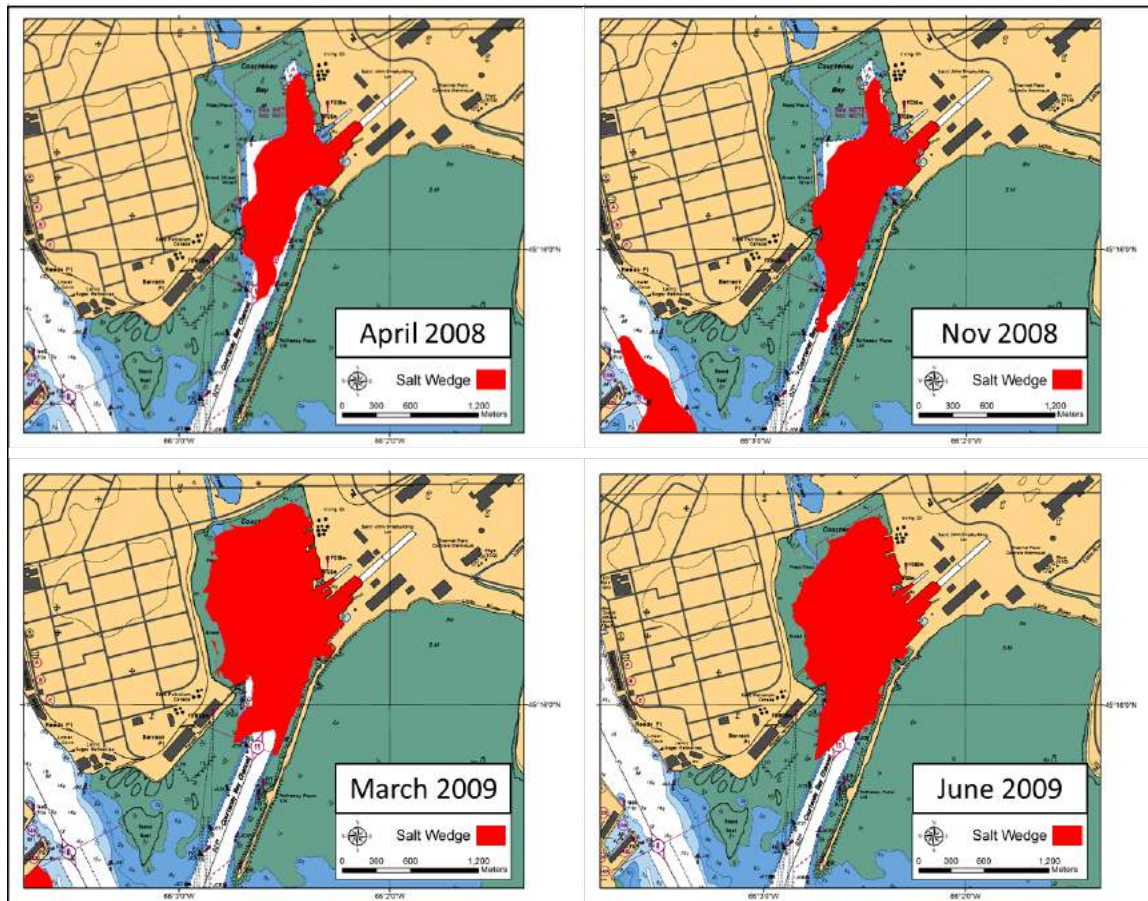


Figure 60 – Salt Wedge Distribution in Courtney Bay Turning Basin at Low Tide

Figure 60 displays the annual variations in the low tide extent of the orphaned zone of saline water in the Courtney Bay Turning Basin. The salt wedge is defined for display purposes as waters with a salinity of greater than 20 psu. The extent of the salt wedge is similar for March and June and for November and April with the primary variation being the lateral extent of the salt water coverage over the shallow regions of the Turning

Basin. The orphan salt wedge extent is maximized during the low river discharge periods and the potential for deposition of sediment in Courtney Bay will be greatest at these low river discharge times.

5.3. Optical Backscatter Observation Overview

The existing hydrodynamic model does not inherently predict suspended sediment load associated with the water mass however optical backscatter observation profiles, which provide an estimate of suspended sediment, were provided for the Main Harbour Channel and Courtney Bay in Toodesh (2012). The profiles were measured for the April, November and March observational periods, but are missing for June due to a sensor malfunction. The figures in Toodesh (2012) lacked detail and have thus been reproduced with greater scale, magnification and contours within this section. Profiles for the three observational periods are provided at low, flood, high and ebb tide in units of suspended sediment. Additionally, a cross-plot of suspended sediment against salinity has been generated to show the correlation between suspended sediment loads and the water mass.

Determining the location and source of the suspended sediments in the physical observations are essential components to understanding the sedimentation of the harbour. With observations alone, the importance of lateral variations in current velocities on the sources of the observed sediment concentrations cannot be established, especially within Courtney Bay where there were no suitable ADCP observations. The model allows for an

improved understanding of the cross channel flows which affect the movement of sediment in the harbour. Notably the model current velocity output described in Section 5.2 indicates that the Courtney Bay sediment sources are primarily lateral contributions either across Round Reef or around the end of the breakwater. Therefore a more detailed view of the distribution of the suspended sediment is required and is presented below.

5.3.1. April 2008

Four representative optical backscatter sections for the Main Harbour Channel in April over a tidal cycle are shown in Figure 61. At low tide the optical backscatter shows high levels of suspended sediment throughout the watercolumn. The highest concentration of optical backscatter is shown in the fresh waters, with values ranging from 40 to 60 mg/l, while the values decrease through the mixed waters to a minimum value of 20 mg/l near 30 psu. This represents the highest levels of freshwater optical backscatter observed throughout the year. At the harbour entrance lower levels of suspended sediment are visible. On the flood tide the optical backscatter is observed to be highest in the salt wedge and decreasing in the surface waters. At high tide the optical backscatter levels have decreased overall in the salt wedge but a higher concentration of suspended sediment is visible at the head of the salt wedge, forming a turbidity maximum [Dyer, K. R., 1997]. The salt wedge on the ebb tide now has a reduced level of suspended sediment, as the optical backscatter values have decreased throughout the entire water column.

This turbidity maximum visible at high tide is the result of both the resuspension of sediments by the incoming salt wedge and flocculation of river borne particles as they come in contact with waters of elevated salinity. Suspended clay particles present in the fresh river water meet the incoming salt wedge along the halocline and the increase in salinity causes the clay particles to flocculate [Eisma, 1986]. The increased size of the flocs causes them to deposit into the salt water layer which is flowing upstream due to entrainment. The general upstream flow of salt water directs the suspended sediment into the nose of the salt wedge.

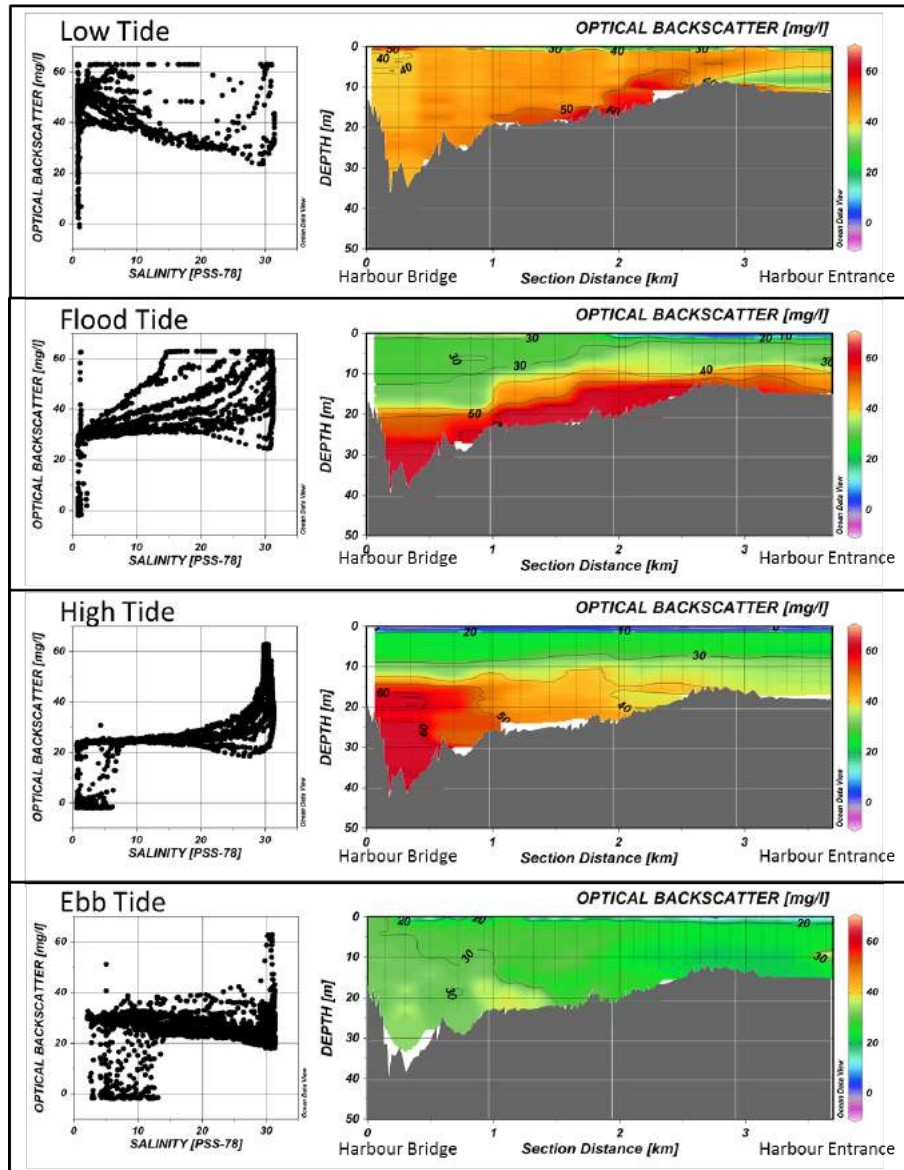


Figure 61 – April 2008 Optical Backscatter Profiles from Main Harbour Channel

The Courtney Bay channel section stretches from the intersection with the Main Harbour Channel to the Turning Basin as shown in Figure 13. Optical backscatter for April 2008 are plotted along this section in Figure 62. At low tide within the Courtney Bay Channel section for April, the optical backscatter is highest at the intersection with the Main

Harbour channel. This area is past the end of the breakwater in the fresh waters crossing the mouth of the Courtney Bay Channel. The area of high optical backscatter can be explained through examination of the seabed and surface currents velocities from section 5.2.2.1 (Figure 47 and Figure 48). Both the surface and seabed waters are originating from the Main Harbour Channel at this stage of the tide. On the flood tide high optical backscatter values are propagating into the channel in two distinct areas. As was observed in the Main Harbour channel, the intruding salt wedge contains high levels of suspended sediment, but it remains outside the breakwater while areas of elevated optical backscatter appear in the fresh surface waters within Courtney Channel. As the flood tide continues, after the maximum rate of flood, more salt water is being pushed into the channel and it is carrying high levels of suspended sediment. The concentration of suspended sediment in the fresh surface layer, that was apparent at the beginning of the flood, is decreasing over time, but the area remains clearly separated from the sediment rich lower saline waters. At high tide the optical backscatter profile shows relatively low values throughout the channel, with the exception of near the seabed in the Turning Basin and at the end of the breakwater. In examination of the model current velocity data at this stage of the tide, as shown previously in section 5.2.2.1, strong currents can be observed at the seabed entering Courtney Channel from around the end of the breakwater which explains the anomalous region of suspended sediment. On the ebb tide, the area of elevated optical backscatter at the end of the breakwater has grown in size and concentration. As shown in section 5.2.2.1, the near seabed currents which originate from around the end of the breakwater are at their maximum magnitudes between high and ebb tide.

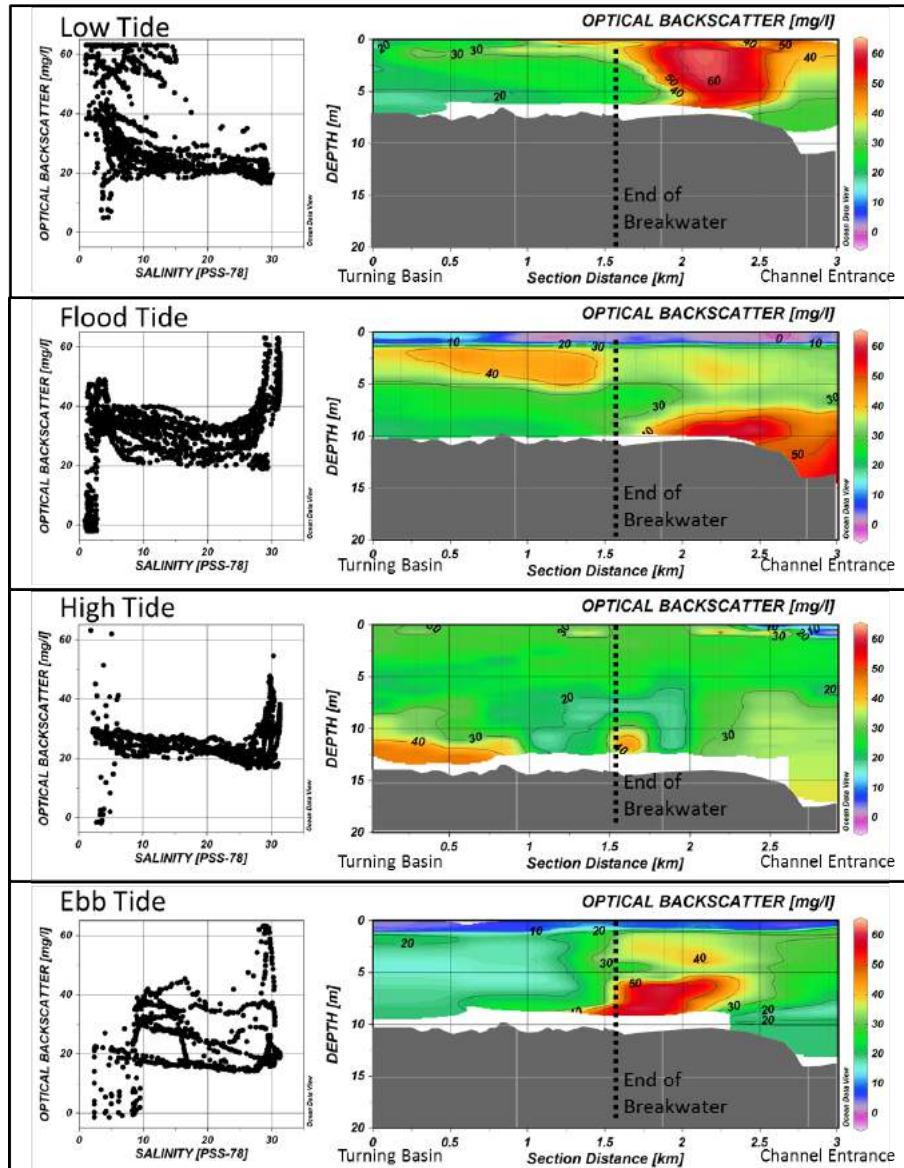


Figure 62 – April 2008 Optical Backscatter Profiles from Courtney Bay Channel

5.3.2. November 2008

The optical backscatter sections for November over a tidal cycle are shown in Figure 63 for the Main Harbour Channel section, as described by Figure 13. At low tide, an area of low optical backscatter is visible under the Harbour Bridge and optical backscatter levels generally correlate well with salinity based on the plot of optical backscatter and salinity in Figure 63. On the flood tide the optical backscatter is predominantly low in the freshwater layer but high in the nose of the salt wedge (Figure 16), similar to conditions observed on the flood tide in April. Near the channel entrance the values appear low, but likely the optical backscatter probe on the MVP instrument could not get close enough to the seabed to sample the suspended sediment. As the flood continues the optical backscatter decreases in the channel downstream of the harbour bridge as the salt wedge continues to propagate into the estuary. As will be discussed in Section 5.4, the area of elevated optical backscatter follows the nose of the salt wedge and has propagated upstream of the Main Harbour bridge. At high tide the optical backscatter levels are decreasing downstream of the Main Harbour bridge as the sediments are being brought in with the turbidity maximum in the salt wedge towards to the Reversing Falls, similar to observations in April. On the ebb tide, the optical backscatter values have decreased throughout the channel, although the section still contains predominantly salt water, as discussed previously in section 5.1.

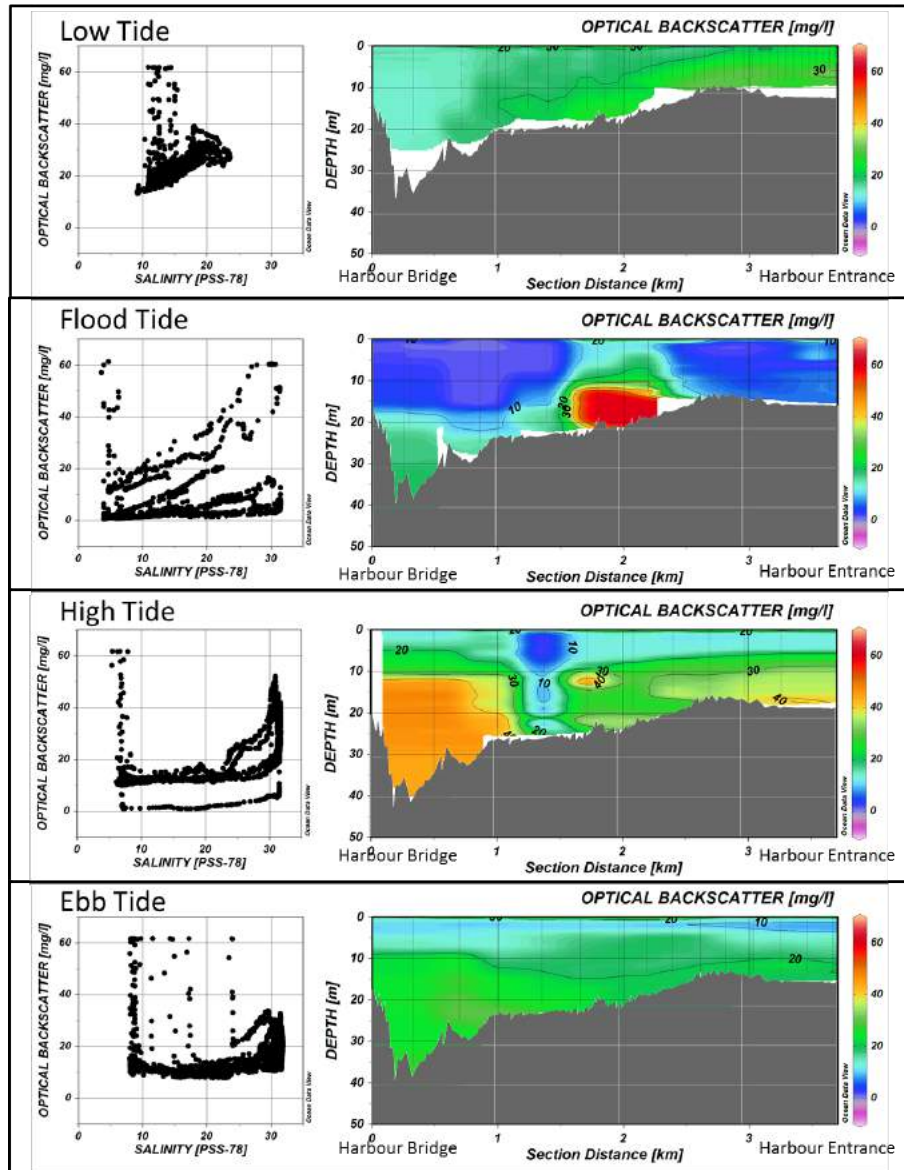


Figure 63 – November 2008 Optical Backscatter Profiles from Main Harbour Channel

At low tide within the Courtney Bay Channel section for November, shown in Figure 64, moderate optical backscatter values exist throughout the water column, with levels decreasing towards the seabed, correlating with the presence of salt water (Figure 24). This shows that there are higher concentrations of suspended sediment in the fresh water

than salt water at this time. Within the Turning Basin area at the surface a very thin layer of high optical backscatter is visible, which may correlate to sediment in the buoyant freshwater output of Marsh Creek. Two distinct areas of high optical backscatter exist within the channel on the flood tide, one within the breakwater and the other at the intersection of the Main Harbour channel. The area of high optical backscatter within the breakwater does not correlate with the salinity distribution.

Examination of the model output for the November simulation in section 5.2.2.2 (Figure 51 and Figure 52) at the same stage of flood tide as the observations in Figure 64 reveals the source of the two areas of high optical backscatter. The surface waters are still propagating downstream and are passing over the shallow reef between the two channels leading to the area of elevated optical backscatter to the left of the end of the breakwater in Figure 64. At the seabed the incoming salt waters are originating from around the end of the breakwater and producing the area of elevated optical backscatter to the right of the end of the breakwater near the seabed in Figure 64.

At high tide, there are multiple areas of high concentrations of suspended sediment in the channel, as shown in Figure 64. One area is within the breakwater, on the left side of the limit of the breakwater in Figure 64, and one is outside of the end of the breakwater.

Examination of the model current velocities at the seabed at high tide (Figure 51) reveals that the bottom waters are propagating into the channel from around the end of the breakwater. This bottom water is likely also the source of the areas of high suspended sediment shown in the channel.

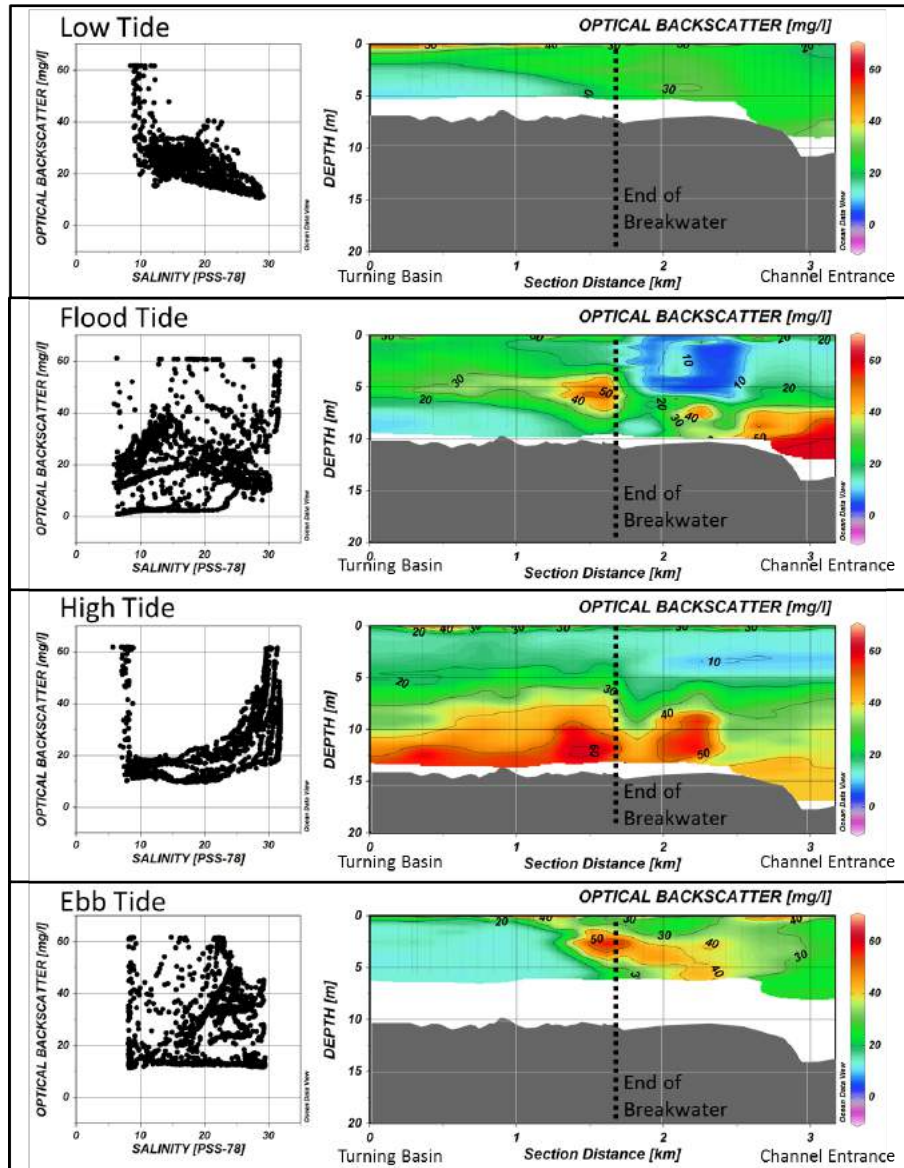


Figure 64 – November 2008 Optical Backscatter Profiles from Courtney Bay Channel

During the ebb tide, the optical backscatter values decrease in the channel suggesting that the suspended sediment has deposited. On the ebb tide, as shown in Figure 64, a plug of high optical backscatter becomes apparent near the surface just to the left of the end of the breakwater in the section. Optical backscatter levels are moderately elevated

throughout the waters downstream of the end of the breakwater. Examination of the model surface current data (Figure 52) reveals the source of the area of high optical backscatter inside the breakwater to be the waters flowing out of Courtney Bay.

5.3.3. March 2009

At low tide the optical backscatter section for the Main Harbour Channel in Figure 65 displays low values overall, with very low values in the mixed surface waters. At flood tide high optical backscatter levels are present in the nose of the salt wedge (Figure 18), but very low values are present in the upper layer. The area of high optical backscatter advances further upstream with the salt wedge in the form of a turbidity maximum as the flood tide continues. At high tide the optical backscatter levels have decreased overall in the observed section as the nose of the salt wedge has propagated upstream of the Harbour Bridge, but levels can still be observed to increase towards the seabed. On the ebb tide the optical backscatter values have lowered slightly from levels observed at high tide throughout the channel.

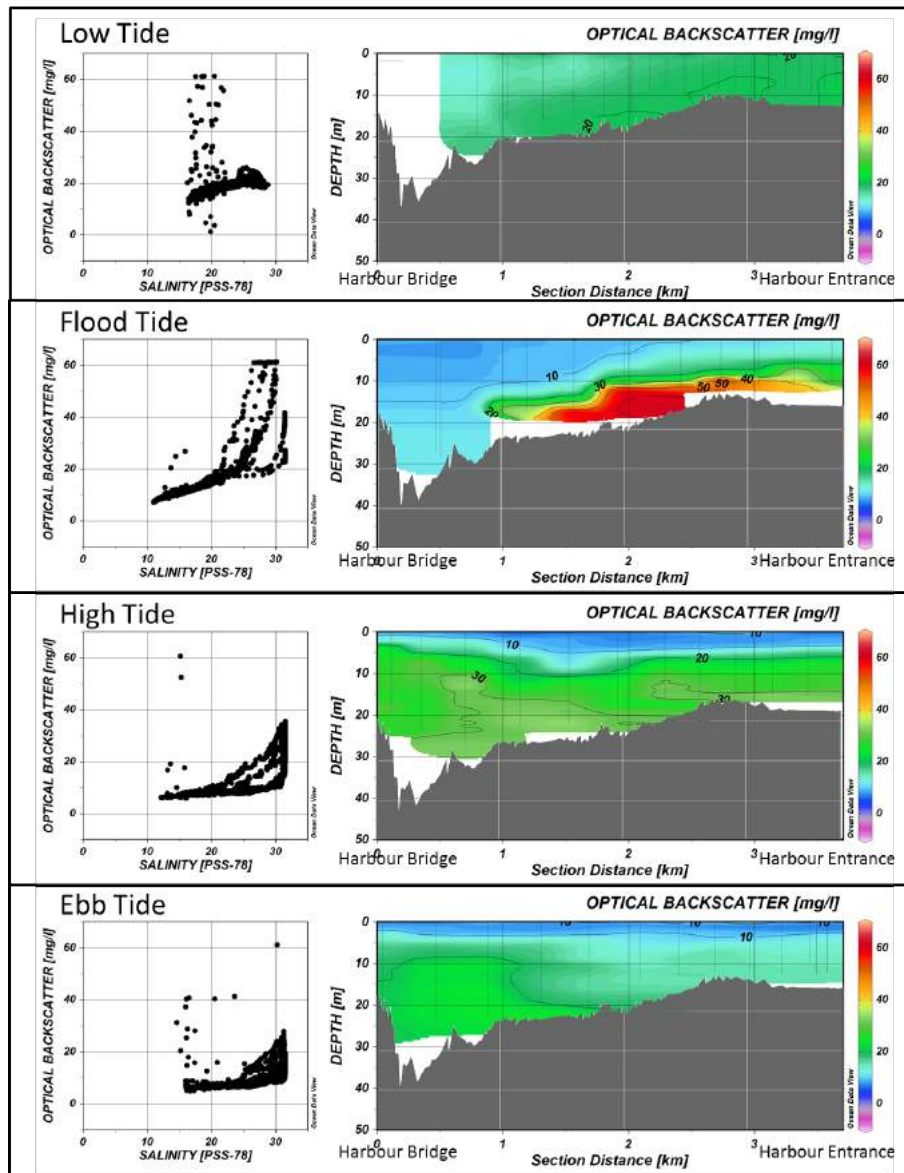


Figure 65 – March 2009 Optical Backscatter Profiles from Main Harbour Channel

At low tide within the Courtney Bay Channel section for March, as shown in Figure 66, an area of elevated optical backscatter is only visible downstream of the breakwater near the intersection of the Main Harbour Channel. The section within the channel upstream of the breakwater contains near uniform low values.

During the flood tide two areas of high optical backscatter values are apparent at the entrance of the Courtney Bay channel (Figure 66). The high optical backscatter area is not directly correlated to the salinity in the form of a turbidity maximum, but is contained predominantly below the halocline (Figure 26). Examination of the current velocities from the March model simulation data (Figure 54) reveals the source of the area of elevated optical backscatter. On the flood tide there are strong currents near the seabed propagating both around the end of the Courtney Bay breakwater and across the mouth of the Courtney Bay channel into the Main Harbour. The anomalous areas of elevated optical backscatter correspond to these two areas of near seabed currents. Further into the channel, near the Turning Basin, optical backscatter values are low near the seabed, but elevated near the surface in the mixed layer. This anomalous area could result from suspended sediment input from Marsh Creek or wave driven resuspension of sediments within the tidal flats.

At high tide the two areas of elevated optical backscatter appear to have propagated further up the channel towards the Turning Basin. This corresponds to the model output at this time, which shows that seabed currents are pushing waters up the channel. The distribution of optical backscatter values roughly correlates with the salinity distribution shown in Figure 26.

On the ebb tide the area of elevated suspended sediment that was propagating up the channel is now gone and has likely settled to the seabed. The area at the intersection of

the Main Harbour channel and Courtney Bay channel contains moderately elevated levels of suspended sediment. This anomaly is a remnant of the incoming salt wedge whose velocities are decreasing on the ebb tide (Figure 54).

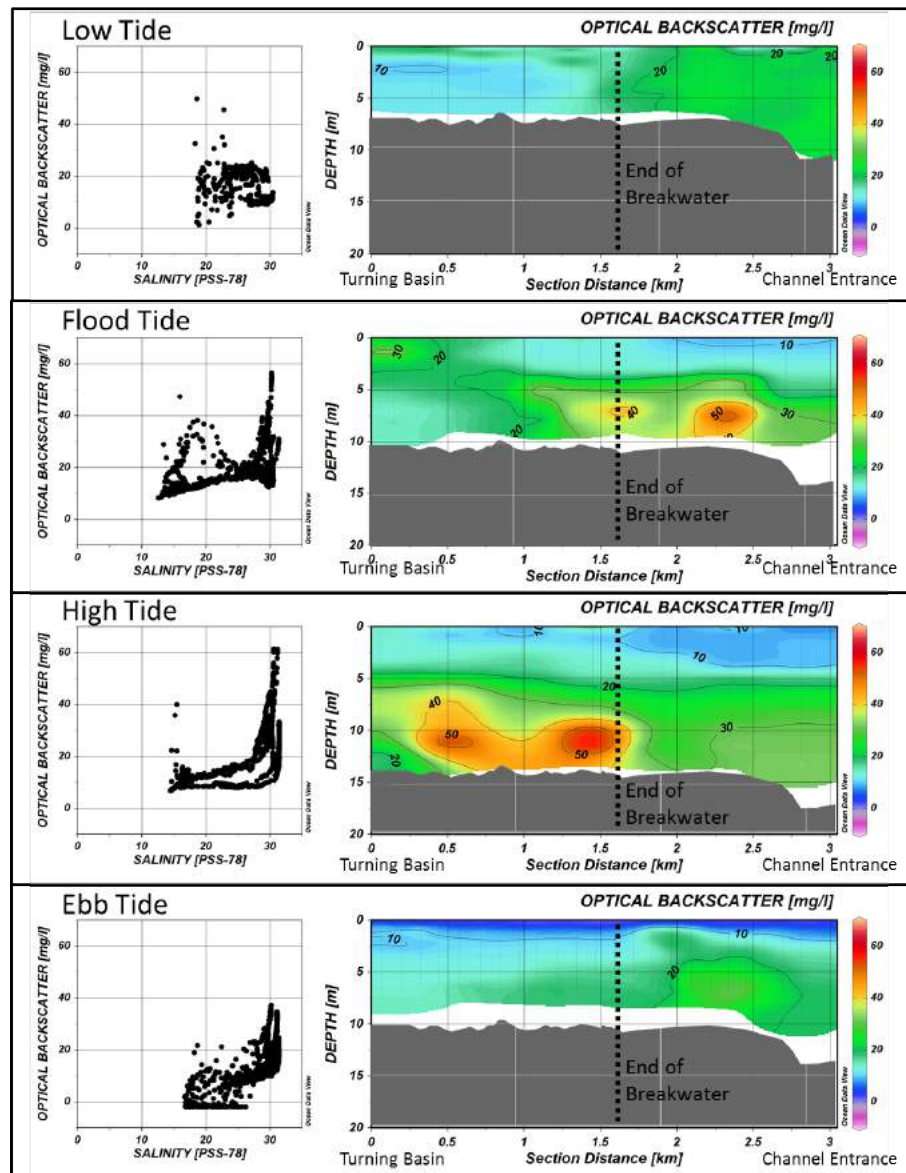


Figure 66 – March 2009 Optical Backscatter Profiles from Courtney Bay Channel

5.4. Estuarine Circulation and Optical Backscatter Upstream of Harbour Bridge

The physical oceanographic sections described in Toodesh (2012) covered only the waters of the Main Harbour Channel downstream of the Harbour Bridge, as shown in Figure 13. Additional observations however, from the Heron, were taken at that time upstream of the Harbour Bridge whenever conditions allowed for safe navigation. These are presented here for the first time. Due to the strong currents, this area was transited only during times of slack water, the timing of which depended on the tidal and river elevations. With the limited observations alone, the circulation of this section of the estuary could not be fully described. The model output however, allows for the estuarine circulation above the Harbour Bridge to be described for periods when observations are not possible. Thus further insights, impossible to obtain by physical observation, can be made.

5.4.1. April 2008

April corresponds to the time of the spring freshet, when river discharge is maximized. Due to the elevated river levels, the salt wedge is pushed further downstream in the harbour relative to average conditions. Above the harbour bridge, at both low and flood tide, the salt wedge is never present, as shown in the model profile of Figure 67. The salinity profile corresponds to the section between the Harbour Bridge (right hand side of the figure) and the Reversing Falls sill (left hand side of the figure).

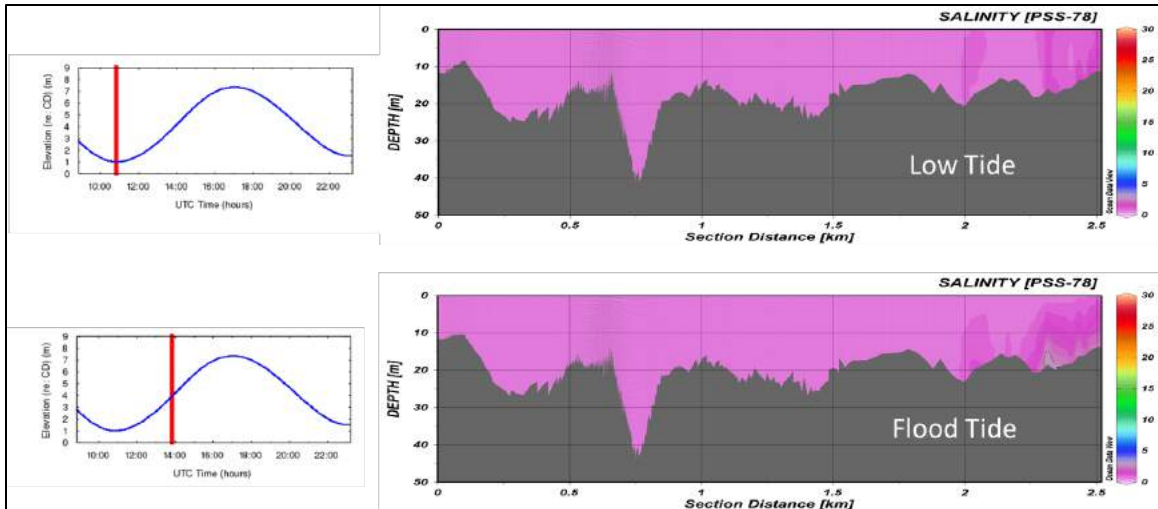


Figure 67 – April 2008 Model Salinity Output Upstream of Harbour Bridge at Low and Flood Tide.

Section begins at the Reversing Falls sill and terminates at the Harbour Bridge.

At high tide the Main Harbour Channel between the Harbour Bridge and the Reversing Falls is heavily stratified with fresh water overlaying the salt wedge throughout the estuary, as shown in Figure 68. The optical backscatter indicates that the suspended sediment concentrations are almost perfectly correlated with the salinity distribution and are highest in the salt wedge, up to 60 mg/l, and around 20 mg/l in the freshwater layer. Within a few metres of the surface, the optical backscatter indicates very low sediment concentration, of approximately 10 mg/l, which does not correlate with a change in salinity. The acoustic backscatter shows a clear and narrow impedance contrast between the fresh and saltwater layers. Within the upper freshwater layer, the acoustic backscatter also shows a contrast in impedance which divides the layer. This upper interface does not correlate with any of the measured variables (Temperature, Salinity and Velocity), but could be related to the low optical backscatter observed near the surface.

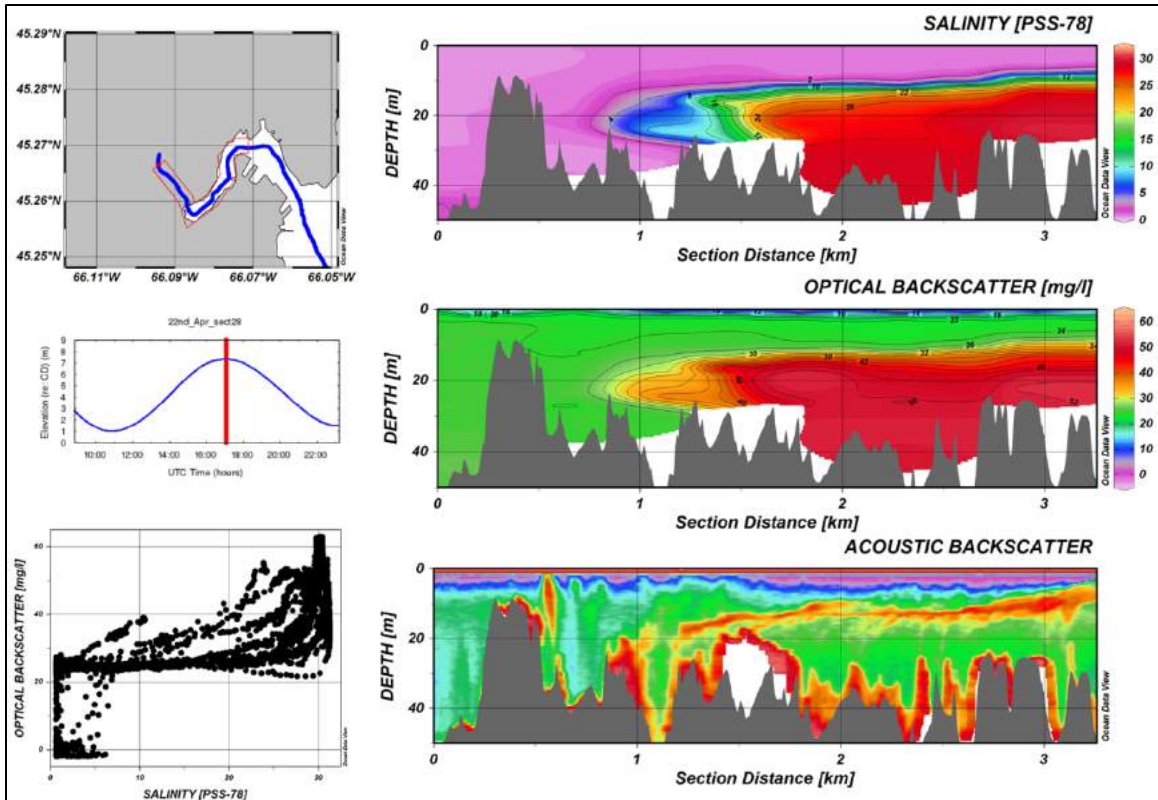


Figure 68 – April 2008 Oceanographic Observations Upstream of Harbour Bridge at High Tide.

Section begins at the Reversing Falls sill and terminates at the Harbour Bridge.

As the tide passes high tide and begins to ebb, the salt wedge reaches the Reversing Falls, but is not able to propagate past the sill to continue further upstream. This time period is represented by the observational profile in Figure 69, but as there are data missing in the vicinity of the falls, the same time period is represented by the model output profile in Figure 70 and plan view of the salt wedge in Figure 71. The combination of fresh water discharge from the river and the bathymetric restriction of the Reversing Falls halt the salt wedge from progressing further upstream.

On the start of the ebb tide, the observational profile in Figure 69 shows that the salt water begins to mix with the upper fresh layer water, although there is still a strong salinity gradient between the layers. The optical backscatter in the salt wedge indicates the presence of significantly lower values of suspended sediment than observed at high tide. As sediment concentrations in the fresh surface waters have not increased, this implies that the sediment has likely settled into the deep channel between the Reversing Falls and the Harbour Bridge. The acoustic backscatter indicates that there is mixing between the salt and fresh waters as the turbulent area of high impedance contrast is thickening.

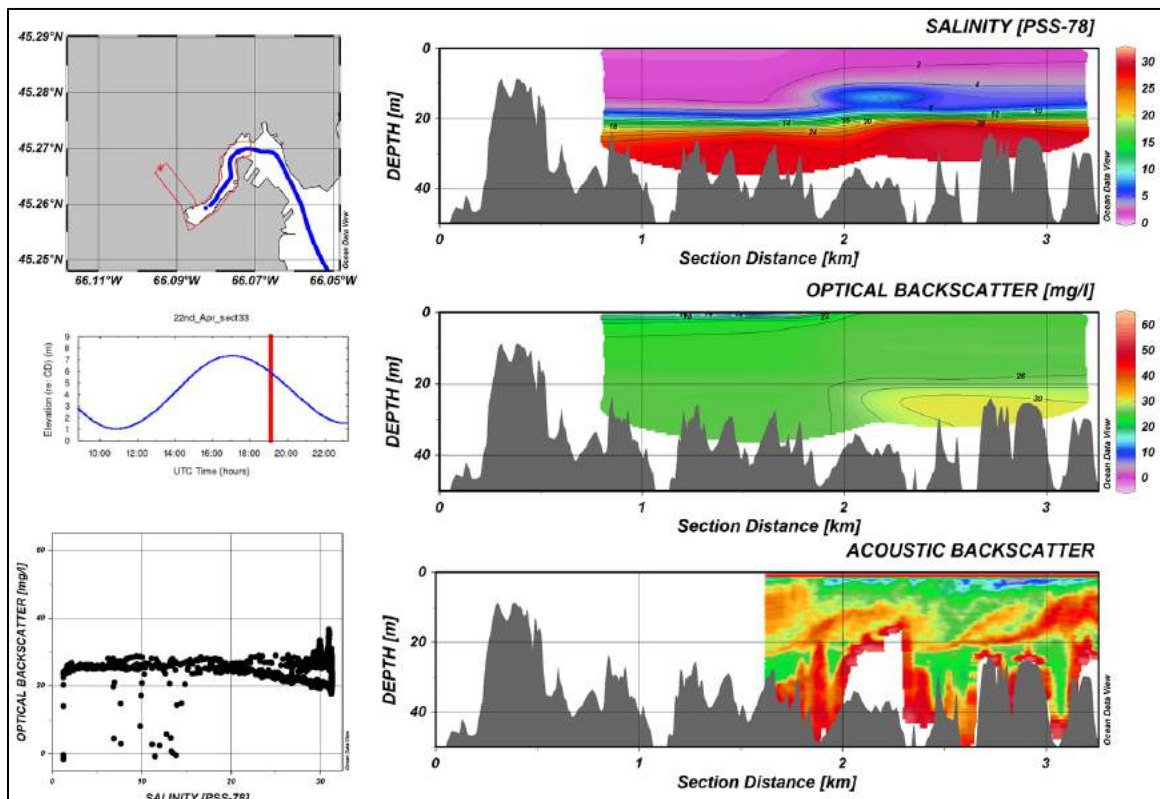


Figure 69 – April 2008 Oceanographic Observations Upstream of Harbour Bridge at the start of the Ebb Tide. Section begins at the Reversing Falls sill and terminates at the Harbour Bridge.

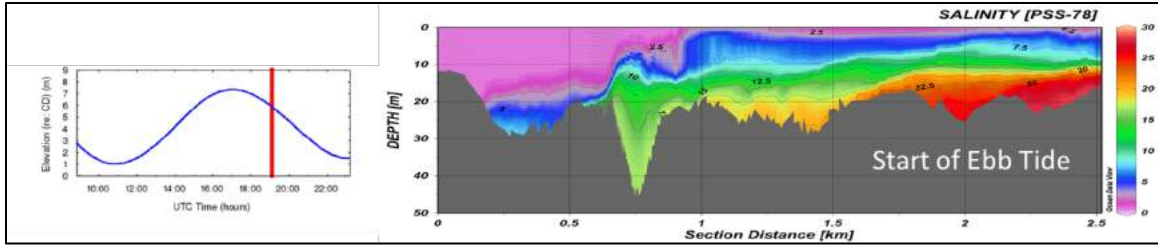


Figure 70 – April 2008 Model Salinity Output Upstream of Harbour Bridge at the Start of Ebb Tide.

Section begins at the Reversing Falls sill and terminates at the Harbour Bridge.

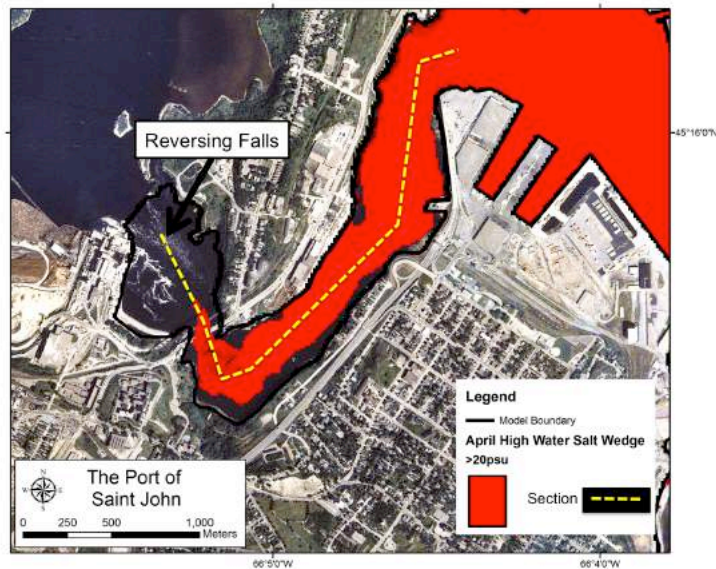


Figure 71 – April 2008 Modelled Salt Wedge at High Tide at Reversing Falls

On the ebb tide, the fresh water output from the river pushes the salt wedge further downstream below the harbour bridge and the area upstream of the bridge is composed of entirely fresh water. The model output at this stage of the tide is shown in Figure 72.

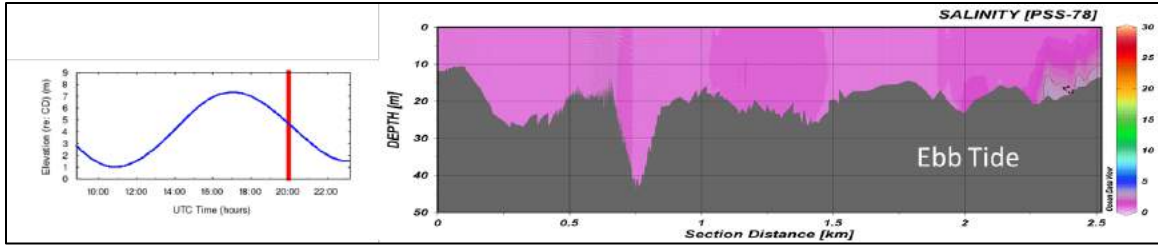


Figure 72 – April 2008 Model Salinity Output Upstream of Harbour Bridge on Ebb Tide. Section begins at the Reversing Falls sill and terminates at the Harbour Bridge.

5.4.2. November 2008

For the November 2008 time period, the model reveals that the salt wedge has not penetrated beyond the harbour bridge on the flood tide, as shown in Figure 73. Similar to the low and flood tide sections for April, the waters between the Reversing Falls and the Harbour Bridge are entirely fresh.

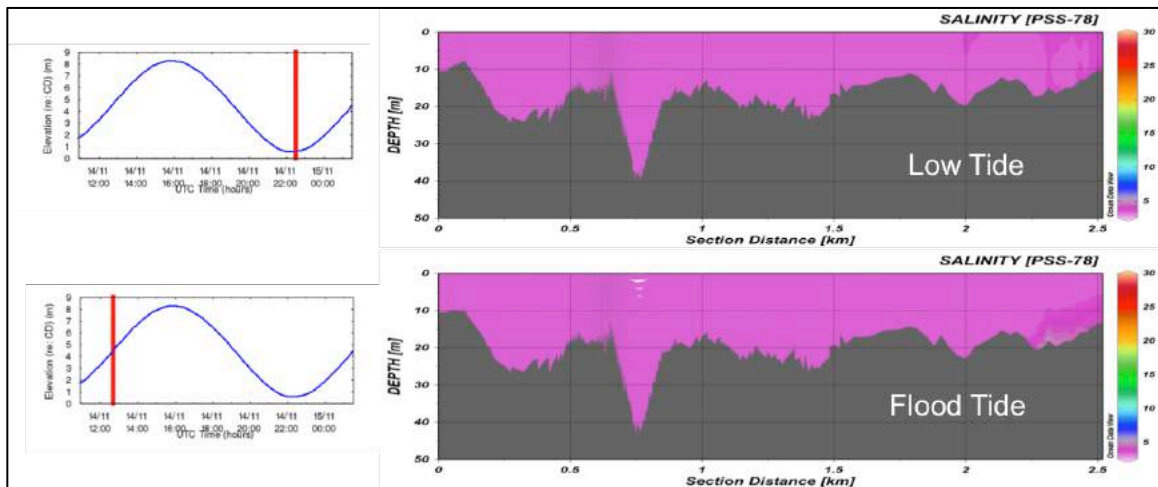


Figure 73 – November 2008 Model Salinity Output Upstream of Harbour Bridge at Low and Flood Tide. Section begins at the Reversing Falls sill and terminates at the Harbour Bridge.

At the end of the flood tide, as shown with observational data in Figure 74, the salt wedge has now propagated up towards the Reversing Falls. The halocline is observed near the surface with fresh waters flowing over the salt wedge down through the harbour. The optical backscatter shows high levels of suspended sediment in the salt wedge and weak levels in the fresh water coming through the reversing falls. The interface between the salt and fresh water layers is less clearly defined in the acoustic backscatter, likely due to the low gradient of the halocline, but mixing is apparent along the interface.

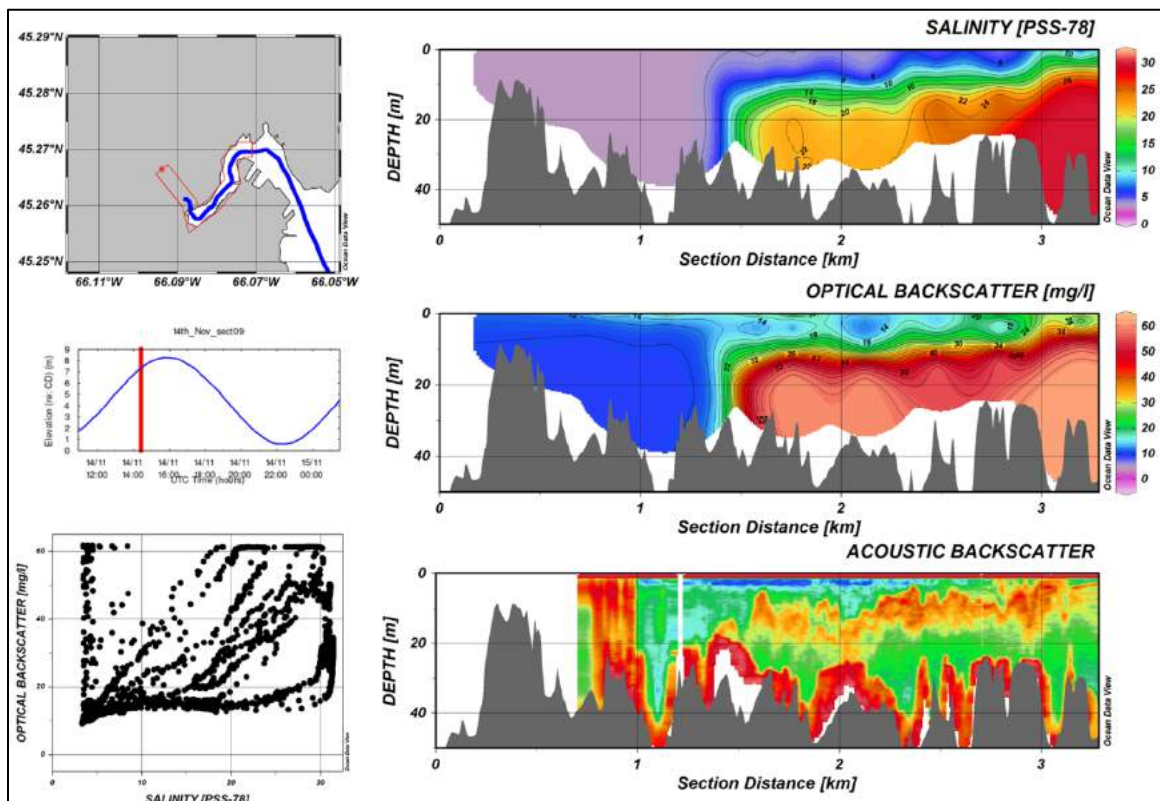


Figure 74 – November 2008 Oceanographic Observations Upstream of Harbour Bridge at end of Flood Tide. Section begins at the Reversing Falls sill and terminates at the Harbour Bridge.

The model provides missing information on the estuarine circulation at high tide and the start of the ebb tide, as shown in Figure 75. Within this time period the salt water continues to advance upstream and, unlike in April, propagates over the Reversing Falls. At high tide a fresh surface layer is visible in the profile, which thins at the start of the ebb tide.

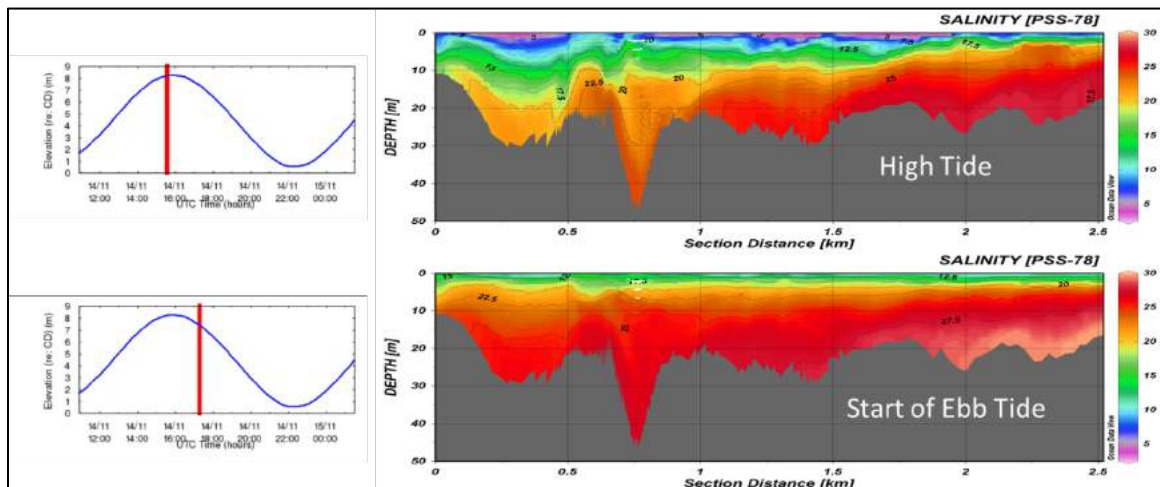


Figure 75 – November 2008 Model Salinity Output Upstream of Harbour Bridge at High Tide and the Start of Ebb Tide. Section begins at the Reversing Falls sill and terminates at the Harbour Bridge.

On the ebb tide, as shown in Figure 76, the salt wedge is pushed towards the surface of the water column and there is little stratification. The optical backscatter has decreased in the channel compared to the levels observed on the flood tide, suggesting deposition of suspended sediment in the deep channel during slack water as observed previously in April. The acoustic backscatter shows that the magnitude of the turbulence has decreased but is still present along the halocline.

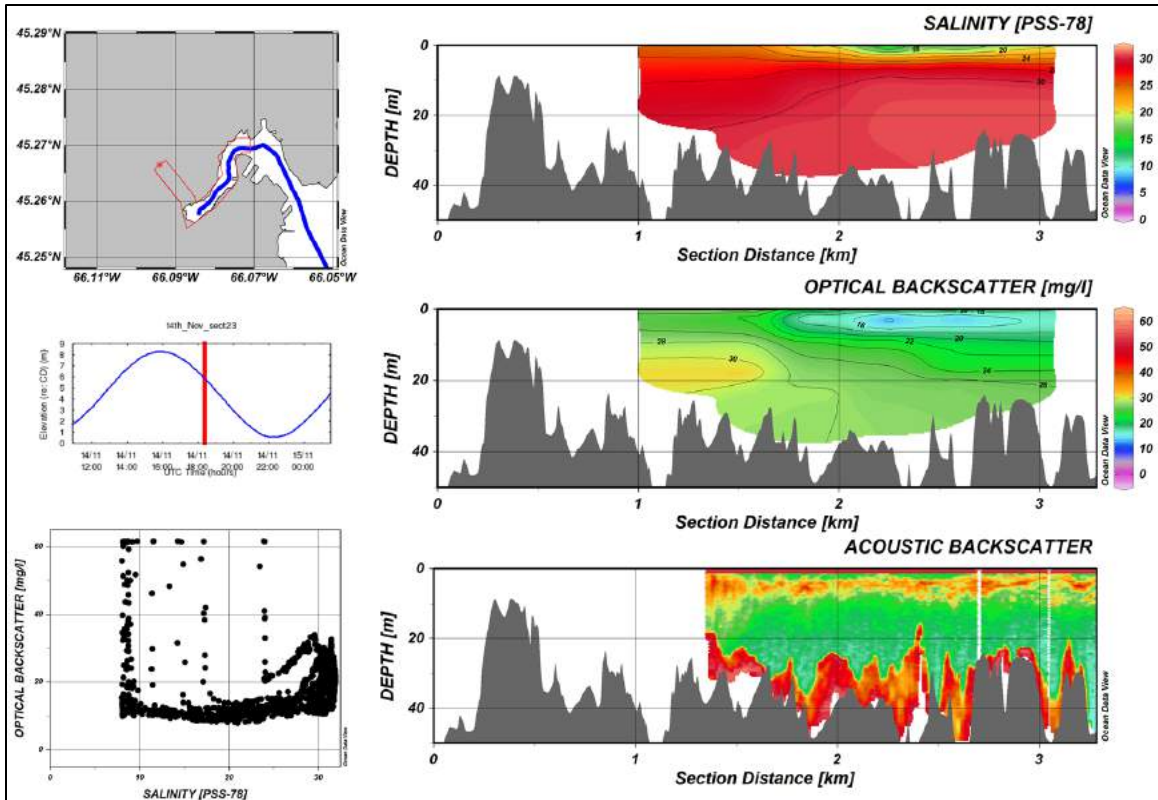


Figure 76 – November 2008 Oceanographic Observations Upstream of Harbour Bridge on Ebb Tide.

Section begins at the Reversing Falls sill and terminates at the Harbour Bridge.

5.4.3. March 2009

The model output at low tide for the section upstream of the harbour bridge (Figure 77) indicates that the waters in the area are completely mixed with a salinity of approximately 12 psu. Note that this matches the river salinity levels at this time of year, and is a result of entrainment occurring upstream of the Reversing Falls. By flood tide, the nose of the salt wedge is beginning to propagate upstream of the Harbour Bridge. At high tide the

salt wedge has propagated upstream past the constriction of the Reversing Falls and into the Saint John River gorge.

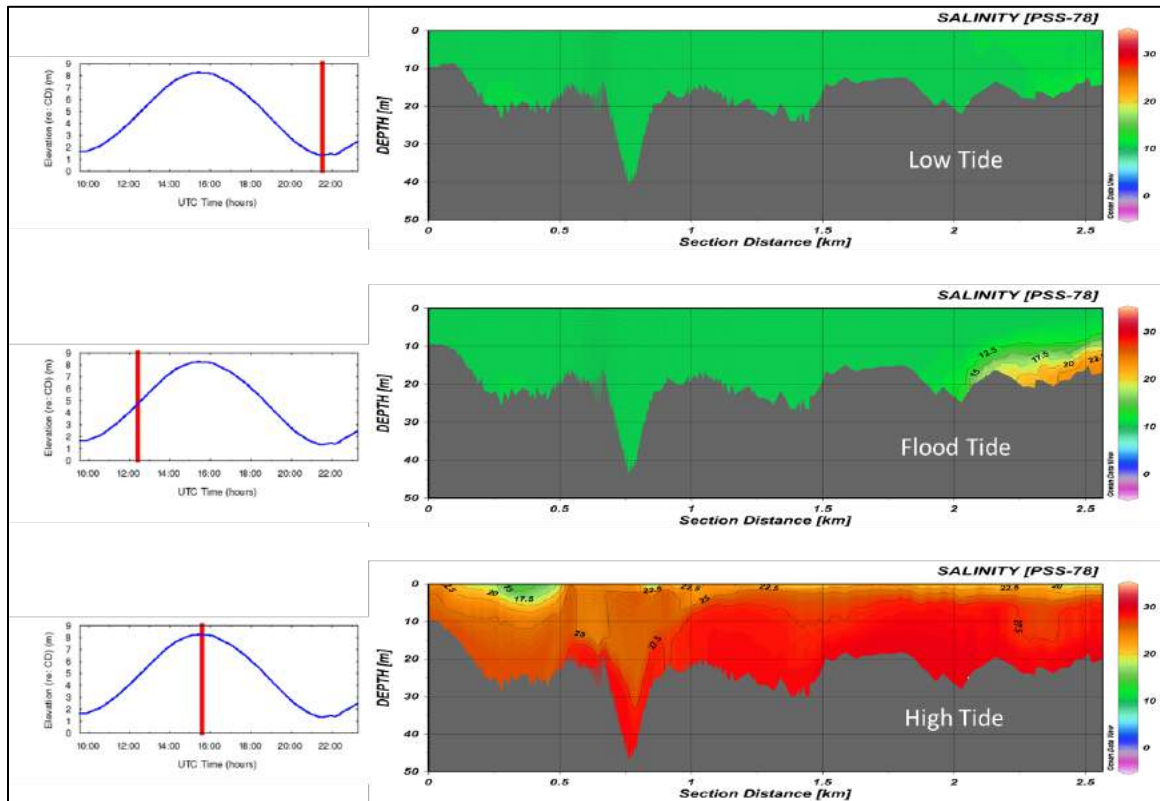


Figure 77 – March 2009 Model Salinity Output Upstream of Harbour Bridge at Low, Flood and High Tide. Section begins at the Reversing Falls sill and terminates at the Harbour Bridge.

Observations within the upstream portion of the Main Harbour Channel for March were available only during the start of the ebb tide, as shown in Figure 78. During this time, the channel is saturated by the salt wedge. Optical backscatter values within the profile follow the concentration of the local salinity. To extend the observations throughout the channel, the model output for the same time periods is shown as the top pane in Figure

79. This figure provides a close match the limited observations in Figure 78 and confirms that the salt wedge is still reaching over the Reversing Falls sill at this time.

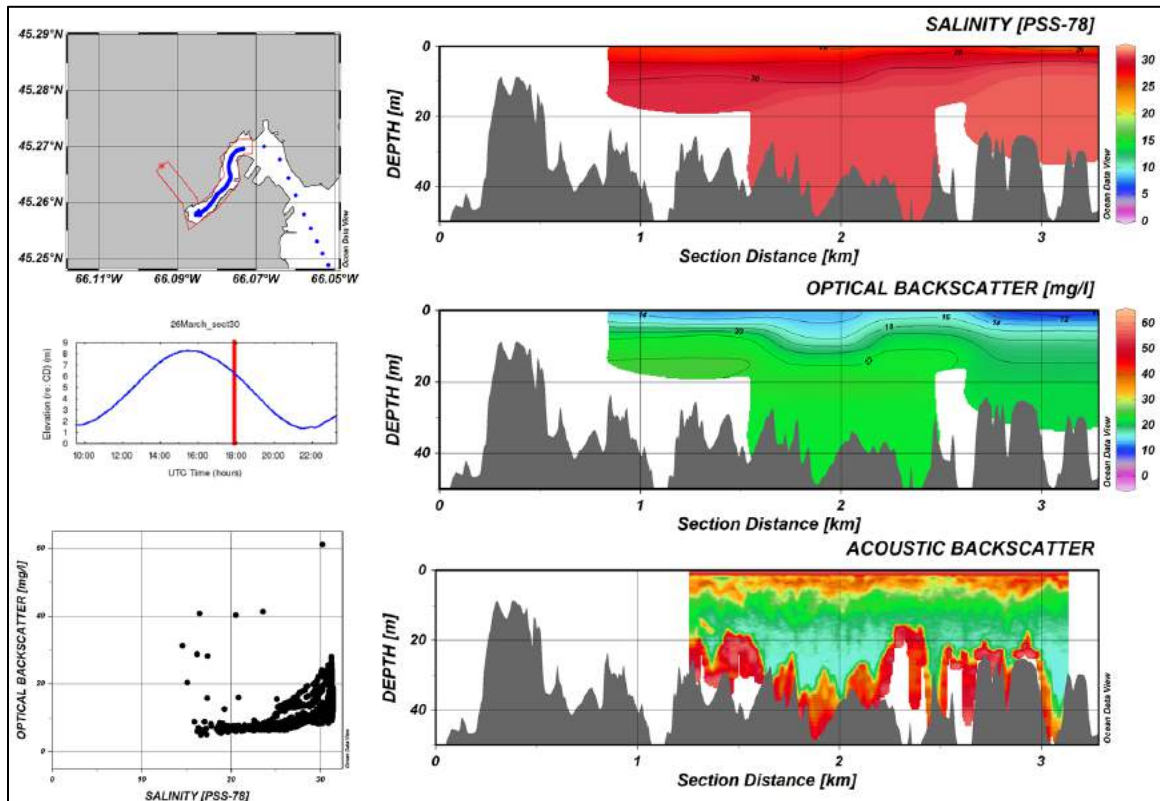


Figure 78 – March 2009 Oceanographic Observations Upstream of Harbour Bridge on Ebb Tide.

Section begins at the Reversing Falls sill and terminates at the Harbour Bridge.

The lower pane of Figure 79 displays the modelled salinity profile for ebb tide, where the fresh water is beginning to propagate into the channel. The relatively fresh river waters are mixed from the waters that originated from upstream of the falls with a salinity of 12 psu.

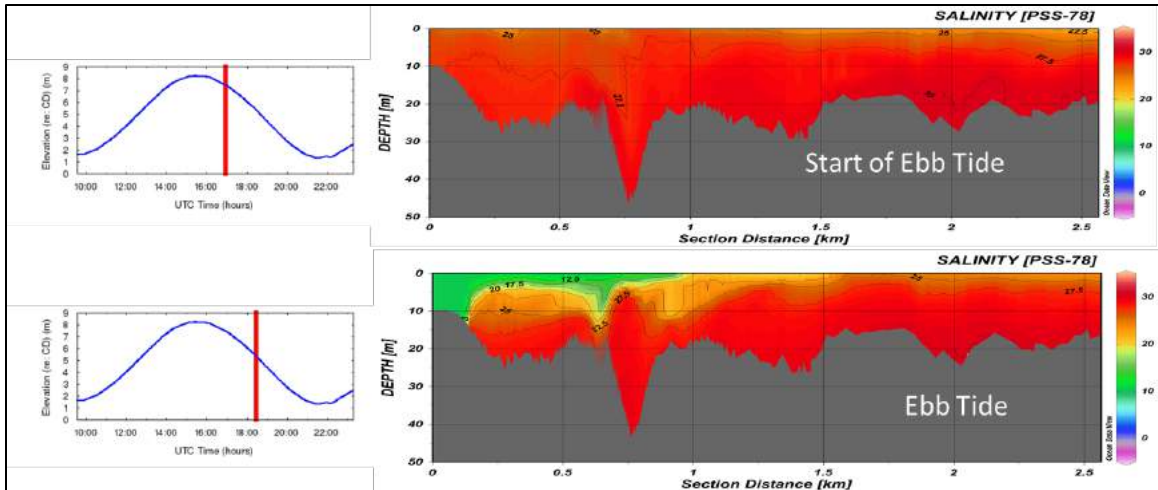


Figure 79 – March 2009 Model Salinity Output Upstream of Harbour Bridge at the Start of Ebb and Ebb Tide. Section begins at the Reversing Falls sill and terminates at the Harbour Bridge.

5.4.4. June 2009

In June at low tide the section upstream of the Reversing Falls contains relatively fresh river waters with a salinity concentration of approximately 10 psu, as shown in the model output section of Figure 80. On the flood tide, the salt wedge has not yet propagated past the Harbour Bridge. At high tide the salt wedge has reached the Reversing Falls and is starting to pass over the constriction.

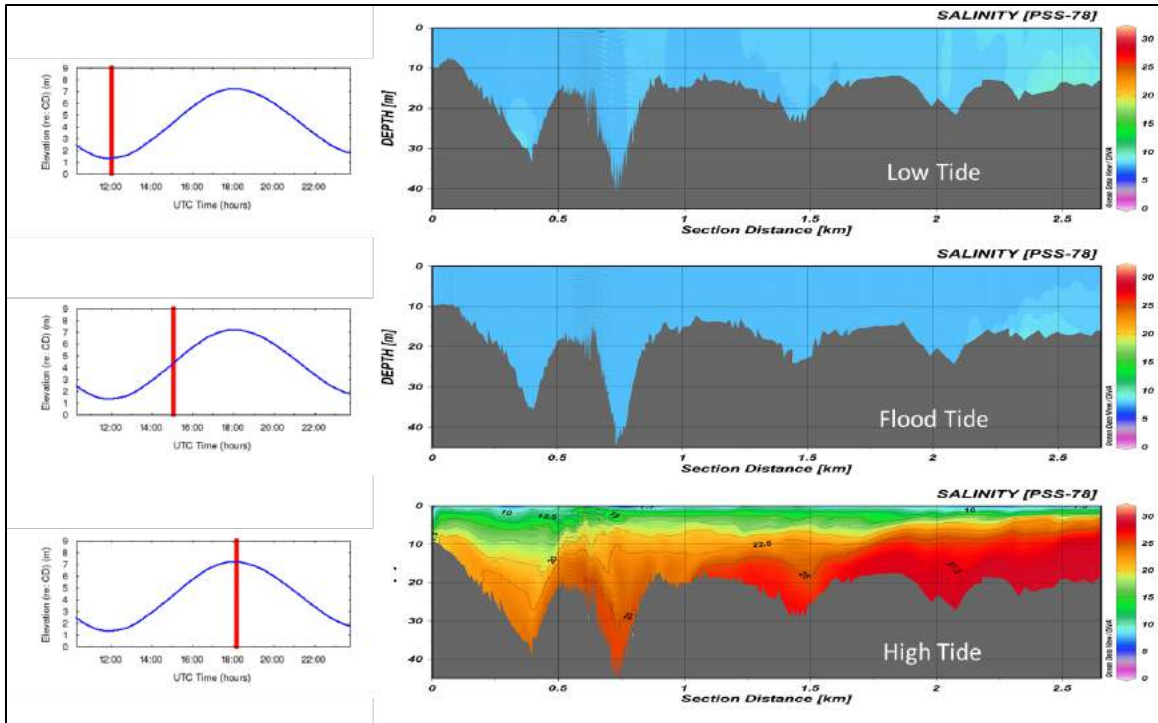


Figure 80 – June 2009 Model Salinity Output Upstream of Harbour Bridge at Low, Flood and High Tide. Section begins at the Reversing Falls sill and terminates at the Harbour Bridge.

Observations were available only for the start of the ebb tide in June for the channel upstream of the Reversing Falls, as shown in Figure 81. At this time the salt water has moved into the channel upstream of the Harbour Bridge and some mixed water has made its way over the sill of the Reversing Falls. The acoustic backscatter profile shows the strong mixing occurring as waters pass over the Reversing Falls sill. As the ebb tide continues, as shown in the model output profile of Figure 82, the fresh river water starts to replace the salt waters within the channel.

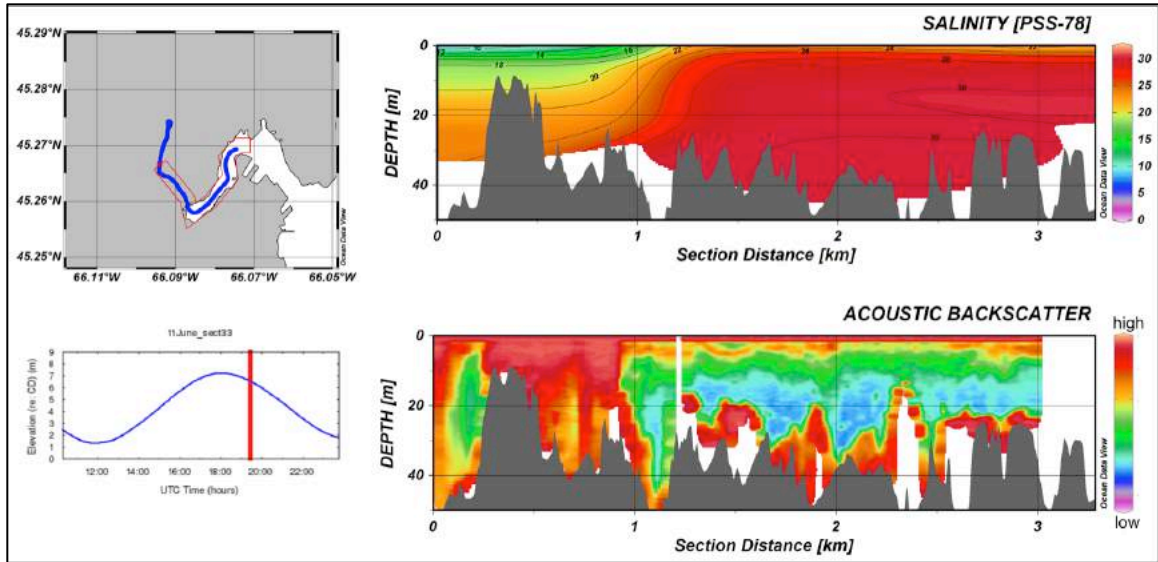


Figure 81 – June 2009 Oceanographic Observations Upstream of Harbour Bridge on the start of the Ebb Tide. Section begins at the Reversing Falls sill and terminates at the Harbour Bridge.

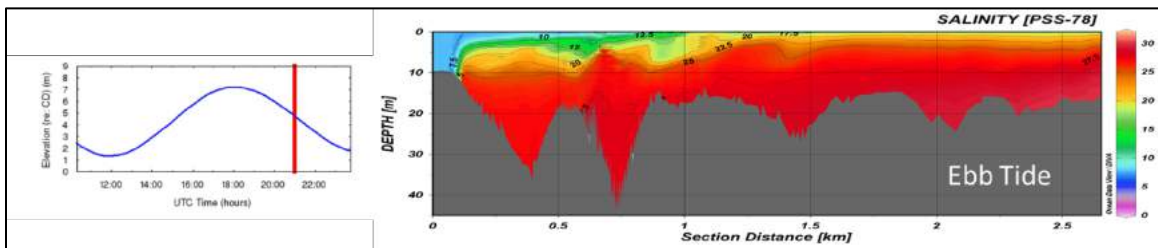


Figure 82 – June 2009 Model Output Upstream of Harbour Bridge on Ebb Tide. Section begins at the Reversing Falls sill and terminates at the Harbour Bridge.

5.5. Discussion of Circulation

The observations described in this chapter confirm that the estuarine circulation in the Port of Saint John depends heavily on the interaction between the large Bay of Fundy

tidal range and river discharge. During 2008, the spring freshet was sufficiently strong to arrest the salt wedge prior to reaching the Reversing Falls gorge upstream of the depth constriction of the falls. Previous studies of the Saint John River estuary have observed a similar phenomenon [RW.ERROR - Unable to find reference:292]. The point of arrest of the salt wedge changes the mixing characteristics of the waters moving over the falls and downstream between the falls and the Harbour Bridge.

Examination of the suspended sediment profiles for the April 2008 spring freshet condition suggest that there are elevated levels of suspended sediment in the nose of the salt wedge. The salt wedge approaches the Reversing Falls at high tide and the salt wedge slows down before it is arrested downstream of the falls. As the velocity of the salt wedge decreases, the sediments observed in the turbidity maximum fall out of suspension and are deposited in the channel between the Harbour Bridge and the Reversing Falls. On the ebb tide as the salt water is pushed out of the channel by the fresh river waters, the seabed is exposed to the overlying outgoing fresh water and the sediment is being resuspended by the strong currents. The fresh waters flowing out through the harbour carry high concentrations of suspended sediment originating from both the river and those recently and briefly deposited by the turbidity maximum of the salt wedge. Some of the resuspended sediment flows into side eddies of the Main Harbour Channel where they decelerate and settle into the berths, while the rest continues to flow downstream. A fraction of the downstream flow diverges to the East over the submerged mudflats which separate the Main Harbour and Courtney Bay. Within this area of inter-channel mudflats, known as Round Reef, the already sediment laden waters likely pick up more sediment

which recently settled out of suspension at high tide. The fresh surface waters collide with the Courtney Bay breakwater, as observed in the model output, and a portion of the sediment-laden water is sent up into Courtney Bay. The velocity of the fresh water layer decreases as it reaches the Turning Basin and the deceleration causes the sediments fall out of suspension. This process explains the source of the elevated levels of suspended sediments observed in the fresh waters of Courtney Bay in April 2008.

Elevated levels of suspended sediment are also visible in the fresh surface waters of Courtney Bay in November, but in weaker concentrations than in April. In November, high concentrations of suspended sediment are not visible in the fresh waters of the Main Harbour Channel on the ebb tide, which suggests that the primary source of the suspended sediment observed in the fresh water of Courtney Bay is not the Main Harbour Channel but the mudflats of the Round Reef area. The elevated current velocities flowing from the Main Harbour Channel to Courtney Bay over Round Reef may be of a sufficient magnitude to resuspend the deposited fine-grain sediments that reside on the mudflats and provide a contribution to the observed suspended sediment. The fine grain sediments near Round Reef are likely deposited at times of low current velocity as observed in section 5.2.2.1.

In March, there is no visible sediment concentration in the fresh water surface layer of the Courtney Bay Channel. In June, lack of optical backscatter observations prevents a definitive statement, but by analogy with March, a similar process is inferred.

At the end of the Courtney Bay breakwater, an area of strong current velocity is observed to wrap around the end of the breakwater coming from the mudflats to the East of the breakwater. This circulation pattern is observed at all times of the year between flood and high tide and is accompanied by a high concentration of suspended sediment. During times of strong storm wave resuspension outside the harbour, increased concentrations of suspended sediment would be observed in this area, as discussed in Melanson (2012),.

Observations indicate that the salt wedge often contains high levels of suspended sediments in both channels at all times of the year. The upstream extent of the salt wedge, however, changes throughout the year and is dependent on the output of fresh waters of the river. Two factors control the position of the salt wedge in the estuary. The first is the relative strength of the river discharge and the corresponding spring or neap tidal range. The second, which is actually correlated with the first, is the amount of entrainment along the halocline. The reach of the salt wedge in the Main Harbour channel also influences the location of mixing in the estuary. For example, in April the salt wedge does not pass over the Reversing Falls and so the mixing of the fresh and salt waters is observed in the channel between the Harbour Bridge and the Reversing Falls as shown by the large Kelvin-Helmholtz instabilities observed on the ebb tide (Figure 69). During the observation periods of November, March and June, the salt wedge passes over the Reversing Falls constriction and mixing continues to occur upstream of the falls.

CHAPTER 6: Residual Model Circulation

The current velocities obtained from the model runs can be averaged over a tidal cycle to obtain the residual circulation throughout the harbour. The residual circulation represents sub-tidal estuarine circulation in the harbour. The model computes north and east velocity components at the centre of each element for every time step at all layers. The mean of the velocities over a tidal cycle then provides the residual flow, which within the bottom layer of the model output, next to the seabed, provides a proxy for potential sediment transport [Leys and Mulligam, 2011]. Most of the dredged material is composed of sandy silts and clayey sands, which have low settling speeds of 1 and 0.1 mm/s respectively [Leys and Mulligam, 2011]. These particles are likely to be maintained in suspension for most of the tidal cycle. The residual velocity within the bottom seabed layer of the model was examined to determine the residual interactions of the salt and fresh waters with the seabed sediment. Both the outgoing fresh water flow from the Saint John River and the incoming salt wedge from the Bay of Fundy interact with the seabed to modify the residual circulation. The quantity of fresh water consequently changes the residual flow regime and each model simulation period provides a unique seabed residual circulation pattern.

6.1. April 2008

As the fresh water output from the Saint John River is greatest in April, the residual flow near the seabed through the Main Harbour channel upstream of the Harbour Bridge is strong in the downstream direction, as shown in Figure 83. Residual seabed current velocities rise to a maximum of almost 3 m/s in the channel. Downstream of the Harbour Bridge a series of horizontal eddies develop throughout the harbour. These eddies are residual eddies, unlike those described previously in Section 5.2. A small counter clockwise residual eddy develops just south of the Harbour Bridge, upstream of the berths on the west side of the channel, labelled as area A in Figure 83. A larger counter clockwise residual eddy develops at the northern tip of the Main Harbour channel, east of the harbour bridge, along the face of long wharf, labelled as area B in Figure 83. The largest residual eddy in this section of the harbour is rotating clockwise and is developed across the breadth of the harbour spanning between the eastern piers and the berths on the west side of the channel, labelled as area C in Figure 83. It can be noted that residual currents reach 0.75 m/s along the face of the eastern piers, on the eastern side of the channel. In all cases much lower residual velocities branch off these eddies into the docks, implying potential sinks of sediment.

The eddy developed at location B in Figure 83 feeds sedimentation along the north east docks in the Main Harbour Channel, while eddy C feeds the western docks. In both of these areas the strong residual currents, which carry sediment laden water down through the Main Harbour Channel from the Reversing Falls, quickly decelerate and are able to

deposit sediment into the docks. These dock areas both require annual dredging [Leys, 2007].

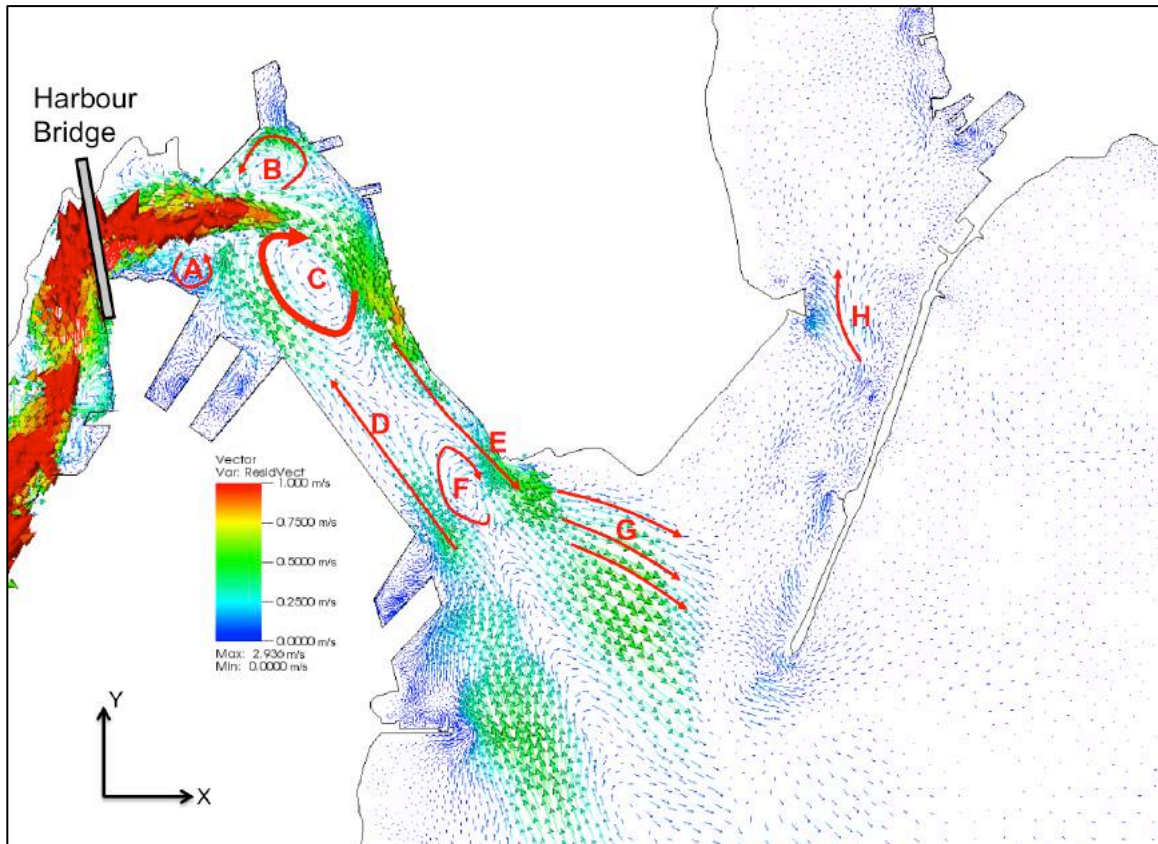


Figure 83 – April 2008 Model Tidal Residual Currents at the Seabed

Further downstream, the western side of the channel is dominated by the inflow of the salt wedge, while the eastern side of the channel is dominated by the outflowing fresh water, labelled as areas D and E in Figure 83. Changes in lateral channel geometry cause the formation of another eddy in the centre of the Main Harbour Channel between the end of the eastern piers and the downstream end of the western piers, labelled as area F in

Figure 83. Downstream of the east piers, a strong outflowing residual circulation pattern can be observed over the mud flats between the Main Harbour Channel and Courtney Bay Channel with near seabed current velocities reaching 0.5 m/s, labelled as area G in Figure 83. This pattern is quickly attenuated when it reaches the Courtney Bay channel implying residual deceleration and thus potential deposition of sediment.

Within Courtney Bay, in April, the residual current velocities at the seabed are weak with upstream magnitudes of approximately 0.1 m/s. Velocities increase slightly as the water from the channel enters the Turning Basin, labelled as area H in Figure 83. The direction of the near seabed residual currents is predominantly into Courtney Bay. In the case of Courtney Bay, no erosion is envisaged as sediments originating from areas of higher velocity already in suspension are now decelerating and depositing.

6.2. November 2008

Fresh water output from the Saint John River is at fall freshet levels in November, which are less than levels observed in April. The flow in the channel between the Reversing Falls and the Harbour Bridge has diminished to a maximum of 1.6 m/s (Figure 83), but the flow direction is still downstream. Downstream of the Harbour Bridge, the seabed residual circulation has notably changed compared to patterns observed April. Out of the three eddies observed in April (Figure 83), only the one observed at the head of the Main Harbour Channel still exists in November, labelled as area A in Figure 84. The

predominant direction of residual velocity vectors is now pointing upstream in this area and is influenced more by the incoming salt wedge than the outgoing fresh water, labelled as area B in Figure 84.

The restricted downstream extent of the fresh water related residual current vectors and disappearance of the channel wide eddy could have a significant impact on sediment transport in the Main Harbour Channel in November. The disappearance of the eddy implies that suspended sediment will no longer quickly decelerate and settle in the western berths, like it did in April. As the residual currents in the Main Harbour Channel are now in the upstream direction, suspended sediment is able to move into the channel and settle as it decelerates upon meeting the seabed residual extent of the downstream flow. This would cause deposition of suspended sediments in the centre of the Main Harbour Channel.

The magnitude of the velocity vectors along the east piers in Figure 84 has decreased compared to April and the channel residual velocities are now dominated by the incoming salt wedge. The small eddy at the entrance of the harbour, labelled area F, is still apparent but has move slightly to the east. Over the mudflats which separate the Main Harbour Channel and Courtney Bay, the velocity vectors resemble those of April, yet their magnitudes have decreased to approximately 0.25 m/s, labelled as area C in Figure 84. The lower velocities would affect the composition and concentration of the sediment, which is able to stay in suspension as waters pass over the area. At the intersection of the two channels and within the Courtney Channel and Turning Basin, the

structure of the velocities is relatively the same as in April, with the exception of the area at the end of the breakwater, labelled as area D in Figure 84. In November, the flow around the end of the breakwater, from east to west coming into the channel, is notably more developed than it was in April. This flow corresponds to an area of erosion on the seabed in the channel (section 6.5) and could carry suspended sediment from both offshore and the mudflats east of the breakwater up into Courtney Bay [Melanson, 2012]. This sediment rich flow is likely a major source of sedimentation in Courtney Bay.

As observed in April, velocities increase slightly as the water from the Courtney Channel enters the Turning Basin, labelled as area H in Figure 66.

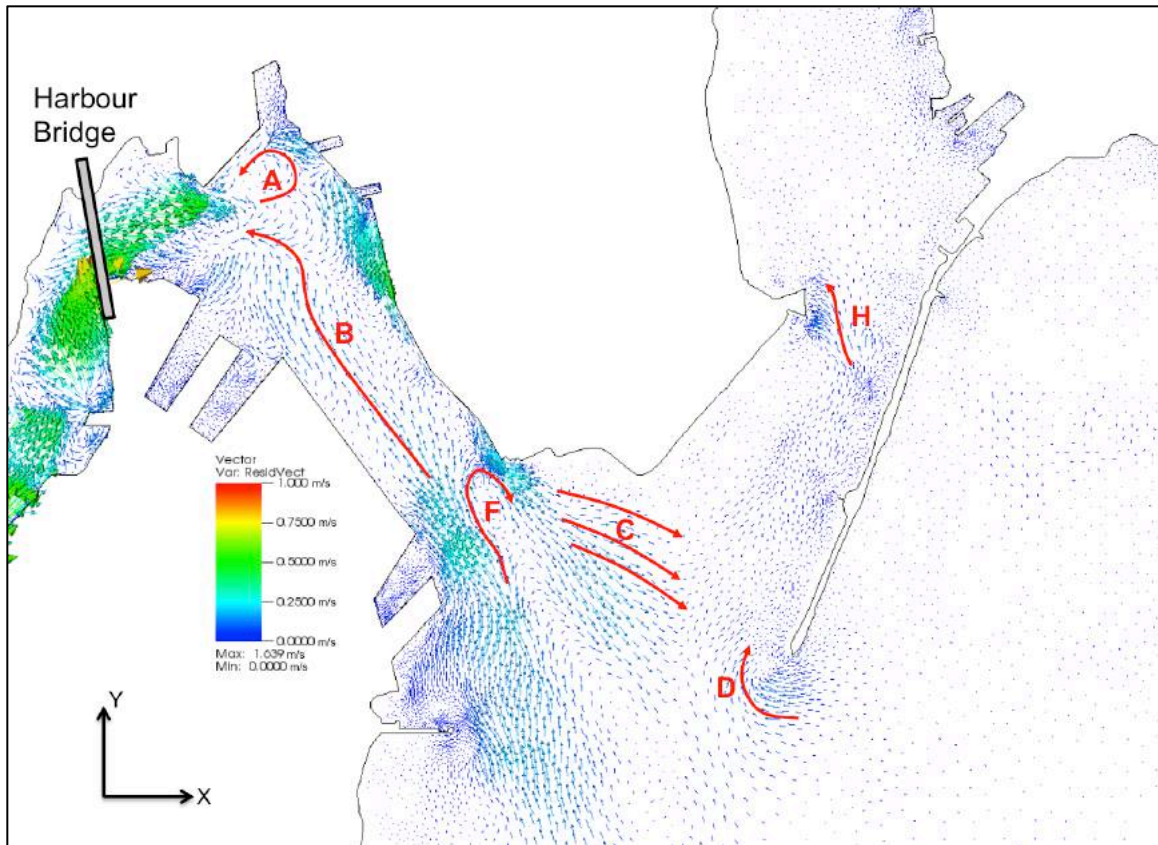


Figure 84 – November 2008 Model Tidal Residual Currents at the Seabed

6.3. March 2009

The period of minimum fresh water output for the Saint John River is in the winter. The March simulation thus corresponds to the period when the incoming salt wedge has the most influence on the residual circulation, as shown in Figure 85. Near seabed residual velocities in the channel between the Reversing Falls and the Harbour Bridge are predominantly upstream and an eddy has developed near the Marine Wharf, labelled as area A in Figure 85. Downstream of the Harbour Bridge the eddy that was visible in

November at the north end of the channel has disappeared, to be replaced by the weak currents associated with the upstream residual flow. No eddies are developed in the Main Harbour below the Harbour Bridge and the only downstream flow is visible along the northern and southern most east piers. Due to the terrain following nature of the vertical model coordinates, these flows could be in shallower water outside of the primary salt wedge where there is more influence from the surface flows. The downstream cross-channel flow is still visible over the mudflats between the Main Harbour and the Courtney Channel, labelled as area B in Figure 85, though the magnitude is weaker than observed in April and November at approximately 0.12 m/s.

The residual flow around the end of the breakwater, which was first observed in November, is even stronger and more developed in March, labelled as area C in Figure 85. The residual flow in Courtney Channel and the Turning Basin is very similar to the fields observed in November and April.

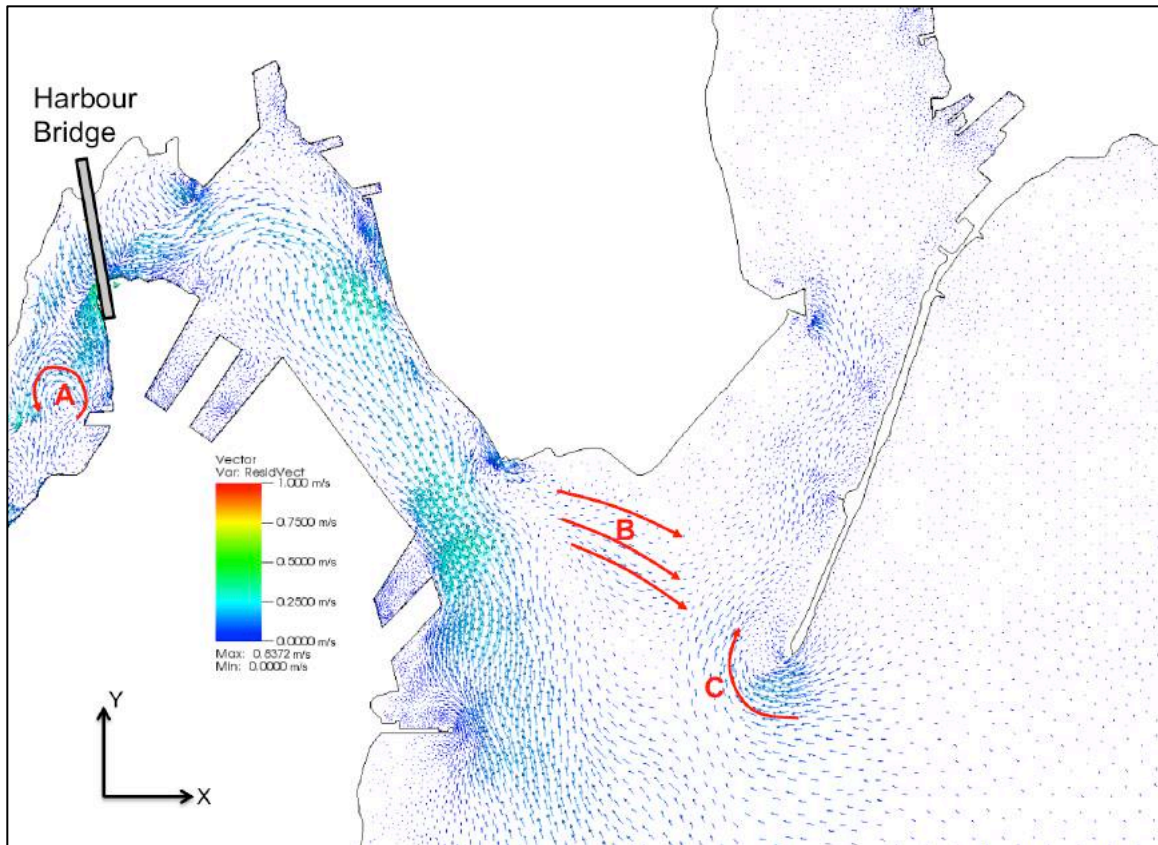


Figure 85 – March 2009 Model Tidal Residual Currents at the Seabed

6.4. June 2009

In June, the water levels are at a summer minimum, and the residual circulation pattern resembles the patterns observed in March and November, as shown in Figure 86. A general upstream flow is apparent through the Main Harbour Channel, with a weak cross channel flow over Round Reef. An enhanced residual flow around the end of the breakwater is visible, similar to March 2009, and is responsible for transporting sediment rich waters from east of the breakwater into Courtney Channel. In contrast to the March

residual circulation, the Round Reef velocities are elevated and the inflowing waters of the Main Harbour Channel meet the outflowing waters under the harbour bridge.

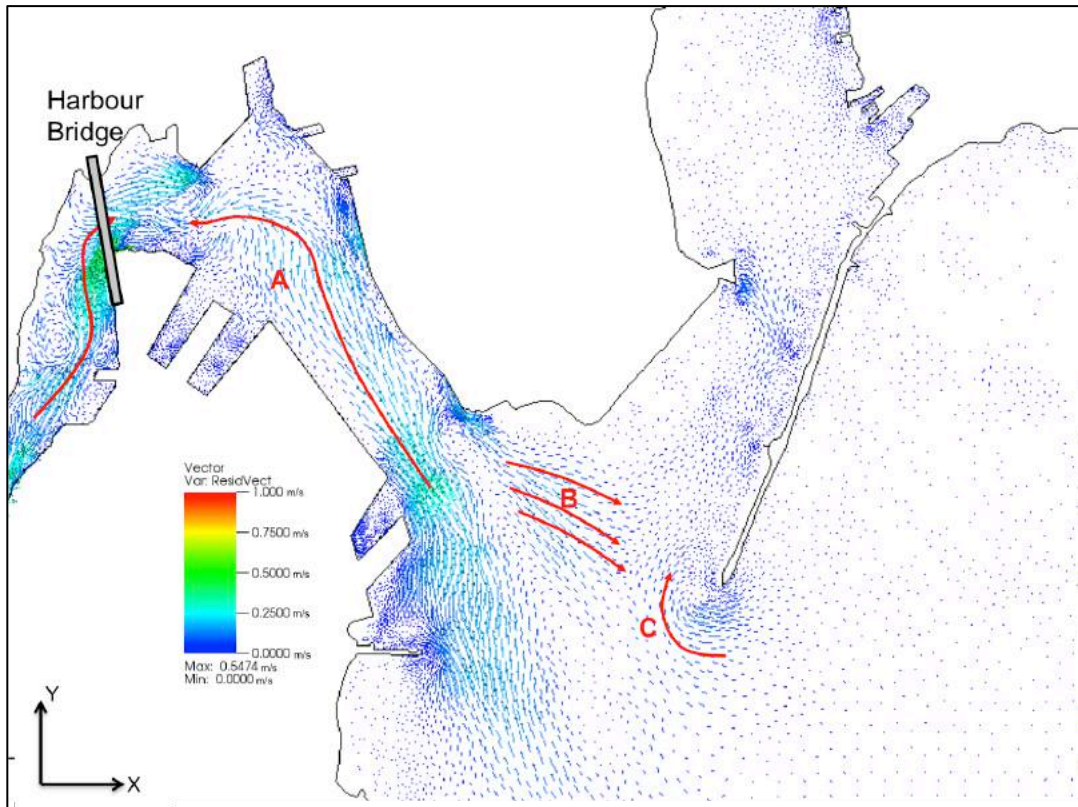


Figure 86 – June 2009 Model Tidal Residual Currents at the Seabed

6.5. Bathymetry Difference Correlation to Residual Circulation

The various multibeam surveys completed throughout the domain of the Port of Saint John can be compared to determine the locations and extent of long-term changes in sediment distribution patterns. These locations of erosion and deposition can then be compared to the residual seabed model current circulation patterns to determine the

effects of the residual circulation on the local seabed. If sufficient current velocities to maintain the suspension of sediments are sustained over a tidal cycle, one would expect sediment to be moved from that area. Regions of accelerating velocity would imply erosion while decelerating velocity would imply deposition.

Multibeam surveys were completed by the Ocean Mapping Group's vessel, the Heron, and the CHS vessels, Pipit and Plover, in 2000, 2001, spring 2008, Fall 2008, spring 2009, fall 2009 and fall 2010, as outlined previously in Figure 9 and below, in time, in Figure 87.

Changes in seabed morphology were obtained through differencing multiple bathymetric surveys to describe how the shape of the seabed is evolving over time, within the accuracy limits of the integrated MBES. Through differencing annual and seasonal multibeam surveys, bulk changes in the locations of seabed materials become apparent.

The MBES surveys are not perfect representations of the seafloor bathymetry and each survey dataset and resulting grid contain a number of artifacts as a result of systematic errors. The grid artifacts can be misunderstood as regions of erosion or deposition and therefore must be understood prior to analysis, as discussed in Section 3.3. The primary sources of errors include tidal errors, long period heave drift and refraction errors. These errors will all manifest themselves as artificial inconsistencies in the multibeam grids.

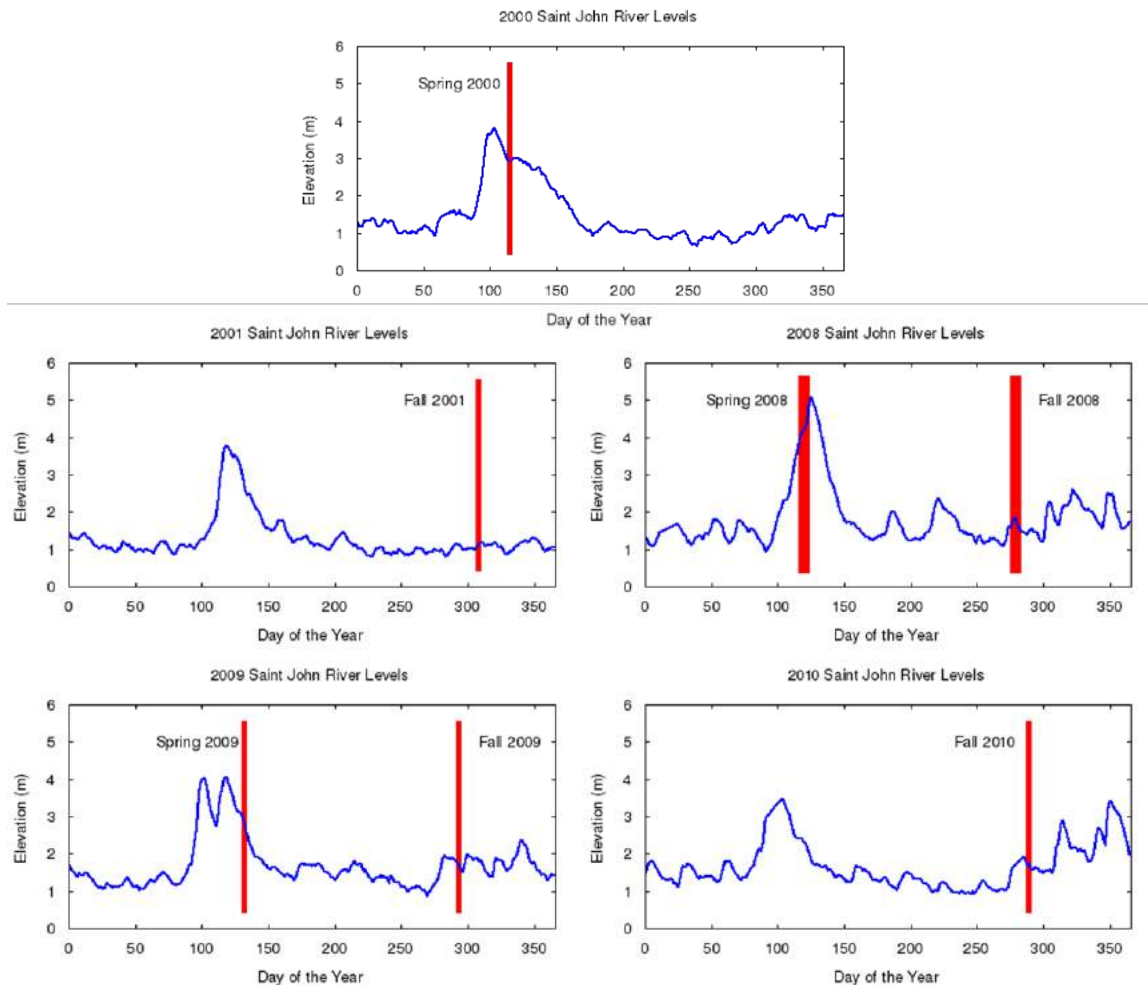


Figure 87 – Saint John Multibeam Survey Times relative to Saint John River level. Line thickness indicates survey duration.

The refraction errors are the most obvious in the difference plots and are revealed as near continuous crests or troughs which run parallel to the survey line directions. These traditionally appear either along or across the main axis of the channel, depending on the survey line orientation. Refraction errors result from an incorrect determination of the local sound speed structure.

Long period heave artifacts are apparent in some of the surveys and usually appear after a speed change due to a rapid change in direction at the end of a survey line. The sudden change in speed alters the draft of the vessel, which the heave sensor cannot model as an impulse response.

Tidal errors in either phase or amplitude will result in vertical offsets between subsequent multibeam survey lines and vessel following depth steps will appear in the grid.

6.5.1. Main Harbour Channel

The Main Harbour Channel is an active area of sedimentation where strong currents continuously modify the erosion and deposition of sediment on the seabed. As discussed previously in this chapter, the residual seabed current patterns change significantly throughout the year and control the areas of seabed change. The formation of eddies, the extent of the fresh water and along and across channel penetration of the competing salt wedge affect the seasonal movement of sediments in this area.

Through analysis of the bathymetry differences in the Main Harbour Channel, it can be noted that the most active area of deposition and erosion of sediment is in the deep basin downstream of the Harbour Bridge (Figure 88). Depending on the tides and the counteracting river discharge the sediments are moved in and out of the deep hole beneath the Harbour Bridge. While this movement of large grain sized bed-load sediment

may not directly affect the dredged areas where minimum under keel clearance is critical, the fine grain portion of the deposited material could affect the dredged areas as a source of suspended sediment. For all difference maps shown in this section, blue areas indicate erosion of up to one metre or greater and red areas indicate deposition of up to one metre or greater.

Figure 88 shows the forward difference in bathymetry between a multibeam survey in the spring of 2009, as rivers levels were decreasing after a spring freshet with two distinct peaks, and spring of 2008, close to the peak of a strong spring freshet. The corresponding river levels are displayed in Figure 87.

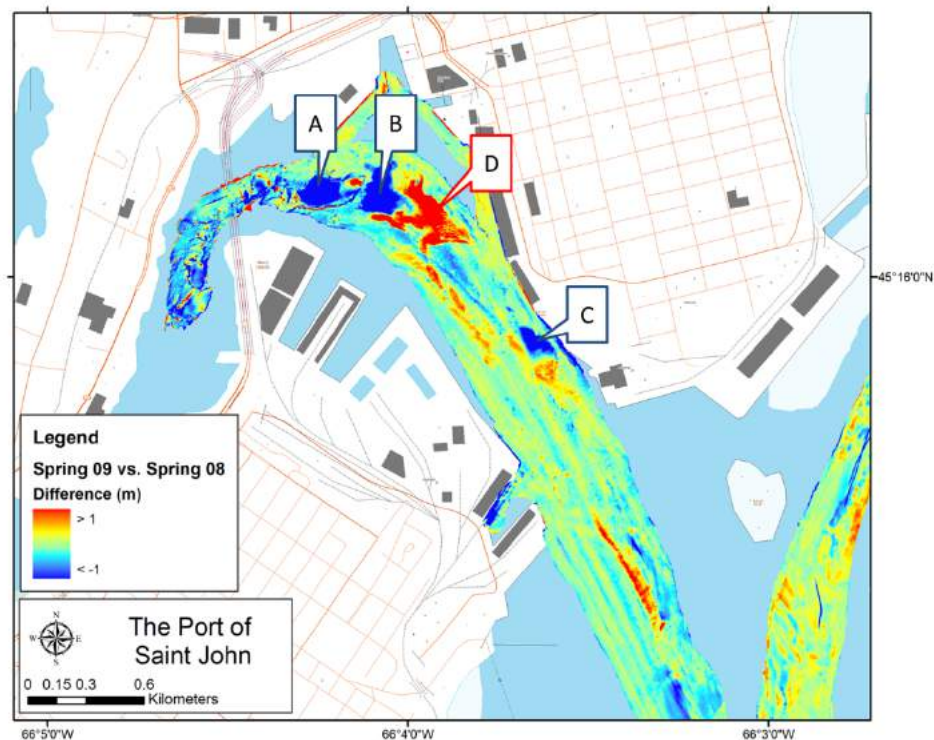


Figure 88 – Bathymetry Difference Main Harbour Channel (Spring 2009 vs. Spring 2008)

There are three areas of erosion in the Main Harbour Channel between these survey times. The first is 450 metres, the second at 750 metres, and the third at 1850 metres downstream of the Harbour Bridge, each marked in Figure 88 as areas A, B and C respectively. Area A describes an erosion of 4.5 metres, area B describes an erosion of 7 metres, area C describes an erosion of 3.5 metres and area D describes an accretion of 4 metres. As this difference map covers a year of changes between freshets, it could be assumed that the differences would be minimal, but the river level difference of over 1 metre between the 2008 and 2009 freshets and the difference in timing between the occurrence of the freshet and the survey likely accounts for the dissimilarity. From the residual current vectors for April 2008, shown in Figure 83, it can be noted that the erosional area at 450 metres exists within the area of strong downstream current coming from under the harbour bridge. As the April simulation was not at the peak of the 2008 freshet, it is likely that the strong residual currents extend further downstream at the peak of the freshet, towards the 750 metre area. The area at 1850 metres also corresponds to an area of increased April current velocities along the face of the eastern pier (area E in Figure 83).

An area of deposition exists approximately 1050 metres downstream of the harbour bridge, marked as area D in Figure 88. This area corresponds to the location of an eddy formed in the April 2008 residual circulation within the Main Harbour Channel.

Figure 89 provides the forward difference maps with a shorter window of time between multibeam surveys in the fall of 2009, during a weak fall freshet, and the spring of 2009,

after the double peak spring freshet. This time period should correspond to the tail end of the freshet together with the summer minimum simulation period of June 2009 and the fall freshet period of November 2008. The residual circulation patterns of June (Figure 86) and November (Figure 84) both indicate that there is a general inflow of water into the Main Harbour Channel, reaching up to the deep hole beneath the harbour bridge. These circulation patterns correspond to the difference map which indicates that during this time there has been a redeposition of sediment of over 3 metres back into the bathymetric lows located at areas A and B downstream of the harbour bridge, as shown in Figure 89. An area of erosion at area D of over 2 metres, 1150 metres downstream of the Harbour Bridge which corresponds to the southern limit of the area of deposition seen in Figure 88, could result from the sediments being pushed back upstream by the salt wedge and deposited back into the depressions at areas A and B. Areas A and B may now be shielded from the high velocity outgoing fresh water by the salt wedge. A small area of deposition of over 1 metre also exists along the eastern pier which corresponds to an area of former erosion from Figure 88, labelled as area C in Figure 89. Note that Figure 89 is almost a mirrored image of the patterns observed in Figure 88.

The spring freshet of 2010 was weak compared to the freshets of 2008 and 2009, with a maximum river level of less than 4 metres, as shown in Figure 87. Examination of the difference in bathymetry between the fall 2010, fall freshet, and spring 2009, post peak freshet, surveys in Figure 90 show that there is further infilling of sediment in the bathymetric depressions downstream of the Harbour Bridge, areas A and B, and along the eastern pier, area C. Corresponding further erosion is also observed at the location 1150

metres downstream of the Harbour Bridge, labelled as areas D in Figure 90. The magnitudes of erosion and deposition in Figure 90 are very similar to those observed in Figure 89. Even with the occurrence of the spring freshet of 2010 amidst the differences of Figure 90, the figure closely resembles Figure 89.

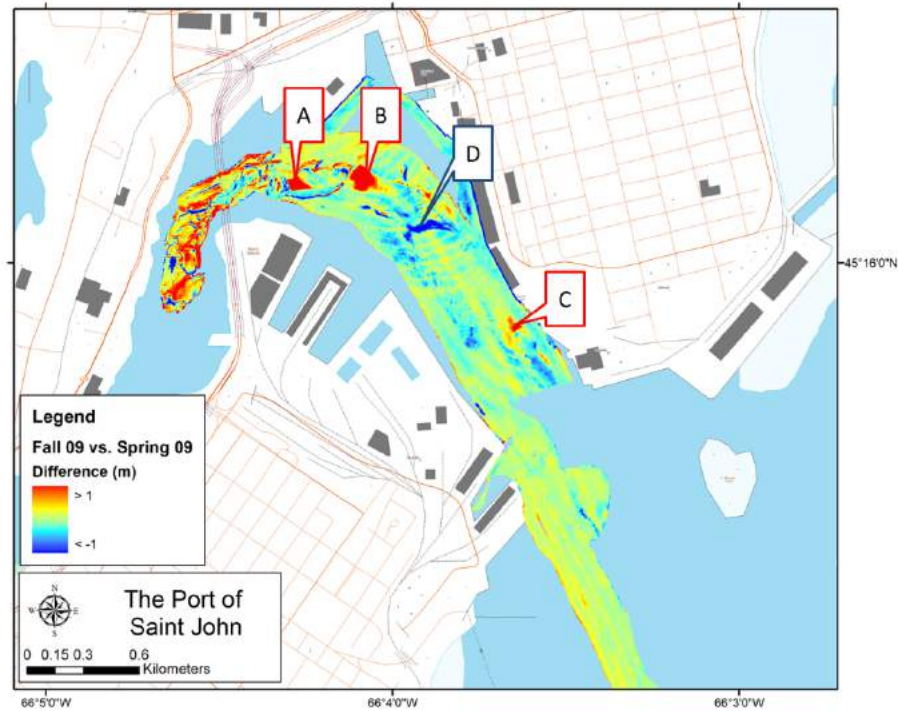


Figure 89 – Bathymetry Difference Main Harbour Channel (Fall 2009 vs. Spring 2009)

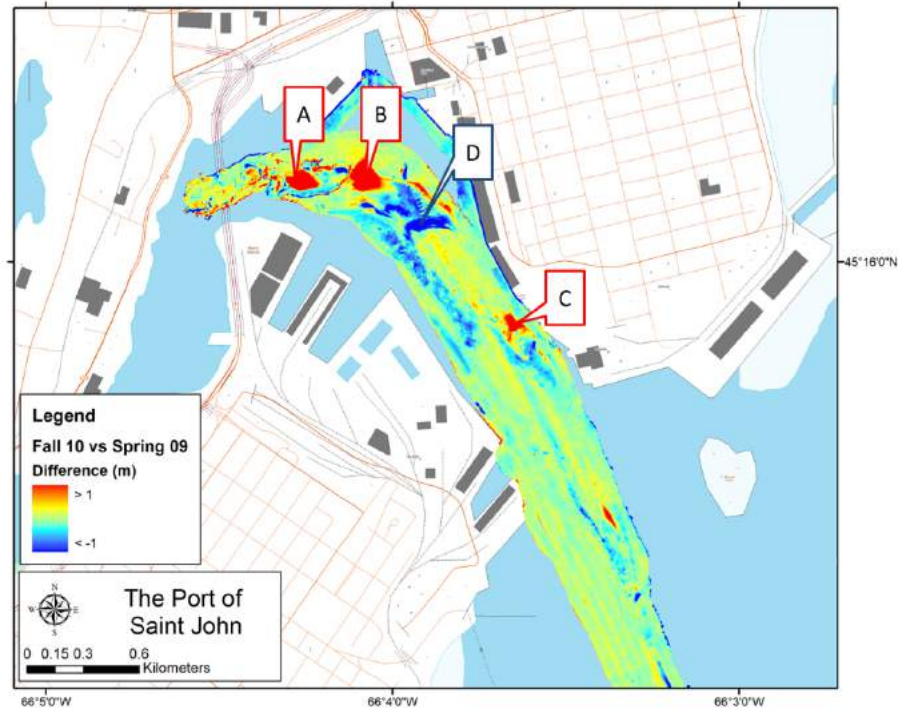


Figure 90 – Bathymetry Difference Main Harbour Channel (Fall 2010 vs. Spring 2009)

Figure 91 shows the difference in bathymetry between fall 2010 and fall 2009, both during the fall freshet. The difference map closely resembles the previous difference map of Figure 90, but the areas of erosion and deposition are smaller in area as they have not had the summer of 2009 to develop.

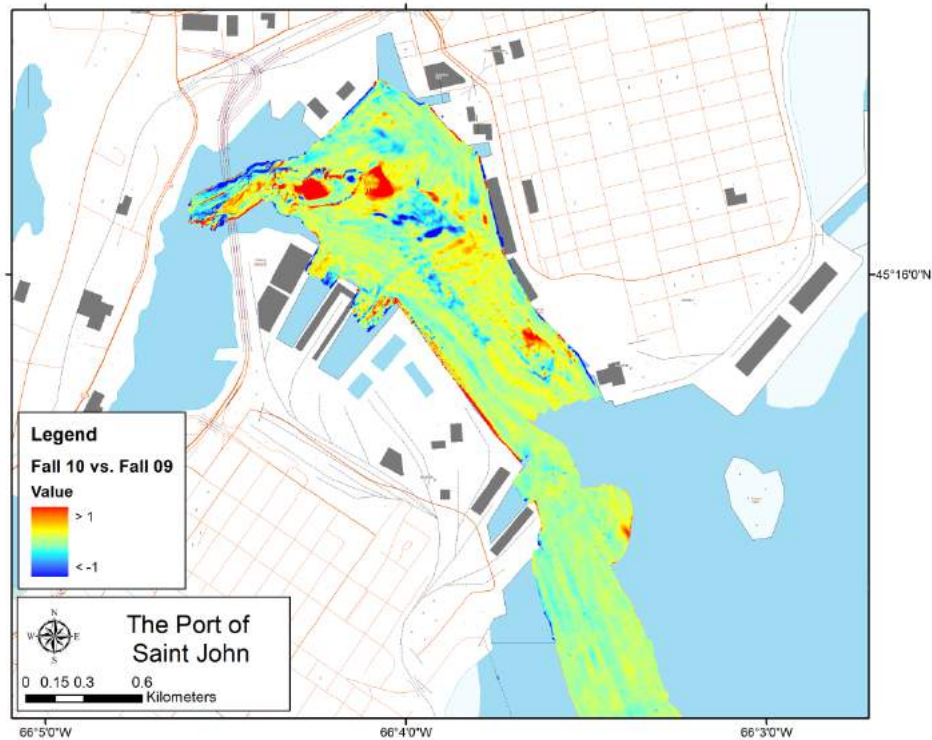


Figure 91 – Bathymetry Difference Main Harbour Channel (Fall 2010 vs. Fall 2009)

To examine longer term trends, the 2000 survey of the Main Harbour Channel was compared to the spring 2008 survey. The 2000 survey was completed during a weak spring freshet, as observed in Figure 87. If the Main Harbour channel was in an equilibrium state, then there should be little difference between bathymetric surveys at a similar time period. The spring 2008 survey was also completed during the spring freshet and the difference between the 2000 and 2008 surveys can be observed in Figure 92. Substantial differences exist between the two surveys in the area downstream of the Harbour Bridge, but many areas have remained largely similar.

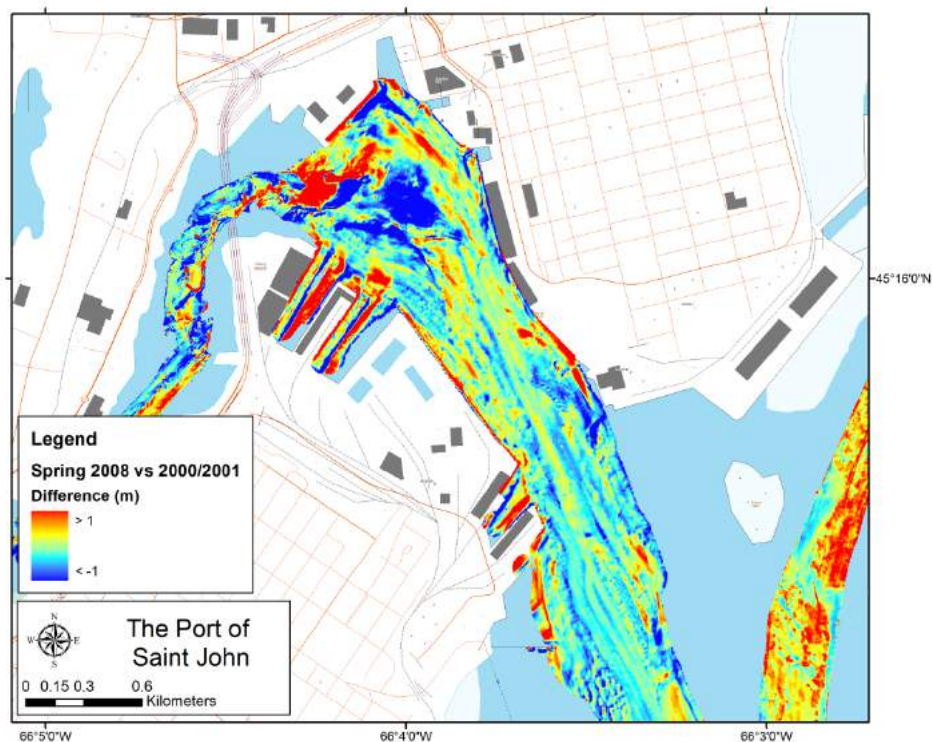


Figure 92 – Bathymetry Difference Main Harbour Channel (Spring 2008 vs. Spring 2000)

6.5.2. Courtney Bay Channel

Figure 93 and Figure 94 represent two distinct time periods in the annual sedimentation cycle of Courtney Bay. Figure 93 represents the seasonal change, between spring of 2008 and fall of 2008, in the channel during the summer, which is almost entirely a deficiency of sediment from dredging. Dredging occurs for most of the summer season to remove the sediments which accumulate in the channel, as discussed in Chapter 2. The anomaly in the dredging pattern is the lack of dredging required along the centre of the channel and in the area south of the breakwater, shown as a red line in Figure 93. The centre of

the channel is likely swept clear by the turbulence generated by the ship propellers which transit through this channel and the main tidal stream. The area south of the breakwater corresponds to a strong residual current that wraps around the end of the breakwater, as discussed previously in this chapter.

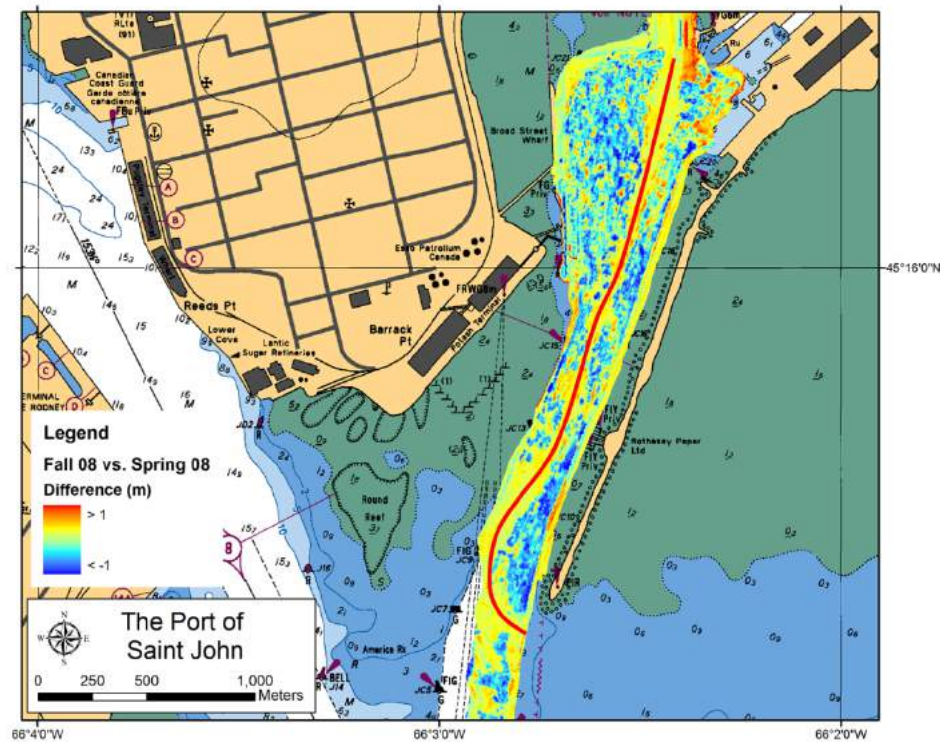


Figure 93 – Bathymetry Difference Courtney Bay Channel (Fall 2008 vs. Spring 2008)

Figure 94 represents the seasonal change over the winter and spring freshet. The pattern observed during this period is similar but opposite to the previous pattern observed over the summer. The sediment is infilling the dredged area upstream of the tip of the Courtney Bay breakwater and starting to fill in the Turning Basin area, shown as areas A

and B in Figure 94. As observed during the summer period, again the centre of the channel and the area south of the breakwater is swept clear of sediment.

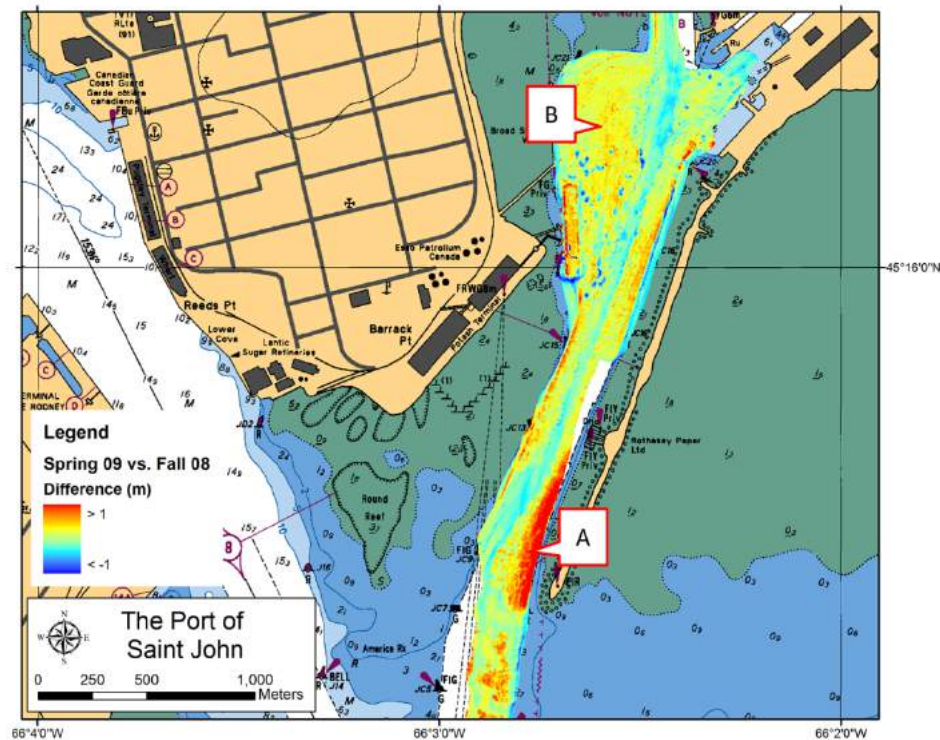


Figure 94 – Bathymetry Difference Courtney Bay Channel (Spring 2009 vs. Fall 2008)

6.5.3. Short Term Seabed Change Analysis

All of the previously examined bathymetry differences are over periods of 6 months or longer. It is unknown then whether the observed changes are due to a slow process or a process that occurs over a few days, for example a result of river surges or spring-neap modulation. To assess this unknown, shorter period differences have been examined. During the spring 2008 multibeam survey, overlapping bathymetry data were collected

over three distinct periods downstream of the Harbour Bridge. The survey times were April 22nd (JD113), April 25th to May 2nd (JD116-123) and May 29th (JD150), as shown in Figure 95. Through examination of the differences between these surveys, the seabed change occurring during the spring freshet was evaluated and compared to the seabed residual circulation observed during the April 2008 simulation.

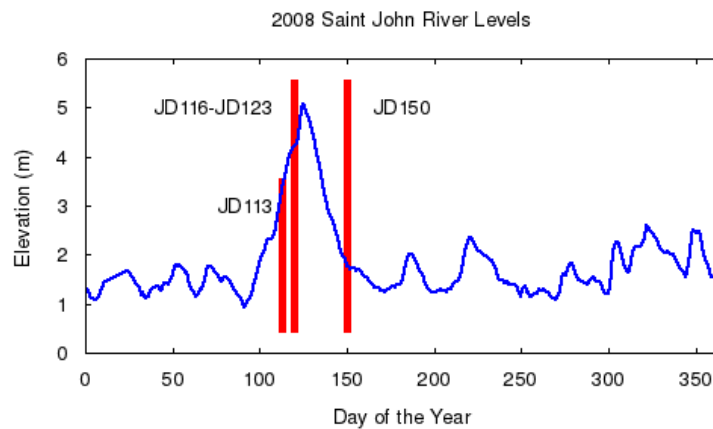


Figure 95 – Spring 2008 Survey Times

Figure 96 shows the difference between the first and second surveys. The seabed is changing rapidly during this time (± 2 metres) which corresponds to increasing strength of the spring freshet, as shown in Figure 95. The primary items to note are the two areas of erosion indicated by the blue areas, which correspond to the bathymetric depression previously discussed at 450 and 750 metres downstream of the Harbour Bridge in Figure 96. The strong river waters of the freshet are able to push the salt wedge out of the harbour so that these areas are exposed to the strong seaward currents on the ebb tide, as described previously in this chapter. The seabed sediments are moved out of the two depressions and some of the sediment is deposited on the seabed directly downstream

(near area D described in Figure 88). Sand waves are starting to appear in the area of deposition further downstream in Figure 96. The area of the sand waves correlates to a region in the seabed residual current field where the downstream velocities are diminished before rising again along the wall of the east pier (Area C of Figure 83).

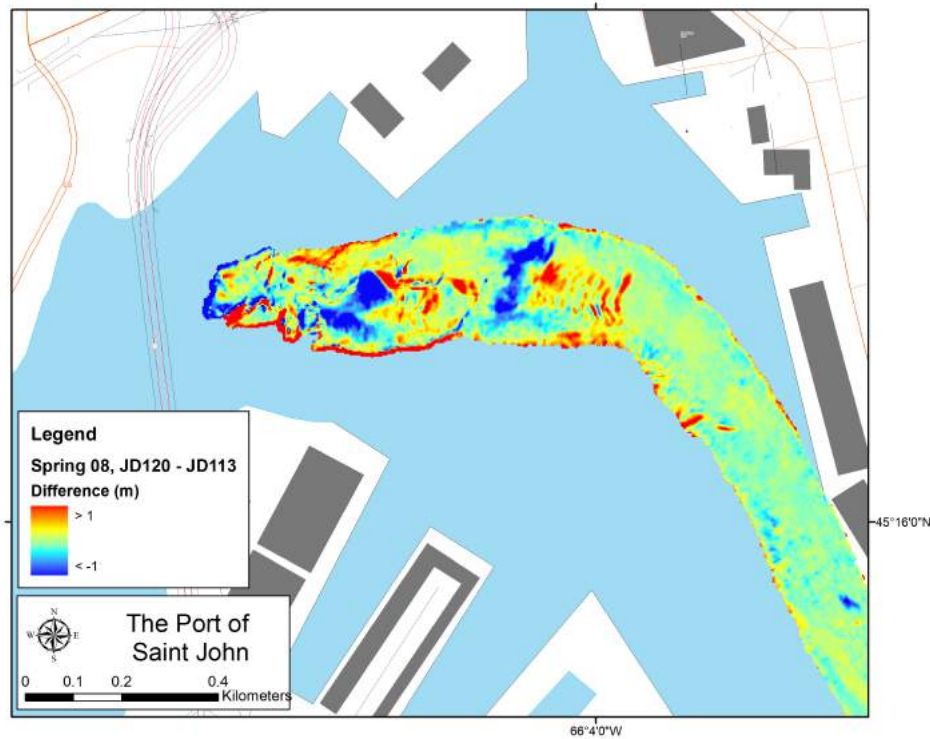


Figure 96 – Bathymetry Difference Main Harbour Channel (Spring 2008, JD120 vs. JD113)

To determine if the sediments eroded from the depressions in Figure 96 are simply deposited downstream in the depositional areas of the same figure, a rough estimation of the volume of the erosional and depositional areas was calculated. The calculation is based on the narrow area of seabed difference coverage shown in Figure 96. It was determined that approximately 12700 m³ of sediment was eroded in this area while only roughly 9900 m³ was deposited, leaving a deficiency of 2800 m³ of sediment.

Figure 97 shows the continuing effects of the spring freshet on the area directly downstream of the harbour bridge. The time range is from prior to the peak of the freshet to the end of the freshet. During this time, as shown in the seabed residual circulation from the April simulation (Figure 83), the seabed residual currents are strong in the downstream direction. Through examination of the bathymetry difference profile in Figure 98, whose location is shown in Figure 97, it can be noted that 4 metres of sediment was eroded from this area over a 30 day period.

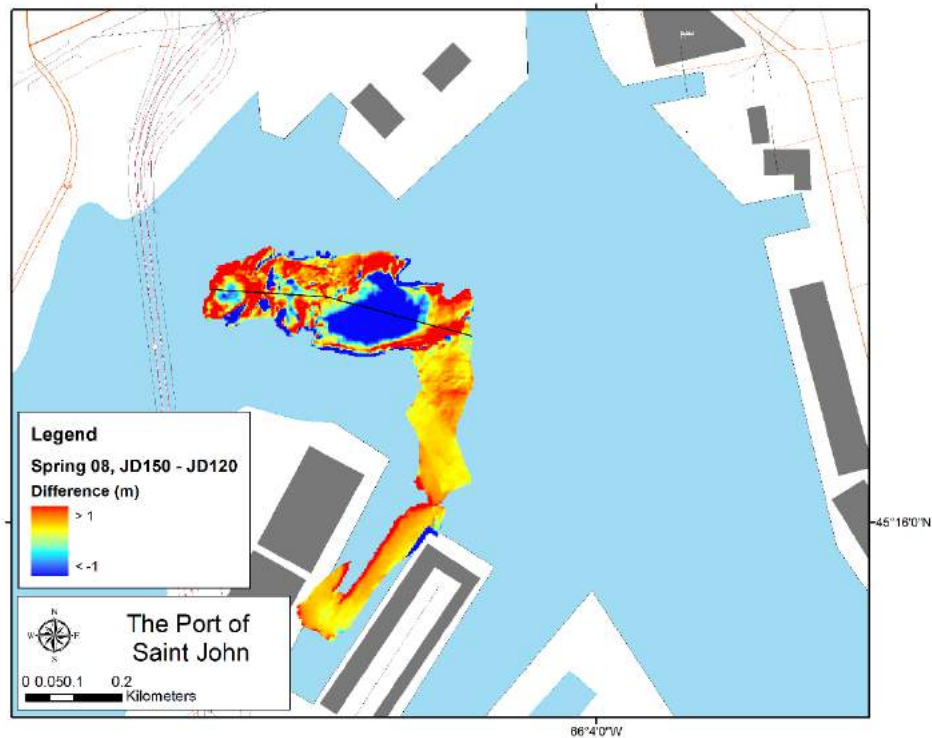


Figure 97 – Bathymetry Difference Main Harbour Channel (Spring 2008, JD150 vs. JD120)

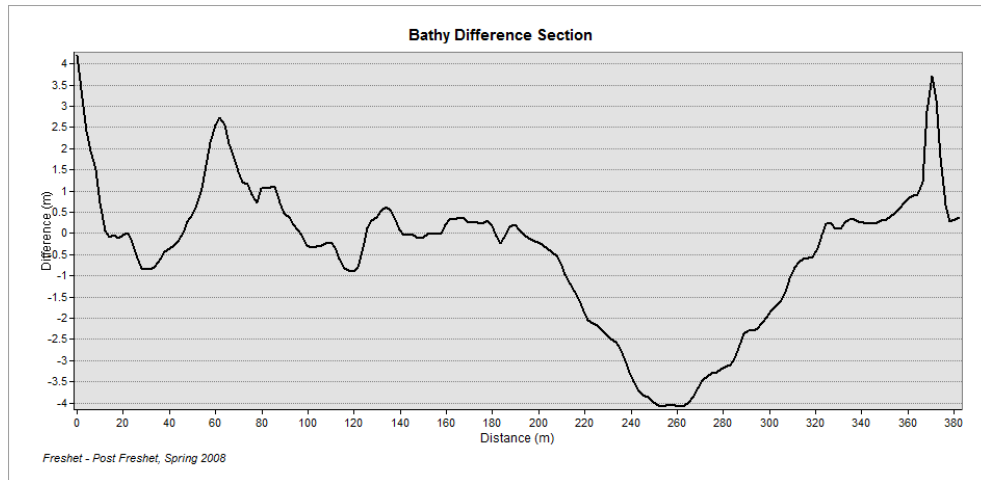


Figure 98 – Bathymetry Difference Profile (Spring 2008, JD150 vs. JD120). Negative differences correspond to areas of erosion, while positive differences correspond to areas of deposition.

6.6. Discussion of Residual Circulation

The tidally averaged residual circulation close to the seabed provides a useful indicator of the local net circulation. During the spring freshet a large residual eddy is developed in the Main Harbour channel downstream of the harbour bridge and bounded by the East and West Piers and Long Wharf. The eddy carries suspended sediment out of the primary high velocity stream in an anti-clockwise pattern towards the west piers where some is deposited by the low velocities within the berths. Leys (2007) confirms that the berth areas are active dredging locations.

The bathymetry difference maps show that the strong residual seabed currents are moving some of the sediment from the area of erosion downstream of the Harbour Bridge. A

portion of the sediment is moving to the area of deposition just downstream, but as was calculated previously through examination of the sediment volume, not all of the sediment is accounted for in the deposition area. Correlating the residual seabed currents and deficiency of eroded sediments places the movement of sediment towards the berth areas along the western piers or further downstream along the eastern piers.

The dredge volumes for just the berths along the West Pier can be compared to the annual maximum river level (Figure 99). As previously discussed in Chapter 2, there was no correlation between river level and total dredge volume for the entire harbour with an R^2 value of 0. The data observed in Figure 99 represents an R^2 value of 0.25, indicating that there is some correlation between the spring freshet and dredge volumes for this area. If the 2006 dredge volume quantity for the berth area is considered an outlier, due to over-dredging of material, then the correlation improves to an R^2 of 0.47.

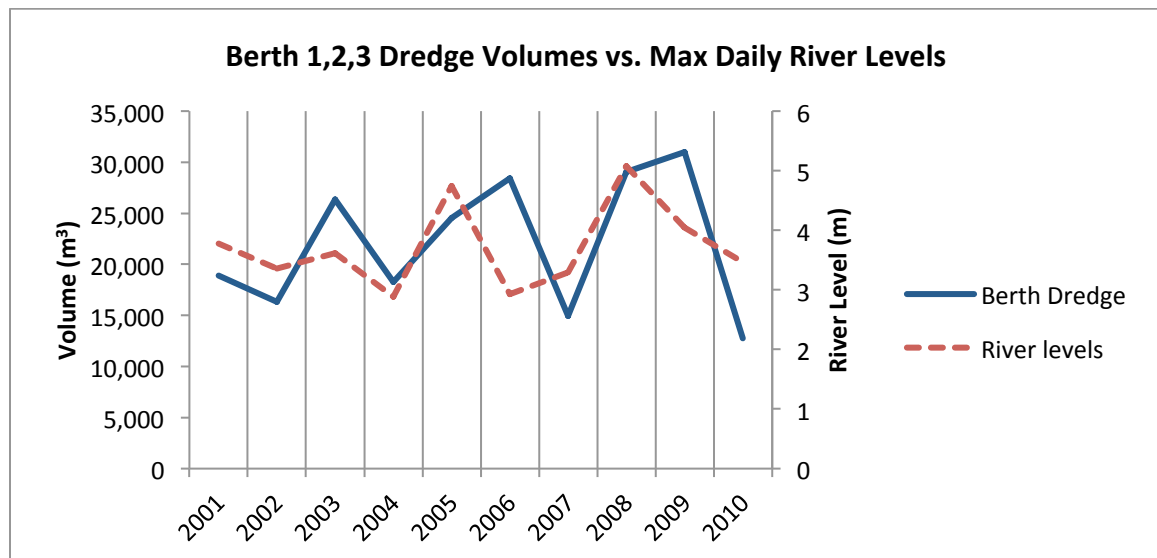


Figure 99 – West Pier Berth Dredge Volumes vs. Maximum Annual River Levels [Saint John Port Authority, 2013]

The residual seabed current velocities of the spring freshet move sediment out of the bathymetric depressions which exist downstream of the harbour bridge, while the residual velocities observed during the remainder of the year move the sediment back upstream to deposit into the depressions. These movements result in an asymmetrical annual pattern of erosion and deposition based on the strength of the spring freshet and the external input of sediments from the salt wedge. Over decadal time scales this area is probably in a state of equilibrium, but is kept annually variable through the fluctuations in the intensity of the spring freshet.

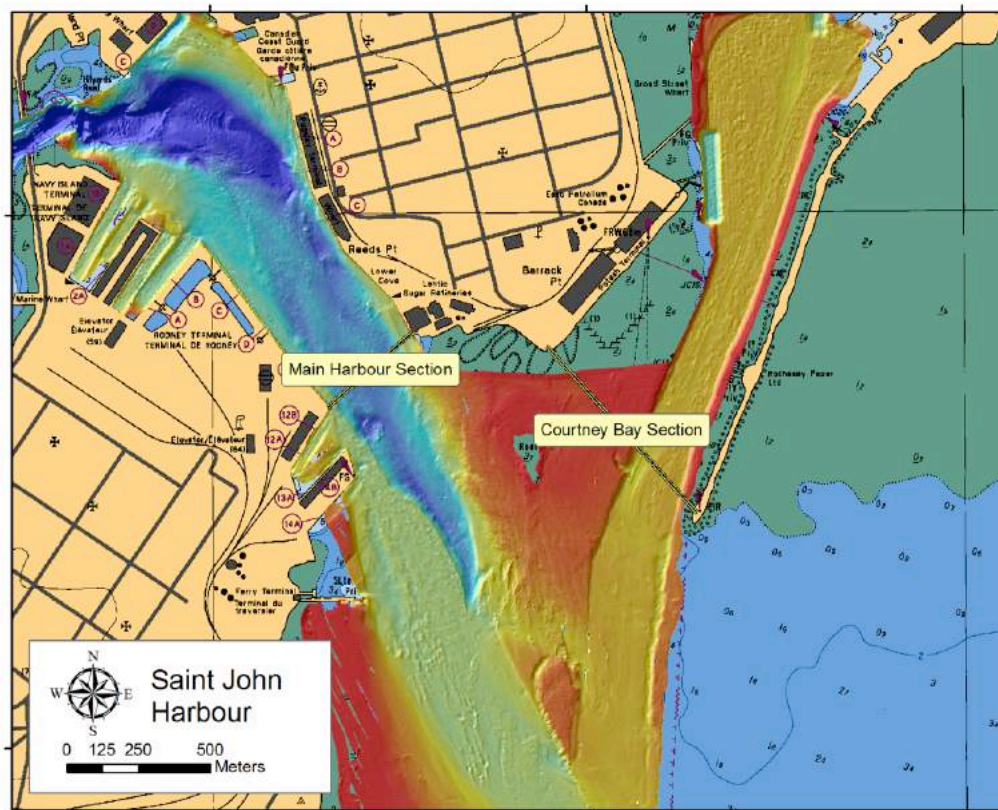
The bathymetry difference maps of Courtney Bay show the effect of the strong residual current which wraps around the end of the Courtney Bay Breakwater. The channel which corresponds to the maximum residual velocities at the end of the breakwater is naturally swept clear, while dredging is required in the surrounding areas. The area of increased deposition observed near the end of the breakwater, which occurs over the winter, corresponds to an area of elevated suspended sediment observed in the March 2009 Courtney Bay optical backscatter profiles, as discussed in section 5.3.1.

CHAPTER 7: Volume Flux Estimation

In order to assess the relative importance of the salt wedge and river input sediments, a better understanding of their relative flux is required [Hughes and Rattray Jr., 1980]. Toodesh (2012) and Melanson (2012) have both previously attempted a flux calculation in the Main Harbour using observations with extrapolation, but their extrapolation does not resolve the cross-channel variations in circulation. In Courtney Bay the velocities were too low to be resolved by Toodesh (2012) and the velocities were measured outside the channel in Melanson (2012). The model developed herein is uniquely capable of calculating the current velocities for the entrance of both channels. While the model lacks the suspended sediment concentrations, the observed backscatter values observed within profiles described in Toodesh (2012) can be extrapolated to model nodes and used for sediment flux calculations.

The model simulation data were used to determine the flux of fresh and salt water over a tidal cycle across a defined section. Through calculation of the fluxes, the mixing of the salt and fresh waters can be examined over a tidal cycle to determine the amount of estuarine transport within the system. The fluxes of salt, fresh and brackish waters were determined at the entrance to both the Main Harbour Channel and the Courtney Bay Channel. The Main Harbour channel section was placed to correspond to the section observed in Toodesh (2012).

The locations of the flux sections are shown in Figure 100. The Main Harbour Channel is the outlet for the Saint John River watershed to the ocean, which is a major source of fresh water. Courtney Bay channel has only a small amount of external fresh water input from Marsh Creek at low tide. As the output from Marsh Creek is small compared to the fresh water input from the Main Harbour Channel, it is reasonable to assume that the source of the fresh and salt waters entering Courtney Bay channel and Turning Basin originate only from the Main Harbour Channel and Bay of Fundy. Thus fresh water input from Marsh Creek was not included in the model.



To illustrate the importance of lateral variations, the fields of salinity and velocity normal to the section for April 2008 are plotted for the Main Harbour Channel section and the Courtney Bay Channel section over a tidal cycle in Figure 101 and Figure 102 respectively. In both figures upstream velocities are presented as negative values. Examining the cross channel fluctuations in salinity and velocity are very important in the calculation of the volume flux over a tidal cycle. As shown previously in Chapter 5, a section across either channel cannot be considered as invariant, something that Toodesh (2012) and Melanson (2012) had no choice but to assume.

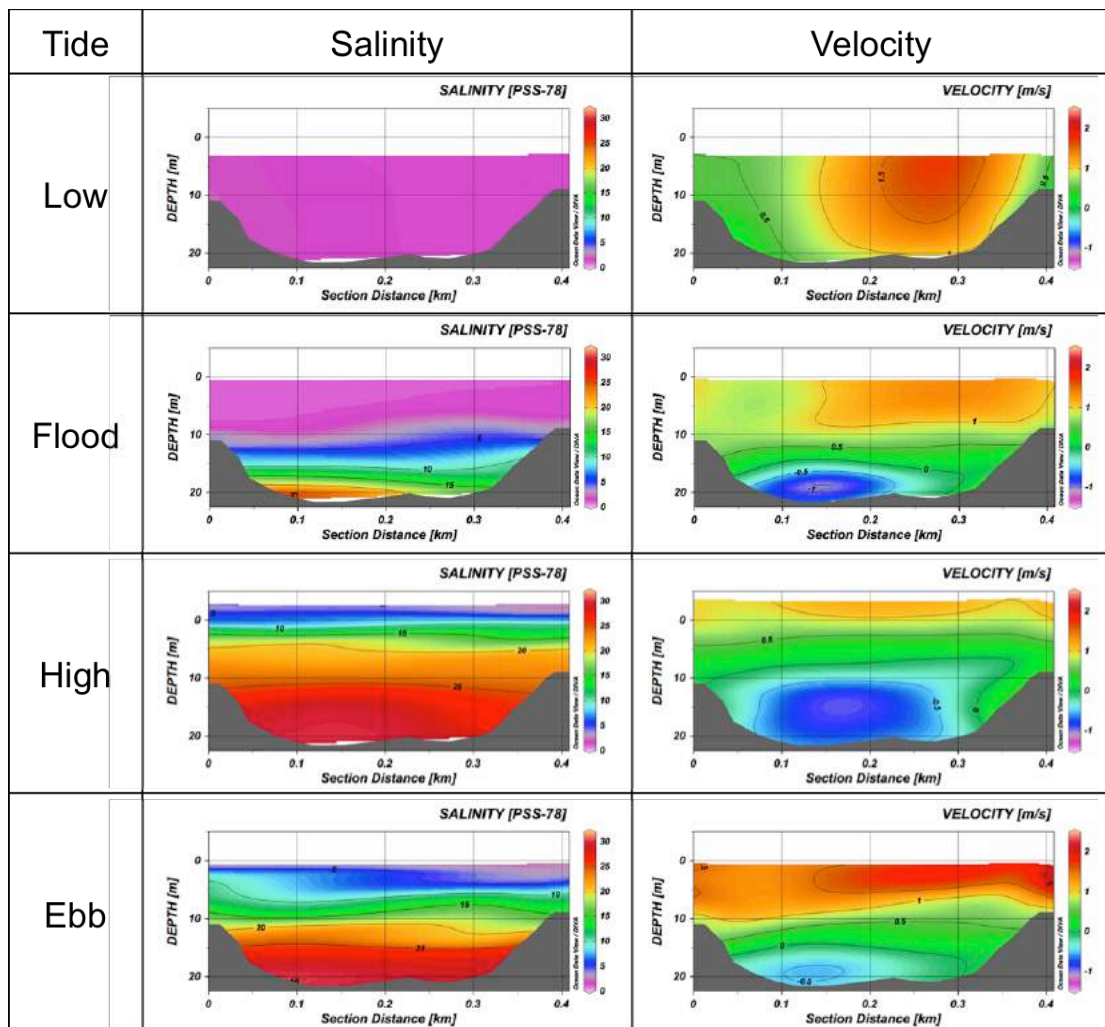


Figure 101 – April 2008 Main Harbour Volume Flux Section at four Stages of the Tide. Section is Presented from West to East Across the Channel. Depths Referenced to Mean Sea Level.

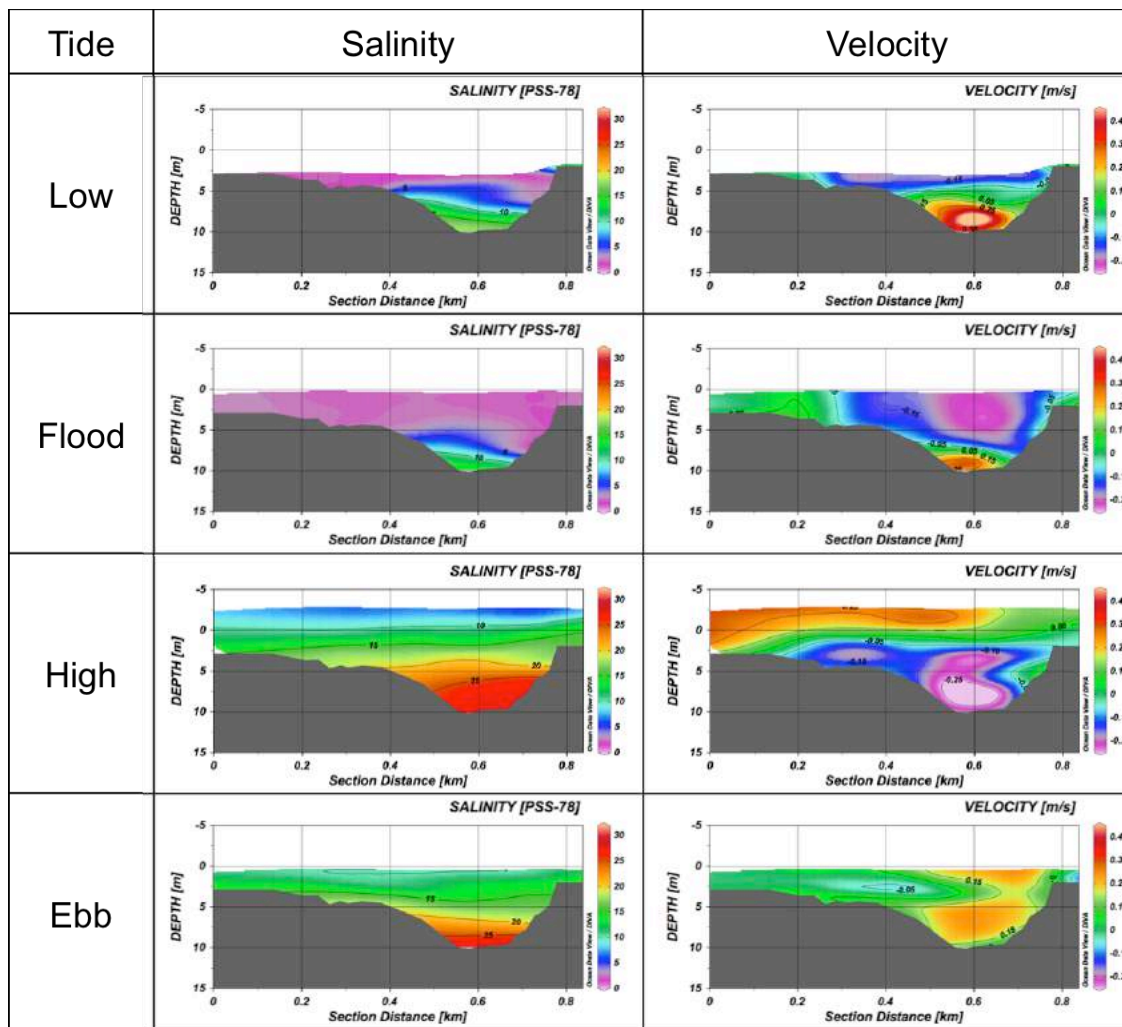


Figure 102 – April 2008 Courtney Bay Volume Flux Section at four Stages of the Tide. Section is Presented from West to East Across the Channel. Depths Referenced to Mean Sea Level.

7.1. Calculation of Model Volume Flux

The model provides velocity data at every element in the mesh at 20 vertical layers and is therefore not tied to specific areas of physical observations to determine volume fluxes, unlike previous flux estimates. To determine the volume flux, the vertical and cross

channel changes in velocities and salinity of the water masses that are predicted by the model are taken into consideration. To calculate the volume flux from the model output, coordinates are chosen for the start and end of the line. The closest nodes by distance to the specified coordinates are then chosen to represent the start and end points of the flux section. The line is divided into small segments to discretize the calculation of the areas along the line. For this investigation, the flux section was divided into 100 segments of equal length. For the Main Harbour Channel this resulted in a segment length of 3.8 metres, while the longer flux section across Courtney Bay resulted in a segment length of 7.5 metres. For each horizontal segment along the line the three closest nodes and elements by distance from the centre of the segment are determined from the model output for the flux calculation (Figure 103). The section salinity, and north and east velocity values are interpolated to the centre of the segment using an inverse distance weighted mean value from the surrounding three nodes and elements respectively. The weighted mean calculation for the three closest nodes or elements is shown in equation (2), where V represents either the salinity or component velocity variables and d represents the distance to the node or element.

$$V' = \frac{\left(\frac{1}{d_1}\right)V_1 + \left(\frac{1}{d_2}\right)V_2 + \left(\frac{1}{d_3}\right)V_3}{\left(\frac{1}{d_1}\right) + \left(\frac{1}{d_2}\right) + \left(\frac{1}{d_3}\right)} \quad (2)$$

For each segment, the vertical component is divided by the number of layers in the model and the areas of each of the resulting polygons are calculated, as shown by the blue area segment in Figure 104. Velocities along the line for each area are divided into normal and

tangential components and the normal component is multiplied by the area of the discrete area segment to obtain the volume flux. The fluxes of all the segments are then grouped into categories based on the salinity of the area segment. For this study fresh water is classified as having a salinity of less than 10 psu, brackish between 10 and 20 psu and saline as greater than 20 psu. The fluxes of each category are then summed over a tidal cycle to calculate a net residual volume flux.

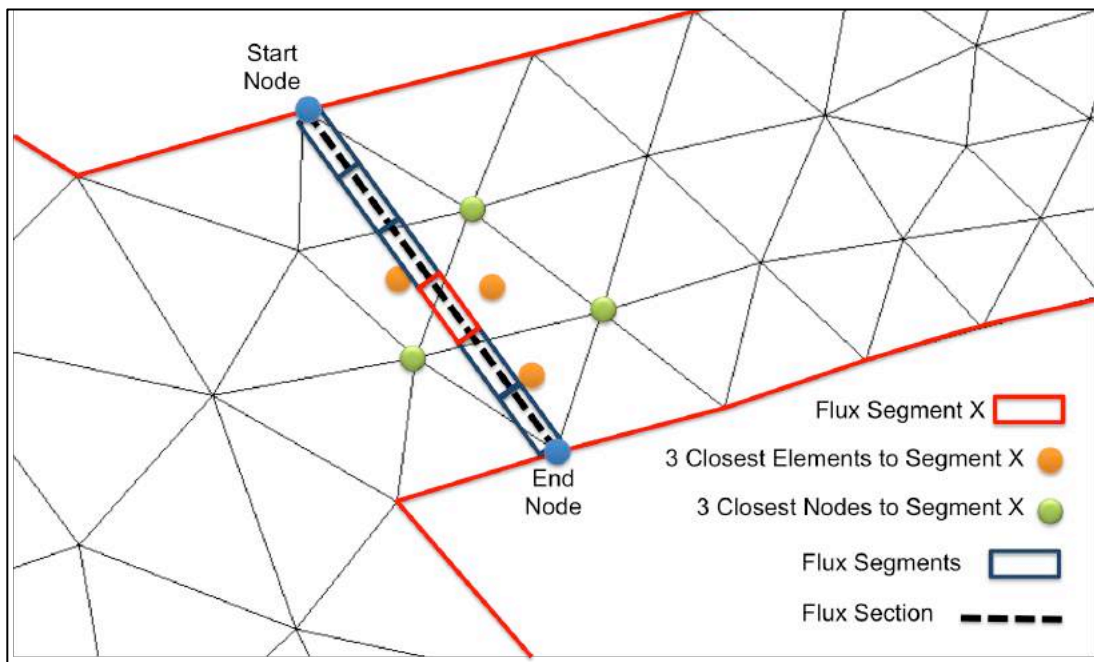


Figure 103 – Flux Segment Node and Element Averaging

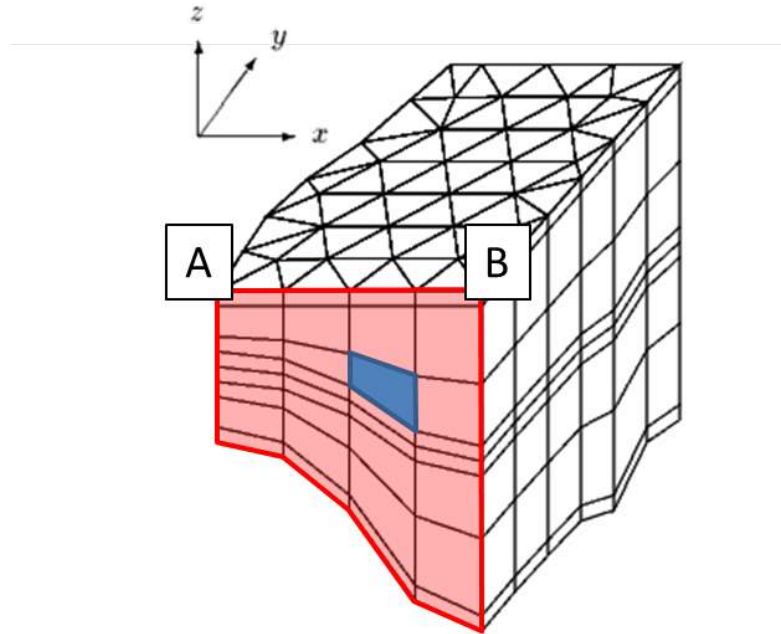


Figure 104 – Volume Flux Calculation, Modified from Ip and Lynch [1995]

The suspended sediment values from the optical backscatter probe offered by Toodesh (2012) were combined with the model volume flux calculations to provide sediment flux across each of the sections. The calculation of the flux at each node used the closest optical backscatter observation in space, time and depth, within a maximum time and space limit. The chosen suspended sediment value was then multiplied by the volume flux and categorized based on salinity to fresh, brackish or salt. The sediment concentration value was converted from milligrams per litre to kilograms per metre cubed to result in a flux estimate of kilogram per second. The sediment flux calculation required the strictly incorrect, but unavoidable, assumption that the sediment concentration did not vary in the cross channel direction.

The calculation of the model volume flux within the channels is performed with two assumptions. The first is that the sum of discrete time steps of the model simulation output corresponds exactly to a tidal cycle and second that there is no asymmetry in the tides which could lead to an imbalance in the mean flux over a tidal cycle. The model outputs data at defined time intervals, which were 30 minute intervals for the Port of Saint John simulation. As the M2 tidal cycle is 12.42 hours, the output time step of data at 12.5 hours is advanced by 0.08 hours. The high and low tides do not describe a perfect sine wave as the observed tide, or predicted tide with all available constituents, were used to force the model boundary conditions and create an asymmetry between the high and low tides. Due to these assumptions the mean volume flow in Courtney Bay may not be zero over a tidal cycle, although it should be as it is modelled as a closed basin.

7.2. Model vs. Observation Flux Comparison

The volume flux of water through the Main Harbour Channel constriction of the Saint John Harbour was examined from the output of the model simulations and compared to the results for the same time periods as the study performed in Toodesh (2012). The comparison reveals the importance of the lateral velocity and water mass variations on the flux calculation. As the model does not contain estimates of suspended sediment, only the total amount of fresh, brackish and saline water moving through the constrictions can be examined directly from the output. The observed suspended sediment was combined with the flux observations to obtain an estimate of sediment flux. At the entrance of the

Courtney Bay channel, flux estimates could not be calculated in Toodesh (2012) due to signal to noise limitations associated with the underway ADCP measurement of weak current velocities.

The volume flux calculations for the Main Harbour Channel are compared to the results from Toodesh (2012) in the following section. The majority of the observed differences in the results can be explained through the fact that the observations were only collected at one point along the cross section and that the ADCP has two large blanking zones in which no data were observed, as discussed in section 3.1. The upper blanking zone is the distance between the surface of the water and the start of ADCP signal reception. The lower blanking zone is due to side lobe interference with the seabed and therefore depends on the beam geometry. As the surface fresh water layer could be entirely within the upper blanking zone and the near seabed peak suspended sediment can be within the lower blanking zone, this is a major omission.

7.2.1. Main Harbour Channel Section

The section across the Main Harbour channel went from 45.26062° N 66.06155° W (WGS84) to 45.26296° N 66.05775° W (WGS84), as shown previously in Figure 100 and Figure 101. The tables in the following sections show the results of the flux calculations. The total mean flux and the volume and sediment fluxes of the three salinity layers are presented. A positive flux value indicates that the flow is out to sea, in a south east

direction, perpendicular to the segment. A negative value indicates that the flow was into the Harbour. As the Main Harbour channel has the influx of the Saint John River at all times of the year, the mean volume flux over a tidal cycle should always be positive. Figure 101 illustrates that the maximum depth of the section is 17m below chart datum and the width of the section is slightly greater than 400 metres.

7.2.1.1. April 2008

Table 14 shows the results of the model volume flux calculation, the results from Toodesh (2012) and the associated difference for April 2008 along the Main Harbour section. The results are divided into layers relative to the salinity of the water masses.

The model results in Table 14 indicate that fresh waters dominate the section in April. The residual flow of salt water is going into the Harbour, and is leaving in the form of mixed brackish waters. The flux of fresh water through the section is greater than, but close to, levels of the mean maximum river discharge of $2360 \text{ m}^3/\text{s}$ measured further upstream, as discussed in section 2.1. Results presented in Toodesh (2012) describe more fresh water exiting the system and more salt water entering, with less mixing to brackish water. Profiles of salinity discussed in Chapter 5 show that mixing is occurring on both the flood and ebb tide.

Table 14 – Residual Flux Results for April 2008 in Main Harbour Channel. Positive flux indicates downstream direction, towards the Bay of Fundy.

Residual Volume Flux	Model		Toodesh (2012)		Difference	
<i>Mean Volume Flow</i>	3790.82	m ³ /s	4704.00	m ³ /s	-913.18	m ³ /s
<i>Fresh <10 psu</i>	3644.21	m ³ /s	5156.00	m ³ /s	-1511.79	m ³ /s
<i>Brackish >10 && <20 psu</i>	537.54	m ³ /s	230.20	m ³ /s	307.34	m ³ /s
<i>Salt >20 psu</i>	-390.93	m ³ /s	-682.60	m ³ /s	291.67	m ³ /s

The sediment flux model estimate is presented in Table 15. The table shows that while 29 kg/s of sediment is moving into the Main Harbour Channel with the salt wedge, 114 kg/s is moving out in the fresh and brackish waters. The results from the observations of Toodesh (2012) provide similar directions and magnitudes to the model results.

Table 15 – Residual Sediment Flux Results for April 2008 in Main Harbour Channel. Positive flux indicates downstream direction, towards the Bay of Fundy.

Residual Sediment Flux	Model		Toodesh (2012)		Difference	
<i>Mean Sediment Flux</i>	92.03	kg/s				
<i>Fresh <10 psu</i>	114.35	kg/s	166	kg/s	-51.65	kg/s
<i>Brackish >10 && <20 psu</i>	6.82	kg/s	6	kg/s	0.82	kg/s
<i>Salt >20 psu</i>	-29.14	kg/s	-33	kg/s	3.86	kg/s

The evolution of the volume flux of each of the water masses can be examined over a tidal cycle for the section, as shown in Figure 105, for April 2008. At high tide the section is mostly salt water moving into the harbour, but some fresh water is still passing over the salt water to move out of the harbour. On the ebb tide, the volume of fresh water moving out of the harbour decreases, as does the amount of salt water moving in, but the brackish waters are being pushed out of the harbour. As the ebb tide finishes and tide

water levels lower, the fresh water discharge increases and dominates the flow until the salt water moves back into the harbour on the flood tide.

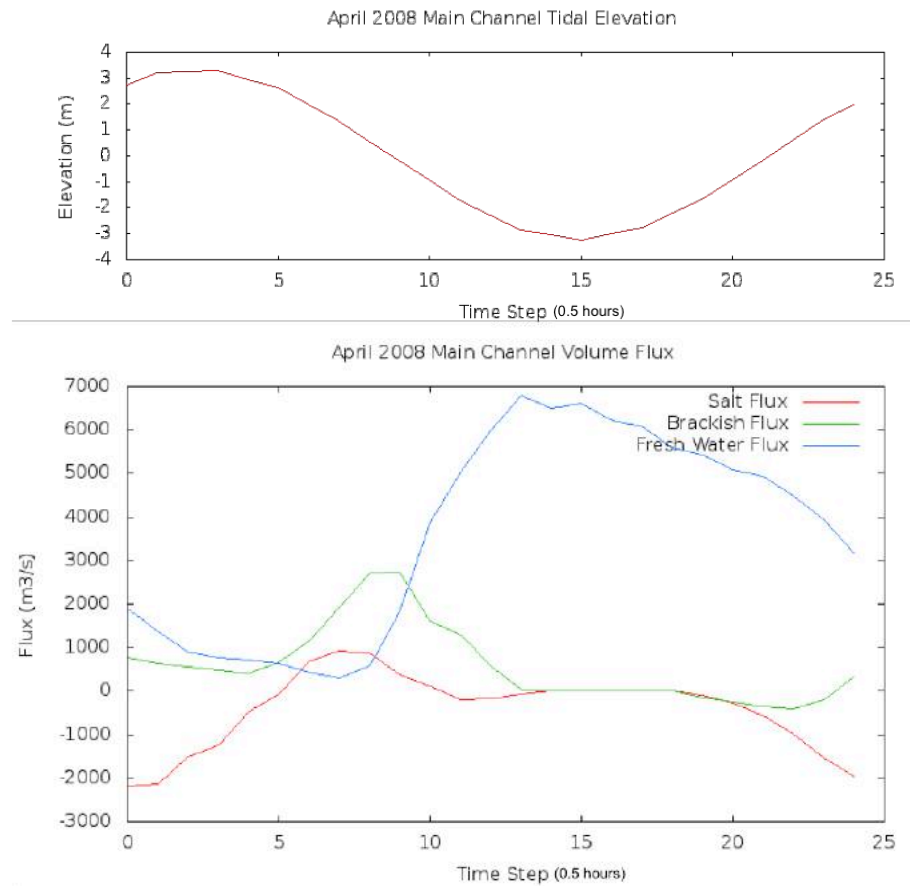


Figure 105 – April 2008 Volume Flux over a Tidal Cycle in Main Harbour

7.2.1.2. November 2008

Table 16 shows the results of the model volume flux calculations, the results from Toodesh (2012) and the associated differences for November 2008 along the Main

Harbour section. The results are divided into layers relative to the salinity of the water masses.

In November 2008 the fresh water makes up most of the residual flux through the Main Harbour Channel. This is a departure from the results obtained by Toodesh (2012), but is likely partially a result of the near surface layer which is missed by the ADCP and MVP due to instrument draft and the blanking distance as shown in Section 5.4.2. The residual fresh water output is lower than in April 2008, which is to be expected as the river level has decreased significantly from the levels observed during the spring freshet, as shown in Figure 7. The model prediction of the flux of residual mixed waters coming out of the harbour are similar to results from April 2008 and indicate that a similar amount of mixing may be occurring upstream of the section.

Table 16 – Flux Results for November 2008 in Main Harbour Channel. Positive flux indicates downstream direction, towards the Bay of Fundy.

Residual Volume Flux	Model		Toodesh (2012)		Difference	
<i>Mean Volume Flow</i>	2052.57	m ³ /s	1650.00	m ³ /s	402.57	m ³ /s
<i>Fresh <10 psu</i>	1971.92	m ³ /s	856.60	m ³ /s	1115.32	m ³ /s
<i>Brackish >10 && <20 psu</i>	479.17	m ³ /s	985.10	m ³ /s	-505.93	m ³ /s
<i>Salt >20 psu</i>	-398.52	m ³ /s	-191.60	m ³ /s	-206.92	m ³ /s

The sediment flux model estimate is presented in Table 17. As observed in April 2008, the salt wedge is inputting sediment to the area upstream of the section. The brackish and freshwater layers are carrying the sediment back out of the harbour and downstream of the section. The model shows significantly more sediment in the fresh waters than the

brackish water, which is different from the results of Toodesh (2012) where the distribution was even. This is again likely a result of modelling the near surface fresh water layer.

Table 17 – Residual Sediment Flux Results for November 2008 in Main Harbour Channel. Positive flux indicates downstream direction, towards the Bay of Fundy.

Residual Sediment Flux	Model		Toodesh (2012)		Difference	
<i>Mean Sediment Flux</i>	16.56	kg/s				
<i>Fresh <10 psu</i>	26.04	kg/s	24	kg/s	2.04	kg/s
<i>Brackish >10 && <20 psu</i>	2.71	kg/s	23	kg/s	-20.29	kg/s
<i>Salt >20 psu</i>	-12.19	kg/s	-18	kg/s	5.81	kg/s

Examination of the evolution of the volume fluxes in Figure 106 shows how mixing has changed in the channel compared to the April observation. In November there is a peak of salt water output on the ebb tide, which is not observed in the April flux data. This indicates that the first water mass to move out of the harbour is the salt waters which were not mixed in the channel. Later during the ebb tide there is a peak in the mixed waters which follows the salt waters. This peak is later in the tidal cycle than it was during April. The maximum discharge of fresh water is still at low tide as expected.

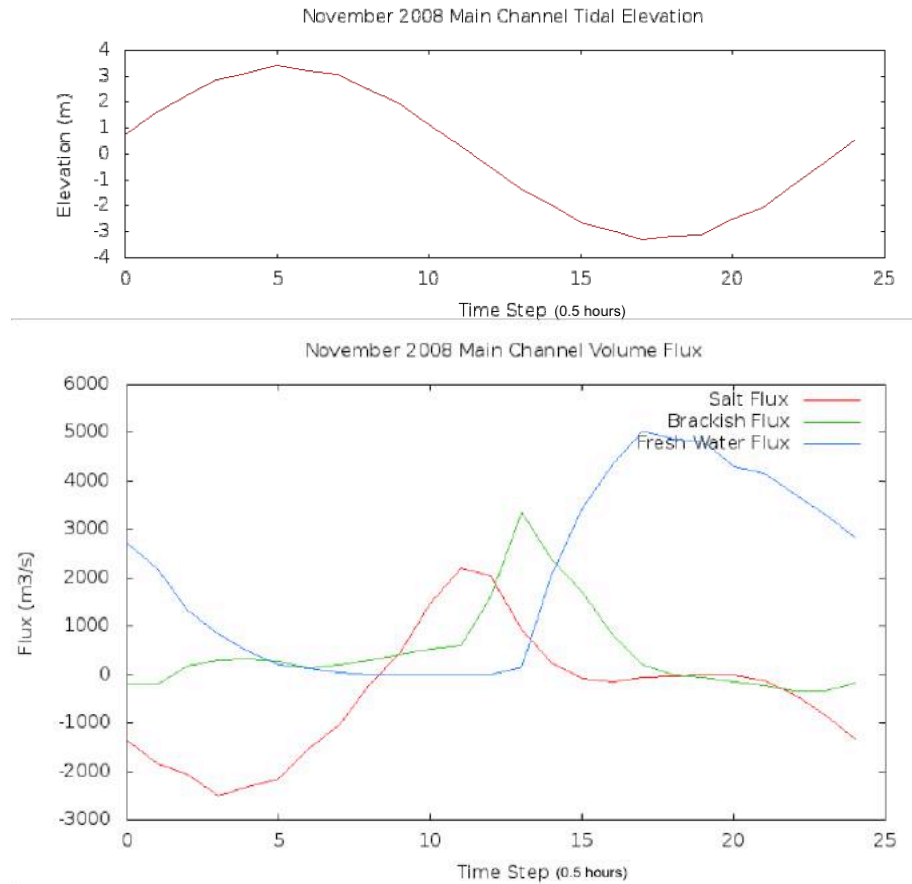


Figure 106 – November 2008 Volume Flux over a Tidal Cycle in Main Harbour

7.2.1.3. March 2009

Table 18 shows the results of the model volume flux calculation, the results from Toodesh (2012) and the associated difference for March 2009 along the Main Harbour section. The results are divided into layers relative to the salinity of the water masses.

The distinct feature of the March residual flux analysis is that there is no fresh water

travelling through the section. This is observed in both the model data and in the data from Toodesh (2012). There is a large amount of mixed brackish water exiting the system, which indicates that the fresh water from the river is completely mixed as it exits the channel. This corresponds to observations in Section 5.4.3 which suggest that mixing is occurring upstream of the Reversing Falls. The residual quantity of salt water entering the system is over double the amounts observed in November which indicates that more entrainment is occurring upstream of the section in March which is pulling more salt water into the system. The high values of brackish waters exiting the channel, which are also over double the levels observed in November, can be attributed to mixing from the upstream entrainment. The mean annual minimum river discharge of $250 \text{ m}^3/\text{s}$, as discussed in section 2.1, is similar to, but greater than, the mean volume flow of $131.04 \text{ m}^3/\text{s}$.

Table 18 – Flux Results for March 2009 in Main Harbour Channel. Positive flux indicates downstream direction, towards the Bay of Fundy.

Residual Volume Flux	Model		Toodesh (2012)		Difference	
<i>Mean Volume Flow</i>	131.04	m^3/s	-211.30	m^3/s	342.34	m^3/s
<i>Fresh <10 psu</i>	0.00	m^3/s	0.00	m^3/s	0.00	m^3/s
<i>Brackish >10 && <20 psu</i>	982.48	m^3/s	657.20	m^3/s	325.28	m^3/s
<i>Salt >20 psu</i>	-851.44	m^3/s	-868.50	m^3/s	17.06	m^3/s

The sediment flux model estimate is presented in Table 19. In March, the inflow of high suspended sediment salt water is not compensated by a strong outflow of sediment laden fresh water. Therefore the mean sediment flux results in movement upstream into the

harbour. The model results provide a close relationship with the results of Toodesh (2012).

Table 19 – Residual Sediment Flux Results for March 2008 in Main Harbour Channel. Positive flux indicates downstream direction, towards the Bay of Fundy.

Residual Sediment Flux	Model		Toodesh (2012)		Difference	
<i>Mean Sediment Flux</i>	-11.64	kg/s				
<i>Fresh <10 psu</i>	0.00	kg/s	0	kg/s	0.00	kg/s
<i>Brackish >10 && <20 psu</i>	6.64	kg/s	9	kg/s	-2.36	kg/s
<i>Salt >20 psu</i>	-18.27	kg/s	-34	kg/s	15.73	kg/s

Examination of the evolution of the volume fluxes in Figure 107 shows how the water masses are moving during a tidal cycle. Similar to November, a peak of salt water outflow is visible, which indicates that the mixing is occurring further upstream than it was in April. The maximum flow of brackish waters is at low tide.

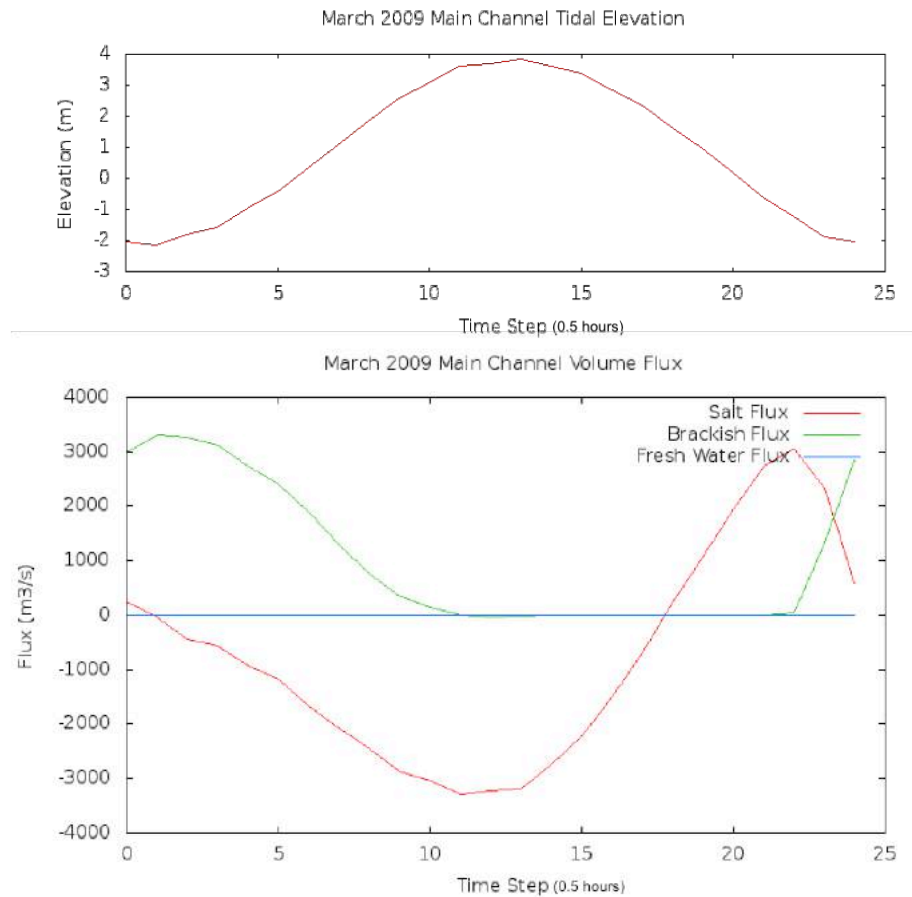


Figure 107 – March 2009 Volume Flux over a Tidal Cycle in Main Harbour

7.2.1.4. June 2009

Table 20 shows the results of the model volume flux calculation, the results from Toodesh (2012) and the associated difference for June 2009 along the Main Harbour section. The results are divided into layers relative to the salinity of the water masses.

The residual quantity of salt water entering the Main Harbour Channel in June is similar to the quantities observed in April 2008 and November 2008, while the quantity of mixed brackish water exiting the Main Harbour Channel is close to the levels observed in March 2009. The quantity of fresh water exiting the system is low compared to April and November, as would be expected considering the observed river levels. There is however, a fresh water layer present, unlike the March simulation period. The model describes a lower quantity of fresh waters exiting the Harbour compared to observations by Toodesh (2012), but greater brackish and salt water flux. The difference in the salt water flux is likely accounted for by the limitations in physically sampling the near seabed layers. Sediment fluxes could not be calculated for June 2009 due to a malfunction of the optical backscatter probe.

Table 20 – Flux Results for June 2009 in Main Harbour Channel. Positive flux indicates downstream direction, towards the Bay of Fundy.

Residual Volume Flux	Model		Toodesh (2012)		Difference	
<i>Mean Volume Flow</i>	580.61	m ³ /s	759.90	m ³ /s	-179.29	m ³ /s
<i>Fresh <10 psu</i>	113.46	m ³ /s	293.10	m ³ /s	-179.64	m ³ /s
<i>Brackish >10 && <20 psu</i>	806.02	m ³ /s	611.80	m ³ /s	194.22	m ³ /s
<i>Salt >20 psu</i>	-338.87	m ³ /s	-145.00	m ³ /s	-193.87	m ³ /s

Figure 108 displays the volume flux over a tidal cycle for June. On the ebb tide, there is a plug of salt, brackish and fresh water exiting the harbour in succession. As there is still a fresh water surface layer in June, unlike March, the fresh water appears at low tide when it is moving out through the Main Harbour Channel. The presence of the fresh water outflow is short lived as it is suppressed by the rising tide.

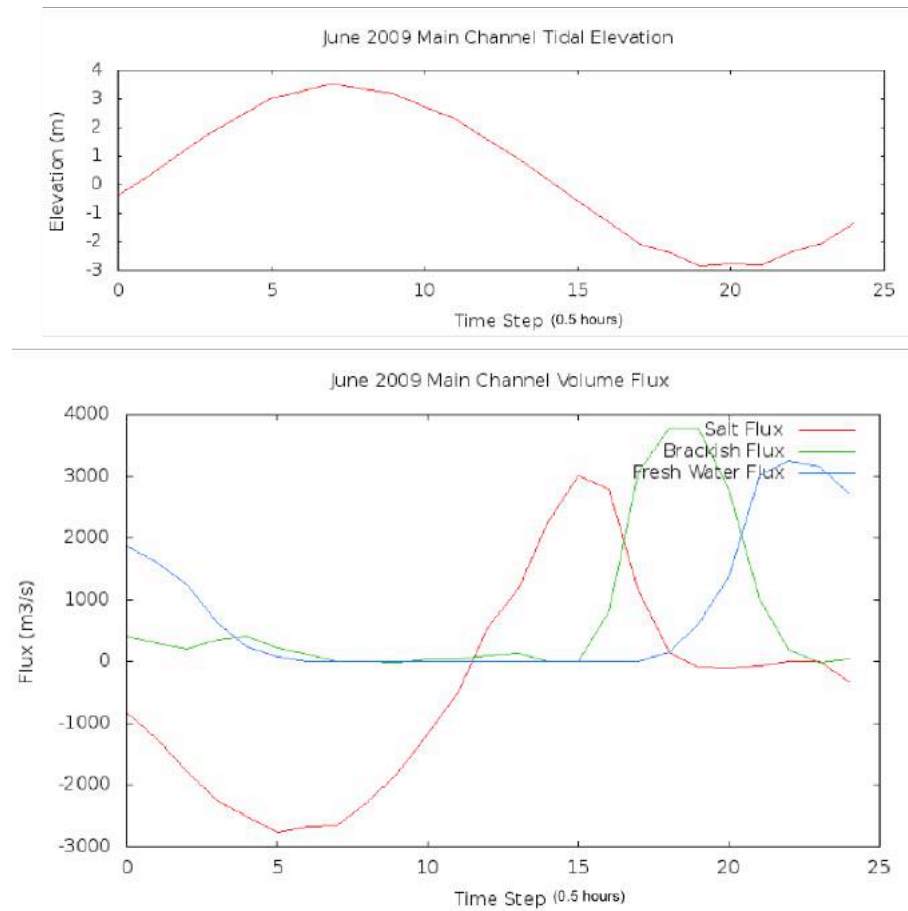


Figure 108 – June 2009 Volume Flux over a Tidal Cycle in Main Harbour

7.2.2. Courtney Bay Section

The flux across the mouth of Courtney Bay has not been calculated in previous studies, but as most of the dredging occurs within this area the flux estimates here are the most critical. The ADCP current observations from Toodesh (2012) held too little a signal to noise ratio to extract usable data and the bottom mounted ADCP observations of Melanson (2012) were taken outside the channel, south of the end of the breakwater. The

model resolves the low current velocities and includes the variations in flow over the intertidal areas.

The flux section across the Courtney Bay Channel went from 45.26248° N 66.05184° W (WGS84) to 45.25725° N 66.04520° W (WGS84), as shown previously in Figure 102.

The tables in the following sections reveal the results of the flux calculation including the total mean flux and the flux of the three layers. A positive flux value indicates that the flow is out to sea, in a southwest direction, perpendicular to the segment. A negative value indicates that the flow is into Courtney Bay. Figure 102 shows that the maximum depth of the section approximately 7 metres below chart datum and the width of the section is more than 600 metres.

7.2.2.1. April 2008

Table 21 shows the residual volume flux in Courtney Bay for April 2008. Averaged over an approximate semi-diurnal tidal cycle, the fresh river waters coming from the Saint John River and the salt waters of the Bay of Fundy are moving into the bay. After the two water masses enter the bay, they are mixed and flow out as brackish waters.

Table 21 – Flux Results for April 2008 in Courtney Bay

Residual Volume Flux	Model	
<i>Fresh <10 psu</i>	-64.89	m ³ /s
<i>Brackish >10 && <20 psu</i>	124.94	m ³ /s
<i>Salt >20 psu</i>	-82.62	m ³ /s

The sediment flux model estimate is shown in Table 22. In April sediment is input to Courtney Bay through both the fresh and salt water layers. Only a portion of the sediment is flushed back out of the bay with the brackish waters. The elevated levels of sediment from the fresh and salt water layers results in a net sediment flux of 5.69 kg/s into Courtney Bay.

Table 22 – Sediment Flux Results for April 2008 in Courtney Bay

Residual Sediment Flux	Model	
<i>Mean Sediment Flux</i>	-5.69	kg/s
<i>Fresh <10 psu</i>	-3.95	kg/s
<i>Brackish >10 && <20 psu</i>	1.11	kg/s
<i>Salt >20 psu</i>	-2.85	kg/s

Figure 109 displays the volume flux of the water masses over a tidal cycle. At high tide, the fresh river waters are leaving the area as the salt wedge enters the channel. As the ebb tide begins, the brackish waters replace the fresh waters exiting the section. At the end of the ebb tide, the brackish waters are joined by some salt waters leaving the area. At low tide, and continuing until the end of the flood tide, fresh waters are entering the bay.

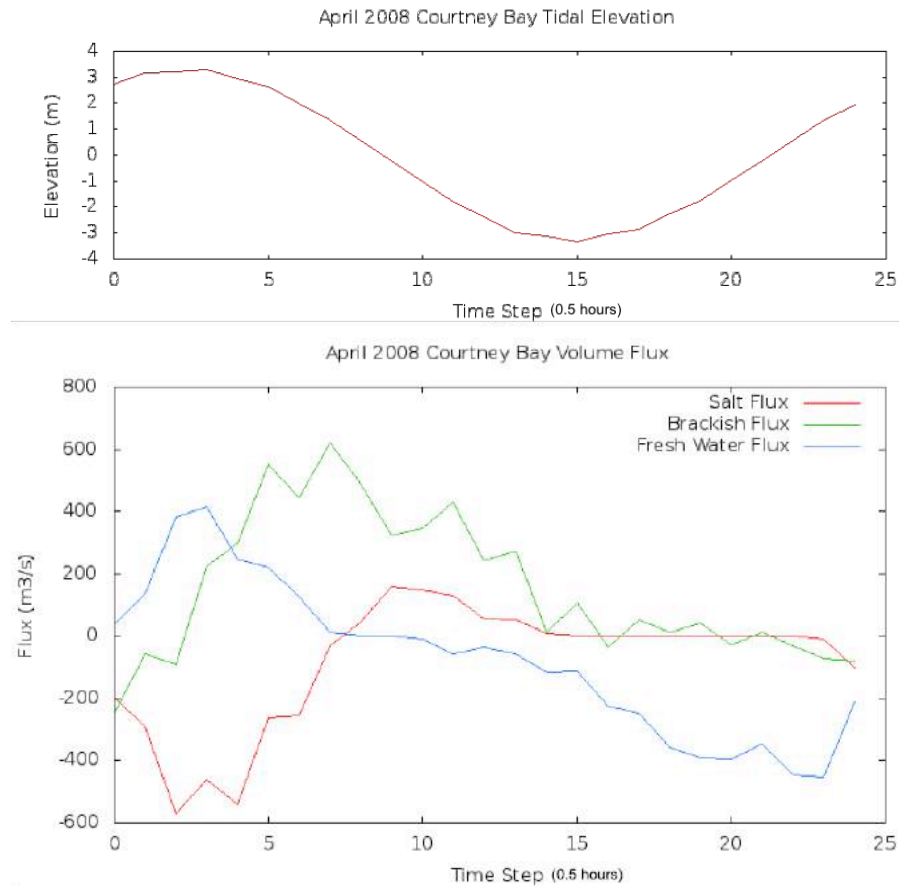


Figure 109 – April 2008 Volume Flux over a Tidal Cycle in Courtney Bay

7.2.2.2. November 2008

In November 2008, the residual flux of fresh water moving into the bay is higher than it was in April 2008, as shown in Table 23. Examining the evolution of the flux of fresh water for April 2008 (Figure 109) and November 2008 (Figure 110) reveals that very little fresh water is exiting Courtney Bay in November, which leads to the increased upstream flux of fresh water observed in Table 23. The mean flux of salt water is very close the calculated values for April 2008.

Table 23 – Flux Results for November 2008 in Courtney Bay

Residual Model Flux Results		
<i>Fresh <10 psu</i>	-102.81	m ³ /s
<i>Brackish >10 && <20 psu</i>	153.75	m ³ /s
<i>Salt >20 psu</i>	-84.87	m ³ /s

Table 24 displays the sediment flux results estimated from the model output. In November 2008 the sediment flux out of Courtney Bay in the brackish water layer is greater than it was in April, while the incoming sediment flux in the fresh and salt water layer is weaker. This results in a smaller mean flux result of 2.38 kg/s into the bay.

Table 24 – Sediment Flux Results for November 2008 in Courtney Bay

Residual Model Sediment Flux Results		
<i>Mean Sediment Flux</i>	-2.38	kg/s
<i>Fresh <10 psu</i>	-1.87	kg/s
<i>Brackish >10 && <20 psu</i>	1.21	kg/s
<i>Salt >20 psu</i>	-1.72	kg/s

Examination of the evolution of the fluxes in November over a tidal cycle is shown in Figure 110. The primary difference in comparison to the April flux evolution is the diminished fresh water output through the section at high tide. The peak level of brackish water output and salt water input are very similar to April.

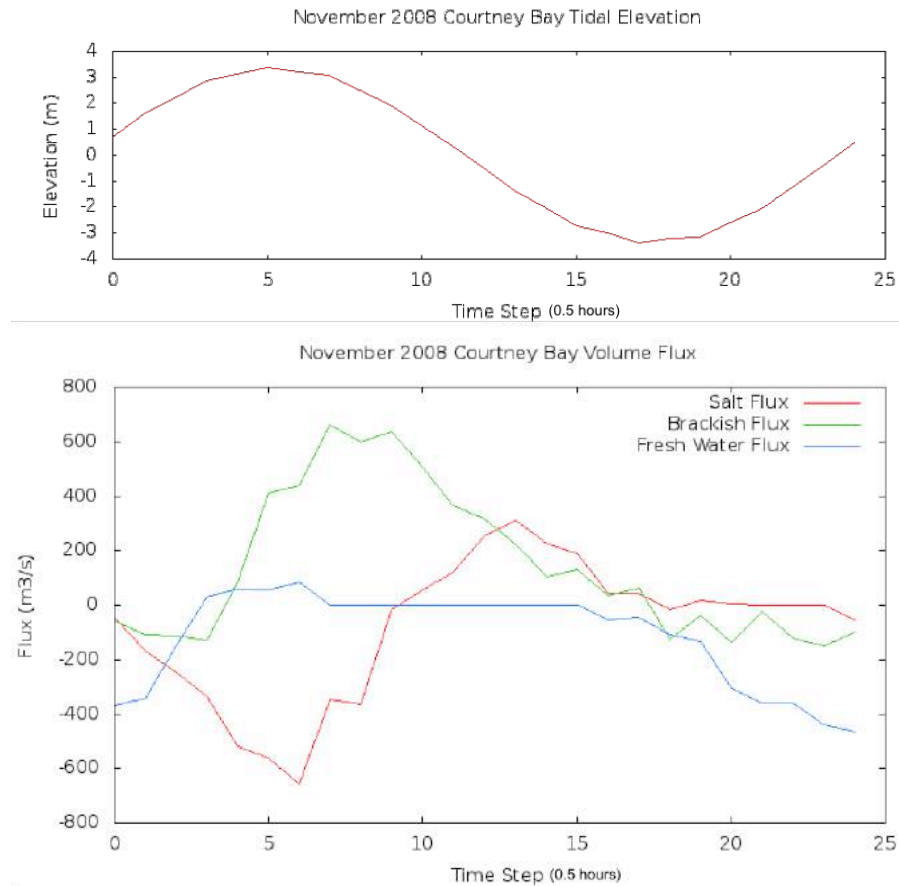


Figure 110 – November 2008 Volume Flux over a Tidal Cycle in Courtney Bay

7.2.2.3. March 2009

The minimum salinity value observed in March 2009 is approximately 10 psu, therefore the previously established ranges for salt, brackish and fresh water will not identify the sources of incoming waters in the flux calculation. Dividing the range of salinities into three equal parts for March yields fresh water with a salinity of less than 17 psu and salt water with salinity of greater than 24 psu. This range was not used for the previous flux

estimates through the Main Harbour Channel for March as the flux through that section was compared to pre-existing ranges established in Toodesh (2012).

The volume flux results for March 2009 based on the new ranges are shown in Table 25. As previously observed in April 2008 and November 2008, waters originating from the river through the Main Harbour Channel and waters from Bay of Fundy are entering the Courtney Bay Channel. The fresher surface waters and saline lower waters are mixing within the channel and exiting as brackish water.

Table 25 – Flux Results for March 2009 in Courtney Bay

Residual Model Flux Results		
<i>Fresh <17 psu</i>	-134.70	m ³ /s
<i>Brackish >17 && <24 psu</i>	61.57	m ³ /s
<i>Salt >24 psu</i>	-104.66	m ³ /s

Table 26 displays the sediment flux estimates for March from the model output. Sediment is moving into the channel through both the fresh and saline layers, while very little sediment is leaving the channel in the brackish layer. During this time of year, unlike April and November, there is more sediment moving into the Courtney Bay Channel through the salt water layer rather than the fresh surface waters. The mean flux of sediment is only slightly less than levels observed in November.

Table 26 – Sediment Flux Results for March 2009 in Courtney Bay

Residual Model Sediment Flux Results		
<i>Mean Sediment Flux</i>	-1.86	kg/s
<i>Fresh <17 psu</i>	-0.51	kg/s
<i>Brackish >17 && <24 psu</i>	0.03	kg/s
<i>Salt >24 psu</i>	-1.38	kg/s

Figure 111 shows the flux of fresh, brackish and saline waters over a tidal cycle for March. The relative timing of the inflow and outflow of fresh, brackish and saline waters are similar to profiles in November and April, although the magnitudes are less.

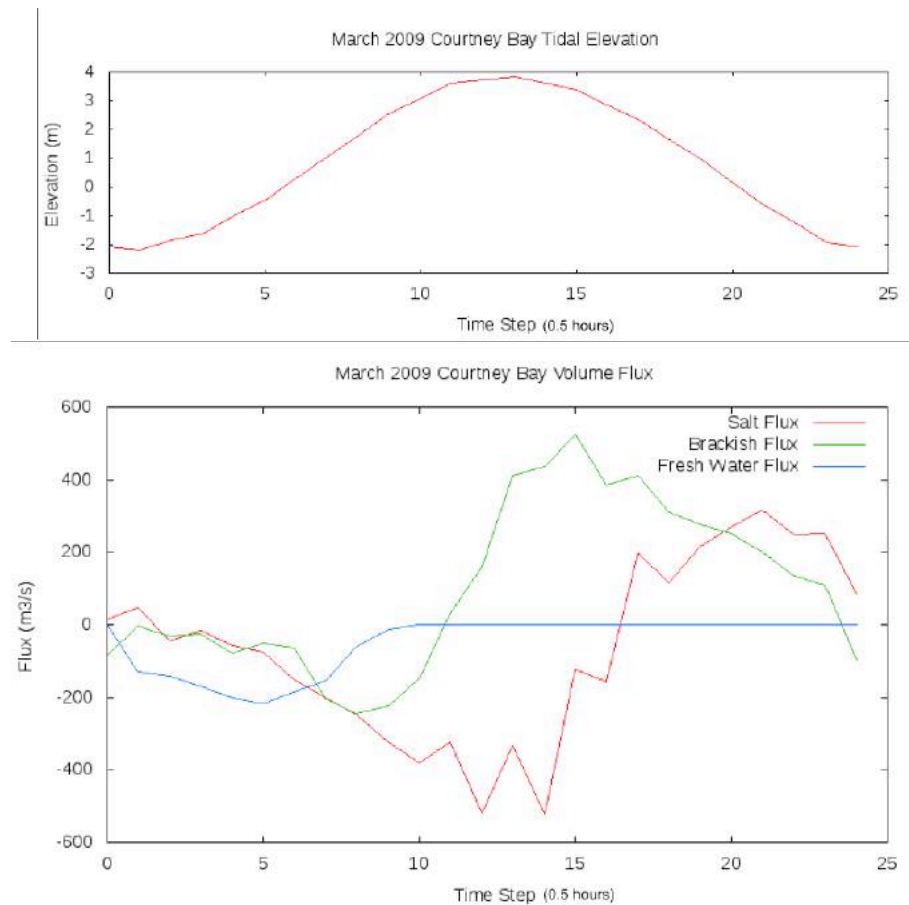


Figure 111 – March 2009 Volume Flux over a Tidal Cycle in Courtney Bay

7.2.2.4. June 2009

Table 27 shows the residual flux results for the June 2009 simulation. For June the defined ranges of fresh, brackish and saline water from March have been used for analysis. Similar to March 2009, the minimum salinity observed is approximately 8 psu. The residual flux of brackish water is out of the harbour and the flux of salt and fresh waters are into the harbour, averaged over a tidal cycle. This indicates that incoming saline and fresh water masses are mixing in the channel and resulting in a brackish flow out of the channel. The nature of the mixing is similar to the other simulation times. As there were no observations of optical backscatter in June, a sediment flux cannot be calculated.

Table 27 – Flux Results for June 2009 in Courtney Bay

Residual Model Flux Results		
<i>Fresh <17 psu</i>	-64.89	m ³ /s
<i>Brackish >17 && <24 psu</i>	124.94	m ³ /s
<i>Salt >24 psu</i>	-82.62	m ³ /s

Figure 112 illustrates the progression of the water masses over a tidal cycle. The fresh water enters the channel only near low tide when fresh water is flowing out of the Main Harbour Channel. On the flood tide, the fresh water is been pushed back out of the channel until it has been replaced by a downstream flow of brackish waters leaving the

channel at high tide. High tide is also when the maximum inflow of saline water is observed. Approaching low tide both saline and brackish waters are exiting the channel.

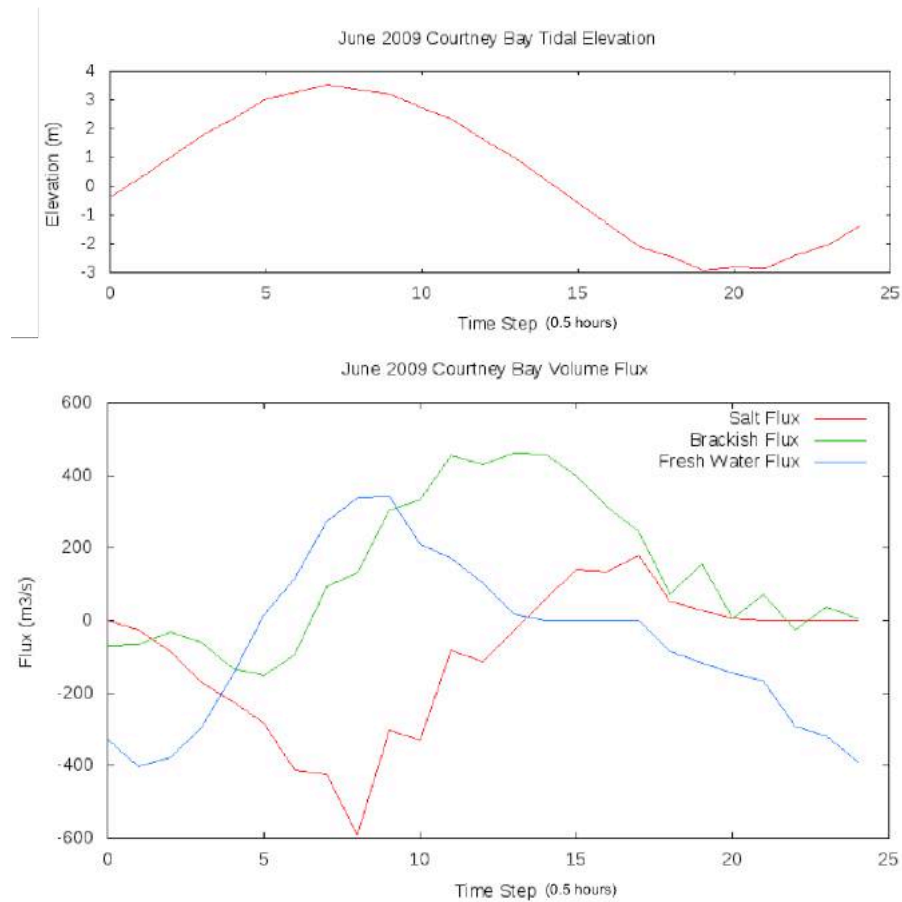


Figure 112 – June 2009 Volume Flux over a Tidal Cycle in Courtney Bay

7.3. Discussion of Model Flux Estimates

Examination of the timing and flux of salt, fresh and brackish waters through the Main Harbour Channel and Courtney Bay allows for an improved understanding of the mixing

within the respective areas. The estuarine mixing of fresh river water with the salt wedge has been analyzed within the Main Harbour channel to determine the predominant location of mixing and the tidal influence. In Courtney Bay the quantity of mixing within the closed basin has been evaluated to determine the relative effects of the fresh and salt waters. Through the addition of suspended sediment observations to the model flux estimates, an improved understanding of the movement of the sediment laden water was developed. This is especially true within Courtney Bay, where insufficient data coverage and quality has not allowed for these quantities to be previously calculated.

The sediment flux results for the Main Harbour Channel in the salt wedge are similar for all three times of the year with values ranging from 12 to 29 kg/s of sediment moving upstream. The maximum amount of sediment moving out of the Main Harbour Channel is observed in April at 114.35 kg/s. In November only a quarter of the April sediment magnitude is moving out of the harbour averaged over a tidal cycle. In March, the sediment is moving upstream in the Main Harbour Channel and is therefore settling within the estuary, likely to be resuspended during the April spring freshet.

In Courtney Bay any suspended sediment that is moving into the bay, and is not flushed out again, must be settling within the bay. Examining the mean sediment flux across the Courtney Bay section reveals an estimate of the annually varying quantity of suspended sediment settling within the area upstream of the section. The maximum value of the calculated sediment flux is in April, while the lowest rate is in March. In March the salt

wedge provides more influence on the input sediment than the fresh water, while the opposite is found in November and April.

In April the mixed waters which flow out through the Main Harbour exit earlier in the tidal cycle than during the other simulation periods. This is because the mixing of the fresh river waters and the salt wedge occurred between the Harbour Bridge and the Reversing Falls in April, while it occurred further upstream during the other periods. For the November, March and June simulation periods a significant component of the mixing is likely happening after the salt wedge has passed over the Reversing Falls. These observations are confirmed by the salinity profile analysis of section 5.4. For the flux assessment associated with those periods, the unmixed salt wedge comes down through the harbour first, followed by the mixed waters of the estuary above the Reversing Falls.

As any net salt water inflow must reflect tidally averaged entrainment, the residual salt water flux for each simulation period provides a proxy for the overall entrainment flux associated with the mixing of salt and fresh waters within the estuary. The annual variations in the salt flux through the Main Harbour Channel section are minimal indicating that the entrainment flux is also relatively constant. The reach of the estuary varies significantly over each of the simulation periods as described in Delpeche (2007) and Metcalfe (1976). This then implies that in April the quantity of mixing within the relatively short distance between the Main Harbour Bridge and the Reversing Falls is similar to the overall mixing in November, March and June where the salt wedge progresses much further up the river.

The source of the fresh water that enters Courtney Bay is entirely from the Main Harbour Channel via the Round Reef area between the two channels. Examination of the flux values of the fresh waters over a tidal cycle through each of the sections reveals the relative quantity of fresh water from the Main Harbour Channel that enters Courtney Bay for each simulation period. The fresh water which enters Courtney Channel depends on the interaction of the fresh waters from the Main Harbour Channel and the outflowing waters of Courtney Bay, as shown in Section 5.2, which are a function of the Saint John River discharge and the tidal range. Table 28 shows the maximum modeled relative quantity of fresh water entering Courtney Bay from the Main harbour Channel for the April and November simulation periods over a tidal cycle. The March and June periods were omitted as very little fresh water is present at those times and they used a different reference scale for water mass calculation in Courtney Bay. The table reveals that conditions in November, during the fall freshet and neap tides, allowed for the maximum relative quantity of fresh water to flow in Courtney Bay. If the spring freshet had occurred at a time of neap tides in 2008 the relative influence of fresh waters for the April simulation may have been greater.

Table 28 – Relative Influence of Fresh water in Courtney Bay from Main Harbour

Simulation Period	Relative Influence	Tidal Period at Maximum Exchange
<i>April 2008</i>	12 %	Mid Flood Tide
<i>November 2008</i>	16 %	Mid Flood Tide

CHAPTER 8: Hydrographic Vertical Uncertainty Assessment

Hydrographic MBES surveys within the Port of Saint John are plagued with systematic errors associated with not sufficiently capturing variations in the sound speed field as discussed in section 6.5. The sound speed structure changes rapidly over a tidal cycle and the surveyor may not be able to accurately capture the variations. The error in sound speed will result in depth errors in the bottom detections of the multibeam system and restrict the achievable swath width of a survey. Narrow swath widths require additional lines to be collected to ensure 100% coverage of the seabed and frequent stops to collect updated sound speed profiles leads to inefficiencies in data collection. In the Port of Saint John, hydrographic multibeam surveys of the dredge areas are performed on a regular basis to monitor the dredge volumes and to guide operations. For that application, the allowable uncertainty in depth soundings must be restricted to the sub-decimeter level to resolve changes in harbour morphology and to ensure that dredge volumes are measured accurately for invoice calculations.

To understand the consequence of uncertainty in model output variables, as discussed in Chapter 4, the results can be described in terms of a potential application of the model output. The accuracy of MBES surveys depends on many factors, but knowledge of the spatial and temporal variations in the sound speed field and tidal elevations are two of the largest sources of error. Capturing the true variability of the sound speed field by measurement in the port is difficult as the estuarine circulation can change the character

of the field quickly and physical sampling from the survey vessel may not be able to capture the true shape of the field, especially without an underway profiling system. A potential solution to the aliasing caused by insufficient physical sampling is integrating the model output with the data processing and collection streams as a substitute or proxy for real observations.

Temperature and salinity are native outputs of the model, each represented at every model node and vertical layer. With knowledge of the temperature, salinity and depth variables sound speed may be calculated and added to the model data variables. Sound speed is calculated using the UNESCO standard Chen and Millero formula, as discussed in section 3.3, [Fofonoff and Millard, 1983]. Through calculation of the sound speed distribution within the model domain at every output time step, the variability of the sound speed field can be estimated for the entire Port of Saint John. Knowledge of the potential sound speed field at the time of a hydrographic survey allows for advances in data collection and data processing. Survey planning could be improved through evaluation of potential beam refraction errors as a result of strong sound speed gradients and comparisons to single observations of sound speed at a position close to the survey. This could allow for improved planning of physical sampling of the sound speed field. Artificial sound speed casts could also be generated to improve data collection in real time and limit refraction errors.

A spatially varying model of sound speed variability in an area of complex estuarine circulation must be evaluated prior to use and the uncertainty associated with the model

output quantified. The physical sampling campaign of Toodesh (2012) provides an excellent data set for evaluation of the model output for such an application. The differences between the model data and the observations have been evaluated in Chapter 4, and now the consequence of those differences in terms of resulting depth error will be assessed.

8.1.1. Model Surface Elevations

The model calculates surface elevations throughout the domain of the Port of Saint John. Using the location of a permanent tide gauge at the Bay Ferry Terminal Dock in the port as a reference (Figure 1), the effects of the changing tide on the maximum potential vertical elevation uncertainty can be determined by examining the amplitude and phase of the M2 component of the tide throughout the model domain. The M2 constituent values were extracted from the model output for the April 2008 period using the T_TIDE harmonic tidal analysis software [Pawlowicz et al., 2002]. The semi-diurnal M2 constituent is the most influential constituent in the Port of Saint John and the April 2008 observation and simulation period represents a spring tide condition.

The maximum difference in tidal amplitude between the tide gauge and the upper limits of Courtney Bay as predicted by the model is only 0.01m, and between the gauge and the Harbour Bridge is 0.06m. Beyond the Harbour Bridge to the start of the Reversing Falls, the amplitude of the tide changes by an additional 0.4m.

The maximum tidal phase difference between the tide gauge and the upper limits of Courtney Bay as described by the model is 0.3 degrees (37 seconds for M2), and between the gauge and the Harbour bridge is 1 degree (124 seconds for M2). Beyond the Harbour Bridge to the start of the Reversing Falls, the phase changes by an additional 0.8 degrees (99 seconds for M2).

The total potential tidal error is calculated using Fermat's Theorem which states that the local maximum, or minimum, of the difference function, as shown in Equation (3), is found when the differential of that function is set to zero [Stewart, J., 1999]. The difference function shown in Equation (3) describes the vertical difference between two tidal waves where A_1 is the tidal amplitude at the tide gauge location, A_2 is the tidal amplitude at another point in the model domain, ω is the M2 constituent speed, φ_1 is the tidal phase at the tide gauge location and φ_2 is the tidal phase at another point in the model domain.

$$\Delta_{Elev}(t) = A_1 \cos(\omega t - \varphi_1) - A_2 \cos(\omega t - \varphi_2) \quad (3)$$

For a survey constrained by the limits of the Harbour Bridge, the maximum potential vertical error due to the tidal difference in amplitude and phase would equate to 0.08 m, while a survey constrained by the start of the Reversing Falls could see a maximum tidal vertical error of 0.41 m. Harbour dredging is constrained exclusively to below the harbour bridge, therefore the maximum tidal uncertainty should be below 0.08m, which is below the decimeter level dredging accuracy limit, but could still prove important in

the overall error budget when other error sources are considered. These results are only relevant to those surveys using the Saint John tide gauge for vertical reference.

Ellipsoidally referenced surveys, which are not related to local chart datum, would be independent of these error sources, although they are susceptible to their own vertical referencing errors.

8.1.2. Model Sound Speed Comparison to Observations

Sound speed was calculated from the model results for every node and layer in the domain at each output time step. Temperature and salinity were used at each of the depth layers to calculate the sound speed. Sound speed values were also observed from the MVP-30 during each of the tidal cycle observation periods of Toodesh (2012) throughout the domain of the Port of Saint John. The observed values of sound speed can be compared to the model sound speed values to determine the effect of the differences on ray-tracing uncertainty over the depth and oblique geometries encountered in a traditional MBES survey.

The vertical ray tracing uncertainty between the model and the observations was calculated in a number of stages. First the location of the observed sound speed profile was determined in the model coordinate system through projection of the geographic coordinates from the MVP profile. The closest model node to the projected observation location was then determined along with the tide corrected depth at that location. The

modelled tide at the node was used for tidal correction. The tide corrected depth, modelled sound speed profile and prescribed transducer draft at the chosen node were used to establish a two-way travel time required for an acoustic ray to propagate through the medium at a specified swath angle. The modelled two-way travel time is then applied to the same acoustic ray, but now using the observed sound speed profile to arrive at an observed profile depth. As this procedure is designed to simulate a hydrographic multibeam survey, it is assumed that the vessel is equipped with a surface sound speed probe and the model sound speed at the depth of the transducer is used for the initial launch angle in both simulations. The result is a depth calculation at a specified swath angle for both the model profile and the observed profile, which allows for the associated vertical error to be extracted.

The vertical error associated with the comparison of the model sound speed profile and the observed sound speed profile is calculated at the location of each MVP profile. Error statistics can then be calculated based on the number of observations in a tidal cycle. The minimum number of observations was 667 profiles from the June survey, while the maximum was 906 profiles from the November survey. The error statistics were calculated as mean and standard deviation at one sigma values based on an absolute depth difference and a percentage of water depth difference, and a central frequency limit value based on both the IHO S-44 order levels and the 10cm dredging accuracy requirement . As the Port of Saint John is a shallow harbour where under keel clearance is critical, the Special Order level for Total Vertical Uncertainty (TVU) is used for evaluation. The

Special Order level for TVU is defined at 95% as follows in Equation (4), where d is the depth in metres [International Hydrographic Organization, 2008].

$$\pm\sqrt{0.25^2 + (0.0075 * d)^2} \quad (4)$$

8.1.3. Model vs. Observations

To evaluate the consequence of the difference between the model and observed sound speed profiles, the absolute depth error associated with ray tracing the beams of a multibeam sonar up to 60 degrees is examined. This method of evaluation emphasizes the significance of the differences between the model output and observations for a standard hydrographic survey.

Table 29 shows the mean difference and standard deviation between the ray-tracing result from the MVP-30 data and the model data for each of the four survey periods. The number of MVP-30 casts used in the calculation and the percentage of the differences which fall within the 10 cm dredging accuracy limits and 50% of the Special Order TVU limits are also presented in Table 29. The Special Order error limits are depth dependant, so the limit is calculated independently for each observation. The Percentage of Water Depth Error presented in the table relates the absolute depth error to the local water depth to provide a statistic which is independent of water depth variations.

Table 29 – Cumulative Statistics up to 60 deg of MVP-30 Casts vs. Model Output

Survey	Value	Mean	SD	Count	CF: 50% of Special Order TVU limits	CF: 10cm dredging limit
<i>April 2008</i>	Absolute Depth Error (m)	0.001	0.097	750	92%	86%
	Percentage of Water Depth Error (%)	-0.024	0.513	750		
<i>November 2008</i>	Absolute Depth Error (m)	-0.007	0.045	906	98%	96%
	Percentage of Water Depth Error (%)	-0.061	0.299	906		
<i>March 2009</i>	Absolute Depth Error (m)	-0.002	0.063	685	95%	93%
	Percentage of Water Depth Error (%)	0.007	0.320	685		
<i>June 2009</i>	Absolute Depth Error (m)	-0.006	0.017	806	100%	100%
	Percentage of Water Depth Error (%)	-0.051	0.143	806		

The non-cumulative beam based standard deviation at 95%, or two-sigma, is shown in Figure 113. As would be expected, the uncertainty errors cancel at 45 degrees and rise quickly after 55 degrees. The maximum standard deviation values are observed in April, when there is a large difference between the fresh and salt water masses. The standard deviation at 95% can be compared directly to the IHO special order TVU limit. With an average depth of 9.89 metres within the bounds of the model area in the Port of Saint, the Special Order TVU limit is calculated as 0.25 metres using Equation 2.

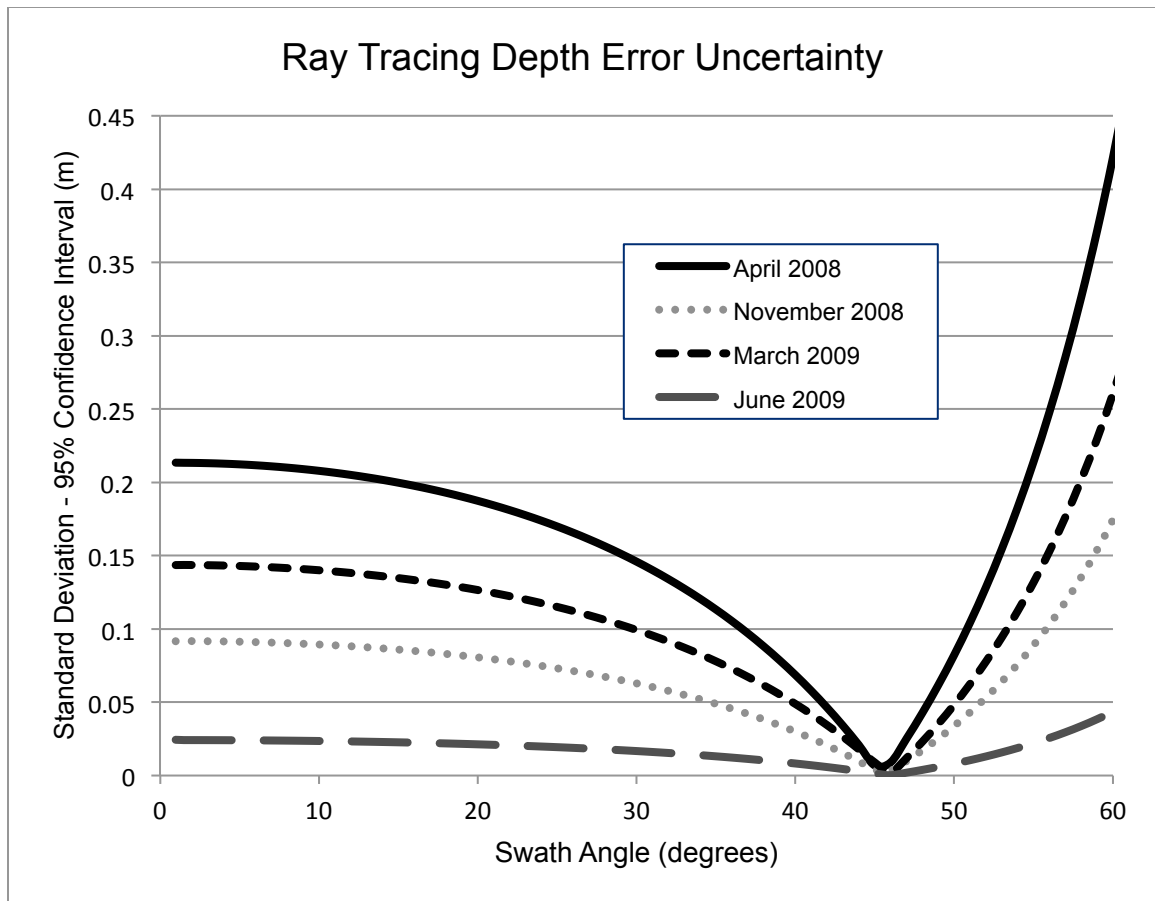


Figure 113 – Beam Angle Standard Deviation based on Difference Statistics

The cumulative vertical ray tracing depth errors are presented along with the error based on a percentage of water depth up to 60 degrees for each set of tidal cycle observations in Figure 114, Figure 115, Figure 116 and Figure 117. The figures describe 30 bin histograms of the differences along with the mean value of the distribution and the 10 cm dredging accuracy limits. The figures graphically show the mean and CF 10cm accuracy limits as described in Table 29.

The absolute depth error for April 2008, as shown in the left pane of Figure 114, is the only dataset of those shown in figures Figure 114, Figure 115, Figure 116 and Figure 117 which does not pass the Kolmogorov-Smirnov test for normality [Chakravarti, I. M., R. G. Laha and J. Roy , 1967]. In the case where the distribution is not normal, the CF provides a more useful statistic than the standard deviation.

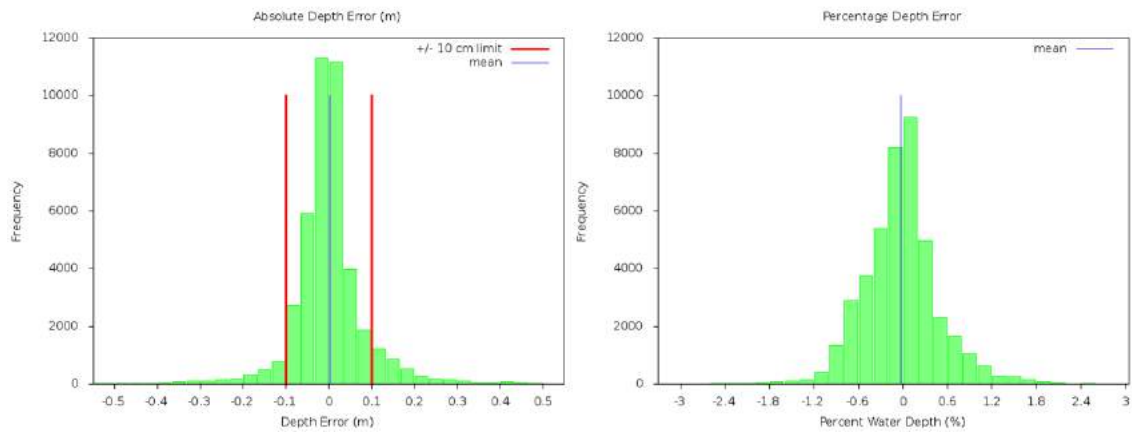


Figure 114 – April 2008 Absolute and Percentage Depth Error Histograms

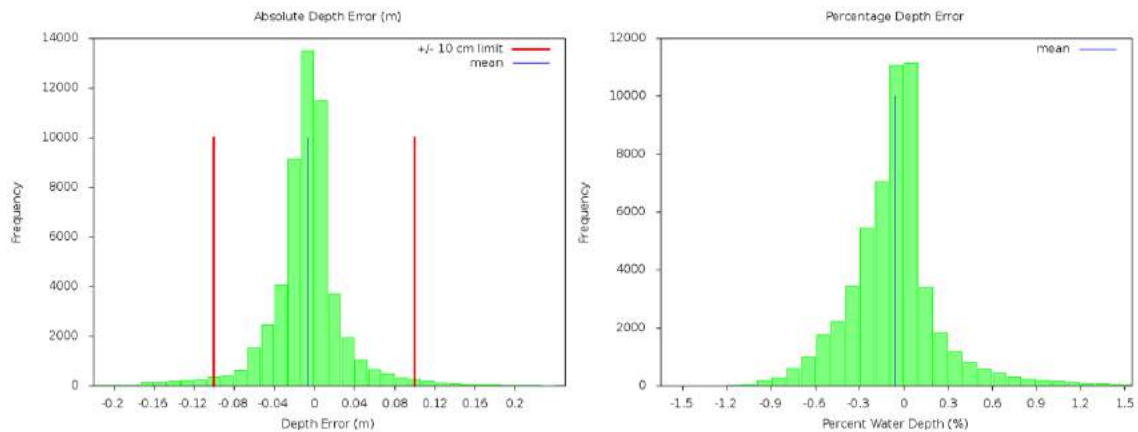


Figure 115 – November 2008 Absolute and Percentage Depth Error Histograms

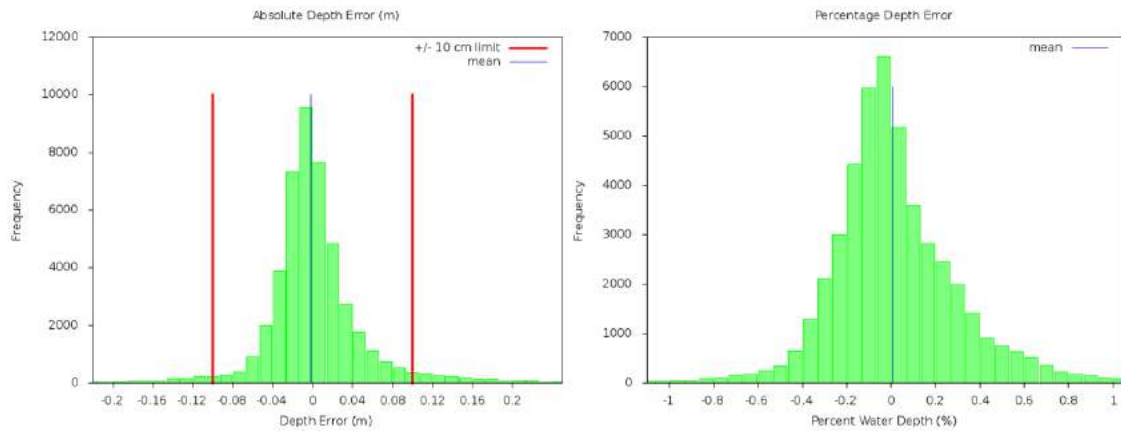


Figure 116 – March 2009 Absolute and Percentage Depth Error Histograms

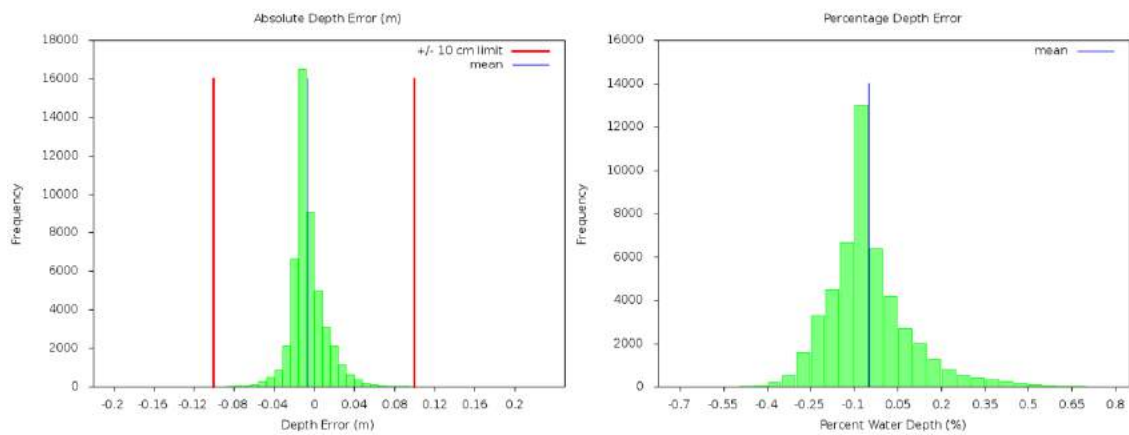


Figure 117 – June 2009 Absolute and Percentage Depth Error Histograms

8.1.3.1. Estimating Potential Error Distributions

Most hydrographic survey vessels do not have underway sound speed profiling capability. Therefore it is practical to compare the model output to an occasional static sound speed profile. Comparison of a single profile to a spatially and temporally varying

field of sound speed from the model output provides insight to the uncertainty associated with conventional hydrographic data collection.

To examine the variability of the sound speed field over time, the consequence of using a single sound speed profile over a certain area and time period instead of constantly varying the profile based on the model output data is analyzed. Assuming that a single profile is input to a multibeam system at a specified time and place, the effects of using that profile over a specified time period and survey area (the entire model domain) can be evaluated as the difference between the ray tracing results using the input profile and the modelled profile at the actual real-time location of the vessel. It is assumed that the vessel has a surface sound speed sensor to correct beam steering angles; therefore the calculation of the difference uses a varying surface sound speed that corresponds, to the model result at the depth of the transducer. This provides a depth error that results from the differences in the water masses. The depth error is converted to a percentage of water depth error and an associated level of IHO S-44 order [International Hydrographic Organization, 2008]. It is assumed that 50% of the uncertainty error budget is allocated for sound speed errors, while the other 50% may be occupied by sensor specific and tidal errors.

Examining the potential error field not only provides an estimate of sounding uncertainty throughout the domain, it also adds a planning capability to the model output. Regions can now be determined where if a single sound speed profile is used then depth errors will be below a certain threshold. Polygons could be generated for certain stages of the

tide which show zones of minimum and maximum errors based on a specified initial sound speed cast location.

As an example, Figure 118 shows the worst-case associated IHO acceptance levels with contours indicating vertical errors within Special Order, within Order 1, within Order 2 and larger than the limits of Order 2 based on a single sound speed profile over a tidal cycle. This clearly shows that a sound speed profile collected at the “Reference Cast Location” near the intersection of the Courtney Bay and Main Harbour Channels is only representative of a portion of the Port of Saint John area. Special order is maintained around the location of the cast and up into Courtney Bay. Uncertainties beyond the limits of Order 2 result in the Main Harbour channel.

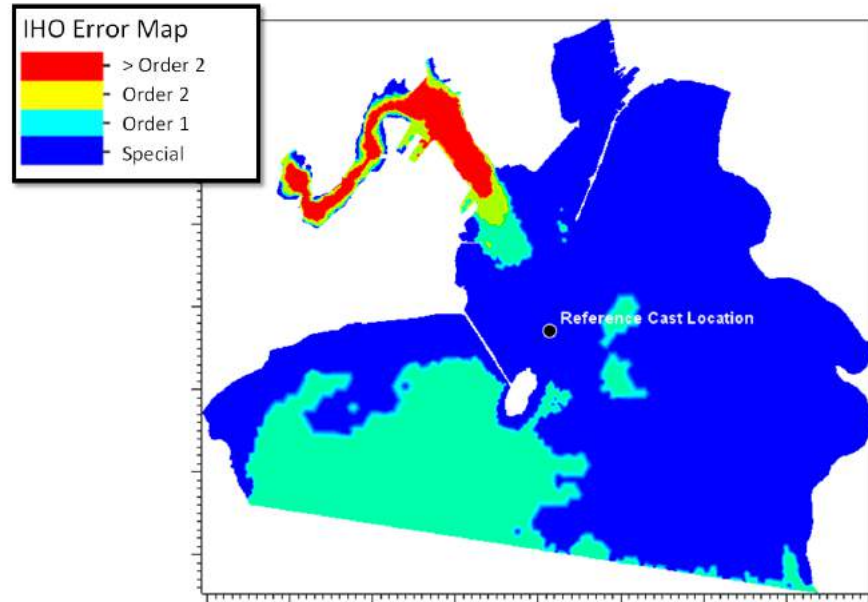


Figure 118 – November 2008 IHO Order Distribution

8.2. Discussion

Baroclinic hydrodynamic models provide a three dimensional temporal overview of the temperature and salinity conditions for a specified area. Sound speed fields can be calculated from these variables which provide a method for analyzing potential sound speed uncertainty. The optimal frequency and locations of sound speed casts, the consequences of using a cast from a specific area and the creation of synthesized casts can all be determined from the model output. The simulations for the four periods illustrate the influence of the estuarine conditions on the potential sound speed uncertainty.

For an area of complex oceanography, such as the Saint John Harbour, the model provides an alternative to high density collection of sound speed profiles. As the model results will never perfectly match the observations, the significance of the difference must be determined. The model provides a ray tracing solution which matches the observed profile within a maximum standard deviation of 10 cm up to a swath width of 60 degrees 86% of the time for the April survey, while the fit is much better for other times of the year due to the weaker sound speed gradients.

Testing the model output for hydrographic data processing for the Port of Saint John shows promising results. The majority of the time, the model could substitute actual observations with little effect on ray-tracing uncertainty. Areas of acceptable uncertainty

resulting from CTD cast locations can be determined through examination of the error fields in terms of IHO uncertainty levels at each time of year.

CHAPTER 9: Discussion

Discovering the exact source of sedimentation in the Port of Saint does not have a simpler answer. The distribution of sediment in the complex estuary is ultimately driven by a combination of the varying river discharge, strong hyper-tidal current velocities and the estuarine circulation. Examination of the physical oceanographic observations, three-dimensional baroclinic hydrodynamic modelling output and bathymetric survey differences, as presented in this thesis, adds to understanding the complexity of the environment.

A number of previous studies have examined the relationship between three dimensional model output and physical oceanographic observations. Most studies include qualitative time series comparisons of water levels, salinity and velocity and basic RMS quantitative statistics [Levasseur et al., 2007; Yang and Khangaonkar, 2009; Weisberg and Zheng, 2006; Zheng and Weisberg, 2010]. A more comprehensive analysis of the Hudson River estuary is provided in Warner et al. (2005). In that study the model skill of three-dimensional baroclinic model output is assessed using a predictive skill assessment metric, which provides an index of agreement between the model and the observations. The index of agreement is calculated as the ratio between the mean square error and the potential error, multiplied by the number of values and subtracted from unity, as shown in equation (5), where P is the model simulated data, O is the observed data and N is time increment [Legates and McCabe, 1999]. The resulting correlation value varies from zero

to one, where one is perfect agreement and zero is complete disagreement [Wei and Zhang, 2011]. This determination is sensitive to extreme values and outliers due to the squared differences and does not rely on comparison to physical limits, unlike the qualitative statistics of section 4.2. For a qualitative comparison Warner et al. (2005) examines profiles of salinity and velocity over a tidal cycle, and longitudinal salinity distributions for the model and observations, similar to figures presented in section 4.1. Warner et al. (2005) also provides a simple overview of salt flux for a cross section of the estuary and compares to observed flux.

$$d = 1.0 - \frac{\sum_{i=1}^N (O_i - P_i)^2}{\sum_{i=1}^N (|P_i - \bar{O}| + |O_i - \bar{O}|)^2} \quad (5)$$

The evaluation of the relationship between the observed data and the model output presented in this thesis extends beyond the comparisons of previous studies and examines the goodness of fit of the model from multiple perspectives. The comparison values prove to provide a close relationship for both qualitative and quantitative metrics. The spatial correlation of the differences change depending on the time of year, but averaged over the four simulation periods the best fit between the observations and the model results is found within the Courtney Bay Channel. The Courtney Bay Turning Basin provides the weakest fit.

The estuarine circulation within the waters between the Harbour Bridge and the Reversing Falls was shown to be essential in understanding the annual mixing regime.

The circulation within this area is especially significant during April, the spring freshet time period. The spring freshet is the only time of year when the salt wedge does not pass over the Reversing Falls. This completely changes the mixing regime within this short section. The volume flux indicates that a similar quantity of salt water is being entrained into the upper fresh water layer independent of the simulation period; therefore a similar quantity of mixing and entrainment is occurring during the spring freshet, just between the Harbour Bridge and the Reversing Falls, as there is at other times of the year when the reach of the estuary is up to 20 km upstream.

The suspended sediment within the port is contained both within the incoming salt wedge and the outflowing freshwaters. The highest concentrations of sediment are within the salt wedge, as described by the optical backscatter profiles, but in the Main Harbour Channel these sediments are deposited in the estuary and resuspended by the outflowing fresh water. Sedimentation in the port is not controlled solely by river discharge, but the combination of the salt wedge sediment concentration and the discharging river. This is why there is no direct correlation between river discharge and dredge volumes. The sediment flux estimates reveal that the maximum amount of sediment moving through the fresh water in the Main Harbour Channel is during the April simulation. In Courtney Bay during the March simulation period the salt wedge carries the majority of the sediment while the opposite is observed in April and November. During those times a greater quantity of suspended sediment is observed in the fresh water than the lower salt water layer.

The sediment in the salt wedge partially comes in from offshore as Melanson (2012) showed in the correlation between dredge volumes and winter storms. Another source of sediment is the mud flats within the domain of the harbour. There are two areas of focus in this thesis; the inter-channel mudflats near Round Reef and the area east of the Courtney Bay breakwater.

The Round Reef area acts as both a source and sink of sediment for the waters that flow from the Main Harbour Channel into Courtney Bay. At certain stages of the tide the current velocities decrease dramatically as they pass over this area, as discussed in Section 5.2. This causes deposition of fine grained sediments which were in suspension as they left the Main Harbour Channel. At other stages of the tide the velocities increase and resuspend the recently deposited fine grained sediments to propagate them into Courtney Bay.

The area east of the breakwater is a source of sediment for the salt water which was shown to wrap around the end of the breakwater and flow into Courtney Bay. This area is not well protected from strong south-easterly winds and sediment re-suspension is likely partially driven by strong wave activity. The fresh and salt waters which flow into Courtney Bay both slow down dramatically once they reach the Turning Basin. They sit nearly stagnant for a period of over an hour when the optical backscatter shows the suspended sediment disappears, presumably by deposition.

The salt wedge comes into the Main Harbour Channel with increased suspended sediment concentration at the nose of the wedge on the flood tide. As the tide reaches its maximum and starts to ebb, the salt wedge slows down and much of the sediment is deposited to the seabed. Where this sediment is deposited has an impact on the sedimentation in the port of Saint John. In April, when the river discharge is high, the sediment is deposited in the channel between the Reversing Falls and the harbour bridge. At other times of the year, when river discharge is lower, the salt wedge moves over the Reversing Falls and the turbidity maximum deposits sediment upstream of the Reversing Falls. In April the river discharge is sufficiently strong that it picks up the fine-grained sediment that was deposited by the salt wedge and moves it back out of the harbour on the ebb tide. Some of the suspended sediments are trapped in lateral eddies formed in the Main Harbour channel which redirect and deposit within the berths along the west piers where the current velocities drop. The large eddy in the Main Harbour Channel is clearly shown in the seabed residual circulation plots for April in Chapter 6. The strong residual currents in this area affect the erosion and disposition of sediments throughout the channel. That eddy is either poorly or not at all developed at other times of the year.

After the sediment rich fresh water has left the Main Harbour Channel, a portion of it moves across Round Reef, where it places more sediment into suspension and collides with the incoming flow from around the breakwater and decelerates. The combined flow then travels up the Courtney Bay Channel to the head of the bay, in the Turning Basin, where the velocity drops and the sediments are deposited.

In April and November the residual flux of suspended sediment indicates that sediment is leaving the Main Harbour Channel and propagating into Courtney Bay and the Outer Harbour. In March, the Saint John estuary is a sediment sink as more sediment is entering the river through the salt wedge than is able to be flushed out. Independent of the time of year the Courtney Bay channel acts as a sediment sink. Compared to the other times of the year, the least amount of residual suspended sediment is entering the Courtney Bay Channel in November. November is also the time when the largest percentage of fresh water is entering Courtney Bay. This correlation implies that increasing the fresh water input to Courtney Bay could improve the flushing of sediment laden waters.

The area of the harbour with the most significant seabed change is downstream of the Harbour Bridge within the Main Harbour Channel. The minimum reach of the salt wedge near low tide influences the erosional and depositional patterns of this area. The area is actively eroded during the spring freshet, but the residual inflow of seabed currents fills in the depression the remainder of the year. The area represents the deepest point in the domain of port; therefore it is not of navigational significance. However, the residual flow suggests that some of the finer materials may be redirected into the berths along the channel.

The model output has been shown to be applicable to use with hydrographic data processing. The model output can be used in place of high density physical observations which may not be possible due to the logistical constraints associated with working in a

busy commercial harbour. It can also act as a prediction tool to estimate optimal acoustic survey conditions when ray tracing errors will be minimized.

9.1. Recommendations for Future Work

Based on the work of this thesis, suggestions for potential topics of future study in the Port of Saint John are presented below. These focus on areas beyond the scope of this work.

- Alter the model grid to include additional vertical layers in an effort to improve the mixing estimate along the halocline
- Look at the potential source of sediment in the salt water layer through the integration of a sediment transport model to a lower resolution hydrodynamic model which stretches out into the Bay of Fundy. Examine the possibility that suspended sediment is originating from the Black Point disposal site, inshore shallows, further offshore, or local banner banks.
- Model the effects of the breakwater modification suggestions in Neu, 1960 (Figure 6). Especially those which alter the influence of the river on the Courtney Bay channel.

- Perform more frequent regional bathymetric surveys of the domain of the port at a minimum of monthly time intervals, ensuring to observe the state of sediment distribution before, during and after the spring (and fall) freshets. A focus should be made on the areas downstream of the Harbour Bridge (Areas A, B, C and D in Figure 88), the berths along the western pier, the Courtney Bay channel and the Turning Basin. This would establish when the sediment is arriving in the port (during the winter or during the freshet)
- Collect long term observations of the sediment concentrations and current velocities in the salt wedge at each of these periods from a cabled ADCP in the Courtney Bay Channel or from sensors located on the anchor chain of a navigation buoy.
- Perform additional oceanographic tidal cycles at similar times of year as the Toodesh (2012) surveys, but planned for both spring vs. neap tides. This would give more reliable volume flux estimates where the effects of the tidal range could be evaluated.
- Establish an operational nowcast and forecast model for the Port of Saint John. The model could use observed and predicted river and harbour water levels to force open boundary elevations. Forecasts of the sound speed field could be generated ahead of MBES survey operations. As a by-product, the model

forecasts would allow for better prediction of slack water through the Reversing Falls by accounting for variations in river levels.

CHAPTER 10: Conclusions

A three-dimensional baroclinic hydrodynamic model has been developed for the Port of Saint John to extend beyond physical observations of temperature, salinity and current velocity to the entire domain of the port. The model allows for an understanding of the estuarine circulation over a tidal cycle in areas where observations are not feasible. The model simulations were run during four times of the year which represented the breadth of river discharge and spring/neap tidal range.

Qualitative and quantitative assessments of the model were completed through comparison of model output to the physical observations of Toodesh (2012). The observational data provided spatially and temporally distributed statistics for the fit between the model and observational variables of salinity, temperature, derived sound speed and current velocity. Deficiencies of the model in estuarine mixing were found, but overall the model was shown to provide a close approximation to the observations.

Examination of the model output reduces the ambiguities associated with previous oceanographic studies within the Port of Saint John. The lateral estuarine circulation, sources of optical backscatter anomalies and correlations with bathymetric change can now be determined. The cross-channel circulation is significant throughout the domain of the port. The geometry of the Main Harbour Channel impacts the salinity distribution and eddy development over a tidal cycle, which both impact sedimentation in the port. The

inter-channel area between the Main Harbour and Courtney Bay channels provides a route for the fresh waters to interact with Courtney Bay and acts as a source of suspended sediment. The dynamics of flow for the waters that enter Courtney Bay from around the end of the breakwater can also now be understood.

The model is able to fill in the gaps in understanding of the circulation between the Harbour Bridge and the Reversing Falls, an area that can only be accessed by vessels safely at slack water. Understanding the estuarine circulation within this area is important, especially during the spring freshet when the salt wedge is not able to propagate over the Reversing Falls.

Volume flux estimates were calculated based on the model output without the deficiencies of the calculations in previous studies. The model allows for the secondary circulation patterns within the channels to be included in the flux estimate, does not mask the near surface or seabed layers and is able to resolve the weak current velocities within Courtney Bay. Incorporation of observed suspended sediment allows for sediment flux estimates within both the Main Harbour Channel and Courtney Bay.

An application of the hydrodynamic model output is the prediction of variations in sound speed structure and tidal amplitude and phase for hydrographic MBES data processing. The model is shown to adequately represent the sound speed field and could be used reliably as both a source of sound speed information and predictive survey planning tool. The observational sound speed data also provides a benchmark for determining the

consequences of deficiencies in the model representation of the estuary in terms of a practical application.

The development of a three dimension baroclinic hydrodynamic model for the Port of Saint John has greatly improved our understanding of the estuarine circulation within the Port. The model allows for uncertainties associated with previous studies to be diminished and provides a more complete picture of the complex interaction between the Saint John River discharge and Bay of Fundy tides.

Bibliography

ACEnet(2011). "About ACEnet - ACEnet." [On-line] 3/26/2012, 2012. http://www.ace-net.ca/wiki/About_ACEnet .

Baird, W. F. (1987). "Evaluation of the sedimentation processes in Saint John Harbour/Courtenay Bay New Brunswick." *Rep. No. T8080-6-3027*, W.F. Baird & Associates Coastal Engineers Ltd., Ottawa, Ontario.

Canadian Hydrographic Service (2009). "Saint John Harbour and Approaches / et les approches. (Chart 4117)." 1:15000(Saint John, NB), Government of Canada, Ottawa, Ontario.

Chaffey, J. D., and Greenberg, D. A. (2003). "resolute: A Semi-Automated Finite Element Mesh Generation Routine." *Rep. No. 225 Canadian Technical Report of Hydrography and Ocean Sciences*, Ocean Sciences Division, Bedford Institute of Oceanography, Department of Fisheries and Oceans, Dartmouth, Nova Scotia, Canada.

Chakravarti, I. M., R. G. Laha, and J. Roy (1967). *Handbook of methods of applied statistics*. Wiley, New York, New York.

Chen, C. (2013). "An Unstructured Grid, Finite-Volume Community Ocean Model FVCOM User Manual ." Department of Fisheries Oceanography, School for Marine Science and Technology, University of Massachusetts-Dartmouth, New Bedford, Massachusetts.

Chen, C., R. C. Beardsley, and G. W. Cowles (2006). "An unstructured grid, finite-volume coastal ocean model (FVCOM) system." *Oceanography*, 19(1), pp. 78.

Delpeche, N. (2007). *Observations of advection and turbulent interfacial mixing in the Saint John River Estuary, New Brunswick Canada*. MScEng Thesis, University of New Brunswick, Fredericton, New Brunswick.

Dupont, F., C. G. Hannah, and D. Greenberg (2005). "Modelling the Sea Level of the Upper Bay of Fundy." *Atmosphere-Ocean*, 43(1), pp. 33.

Dyer, K. R. (1997). *Estuaries: a physical introduction*. John Wiley & Sons, New York, New York.

Eisma, D. (1986). "Flocculation and de-flocculation of suspended matter in estuaries." *Netherlands Journal of Sea Research*, 20 pp. 183-199.

Environment Canada(2012). "Environment Canada - Water - Data Products and Services." [On-line] 08/23, 2013. <http://www.ec.gc.ca/rhc-wsc/default.asp?lang=En&n=894E91BE-1>

Fofonoff, N. P., and Millard, R. C. (1983). "Algorithms for Computation of Fundamental Properties of Seawater." *Rep. No. 44*, UNESCO, Paris, France.

Foreman, M. G. G. (2012). "Particle tracking and GOTM files." (Personal Communication).

Godin, G. (1991). "Tidal Hydraulics of Saint John River." *Journal of Waterway, Port, Coastal, and Ocean Engineering*, 117(1), pp. 19-10. ASCE.

Gordon, R. L. (1996). "Acoustic Doppler Current Profiler Principles of Operation A Practical Primer." RD Instruments, San Diego, California.

Hess, K. W., Gross, T. F., Schmalz, R. A., Kelley, J. G., Aikman, F., Wei, E., and Vincent, M. S. (2003). "NOS standards for evaluating operational nowcast and forecast hydrodynamic model systems." *Rep. No. 17*, NOAA Technical Report NOS CS 17, Silver Spring, Maryland.

Hughes, F. W., and M. Rattray Jr. (1980). "Salt flux and mixing in the Columbia River Estuary." *Estuarine and Coastal Marine Science*, 10(5), pp. 479-493.

International Hydrographic Organization. (2008). "IHO Standard for Hydrographic Survey." *Rep. No. Special publication No. 44, 5th edition*, International Hydrographic Bureau, Monaco.

Legates, D. R., and G. J. McCabe (1999). "Evaluating the use of "goodness-of-fit" measures in hydrologic and hydroclimatic model validation." *Water Resources Research*, 35(1), pp. 233-241.

Levasseur, A., L. Shi, N. C. Wells, D. A. Purdie, and B. A. Kelly-Gerreyn (2007). "A three-dimensional hydrodynamic model of estuarine circulation with an application to Southampton Water, UK." *Estuarine, Coastal and Shelf Science*, 73(3-4), pp. 753-767.

Leys, V. (2007). "3D Flow and Sediment Transport Modelling at the Reversing Falls - Saint John Harbour, New Brunswick." *Proceedings of OCEANS 2007*, pp. 1-16.

Leys, V., and Mulligam, R. P. (2011). *Modelling Coastal Sediment Transport for Harbour Planning: Selected Case Studies*. InTech Open Access Publisher, Rijeka, Croatia.

Matheron, D. (2010). *Sedimentation patterns and inferred dynamics in Saint John Harbour*. MScEng Thesis, University of New Brunswick, Fredericton, New Brunswick.

Melanson, J. (2012). *Seasonal and Tidal Variations of Sediment Transport Patterns in the Saint John Inner Harbour*. MScEng Thesis, University of New Brunswick, Fredericton, New Brunswick.

Mellor, G. L., and T. Yamada (1982). "Development of a turbulence closure model for geophysical fluid problems." *Reviews of Geophysics*, 20(4), pp. 851-875.

Metcalfe, C., M. J. Dadswell, G. F. Gillis, and M. L. H. Thomas (1976). *Physical, chemical and biological parameters of the Saint John River estuary, New Brunswick, Canada*. Research and Development Directorate, Biological Station, St. Andrews, New Brunswick.

Natural Resources Canada(2010). "Watersheds." Canada. [On-line] 09/29, 2013. <http://atlas.nrcan.gc.ca/site/english/maps/water.html> .

Natural Resources Canada (2004). "Optical Backscatter calibration data." Personal Communication.

Natural Resources Canada(2003). "Toporama WMS." Government of Canada. Ottawa, Ontario. [On-line] Saint John, NB, 1:50000. http://wms.ess-ws.nrcan.gc.ca/wms/toporama_en?SERVICE=WMS&REQUEST=GetCapabilities .

Neu, H. (1960). "Hydrographic Survey of Saint John Harbour, N.B." National Research Council of Canada, Ottawa, Ontario.

Pawlowicz, R., B. Beardsley, and S. Lentz (2002). "Classical tidal harmonic analysis including error estimates in MATLAB using T_TIDE." *Computers & Geosciences*, 28 pp. 929.

Pond, S., and G. L. Pickard (1983). *Introductory dynamical oceanography*. Pergamon Press, Oxford; New York.

Saint John Port Authority (2013). (Personal Communication).

Saint John Port Authority(2009). "Saint John Port Authority - Media Center - Quick Facts." [On-line] 2/27/2012, 2012. http://www.sjport.com/english/media_center/quick_facts.html

Service New Brunswick (2002). "Softcopy Orthophotomap Data Base (SODB)." 1:10000(Saint John, NB), Government of New Brunswick, Fredericton, New Brunswick.

Stewart, J. (1999). *Calculus : early transcendentals*. 4th ed., Thomson/Brooks/Cole, Belmont, California.

Toodesh, R. (2012). *The Oceanographic Circulation of the Port of Saint John over Seasonal and Tidal Time Scales*. MScEng Thesis, University of New Brunswick, Fredericton, New Brunswick.

Umlauf, L., Burchard, H., and Bolding, K. (2012). "GOTM Source Code and Test Case Documentation, Version 4.0." (<http://www.gotm.net/index.php?go=documentation>).

Warner, J. C., W. R. Geyer, and J. A. Lerczak (2005). "Numerical modeling of an estuary: A comprehensive skill assessment." *Journal of Geophysical Research: Oceans*, 110(C5).

Wei, E., and A. Zhang (2011). "The Tampa Bay operational forecast system (TBOFS) model development and skill assessment." U.S. Dept. of Commerce, National Oceanic and Atmospheric Administration, National Ocean Service, Office of Coast Survey, Coast Survey Development Laboratory. Silver Spring, Maryland.

Wei, E., A. Zhang, Z. Yang, Y. Chen, J. Kelley, F. Aikman, and D. Cao (2014). "NOAA's Nested Northern Gulf of Mexico Operational Forecast Systems Development." *Journal of Marine Science and Engineering*, 2(1), pp. 1-17.

Weisberg, R. H., and L. Zheng (2006). "Circulation of Tampa Bay driven by buoyancy, tides, and winds, as simulated using a finite volume coastal ocean model." *Journal of Geophysical Research: Oceans*, 111(C1).

Yang, Z., and T. Khangaonkar (2009). "Modeling tidal circulation and stratification in Skagit River estuary using an unstructured grid ocean model." *Ocean Modelling*, 28(1-3), pp. 34-49.

Zhao, L., C. Chen, and G. Cowles (2006). "Tidal flushing and eddy shedding in Mount Hope Bay and Narragansett Bay: An application of FVCOM." *Journal of Geophysical Research: Oceans*, 111(C10).

Zheng, L., and R. H. Weisberg (2010). "Rookery Bay and Naples Bay circulation simulations: Applications to tides and fresh water inflow regulation." *Ecological Modelling*, 221(7).

Appendix A

Model assessment tables for Courtney Turning Basin, Courtney Channel, Main Harbour Channel (Downstream of Harbour Bridge) and Reversing Falls (Upstream of Reversing Falls).

April 2008

Courtney Turning Basin						
Variable	SSP (m/s)	limit	Temp (deg C)	limit	Sal (psu)	limit
<i>Mean</i>	-0.20		-0.66		2.21	
<i>SD</i>	7.29		0.60		6.58	
<i>RMSE</i>	7.29		0.90		6.94	
<i>Min</i>	-23.93		-2.41		-17.94	
<i>Max</i>	14.39		0.07		14.53	
<i>CF</i>	84.39	10	49.91	0.5	45.35	5
<i>POF</i>	7.16	10	0.00	0.5	36.62	5
<i>NOF</i>	8.46	10	50.09	0.5	18.03	5

Courtney Channel						
Variable	SSP (m/s)	limit	Temp (deg C)	limit	Sal (psu)	limit
<i>Mean</i>	-1.01		-0.19		-0.05	
<i>SD</i>	9.44		0.34		7.55	
<i>RMSE</i>	9.50		0.39		7.55	
<i>Min</i>	-36.46		-2.22		-28.64	
<i>Max</i>	22.40		0.18		19.27	
<i>CF</i>	71.29	10	86.02	0.5	50.72	5
<i>POF</i>	12.91	10	0.00	0.5	26.09	5
<i>NOF</i>	15.80	10	13.98	0.5	23.19	5

Main Harbour						
Variable	SSP (m/s)	limit	Temp (deg C)	limit	Sal (psu)	limit
<i>Mean</i>	-0.76		-0.03		-0.41	
<i>SD</i>	11.94		0.10		9.46	
<i>RMSE</i>	11.97		0.10		9.47	
<i>Min</i>	-38.06		-0.33		-29.87	
<i>Max</i>	33.84		0.24		27.41	
<i>CF</i>	63.71	10	100.00	0.5	47.97	5
<i>POF</i>	17.86	10	0.00	0.5	26.77	5
<i>NOF</i>	18.43	10	0.00	0.5	25.26	5

Main Harbour ADCP				
Variable	North (m/s)	limit	East (m/s)	limit
<i>Mean</i>	0.12		-0.04	
<i>SD</i>	1.33		0.85	
<i>RMSE</i>	1.33		0.85	
<i>Min</i>	-10.47		-8.72	
<i>Max</i>	10.08		11.87	
<i>CF</i>	85.04	1	92.67	1
<i>POF</i>	7.89	1	2.46	1
<i>NOF</i>	7.07	1	4.87	1

Reversing Falls						
Variable	SSP (m/s)	limit	Temp (deg C)	limit	Sal (psu)	limit
<i>Mean</i>	-1.42		-0.02		-0.92	
<i>SD</i>	11.45		0.07		9.00	
<i>RMSE</i>	11.53		0.07		9.04	
<i>Min</i>	-37.22		-0.16		-29.31	
<i>Max</i>	28.77		0.23		22.95	
<i>CF</i>	77.20	10	100.00	0.5	70.95	5
<i>POF</i>	11.32	10	0.00	0.5	15.54	5
<i>NOF</i>	11.49	10	0.00	0.5	13.51	5

Reversing Falls ADCP				
Variable	North (m/s)	limit	East (m/s)	limit
<i>Mean</i>	-0.40		-0.49	
<i>SD</i>	1.16		0.90	
<i>RMSE</i>	1.22		1.03	
<i>Min</i>	-10.69		-11.66	
<i>Max</i>	5.77		2.14	
<i>CF</i>	61.31	1	77.54	1
<i>POF</i>	9.61	1	1.47	1
<i>NOF</i>	29.08	1	20.99	1

November 2008

Courtney Turning Basin						
Variable	SSP (m/s)	limit	Temp (deg C)	limit	Sal (psu)	limit
<i>Mean</i>	0.96		-0.07		1.00	
<i>SD</i>	7.58		0.66		4.68	
<i>RMSE</i>	7.63		0.66		4.78	
<i>Min</i>	-15.78		-3.99		-9.01	
<i>Max</i>	17.01		0.89		11.53	
<i>CF</i>	78.60	10	67.80	0.5	70.79	5
<i>POF</i>	16.37	10	17.80	0.5	23.30	5
<i>NOF</i>	5.03	10	14.40	0.5	5.91	5

Courtney Channel						
Variable	SSP (m/s)	limit	Temp (deg C)	limit	Sal (psu)	limit
<i>Mean</i>	-1.52		-0.06		-1.02	
<i>SD</i>	7.64		0.42		4.98	
<i>RMSE</i>	7.79		0.43		5.08	
<i>Min</i>	-22.86		-1.91		-15.50	
<i>Max</i>	23.81		1.26		15.90	
<i>CF</i>	75.90	10	70.94	0.5	66.13	5
<i>POF</i>	9.36	10	12.55	0.5	13.07	5
<i>NOF</i>	14.74	10	16.52	0.5	20.80	5

Main Harbour						
Variable	SSP (m/s)	limit	Temp (deg C)	limit	Sal (psu)	limit
<i>Mean</i>	-3.09		-0.13		-2.03	
<i>SD</i>	8.06		0.44		5.24	
<i>RMSE</i>	8.63		0.46		5.62	
<i>Min</i>	-24.59		-1.27		-16.07	
<i>Max</i>	23.81		1.25		15.90	
<i>CF</i>	70.03	10	66.84	0.5	62.11	5
<i>POF</i>	7.40	10	10.52	0.5	10.38	5
<i>NOF</i>	22.57	10	22.64	0.5	27.51	5

Main Harbour ADCP				
Variable	North (m/s)	limit	East (m/s)	limit
<i>Mean</i>	0.06		-0.01	
<i>SD</i>	1.03		0.68	
<i>RMSE</i>	1.03		0.68	
<i>Min</i>	-10.73		-3.69	
<i>Max</i>	3.54		7.13	
<i>CF</i>	74.56	1	89.09	1
<i>POF</i>	15.86	1	2.68	1
<i>NOF</i>	9.58	1	8.23	1

Reversing Falls						
Variable	SSP (m/s)	limit	Temp (deg C)	limit	Sal (psu)	limit
<i>Mean</i>	-3.61		-0.17		-2.36	
<i>SD</i>	10.39		0.52		6.89	
<i>RMSE</i>	10.98		0.55		7.28	
<i>Min</i>	-24.97		-1.26		-16.52	
<i>Max</i>	22.88		1.16		15.16	
<i>CF</i>	58.48	10	60.51	0.5	46.33	5
<i>POF</i>	9.37	10	9.62	0.5	12.15	5
<i>NOF</i>	32.15	10	29.87	0.5	41.52	5

Reversing Falls ADCP				
Variable	North (m/s)	limit	East (m/s)	limit
<i>Mean</i>	-0.08		-0.02	
<i>SD</i>	1.28		1.01	
<i>RMSE</i>	1.29		1.01	
<i>Min</i>	-4.40		-7.72	
<i>Max</i>	10.15		2.62	
<i>CF</i>	62.59	1	72.58	1
<i>POF</i>	15.83	1	11.85	1
<i>NOF</i>	21.58	1	15.57	1

March 2009

Courtney Turning Basin						
Variable	SSP (m/s)	limit	Temp (deg C)	limit	Sal (psu)	limit
<i>Mean</i>	-0.25		0.15		-0.69	
<i>SD</i>	8.35		0.67		4.89	
<i>RMSE</i>	8.35		0.69		4.94	
<i>Min</i>	-24.97		-4.02		-8.33	
<i>Max</i>	18.96		1.35		11.29	
<i>CF</i>	77.68	10	59.66	0.5	60.41	5
<i>POF</i>	16.66	10	26.14	0.5	16.38	5
<i>NOF</i>	5.67	10	14.20	0.5	23.21	5

Courtney Channel						
Variable	SSP (m/s)	limit	Temp (deg C)	limit	Sal (psu)	limit
<i>Mean</i>	2.06		0.36		0.35	
<i>SD</i>	6.84		0.44		4.41	
<i>RMSE</i>	7.14		0.57		4.42	
<i>Min</i>	-14.39		-2.35		-12.93	
<i>Max</i>	19.88		1.40		11.85	
<i>CF</i>	82.43	10	63.05	0.5	73.99	5
<i>POF</i>	17.25	10	33.51	0.5	17.52	5
<i>NOF</i>	0.32	10	3.43	0.5	8.49	5

Main Harbour						
Variable	SSP (m/s)	limit	Temp (deg C)	limit	Sal (psu)	limit
<i>Mean</i>	2.80		0.44		0.65	
<i>SD</i>	7.98		0.38		5.61	
<i>RMSE</i>	8.45		0.58		5.65	
<i>Min</i>	-20.24		-0.45		-18.15	
<i>Max</i>	26.86		1.61		17.70	
<i>CF</i>	75.77	10	63.24	0.5	63.62	5
<i>POF</i>	21.46	10	36.76	0.5	22.99	5
<i>NOF</i>	2.77	10	0.00	0.5	13.39	5

Main Harbour ADCP				
Variable	North (m/s)	limit	East (m/s)	limit
<i>Mean</i>	-0.03		-0.02	
<i>SD</i>	0.94		1.09	
<i>RMSE</i>	0.94		1.09	
<i>Min</i>	-4.63		-4.38	
<i>Max</i>	3.55		3.53	
<i>CF</i>	69.68	1	54.87	1
<i>POF</i>	14.70	1	22.44	1
<i>NOF</i>	15.62	1	22.69	1

Reversing Falls						
Variable	SSP (m/s)	limit	Temp (deg C)	limit	Sal (psu)	limit
<i>Mean</i>	-5.71		0.32		-5.35	
<i>SD</i>	2.66		0.15		2.48	
<i>RMSE</i>	6.29		0.35		5.89	
<i>Min</i>	-11.76		0.12		-11.28	
<i>Max</i>	-0.41		0.73		-2.02	
<i>CF</i>	92.75	10	88.41	0.5	52.17	5
<i>POF</i>	0.00	10	11.59	0.5	0.00	5
<i>NOF</i>	7.25	10	0.00	0.5	47.83	5

Reversing Falls ADCP				
Variable	North (m/s)	limit	East (m/s)	limit
<i>Mean</i>	-0.18		0.73	
<i>SD</i>	1.32		0.80	
<i>RMSE</i>	1.34		1.08	
<i>Min</i>	-5.83		-2.01	
<i>Max</i>	2.80		3.85	
<i>CF</i>	58.86	1	54.24	1
<i>POF</i>	18.23	1	44.64	1
<i>NOF</i>	22.91	1	1.13	1

June 2009

Courtney Turning Basin						
Variable	SSP (m/s)	limit	Temp (deg C)	limit	Sal (psu)	limit
<i>Mean</i>	-4.69		-0.75		-1.57	
<i>SD</i>	3.04		1.49		4.29	
<i>RMSE</i>	5.58		1.67		4.57	
<i>Min</i>	-21.96		-4.47		-9.95	
<i>Max</i>	0.63		1.65		9.69	
<i>CF</i>	92.34	10.00	19.70	0.50	68.86	5.00
<i>POF</i>	0.00	10.00	29.46	0.50	10.61	5.00
<i>NOF</i>	7.66	10.00	50.84	0.50	20.54	5.00

Courtney Channel						
Variable	SSP (m/s)	limit	Temp (deg C)	limit	Sal (psu)	limit
<i>Mean</i>	-3.03		-0.14		-2.05	
<i>SD</i>	1.85		1.45		4.70	
<i>RMSE</i>	3.55		1.46		5.13	
<i>Min</i>	-15.78		-4.27		-13.49	
<i>Max</i>	1.12		3.06		11.08	
<i>CF</i>	99.32	10.00	33.30	0.50	63.13	5.00
<i>POF</i>	0.00	10.00	32.49	0.50	8.80	5.00
<i>NOF</i>	0.68	10.00	34.21	0.50	28.07	5.00

Main Harbour						
Variable	SSP (m/s)	limit	Temp (deg C)	limit	Sal (psu)	limit
<i>Mean</i>	-2.04		0.04		-1.74	
<i>SD</i>	1.31		1.52		5.21	
<i>RMSE</i>	2.43		1.52		5.50	
<i>Min</i>	-6.93		-4.81		-16.55	
<i>Max</i>	2.39		4.14		15.60	
<i>CF</i>	100.00	10.00	35.89	0.50	63.23	5.00
<i>POF</i>	0.00	10.00	33.61	0.50	9.96	5.00
<i>NOF</i>	0.00	10.00	30.51	0.50	26.81	5.00

Main Harbour ADCP				
Variable	North (m/s)	limit	East (m/s)	limit
<i>Mean</i>	-0.02		-0.01	
<i>SD</i>	0.52		0.40	
<i>RMSE</i>	0.52		0.40	
<i>Min</i>	-9.59		-3.46	
<i>Max</i>	3.53		5.40	
<i>CF</i>	97.20	1.00	98.34	1.00
<i>POF</i>	1.03	1.00	0.52	1.00
<i>NOF</i>	1.77	1.00	1.14	1.00

Reversing Falls						
Variable	SSP (m/s)	limit	Temp (deg C)	limit	Sal (psu)	limit
<i>Mean</i>	-2.28		0.41		-3.05	
<i>SD</i>	0.97		0.81		2.83	
<i>RMSE</i>	2.47		0.91		4.15	
<i>Min</i>	-5.06		-1.27		-10.86	
<i>Max</i>	0.33		2.43		1.88	
<i>CF</i>	100.00	10.00	33.33	0.50	87.68	5.00
<i>POF</i>	0.00	10.00	50.72	0.50	0.00	5.00
<i>NOF</i>	0.00	10.00	15.94	0.50	12.32	5.00

Reversing Falls ADCP				
Variable	North (m/s)	limit	East (m/s)	limit
<i>Mean</i>	-0.18		-0.57	
<i>SD</i>	1.30		0.83	
<i>RMSE</i>	1.31		1.01	
<i>Min</i>	-9.12		-3.64	
<i>Max</i>	4.92		8.36	
<i>CF</i>	64.86	1.00	74.08	1.00
<i>POF</i>	13.99	1.00	1.39	1.00
<i>NOF</i>	21.14	1.00	24.53	1.00

Curriculum Vitae

Candidate's full name: Ian William Church

Universities attended:

B.Sc.Eng GGE, University of New Brunswick, 2006

M.Sc.Eng GGE, University of New Brunswick, 2008

Publications:

Brucker S., J. Muggah, I. Church, J.E. Hughes Clarke, T. Hamilton, A. Hiroji, W. Renoud, 2013, *Hydrographic efficiencies of operating an 18 m research platform in the eastern Canadian Arctic.*, Proceedings of the US Hydrographic Conference, New Orleans, 2013

Church, I., John E. Hughes Clarke, Susan Haigh, Reenu Toodesh, 2012, *Modelling the estuarine circulation of the Port of Saint John: Visualizing complex sound speed distribution*, Proceedings of the Canadian Hydrographic Conference, Niagara Falls, Ontario, Canada.

Hughes Clarke, J.E., S. Brucker, J. Muggah, I. Church, D. Cartwright, P. Kuus, T. Hamilton, D. Pratomo and B. Eisan, 2012, *The Squamish ProDelta: Monitoring Active Landslides and Turbidity Currents*, Proceedings of the Canadian Hydrographic Conference 2012, Niagara Falls, Ontario, Canada.

Hughes Clarke, J.E., S. Brucker, J. Muggah, T. Hamilton, D. Cartwright, I. Church and P. Kuus, 2012, *Temporal progression and spatial extent of mass wasting events on the Squamish prodelta slope: Landslides and Engineered Slopes: Protecting Society through Improved Understanding*, Eberhardt et al. (eds), Taylor and Francis Group, ISBN 978-0-415-62123-6, p.1091-1096.

Jakobsson, M., L. Mayer, B. Coakley, J. A. Dowdeswell, S. Forbes, B. Fridman, H. Hodnesdal, R. Noormets, R. Pedersen, M. Rebesco, H. W. Schenke, Y. Zarayskaya, D. Accettella, A. Armstrong, R. M. Anderson, P. Bienhoff, A. Camerlenghi, I. Church, M. Edwards, J. V. Gardner, J. K. Hall, B. Hell, O. Hestvik, Y. Kristoffersen, C. Marcussen, R. Mohammad, D. Mosher, S. V. Nghiem, M. T. Pedrosa, P. G. Travaglini, and P. Weatherall (2012). "*The International Bathymetric Chart of the Arctic Ocean (IBCAO) Version 3.0.*" Geophysical Research Letters, 39(12).

Lastras, G., Canals, M., Amblas, D., Lavoie, C., Church, I., De Mol, B., Duran, R., Calafat, A.M., Hughes-Clarke, J.E., Smith, C.J., Heussner, S., and "Euroleón" cruise shipboard party, 2011, *Understanding sediment dynamics of two large submarine valleys from seafloor data: Blanes and La Fonera canyons, northwestern Mediterranean Sea*. Marine Geology, Volume 280, Issues 1–4, Pages 20–39.

Hughes Clarke, J.E., Brucker, S., Muggah, J., Church, I. and Cartwright, D. 2011, *The Squamish Delta Repetitive Survey Program: A simultaneous investigation of prodeltaic sedimentation and integrated system accuracy*, U.S. Hydrographic Conference 2011

Muggah, J., Church, I., Beaudoin, J. and Hughes Clarke, J.E., 2010. *Seamless Online Distribution of Amundsen Multibeam Data*, Paper S7.2, Proceedings of the Canadian Hydrographic Conference 2010, Quebec, Quebec, Canada.

Church, I., Brucker, S., Hughes Clarke, J.E., Haigh, S., Bartlett, J. and Janzen, T., 2009, *Developing Strategies to Facilitate Long Term Seabed Monitoring in the Canadian Arctic using Post Processed GPS and Tidal Models*, U.S. Hydro 2009, oral presentation, Norfolk, Virginia, USA.

Church, I. and Hughes Clarke, J.E., 2008, *Developing Strategies to Improve GPS Positioning and Tidal Information to Facilitate Long Term Seabed Monitoring in the Canadian Arctic*, ArcticNet Annual Scientific Meeting, poster presentation, Quebec City, Quebec, Canada.

Church, I., Hughes Clarke, J.E., Haigh, S., Santos, M., Lamplugh, M., Griffin, J. and Parrott, R., 2008, *Using Globally-Corrected GPS Solutions to Assess the Viability of Hydrodynamic Modeling in the Bay of Fundy*, P4-2, Proceedings of the Canadian Hydrographic Conference and National Surveyors Conference, Victoria, BC

Church, I., Hughes Clarke, J.E. and Haigh, S., 2007, *Applying Predicted Tides from a Local Hydrodynamic Model to Multibeam Bathymetry: A Solution for Seabed Monitoring in Remote Locations*. ArcticNet Annual Scientific Meeting, poster presentation, Collingwood, Ontario, Canada.

Church, I., Hughes Clarke, J.E. and Haigh, S., 2007, *Use of a nested finite-element hydrodynamic model to predict phase and amplitude modification of tide within narrow fjords*. U.S. Hydro 2007, oral presentation, Norfolk, Virginia, USA.

Church I., 2007, *Predicted Tides from Hydrodynamic Models*. U.S. Hydro 2007, The Sixth International Discussion Group Meeting on Uncertainty Management in Hydrography, oral presentation, Norfolk, Virginia, USA.

Church, I., Hughes Clarke, J.E., Haigh, S., and Brucker, S., 2006, *Comparing GcGPS Ellipsoid Height Records, Predicted Tides and a Hydrodynamic Circulation Model for the Pond Inlet, Eclipse Sound and Navy Board Inlet System*. ArcticNet Annual Scientific Meeting, poster presentation, Victoria, British Columbia, Canada.

Church, I., 2006, *Towards a Nested Finite-Element Hydrodynamic Model to Predict Phase and Amplitude Modification of Tide within Narrow Fjords*. Geomatics and Geodesy Student Technical Conference, oral presentation, Fredericton, New Brunswick, Canada.